

NO. ST3
MAY 1956

JOURNAL of the

Structural

Division

PROCEEDINGS OF THE



**AMERICAN SOCIETY
OF CIVIL ENGINEERS**

VOLUME 82

THIS JOURNAL

... represents an effort by the Society to deliver technical data direct from the authors to the reader with the greatest possible speed. To this end, it has none of the usual editing required in more formal publications.

Readers are invited to submit discussion applying to current papers. For papers in this journal the final date on which a discussion should reach the Manager of Technical Publications appears as a footnote with each paper.

Those who are planning papers or discussions for "Proceedings" will expedite Division and Committee action measurably by first studying "Publication Procedure for Technical Paper" (Proceedings Paper 290). For free copies of this paper—describing style, content, and format—address the Manager, Technical Publications, ASCE.

Reprints from this Journal may be made on condition that the full title of the paper, name of the author, page reference (or paper number), and date of publication by the Society are given. The Society is not responsible for any statement made or opinion expressed in its publications.

This Journal is published quarterly by the American Society of Civil Engineers. Publication office at 2500 South State Street, Ann Arbor, Michigan. Editorial and General Offices at 33 West 39 Street, New York 18, New York. \$4.00 of a member's dues are applied as a subscription to this Journal. Second-class mail privileges are authorized at Ann Arbor, Michigan.

Journal of the
STRUCTURAL DIVISION
Proceedings of the American Society of Civil Engineers

STRUCTURAL DIVISION, COMMITTEE ON PUBLICATIONS
Emerson J. Ruble, Chairman; James G. Clark; Elvind Hognestad;
Thomas R. Kuesel; K. W. Lange; N. W. Morgan; Josef Sorkin;
Kenneth White; David M. Wilson.

CONTENTS

May, 1956

Papers

	Number
Specifications for Structures of Aluminum Alloy 6061-T6 Second Progress Report of the Committee of the Structural Division on Design in Lightweight Structural Alloys	970
Specifications for Structures of Aluminum Alloy 2014-T6 Third Progress Report of the Committee of the Structural Division on Design in Lightweight Structural Alloys	971
Discussion	972
Dynamic Stresses in Continuous Plate Girder Bridges by Roy C. Edgerton and Gordon W. Beecroft	973
Earthquake Stresses in Spherical Domes and in Cones by E. P. Popov	974
Limit Design for Buildings by Boyd C. Ringo	986

DIVISION ACTIVITIES

Newsletter	1956-11
----------------------	---------

THE FEDERAL BUREAU OF INVESTIGATION

Report of Special Agent in Charge, New York Office, dated 10/1/41

RE: JAMES EARL RAY, alias, et al.
EDWARD GEORGE BREMER, alias, et al.
EDWARD GEORGE BREMER, alias, et al.

NEW YORK

October 1, 1941

TO DIRECTOR, FBI

Enclosed for the Bureau are two copies of a letterhead memorandum (LHM) dated and captioned as above, and two copies of a letterhead memorandum (LHM) dated and captioned as above.

The LHM dated and captioned as above, is a copy of a letterhead memorandum (LHM) dated and captioned as above, and is a copy of a letterhead memorandum (LHM) dated and captioned as above.

The LHM dated and captioned as above, is a copy of a letterhead memorandum (LHM) dated and captioned as above, and is a copy of a letterhead memorandum (LHM) dated and captioned as above.

The LHM dated and captioned as above, is a copy of a letterhead memorandum (LHM) dated and captioned as above, and is a copy of a letterhead memorandum (LHM) dated and captioned as above.

The LHM dated and captioned as above, is a copy of a letterhead memorandum (LHM) dated and captioned as above, and is a copy of a letterhead memorandum (LHM) dated and captioned as above.

Very truly yours,

Special Agent in Charge, New York Office

Approved and Forwarded: Special Agent in Charge, New York Office

JOURNAL
STRUCTURAL DIVISION
Proceedings of the American Society of Civil Engineers

SPECIFICATIONS FOR STRUCTURES OF
ALUMINUM ALLOY 6061-T6

SECOND PROGRESS REPORT OF THE COMMITTEE OF THE
STRUCTURAL DIVISION
ON DESIGN IN LIGHTWEIGHT STRUCTURAL ALLOYS

FOREWORD

These specifications are a revised version of "Specifications for Structures of a Moderate Strength Aluminum Alloy of High Resistance to Corrosion," published as Proceedings, ASCE, Separate No. 132, May, 1952. A discussion was published in Proceedings, ASCE, Paper No. 765, August, 1955. Publication of these specifications as a progress report of the Committee on Design in Lightweight Structural Alloys has been approved by the Executive Committee of the Structural Division.

SYNOPSIS

These specifications cover allowable stresses, design rules, and fabrication procedures for structures built of the aluminum alloy known commercially as 6061-T6 (formerly 61S-T6). The basic allowable tensile working stress is 15 kips per sq in. based on a minimum yield strength of 35 kips per sq in. and a minimum tensile strength of 38 kips per sq in.

PART I. GENERAL

INTRODUCTION

These specifications cover the allowable stresses, the design rules, and the fabrication procedures for the aluminum alloy most commonly used for structural purposes where a high degree of resistance to corrosion is desired. In the preparation of these specifications the Committee has made use of the available theoretical and experimental work relating to this subject and

Note: Please forward all comments on this report directly to J. W. Clark, Box 772, New Kensington, Pa. Paper 970 is part of the copyrighted Journal of the Structural Division of the American Society of Civil Engineers, Vol. 82, No. ST 3, May, 1956.

particularly to the Committee's previously published¹ "Specifications for Heavy Duty Structures of High-Strength Aluminum Alloy."

These specifications are confined to allowable stresses, design rules, and fabrication. No attempt has been made to cover the loading, erection, inspection, or nontechnical provisions included in many specifications, since such provisions are fairly well established in current good structural practice. Furthermore, no attempt has been made to include design rules which cover every detail of construction but rather those which are different from steel practice or which are needed for the sake of completeness. It is intended, of course, that structures built under these specifications will be designed, constructed, and erected by following the current good practice already well established for steel structures, except as modified herein.

It is believed that the designer can make more efficient use of a set of specifications if he knows the basis for its various provisions. For this reason, Part IV, Explanation of Specifications, has been added. Part IV contains background information and references concerning those paragraphs of the specifications for which some explanation seems required.

When the abbreviation "kip" is used in these specifications it denotes "kilo"-pounds, or "thousands of pounds."

Material

The principal material considered in these specifications is an aluminum alloy having the following nominal chemical composition:

Composition	Percentage by weight
Copper	0.25
Silicon	0.6
Magnesium	1.0
Chromium	0.25
Aluminum	97.9
Total	100.0

This material is covered by the American Society for Testing Materials (ASTM) Specifications Nos. B221-54T(GS11A), B211-54T(GS11A), B209-54T(GS11A), B247-54T(GS11A), B210-54T(GS11A), B235-54T(GS11A), and B241-54T(GS11A). It is produced by several manufacturers under the commercial designation 6061-T6 and is available in the form of sheet, plate, shapes, tubes, rods, bars, rivets and forgings. All these products are given a solution heat treatment and a precipitation heat treatment before being shipped.

The specified minimum tensile strength of this material is 42 kips per sq in. for all products except extruded shapes and forgings, for which the specified minimum tensile strength is 38 kips per sq in. The specified minimum yield strength for all products is 35 kips per sq in. The following are the

1. "Specifications for Heavy Duty Structures of High-Strength Aluminum Alloy," final report of the Committee of the Structural Division on Design in Lightweight Structural Alloys, Transactions, ASCE, Vol. 117, 1952, p. 1253.

lowest of the various specified minimum properties and have been used as a basis for the selection of allowable stresses in these specifications (in kips per square inch):

Description	Stress
Tensile strength	38
Yield strength (offset 0.2%)	35

In addition to the specified minimum tensile properties the engineer will be interested in some of the other mechanical properties not covered by specifications. The following are typical mechanical properties of this alloy:

Shear strength, in kips per square inch	30
Modulus of elasticity in tension and compression, in kips per square inch	10,000
Modulus of elasticity in shear, in kips per square inch	3,800
Poisson's ratio	1/3
Coefficient of expansion per degree Fahrenheit	0.000012
Weight, in pounds per cubic inch	0.098

(The foregoing value of shear strength is typical as determined with steel shearing tools. The value determined by torsion tests is greater.)

Fig. 1 shows tensile and compressive stress-strain curves and the compressive tangent modulus curve for 6061-T6 material having the minimum properties listed in the second paragraph of this section.

Alloy 6061-T6 is the one principally considered in the preparation of these specifications and the one to which the allowable stresses for parts other than bolts apply. However, these specifications may be applied to structures built of other suitable aluminum alloys, provided such alloys meet the specified strengths and elongations listed in the ASTM specifications mentioned in the first paragraph of this section. Whether or not such other alloys need paint protection will depend upon whether they are as resistant to corrosion as 6061-T6. The sections of this specification dealing with welding should not be applied to other alloys unless it has been clearly demonstrated that such alloys are suitable for welding.

Rivets used in fabricating structures designed in accordance with these specifications shall be of aluminum alloy and may be either cold driven or hot driven. The alloy used is indicated in Table 1. Supplementary information on riveting was published² by E. C. Hartmann, M. ASCE, G. O. Hoglund, and M. A. Miller in 1944.

Permanent bolts used in structures designed in accordance with these specifications shall be of the aluminum alloy known commercially as 2024-T4. Such bolts have an expected minimum ultimate shear strength of 37 kips per sq in.

2. "Joining Aluminum Alloys," by E. C. Hartmann, G. O. Hoglund, and M. A. Miller, Steel, August 7, 1944, p. 84.

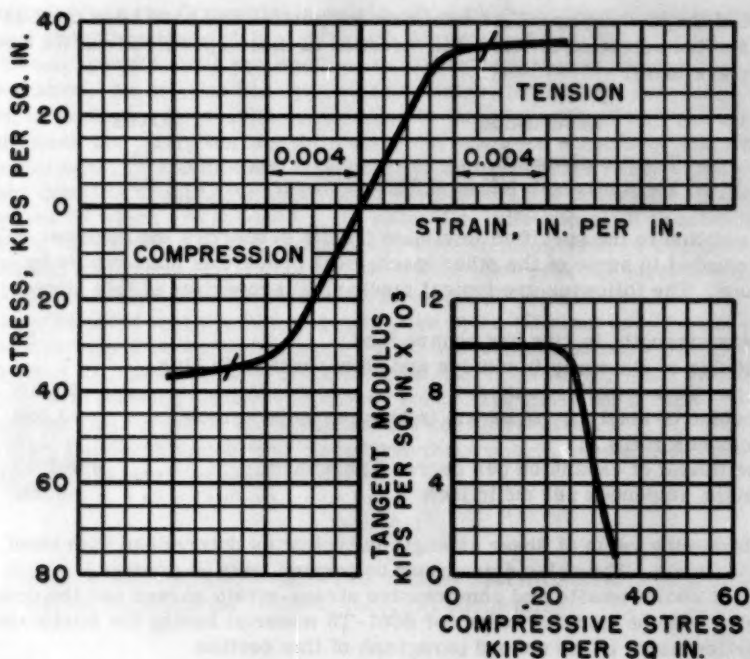


Fig. 1.—Stress-Strain Curves and Tangent Modulus Curve for Alloy 6061-T6 Based on Minimum Properties

TABLE 1.—Alloys to be Used for Rivets

Designation before driving	Driving procedure	Designation after driving	Typical shear strength ^a
6061-T6....	Cold, as received	6061-T6	30
6061-T4....	Hot, 990° F to 1,050° F	6061-T43	24

^a Typical ultimate shear strength of the driven rivet, in kips per square inch.

PART II. SPECIFICATIONS FOR RIVETED AND BOLTED STRUCTURES

Section A. Summary of Allowable Stresses

The allowable stresses to be used in proportioning the parts of a structure shall be as follows:

Specifications

Description

Stress in
kips per
square inch

A-1	Axial tension, net section (see Specification H-4). . .	15
A-2	Tension in extreme fibers, of shapes, girders, and built-up members subject to bending, net section (see Specification H-4)	15
A-3	Axial compression (see Section B)
A-4	Compression in extreme fibers of shapes, girders, and built-up members subject to bending (see Section C)
A-5	Compression in plates, legs, and webs (see Section D)
A-6	Stress in extreme fibers of pins	22
A-7	Shear in plates and webs (see Section E)
A-8	Shear in aluminum alloy 6061-T6 rivets, cold driven (see Tables 4 and 5)	10
A-9	Shear in aluminum alloy 6061-T43 rivets, driven at temperatures of from 990° F to 1,050° F (see Tables 4 and 6)	8
A-10	Shear in turned bolts of aluminum alloy 2024-T4 in reamed holes (see Table 4)	12
A-11	Shear in pins	10
A-12	Bearing on pins	22
A-13	Bearing on hot-driven or cold-driven rivets, milled stiffeners, turned bolts in reamed holes, and other parts in fixed contact (see Section G)	27

Section B. Column Design

B-1. Allowable Compressive Stress in Columns.—The allowable compressive stress on the gross section of axially loaded columns shall be determined from the curves in Fig. 2. Let k be a factor describing end restraint. Ordinarily the curve for partial restraint ($k = 0.75$) shall be used. The curves for pin-ended and fixed-ended columns, also shown in Fig. 2, may be used as a guide in the selection of allowable compressive stresses for those cases in which the degree of end restraint is known to be different from that represented by $k = 0.75$. It is important, however, that no allowable stresses higher than those given for the case of $k = 0.75$ be used in actual design unless a detailed analysis of the structure demonstrates convincingly that a value of k smaller than 0.75 is justified for the member in question.

Columns having cross sections involving webs and outstanding legs of such proportions that local buckling may control the design shall be checked by the method outlined in Section D.

B-2. Columns with Slenderness Ratio Exceeding 120. Because long columns are relatively flexible, they may be appreciably weakened by the presence of lateral loads that would have little effect on the column strength of stiffer members. For this reason, columns with slenderness ratios greater than 120 should not be used unless special care is taken to insure that the effect of any lateral loads to which the member may be subjected, such as wind, dead load, or the weight of workmen and equipment, are taken into account by using the provision for combined compression and bending in Specification B-7.

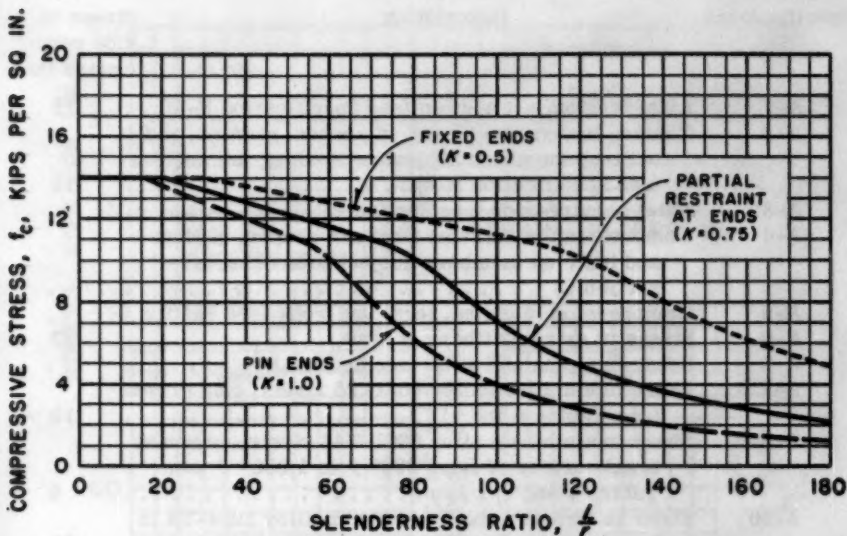


FIG. 2.—ALLOWABLE COMPRESSIVE STRESSES FOR AXIALLY LOADED COLUMNS (GROSS SECTION)

B-3. Connections.—Compression members shall be so designed that the main elements of the section will be connected directly to the gusset plates, pins, or other members.

B-4. Compression Splices.—Members designed for compression, if faced for bearing, shall be spliced on four sides sufficiently to hold the abutting parts true to place. The splice shall be as near a panel point as practicable and shall be designed to transmit at least one half of the stress through the splice material. Members not faced for bearing shall be fully spliced for the computed stress. In either case, adequate provision shall be made for transmitting shear.

B-5. Stay Plates.—On the open sides of compression members, the flanges shall be connected by lacing bars, and there shall be stay plates as near each end as practicable. There shall be stay plates at intermediate points where the lacing is interrupted. The length of the end stay plates shall not be less than one and one-fourth times the distance between rivet lines. The thickness of stay plates shall not be less than one fortieth of the distance between rivet lines.

B-6. Diagonal Lacing.—The slenderness ratio of the part of the flange between the lacing bar connections shall be not more than two thirds of the slenderness ratio of the member.

B-7. Combined Compression and Bending.—The allowable stress in a member that carries bending moment in addition to uniform compression (as, for example, an eccentrically loaded column) shall be determined from the following formula:

$$f_b = f_B \left(1 - \frac{P/A}{f_C}\right) \left(1 - \frac{P/A}{f_{CE}}\right) \dots \dots \dots (1)$$

in which (in kips per sq in.):

f_b is the maximum bending stress (compression) that may be permitted at or near the center of the unsupported length, in addition to uniform compression, P/A ;

P/A is the average compressive stress on the gross cross section, A , of the member, produced by a column load, P ;

f_B is the allowable compressive working stress for the member considered as a beam;

f_C is the allowable working stress for the member considered as an axially loaded column; and

$$f_{CE} = \frac{70,000}{(L/r)^2} \dots \dots \dots (2)$$

in which L/r is the slenderness ratio for the member considered as a column tending to fail in the plane of the bending forces.

B-8. Transverse Shear in Columns.—In designing lacing or shear webs for columns, the maximum shear on the column shall be computed from the formula:

$$V = P \frac{4.5r^2 (f_B - P/A)}{f_C L c} + V_t \dots \dots \dots (3a)$$

but shall not be taken less than

$$V = 0.02 P + V_t \dots \dots \dots (3b)$$

in which:

V is the maximum shear on any transverse section of a column in the outer eighth of the length at each end, in the direction of assumed bending, in kips;

r is the radius of gyration, in inches;

f_C is the allowable compressive working stress taken from Fig. 2, in kips per sq in.;

L is the length of the member, in inches;

c is the distance from the centroidal axis to the extreme fiber, in inches; and

V_t is the shear due to any transverse loads on a column, in kips.

The values of f_B , f_C , L , r , and c must be consistent with the direction of bending assumed.

Section C. Allowable Compressive Stresses in Flanges of Beams and Girders

C-1.—The allowable compressive stress in the extreme fiber (gross section) of single-web rolled shapes, extruded shapes, girders, and built-up sections, subject to bending, shall be determined from the curve in Fig. 3. The terms used in Fig. 3 are defined as follows:

L is the laterally unsupported length of beam (clear distance between

supports at which the beam is prevented from lateral displacement), or, in the case of a cantilever beam with one end free, L is four thirds of the laterally unsupported length, in inches.

TABLE 2.—Allowable Compressive Stress in Beam Flanges
for Various Values of Laterally Unsupported Length
of Compression Flange, L , in Inches

Procedure.—Maximum allowable bending moments are found by multiplying the allowable compressive stresses (in kips per square inch) by the gross section modulus of the beam. The stress on the net section of the tension flange must also be kept within allowable limits.

Depth (in.)	Weight (lb per ft)	Section modulus (in. ³)	Values of L									
			16	32	64	96	128	160	192	256	352	480
(a) I-Beams												
2	0.78	0.481	13.1 ^a	12.1	9.4	5.8	4.2	3.3	2.7	2.0	1.4	1.1
2	1.43	0.782	13.7	12.7	11.4	10.4	8.6	6.8	5.7	4.2	3.1	2.3
2.5	1.80	1.162	13.8	12.9	11.9	11.1	10.3	9.0	7.5	5.6	4.1	3.0
3	1.96	1.68	13.8	12.7	11.1	9.5	7.1	5.6	4.6	3.5	2.5	1.8
3	2.59	1.95	13.9	12.9	11.7	10.8	9.5	7.8	6.5	4.8	3.5	2.6
4	2.64	3.03	13.9	12.8	11.1	9.1	6.6	5.2	4.3	3.1	2.3	1.7
4	3.63	3.59	13.9 ^a	13.0	11.7	10.7	9.3	7.4	6.1	4.6	3.3	2.4
5	3.43	4.90	13.9 ^a	12.9	11.2	9.3	6.7	5.2	4.2	3.1	2.3	1.6
5	5.10	6.09	13.9 ^a	13.2	11.9	10.9	9.8	8.0	6.6	4.9	3.6	2.6
6	4.30	7.36	13.9 ^a	13.1	11.4	9.6	6.9	5.3	4.3	3.1	2.3	1.6
6	5.96	8.77	13.9 ^a	13.2	11.8	10.7	9.1	7.2	5.9	4.4	3.1	2.3
7	5.27	10.48	13.9 ^a	13.2	11.6	10.0	7.2	5.5	4.4	3.2	2.3	1.6
7	6.92	12.12	13.9 ^a	13.3	11.8	10.7	8.8	6.8	5.6	4.1	2.9	2.1
8	6.35	14.39	13.9 ^a	13.4	11.8	10.4	7.7	5.8	4.6	3.3	2.4	1.7
8	8.81	17.18	13.9 ^a	13.4	12.0	11.0	9.6	7.6	6.2	4.5	3.2	2.3
9	7.51	19.09	13.9 ^a	13.5	12.0	10.7	8.2	6.1	4.9	3.5	2.4	1.8
9	10.37	22.75	13.9 ^a	13.5	12.2	11.1	9.8	7.8	6.3	4.6	3.3	2.4
10	8.76	24.68	13.9 ^a	13.6	12.1	10.9	8.8	6.5	5.1	3.6	2.5	1.8
10	12.10	29.41	13.9 ^a	13.6	12.3	11.2	10.1	8.2	6.6	4.8	3.4	2.4
12	10.99	36.35	13.9 ^a	13.6	12.2	11.0	9.2	6.7	5.2	3.6	2.5	1.8
12	17.28	50.81	14.0	13.8	12.6	11.6	10.8	9.6	7.9	5.6	4.0	2.9
(b) H-Beams												
4	4.71	5.36	13.8 ^a	13.6	12.5	11.6	11.0	10.2	9.1	6.8	4.9	3.5
5	6.45	9.53	13.7 ^a	13.7 ^a	12.8	12.0	11.3	10.6	9.7	7.2	5.2	3.7
6	7.81	14.69	13.6 ^a	13.6 ^a	13.1	12.2	11.5	10.9	10.0	7.6	5.3	3.8
6	9.14	15.81	13.6 ^a	13.6 ^a	13.1	12.3	11.7	11.1	10.5	8.5	6.0	4.3
8	11.19	28.23	13.3 ^a	13.3 ^a	13.0 ^a	12.6 ^a	12.0	11.3	10.7	8.6	5.7	3.9
8	12.95	30.23	13.3 ^a	13.3 ^a	13.0 ^a	12.7 ^a	12.1	11.5	10.9	9.3	6.4	4.5

^aThese values are governed by local buckling (see Section D). All other values are determined from Fig. 3, Section C.

S_c is the section modulus for the beam about the axis normal to the web (compression side) in inches cubed;

$$B = I_1 d \sqrt{11.7 + \frac{J}{I_1} \left(\frac{L}{d} \right)^2};$$

I_1 is the moment of inertia for the beam about the axis parallel to the web, in inches to the fourth power;

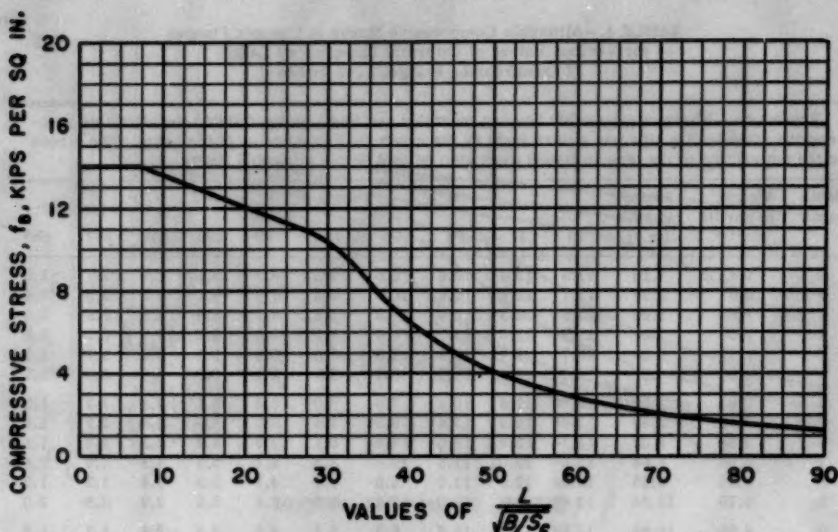


FIG. 3.—ALLOWABLE COMPRESSIVE STRESSES IN BEAM AND GIRDER FLANGES (GROSS SECTION)

J is the torsion factor, in inches to the fourth power; and
 d is the depth of beam, in inches.

In the case of beams having top and bottom flanges of different lateral stiffness, I_1 should be calculated as if both flanges were the same as the compression flange. Values of the torsion factor J are published for many standard shapes.³ Values of J for plates and shapes not published may be calculated by assuming the section to be composed of rectangles and taking the sum of the terms $b t^3/3$ for each rectangle, in which b equals the length and t , the thickness of the rectangle, both in inches. The value of J for a built-up member is the sum of the individual values of J of the sections of which it is composed.

The allowable stresses from Fig. 3 provide a safe margin against the lateral buckling type of failure. The outstanding compression flanges of the beams and girders should be checked for local buckling by the method outlined in Section D.

Table 2 lists values of allowable stress determined from Fig. 3 and Section D for various laterally unsupported lengths of a number of standard I-beams and H-beams. Table 3 lists similar values for standard channels.

Because of their tube-like cross section, double-web box girders are very stiff in torsion compared with single-web girders of comparable size, and, hence, lateral buckling failures such as are considered in Fig. 3 do not occur in such girders. For double-web box girders it is necessary only to check for local buckling of the flanges by the method outlined in Section D.

3. "Alcoa Structural Handbook," Aluminum Co. of America, Pittsburgh, Pa., 1955, pp. 204-226.

TABLE 3.—Allowable Compressive Stress in Channel Flanges
for Various Values of Laterally Unsupported Length
of Compression Flange, L, in Inches

Procedure.—Maximum allowable bending moments are found by multiplying the allowable compressive stresses (in kips per square inch) by the gross section modulus of the beam. The stress on the net section of the tension flange must also be kept within allowable limits.

Depth (in.)	Weight (lb per ft)	Section modulus (in. ³)	Values of L									
			16	32	64	96	128	160	192	256	352	480
3	1.42	1.10	13.5	12.3	10.6	8.0	5.9	4.7	3.9	2.9	2.1	1.5
3	2.07	1.38	13.7	12.8	11.6	10.6	9.2	7.4	6.1	4.6	3.3	2.4
4	1.85	1.92	13.6	12.3	10.4	7.2	5.2	4.1	3.4	2.5	1.8	1.3
4	2.50	2.29	13.7	12.6	11.1	9.4	7.1	5.6	4.7	3.5	2.5	1.8
5	2.32	3.00	13.7	12.4	10.4	7.0	5.0	3.9	3.2	2.6	1.7	1.3
5	3.97	4.17	13.8 ^a	12.9	11.6	10.5	8.9	7.1	5.9	4.4	3.2	2.3
6	2.83	4.37	13.7 ^a	12.6	10.6	7.0	5.0	3.8	3.1	2.3	1.7	1.2
6	4.48	5.80	13.8 ^a	12.9	11.4	9.9	7.6	6.0	4.9	3.7	2.7	1.9
7	3.38	6.08	13.7 ^a	12.8	10.8	7.4	5.1	3.9	3.2	2.3	1.7	1.2
7	5.96	8.64	13.8 ^a	13.0	11.6	10.4	8.5	6.7	5.5	4.1	2.9	2.1
8	4.25	8.46	13.8 ^a	12.9	11.0	8.0	5.4	4.1	3.3	2.4	1.7	1.3
8	6.79	11.34	13.8 ^a	13.1	11.6	10.4	8.2	6.4	5.2	3.9	2.8	2.0
9	4.60	10.60	13.8 ^a	13.0	11.2	8.3	5.5	4.1	3.3	2.4	1.7	1.2
9	8.65	15.75	13.8 ^a	13.2	11.8	10.7	9.0	7.1	5.8	4.3	3.1	2.2
10	5.28	13.47	13.8 ^a	13.1	11.3	8.8	5.8	4.3	3.4	2.4	1.7	1.2
10	10.37	20.69	13.8 ^a	13.3	12.0	10.9	9.5	7.6	6.2	4.6	3.3	2.3
12	7.41	21.97	13.8 ^a	13.4	11.7	12.0	6.8	5.0	3.9	2.7	1.8	1.4
12	12.10	29.94	13.8 ^a	13.5	12.0	10.9	9.2	7.1	5.7	4.1	2.9	2.1

^aThese values are governed by local buckling (see Section D). All other values are determined from Fig. 3, Section C.

Section D. Allowable Compressive Stress for Plates, Legs, and Webs

D-1.—For struts consisting of a single angle or a T-section the compressive stress on the gross area shall not exceed the values given by the curves in Fig. 4 or Fig. 2, whichever is smaller.

D-2.—For compression members other than those consisting of a single angle or a T-section the following procedure shall be followed to provide a suitable margin of safety against the weakening effects of local buckling of flat plates, legs, and webs:

a.—Compute the compressive stress f_c on the flat plate, leg, or web in question, based on the design loads and the gross area, without regard to local buckling. This stress must be within allowable limits as defined in Sections B and C.

b.—Find the limiting value of b/t corresponding to the stress f_c , by the use of Fig. 5 or Fig. 6. If the flat plate, leg, or web has a ratio of unsupported width to thickness not exceeding this limiting value, local buckling is not a problem and the full gross area of the plate, leg, or web may be considered effective.

c.—If the flat plate, leg, or web has a ratio of unsupported width to thickness greater than the limiting $\frac{b}{t}$ -ratio found in step b, only a part of its

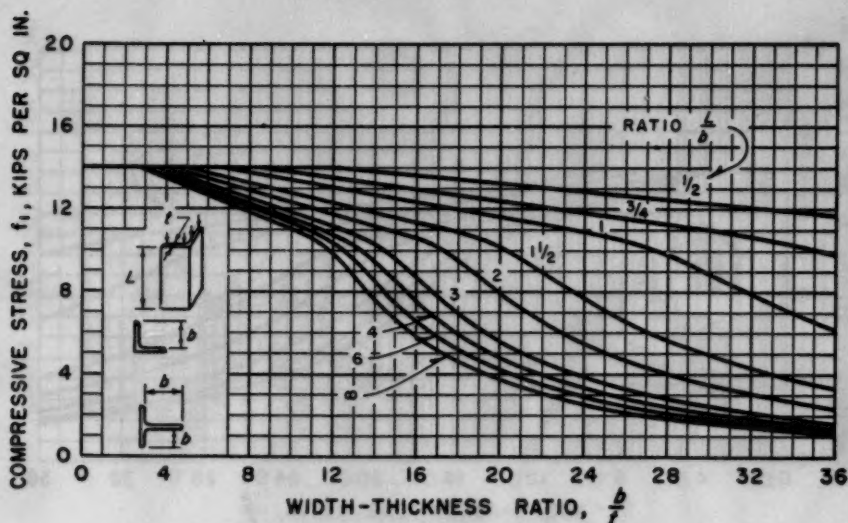


FIG. 4.—ALLOWABLE COMPRESSIVE STRESSES IN OUTSTANDING LEGS OF SINGLE-ANGLE AND T-SECTION STRUTS (GROSS SECTION)

unsupported width shall be included in computing its effective area. The part of the unsupported width of any individual flat plate, leg, or web which may be considered effective shall be found as follows:

$$b_e = b \frac{f_1}{f_c} \dots \dots \dots (4)$$

in which:

b_e is that part of the unsupported width considered effective, in inches;

b is the unsupported width, in inches;

f_c is the compressive stress based on gross area from step (a), in kips per square inch; and

f_1 is the stress found from Fig. 5 or Fig. 6 corresponding to the $\frac{b}{t}$ - value for the plate, leg, or web in question, in kips per square inch.

d.—Compute the compressive stress on the effective area. In the case of an axially loaded column this is simply the axial load divided by the total effective area, which, in turn, is simply the sum of the effective areas of the component parts. In the case of a beam or girder the compressive stress on the effective area shall be determined as follows: Compute the compressive extreme fiber stress f_c for the gross section of the beam or girder and then multiply this value by the ratio of the gross compression flange area to the effective compression flange area, including in each flange area not only the flange proper but also one-sixth of the area of the web.

e.—The compressive stress on the effective area computed in accordance

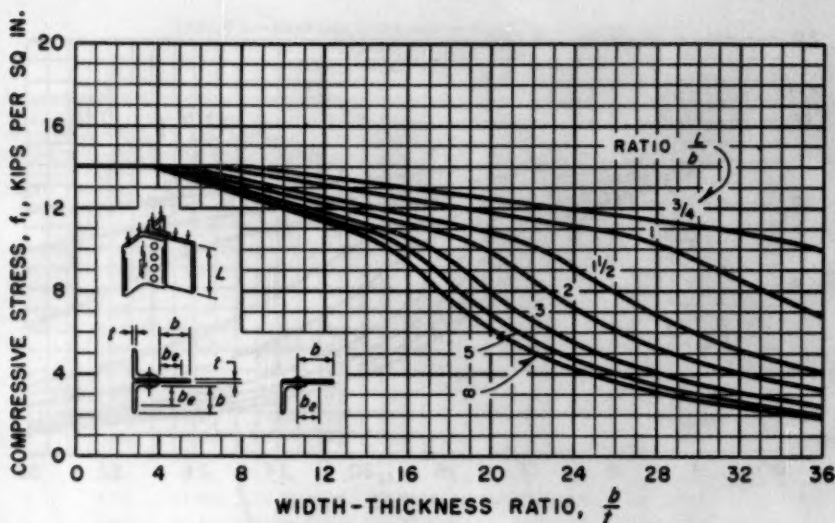


FIG. 5.—CHART FOR DETERMINING EFFECTIVE WIDTH FOR OUTSTANDING LEGS OF ANGLES BUILT INTO OTHER PARTS AND FOR PLATES BUILT IN ALONG ONE EDGE

with step d shall not exceed allowable limits as defined in Section B and C for the gross area.

f.—Steps c, d and e provide a suitable factor of safety against collapse of the member as a whole, but do not necessarily provide complete protection against local buckling of individual flat surfaces at the design load. Where local buckling at the design load cannot be tolerated because of appearance, or for other reasons, the computed compressive stress on the gross area, f_c , shall not exceed $1.5f_1$, where f_1 is the compressive stress given in Fig. 5 or Fig. 6 for the b/t ratio in question. Regardless of whether or not this limitation is placed on f_c , the member must still be checked by the method outlined in Steps a through e to insure an adequate factor of safety against collapse.

Section E. Allowable Shear Stresses in Plates and Webs

E-1.—The allowable shear stress on flat webs shall not exceed the values given by the curves in Fig. 7. The values in Fig. 7 apply to the gross area of the web, but the shear on the net area shall not exceed 10 kips per sq in.

Section F. Plate Girder Design

F-1. Proportioning Plate Girders.—Plate girders shall be proportioned by the moment of inertia method, with the gross section used to determine the moment of inertia.

The stress on the net area of the tension flange shall be found by multiplying the stress on the gross section by the ratio of the gross area of the tension flange to the net area. In determining this ratio the tension flange shall be considered to consist of the flange angles and cover plates plus one-sixth of the web.

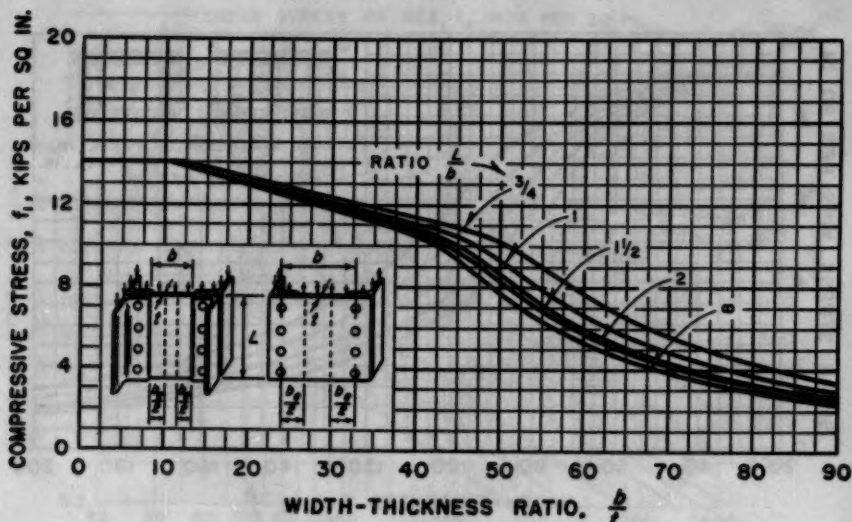


FIG. 6.—CHART FOR DETERMINING EFFECTIVE WIDTH FOR FLAT PLATES BUILT IN ALONG TWO EDGES

F-2. Allowable Flange Stress.—The allowable compressive stress in the extreme fiber of plate girders shall be determined as outlined in Sections C and D. The numerical value of the term $\sqrt{B/S_c}$, used in Fig. 3, is rarely less than one half of the width, in inches, of the compression flange for a plate girder. This fact is useful in preliminary design.

F-3. Flange Cover Plates.—Cover plates shall extend far enough to allow at least two extra rivets at each end of the plate beyond the theoretical end, and the spacing of the rivets in the remainder of the plate shall be such as to develop the required strength of the plate at any section.

F-4. Flange Rivets.—The flanges of plate girders shall be connected to the web with enough rivets to transmit the longitudinal shear at any point together with any load that is applied directly on the flange.

F-5. Flange Splices.—It is preferable that flange angles be spliced with angles and that no two members be spliced at the same cross section.

F-6. Allowable Web Stresses.—The allowable shear stress in the webs of plate girders shall not exceed the values given by the curves in Fig. 7. The longitudinal compressive stress in webs of plate girders at the toe of the compression flange shall not exceed the values given by the curves in Fig. 8.

F-7. Web Splices.—It is preferable that splices in the webs of plate girders be made with splice plates on both sides of the web.

F-8. Spacing of Vertical Stiffeners to Resist Shear Buckling.—The distance, s , between vertical stiffeners shall not exceed the values given by the solid curves in Fig. 9, which are replots of the curves in Fig. 7. The maximum value of the ratio of stiffener spacing to height of web, s/h , in Fig. 9 shall be

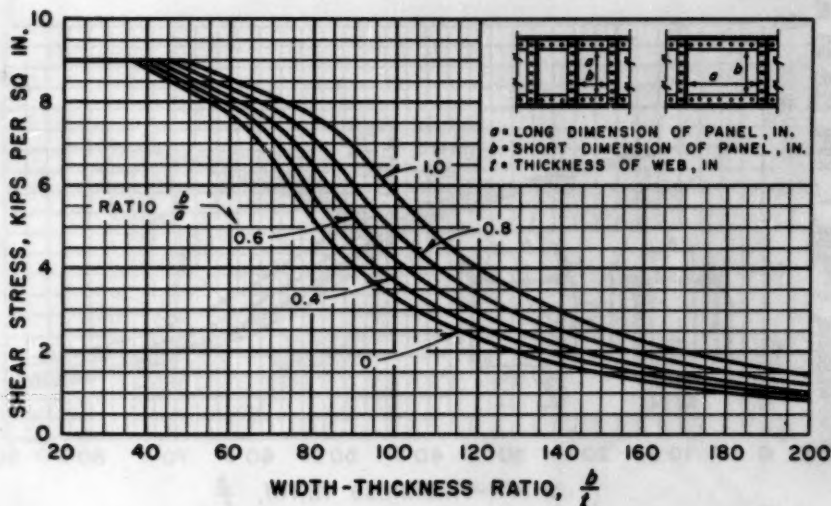


FIG. 7.—ALLOWABLE SHEAR STRESSES ON WEBS; PARTIAL RESTRAINT ASSUMED AT EDGES OF RECTANGULAR PANELS (GROSS SECTION)

determined from the ratio of clear height to thickness, h/t , and the computed shear stress on the girder web. Where a stiffener is composed of a pair of members, one on each side of the web, the distance s shall be the clear distance between the stiffeners. Where a stiffener is composed of a member on

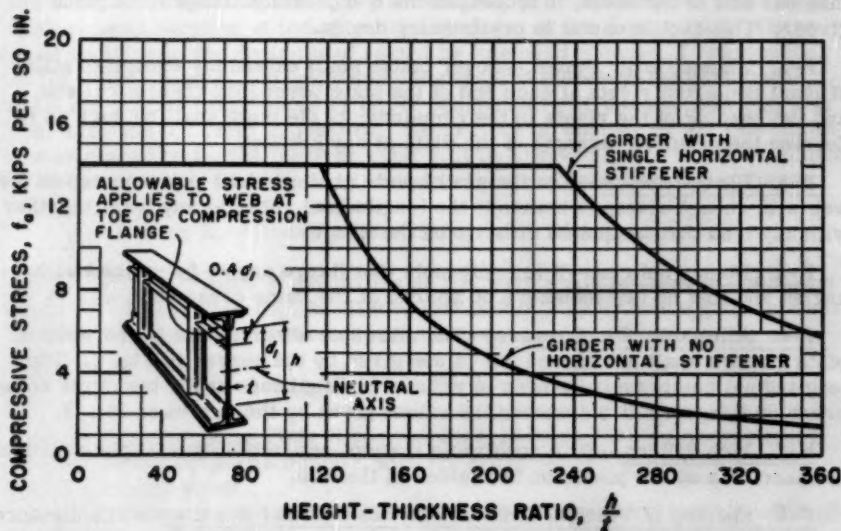


FIG. 8.—ALLOWABLE LONGITUDINAL COMPRESSIVE STRESSES FOR WEBS OF GIRDERS

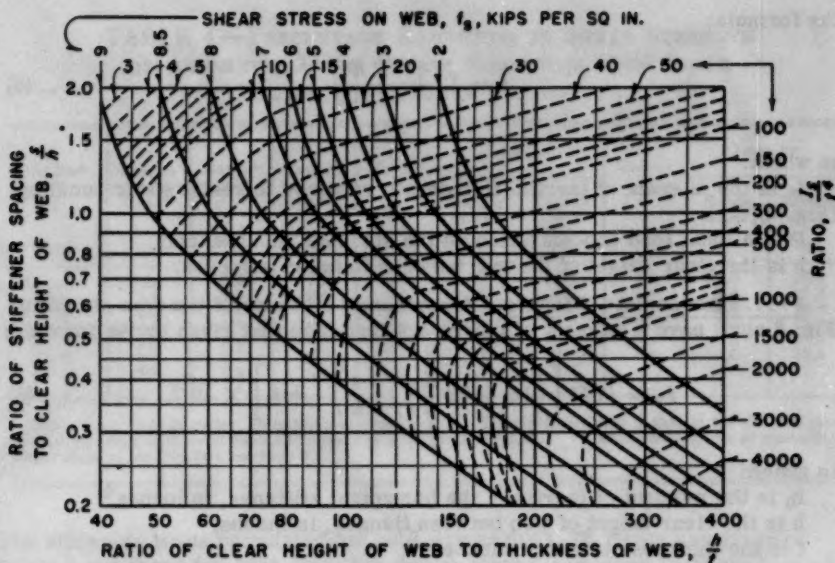


FIG. 9.—SPACING AND MOMENT OF INERTIA OF VERTICAL STIFFENERS TO RESIST SHEAR BUCKLING ON WEBS OF PLATE GIRDERS

one side of the web only, the distance s shall be the distance between rivet lines. In determining the spacing of vertical stiffeners to resist shear buckling in panels containing a horizontal stiffener located as shown in Fig. 8, the distance h in Fig. 9 may be taken as 90% of the clear height between flanges.

F-9. Size of Vertical Stiffeners to Resist Shear Buckling.—Stiffeners applied to plate girder webs to resist shear buckling shall have a moment of inertia not less than the values given by the dotted curves in Fig. 9. The minimum value of the ratio of the stiffener moment of inertia to the fourth power of the web thickness, I_s/t^4 , in Fig. 9, shall be determined from the ratio of height of web to thickness of web, h/t , and the computed shear stress on the girder web.

For a stiffener composed of members of equal size on both sides of the web, the moment of inertia shall be taken about the center line of the web. For a stiffener composed of a member on one side only, the moment of inertia shall be taken about the face of the web in contact with the stiffener. In determining moment of inertia of stiffeners, the term h shall always be taken as the full clear height between flanges, regardless of whether or not a horizontal stiffener is present.

F-10. Vertical Stiffeners at Points of Bearing.—Stiffeners shall be placed in pairs at end bearings of plate girders and at points of bearing of concentrated loads. They shall be connected to the web by enough rivets to transmit the load. Such stiffeners shall have a close bearing against the loaded flanges. Only that part of the stiffener cross section which lies outside the fillet of the flange angle shall be considered effective in bearing.

The moment of inertia of the stiffener shall not be less than that given by

the formula:

$$I = I_s + \frac{P h^2}{70,000} \dots \dots \dots (5)$$

in which:

I_s is the moment of inertia, in inches⁴, required to resist shear buckling (Fig. 9);

P is a local load concentration on the stiffener, in kips; and

h is the clear height of the web between flanges, in inches.

F-11. Horizontal Stiffeners.—A horizontal stiffener of the type shown in Fig. 8 shall have a moment of inertia not less than that given by the formula:

$$I_h = f t h^3 \left[\left(16 + 90 \frac{A_h}{h t} \right) \left(\frac{s}{h} \right)^2 + 6 \right] \times 10^{-7} \dots \dots \dots (6)$$

in which:

I_h is the moment of inertia of the horizontal stiffener, in inches⁴;

h is the clear height of web between flanges, in inches;

t is the thickness of web, in inches;

f is the compressive stress at the toe of the flange angles, in kips per square inch;

s is the distance between vertical stiffeners, in inches; and

A_h is the gross area of cross section of the horizontal stiffener, in square inches.

For a stiffener composed of members of equal size on both sides of the web, the moment of inertia shall be taken about the center line of the web. In the case of a stiffener consisting of a member on one side only, the moment of inertia shall be taken about the face of the web in contact with the stiffener.

Eq. 6 must be solved by trial, since both the moment of inertia, I_h , and the area, A_h , of the stiffener are unknown. It is generally convenient to assume as a first approximation that the ratio $A_h/(h t)$ has the value 0.1.

Section G. Riveted and Bolted Connections

G-1. Allowable Loads.—The allowable loads on rivets and bolts shall be calculated using the allowable shear and bearing stresses listed in Section A with the following exceptions:

a.—If a rivet or a bolt is used in relatively thin plates or shapes the allowable shear stress shall be reduced in accordance with the information given² in Table 4.

b.—If the distance from the center of a rivet or bolt to the edge of a plate or shape toward which the pressure of the rivet or bolt is directed is less than twice the diameter of the rivet or bolt, the allowable bearing stress shall be reduced in accordance with the following:

Ratio of edge distance to rivet or bolt diameter	Allowable bearing stress, in kips per square inch
2 or more	27
1-3/4	25
1-1/2	23

TABLE 4.—PERCENTAGE REDUCTION IN SHEAR STRENGTH
OF ALUMINUM ALLOY RIVETS RESULTING FROM THEIR
USE IN THIN PLATES AND SHAPES

Ratio,* $\frac{D}{t}$	Loss in double shear ^b	Ratio,* $\frac{D}{t}$	Loss in double shear ^b	Ratio,* $\frac{D}{t}$	Loss in:		Ratio,* $\frac{D}{t}$	Loss in:	
					Single shear	Double shear		Single shear	Double shear
(1)	(3)	(1)	(3)	(1)	(2)	(3)	(1)	(2)	(3)
1.5	0	2.2	9.1	2.9	0	18.2	3.5	2.0	26.0
1.6	1.3	2.3	10.4	3.0	0	19.5	3.6	2.4	27.3
1.7	2.6	2.4	11.7	3.1	0.4	20.8	3.7	2.8	28.6
1.8	3.9	2.5	13.0	3.2	0.8	22.1	3.8	3.2	29.9
1.9	5.2	2.6	14.3	3.3	1.2	23.4	3.9	3.6	31.2
2.0	6.5	2.7	15.6	3.4	1.6	24.7	4.0	4.0	32.5
2.1	7.8	2.8	16.9

* Ratio of the rivet diameter, D , to the plate thickness, t . The thickness used is that of the thinnest plate in a single shear joint or of the middle plate in a double shear joint. ^b The percentage loss of strength in single shear is zero for D/t less than 3.0.

The allowable loads calculated for cold-driven 6061-T6 rivets are given in Table 5 and those for 6061-T43, hot-driven rivets, are given in Table 6.

G-2. Effective Diameter.—The effective diameter of rivets shall be taken as the hole diameter but shall not exceed the values of hole diameter given in Table 5 for cold-driven rivets and in Table 6 for hot-driven rivets. The effective diameter of pins and bolts shall be the nominal diameter of the pin or bolt.

G-3. Bearing Area.—The effective bearing area of pins, bolts, and rivets shall be the effective diameter multiplied by the length in bearing; except that for countersunk rivets, half of the depth of the countersink shall be deducted from the length.

G-4. Arrangement and Strength of Connections.—Connections shall be arranged to minimize the eccentricity of loading on the member. Members and connections shall be proportioned to take into account any eccentricity of loading introduced by the connections.

G-5. Net Section.—The net section of a riveted tension member is the sum of the net sections of its component parts. The net section of a part is the product of the thickness of the part multiplied by its least net width. The net width for a chain of holes extending across the part in any straight or broken line shall be obtained by deducting from the gross width the sum of the diameters of all the holes in the chain and adding $\frac{s^2}{4g}$ for each gage space in the chain. In the correction quantity $\frac{s^2}{4g}$:

s is the spacing parallel to direction of load (pitch) of any two successive holes in the chain, in inches; and

g is the spacing perpendicular to direction of load (gage) of the same holes, in inches.

The net section of the part is obtained from that chain which gives the

least net width. The hole diameter to be deducted shall be the actual hole diameter for drilled or reamed holes.

For angles, the gross width shall be the sum of the widths of the legs less the thickness. The gage for holes in opposite legs shall be the sum of the gages from the back of the angle, less the thickness.

For splice members, the thickness shall be only that part of the thickness of the member that has been developed by rivets beyond the section considered.

G-6. Effective Sections of Angles.—If an angle in tension is connected on one side of a gusset plate, the effective section shall be the net section of the connected leg plus one half of the section of the outstanding leg unless the outstanding leg is connected by a lug angle. In the latter case the effective section shall be the entire net section of the angle, and there shall be at least two extra rivets in the lug angle beyond the gusset plate.

G-7. Grip of Rivets.—If the grip of rivets carrying calculated stress exceeds four and one-half times the diameter, the allowable load per rivet shall be reduced. The reduced allowable load shall be the normal allowable load divided by $\left(\frac{1}{2} + \frac{G}{9D}\right)$ in which G is the grip, and D the nominal diameter of the rivet. If the grip exceeds six times the diameter, special care shall be taken in driving the rivets to insure that the holes will be filled completely.

G-8. Pitch of Rivets in Built-Up Compression Members.—The pitch in the direction of stress shall be such that the allowable stress on the individual outside plates and shapes, treated as columns having a length equal to the rivet pitch in accordance with Fig. 2, exceeds the calculated stress. In no case, however, shall the pitch in the direction of stress exceed six times the

TABLE 5.—Allowable Design Load, in Kips per Rivet, (Shear, 10 Kips per Sq In.; and

Dimensions, in Inches	3/8	7/16	1/2	9/16				
Rivet diameter.....	0.386	0.453	0.516	0.578				
Hole diameter.....	W	29/64	33/64	37/64				
Drill size.....								
Thickness of plate, or shape, in inches:	RIVET IN SINGLE SHEAR (ss)							
	ss	ds	ss	ds	ss	ds	ss	ds
1/8	1.17	*1.30 ^b	1.53 ^b	1.53 ^b	1.74 ^b	1.74 ^b	1.95 ^b	1.95 ^b
3/16	1.17	1.95 ^b	1.61	2.29 ^b	2.09	2.61 ^b	2.62	2.93 ^b
1/4	1.17	2.34	1.61	3.06 ^b	2.09	3.48 ^b	2.62	3.90 ^b
5/16	1.17	2.34	1.61	3.22	2.09	4.13 ^c	2.62	4.88 ^b
3/8	1.17	2.34	1.61	3.22	2.09	4.18	2.62	5.25
7/16	1.61	3.22	2.09	4.18	2.62	5.25
1/2	2.09	4.18	2.62	5.25
9/16	2.62	5.25
5/8
3/4
7/8
1

* Assuming distance from center of rivet to edge of member toward which the pressure of the rivet is directed is by bearing. ^b These values are governed by reduced shear strengths as indicated in Table 4. All other values

diameter of the rivets; and for a distance of one and one-half times the width of the member at each end, the pitch in the direction of stress shall not exceed three and one-half times the diameter of the rivets.

G-9. Stitch Rivets.—Where two or more web plates are in contact, there shall be stitch rivets to make them act in unison. In compression members, the pitch of such rivets in the direction of stress shall be determined as outlined in Specification G-8. The gage at right angles to the direction of stress shall not exceed twenty times the thickness of the outside plates. In tension members the maximum pitch or gage of such rivets shall be twenty times the thickness of the outside plates; and in tension members composed of two angles in contact the pitch of the stitch rivets shall not exceed 10 in.

G-10. Minimum Spacing of Rivets.—The distance between centers of rivets shall not be less than three times the diameter of the rivets.

G-11. Edge Distance of Rivets.—The distance from the center of a rivet to a sheared, sawed, rolled, or planed edge shall be not less than one and one-half times the diameter, except in flanges of beams and channels, where the minimum distance may be one and one-fourth times the diameter. For rivets under computed stress, the distance from the center of the rivet to the edge of the plate or shape toward which the pressure of the rivet is directed should normally be at least twice the nominal diameter of the rivet. In cases where a shorter edge distance must be used, the allowable bearing stress shall be reduced in accordance with Specification G-1, exception b.

The distance from the edge of a plate to the nearest rivet line shall not exceed six times the thickness of the plate.

G-12. Sizes of Rivets in Angles.—The diameter of the rivets in angles

For Cold-Driven 6061-T6 Rivets in 6061-T6 Structures
Bearing, 27 Kips per Sq In.^a)

5/8 0.641 41/64		3/4 0.766 49/64		7/8 0.891 57/64		1 1.016 1-1/64		Dimensions, in inches Rivet diameter Hole diameter Drill size
OR IN DOUBLE SHEAR (ds)								Thickness of plate, or shape, in inches:
ss	ds	ss	ds	ss	ds	ss	ds	
2.16 ^b	2.16 ^b	1/8
3.18 ^c	3.25 ^b	3.88 ^b	3.88 ^b	4.51 ^b	4.51 ^b	3/16
3.23	4.33 ^b	4.61	5.17 ^b	6.02 ^b	6.02 ^b	6.86 ^b	6.86 ^b	1/4
3.23	5.41 ^b	4.61	6.46 ^b	6.24	7.52 ^b	8.04 ^b	8.57 ^b	5/16
3.23	6.31 ^c	4.61	7.76 ^b	6.24	9.02 ^b	8.11	10.29 ^b	3/8
3.23	6.45	4.61	8.97 ^c	6.24	10.52 ^b	8.11	12.00 ^b	7/16
3.23	6.45	4.61	9.22	6.24	12.03 ^b	8.11	13.72 ^b	1/2
3.23	6.45	4.61	9.22	6.24	12.39 ^c	8.11	15.43 ^b	9/16
3.23	6.45	4.61	9.22	6.24	12.47	8.11	16.00 ^c	5/8
.....	4.61	9.22	6.24	12.47	8.11	16.22	3/4
.....	6.24	12.47	8.11	16.22	7/8
.....	8.11	16.22	1

not less than twice the nominal rivet diameter (see Specification G-1, exception b). ^b These values are governed by basic allowable shear stress.

whose size is determined by calculated stress shall not exceed one fourth of the width of the leg in which they are driven. In angles whose size is not so determined, 1-in. rivets may be used in 3-1/2-in. legs; 7/8-in. rivets, in 3-in. legs; and 3/4-in. rivets, in 2-1/2-in. legs.

G-13. Extra Rivets.—If splice plates are not in direct contact with the parts which they connect, there shall be rivets on each side of the joint in excess of the number required in the case of direct contact, to the extent of two extra lines for each intervening plate.

If rivets carrying calculated stress pass through fillers, the fillers shall be extended beyond the connected member and the extension secured by enough additional rivets to distribute the total stress in the member uniformly over the combined section of the member and filler.

Section H. Miscellaneous Design Rules

H-1. Reversal of Load.—Members subject to reversal of load under the passage of live load shall be proportioned as follows: Determine the tensile load and the compressive load and increase each by 50% of the smaller; then proportion the member and its connections so that the allowable stresses given in Sections A to G, inclusive, will not be exceeded by either increased load.

H-2. Slenderness Ratio of Tension Members.—Long slender members have little resistance to lateral loads. Therefore, tension members with values of slenderness ratio L/r greater than 150 shall not be used unless special care is taken to insure that such members are designed to resist any lateral loads such as wind, dead load, or the weight of workmen and equipment. Stresses

TABLE 6.—Allowable Design Loads, in Kips per Rivet,
(Rivets Driven at 990° F to 1,050° F; Shear, 8 Kips)

Dimensions, in inches	3/8	7/16	1/2	9/16				
Rivet diameter.....	0.397	0.469	0.531	0.594				
Hole diameter.....	X	15/32	17/32	19/32				
Drill size.....								
	RIVET IN SINGLE SHEAR (ss)							
Thickness of plate, or shape, in inches:	ss	ds	ss	ds	ss	ds	ss	ds
1/8	0.99	1.34 ^b	1.35 ^c	1.58 ^b	1.70 ^c	1.79 ^b	2.00 ^c	2.00 ^a
3/16	0.99	1.85 ^c	1.38	2.37 ^c	1.77	2.69 ^b	2.22	3.01 ^b
1/4	0.99	1.98	1.38	2.68 ^c	1.77	3.31 ^c	2.22	4.00 ^c
5/16	0.99	1.98	1.38	2.76	1.77	3.50 ^c	2.22	4.26 ^c
3/8	0.99	1.98	1.38	2.76	1.77	3.54	2.22	4.43
7/16	1.38	2.76	1.77	3.54	2.22	4.43
1/2	1.77	3.54	2.22	4.43
9/16	2.22	4.43
5/8
3/4
7/8
1

* Assuming distance from center of rivet to edge of member toward which the pressure of the rivet is directed is by bearing. * These values are governed by reduced shear strengths as indicated in Table 4. All other values

caused by the combined bending and tensile loadings shall not exceed allowable limits.

H-3. Stay Plates for Tension Members.—Segments of tension members not directly connected to each other shall be stayed together. The length of the stay plate shall be not less than three fourths of the distance between rivet lines of the segments. Stay plates shall be connected to each segment of the tension member by at least three rivets. The distance between stay plates shall be such that the slenderness ratio of the individual segments of the member between stay plates does not exceed the slenderness ratio of the member as a whole.

H-4. Fatigue.—Tests indicate that riveted members designed in accordance with the requirements of these specifications and constructed so as to be free from severe reentrant corners and other unusual stress raisers will safely withstand at least 300,000 repetitions of maximum live load without fatigue failure regardless of the ratio of minimum to maximum load. Where a greater number of repetitions of some particular loading cycle is expected during the life of the structure, the calculated net section tensile stresses for the loading in question shall not exceed the values given by the curves in Fig. 10. When using the curves in Fig. 10 the reversal-of-load rule in Specification H-1 should be ignored. The final member and connections selected, however, shall be strong enough to satisfy the requirements of Specification H-1.

In considering fatigue action on structures it is well to bear in mind the following points:

a.—The most severe combination of loadings for which a structure is designed (dead load, maximum live load, maximum impact, maximum wind, etc.)

for Hot-Driven 6061-T43 Rivets in 6061-T6 Structures
per Sq In.; and Bearing, 27 Kips per Sq In.^a)

5/8 0.656 21/32		3/4 0.781 25/32		7/8 0.922 59/64		1 1.063 1-1/16		Dimensions, in Inches Rivet diameter Hole diameter Drill size	
OR IN DOUBLE SHEAR (ds)								Thickness of plate, or shape, in inches:	
ss	ds	ss	ds	ss	ds	ss	ds		
2.21 ^b	2.21 ^b								1/8
2.66 ^c	3.32 ^b	3.68 ^c	3.95 ^b	4.67 ^b	4.67 ^b				3/16
2.70	4.43 ^b	3.83	5.27 ^b	5.23 ^c	6.22 ^b	6.82 ^c	7.18 ^b		1/4
2.70	5.06 ^c	3.83	6.59 ^b	5.34	7.78 ^b	7.04 ^c	8.97 ^b		5/16
2.70	5.29 ^c	3.83	7.17 ^c	5.34	9.34 ^b	7.10	10.76 ^b		3/8
2.70	5.41	3.83	7.46 ^c	5.34	9.99 ^c	7.10	12.56 ^b		7/16
2.70	5.41	3.83	7.67	5.34	10.34 ^c	7.10	13.28 ^c		1/2
2.70	5.41	3.83	7.67	5.34	10.61 ^c	7.10	13.69 ^c		9/16
2.70	5.41	3.83	7.67	5.34	10.68	7.10	14.02 ^c		5/8
....	3.83	7.67	5.34	10.68	7.10	14.20		3/4
....	5.34	10.68	7.10	14.20		7/8
....	7.10	14.20		1

not less than twice the nominal rivet diameter (see Specification G-1, exception b). ^b These values are governed by basic allowable shear stress.

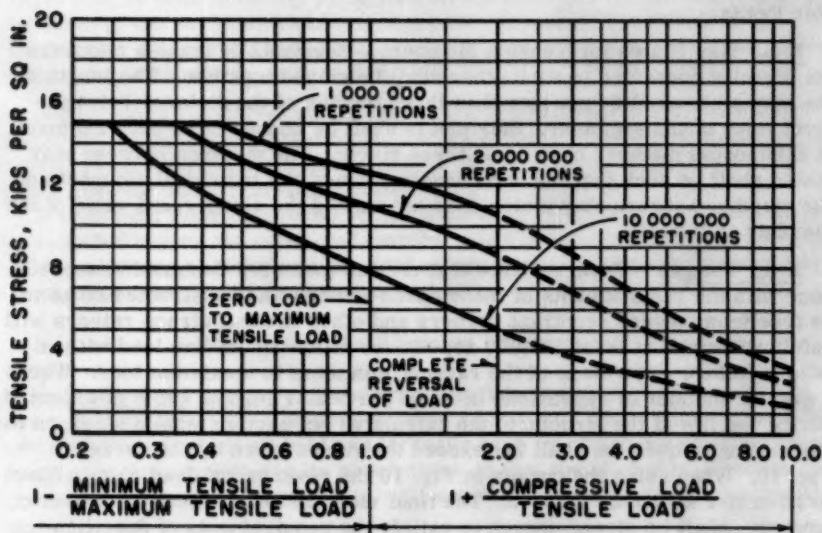


FIG. 10.—ALLOWABLE TENSILE STRESSES ON NET SECTION FOR VARIOUS NUMBERS OF REPETITIONS OF LOAD APPLICATION

rarely occurs in actual service and is of little or no interest from the standpoint of fatigue.

b.—The loading of most interest from the fatigue standpoint is the steady dead load with a superimposed and repeatedly applied live load having an intensity consistent with day to day normal operating conditions.

c.—The number of cycles of load encountered in structures is usually small compared with those encountered in fatigue problems involving machine parts. It takes many years of service to accumulate even 300,000 cycles of any significant stress application in most structures as is indicated by the following examples: 300,000 cycles represent 30 cycles every day for 27 years; 10,000,000 cycles represent 20 cycles every hour for 57 years. Care must be taken not to overestimate grossly the number of cycles for any given load condition.

d.—Careful attention to details in design and fabrication pays big dividends in fatigue life. When a fatigue failure occurs in a structure it is usually at a point of stress concentration where the state of stress could have been improved with little or no added expense.

Section I. Fabrication

I-1. Laying Out.—

a.—Hole centers may be center punched and cutoff lines may be punched or scribed. Center punching and scribing shall not be used where such marks would remain on fabricated material.

b.—A temperature correction shall be applied where necessary in the layout of critical dimensions. The coefficient of expansion shall be taken as 0.000012 per degree Fahrenheit.

I-2. Cutting.—

a.—Material 1/2 in. thick or less may be sheared, sawed, or cut with a router. Material more than 1/2 in. thick shall be sawed or routed.

b.—Cut edges shall be true and smooth, and free from excessive burrs or ragged breaks.

c.—Edges of plates carrying calculated stresses shall be planed to a depth of 1/4 in. except in the case of sawed or routed edges of a quality equivalent to a planed edge.

d.—Reentrant cuts shall be avoided wherever possible. If used they shall be filleted by drilling prior to cutting.

e.—Flame cutting of aluminum alloys is not permitted.

I-3. Heating.—Structural material shall not be heated, with the following exceptions:

a.—Material may be heated to a temperature not exceeding 400° F for a period not exceeding 30 min to facilitate bending. Such heating shall be done only when proper temperature controls and supervision are provided to insure that the limitations on temperature and time are carefully observed.

b.—Hot-driven rivets shall be heated as specified in Section I-5.

I-4. Punching, Drilling, and Reaming.—Rules for punching, drilling, and reaming are as follows:

a.—Rivet or bolt holes in main members shall be subpunched or subdrilled and reamed to finished size after the parts are firmly bolted together. The amount by which the diameter of a subpunched hole is less than that of the finished hole shall be at least 1/4 the thickness of the piece and in no case less than 1/32 in. If the metal thickness is greater than the diameter of the hole punching shall not be used.

b.—Rivet or bolt holes in secondary material not carrying calculated stress may be punched or drilled to finished size before assembly.

c.—The finished diameter of holes for cold-driven rivets shall be not more than 4% greater than the nominal diameter of the rivet.

d.—The finished diameter of holes for hot-driven rivets shall be not more than 7% greater than the nominal diameter of the rivet.

e.—The finished diameter of holes for unfinished bolts shall be not more than 1/16 in. larger than the nominal bolt diameter.

f.—Holes for turned bolts shall be drilled or reamed to give a driving fit.

g.—All holes shall be cylindrical and perpendicular to the principal surface. Holes shall not be drifted in such a manner as to distort the metal. All chips lodged between contacting surfaces shall be removed before assembly.

I-5. Riveting.—

a.—The driven head of aluminum alloy rivets preferably shall be of the flat or the cone-point type, with dimensions as follows:

- 1) Flat heads shall have a diameter not less than 1.4 times the nominal rivet diameter and a height not less than 0.4 times the nominal rivet diameter.
- 2) Cone-point heads shall have a diameter not less than 1.4 times the nominal rivet diameter and a height, to the apex of the cone, not less than 0.65 times the nominal rivet diameter. The included angle at the apex of the cone shall be approximately 127°.

b.—Rivets shall be driven hot or cold as called for on the plans, provision for heating being as follows:

1) Hot-driven rivets shall be heated in a hot air type furnace providing uniform temperatures throughout the rivet chamber and equipped with automatic temperature controls.

2) Hot-driven rivets shall be held at from 990° F to 1,050° F for not less than 15 min and for not more than 1 hour before driving.

3) Hot rivets shall be transferred from the furnace to the work and driven with a minimum loss of time.

c.—Rivets shall fill the holes completely. Rivet heads shall be concentric with the rivet holes and shall be in proper contact with the surface of the metal.

d.—Defective rivets shall be removed by drilling.

I-6. Painting.—Structures of the alloy covered by these Specifications are not ordinarily painted except where (a) the aluminum alloy parts are in contact with, or are fastened to, steel members or other dissimilar materials, or (b) the structures are to be exposed to extremely corrosive conditions. Painting procedure is covered in the following paragraphs, and methods of cleaning and preparation are found in Specification I-7. (Treatment and painting of the structure in accordance with United States Military Specification MIL-T-704 is also acceptable).

a.—Where the aluminum alloy parts are in contact with, or are fastened to, steel members or other dissimilar materials, the aluminum shall be kept from direct contact with the steel or other dissimilar material by painting as described below:

1) Aluminum surfaces to be placed in contact with steel shall be given one coat of zinc chromate primer in accordance with United States Joint Army-Navy Specification JAN-P-735 or the equivalent. Zinc chromate paint shall be allowed to dry before assembly of the parts. Additional protection may be provided by the application of one coat of a suitable nonhardening joint compound, in addition to the zinc chromate primer. The steel surfaces to be placed in contact with aluminum shall be painted with good quality priming paint, such as red lead conforming to Federal Specification TT-P-86a, followed by one coat of paint consisting of 2 lb of aluminum paste pigment (ASTM Specification D962-49, Type II, Class B) per gallon of varnish meeting Federal Specification TT-V-81b, Type II, or the equivalent.

2) Aluminum surfaces to be placed in contact with wood, concrete, or masonry construction, except where the aluminum is to be imbedded in

concrete, shall be given a heavy coat of an alkali-resistant bituminous paint before installation. The bituminous paint used shall meet the requirements of United States Military Specification MIL-P-6883. The paint shall be applied as it is received from the manufacturer without the addition of any thinner.

3) Aluminum surfaces to be imbedded in concrete shall, before installation, be given one coat of zinc chromate primer in accordance with United States Joint Army-Navy Specification JAN-P-735 or the equivalent. The paint shall be allowed to dry before the aluminum is placed in the concrete.

b.—Although structures of the alloy covered by these specifications are not ordinarily painted, there may be applications where the structures are to be exposed to extremely corrosive conditions which make over-all painting advisable. In such instances all contacting metal surfaces shall be painted before assembly with one coat of zinc chromate primer in accordance with United States Navy Joint Army-Navy Specification JAN-P-735 or the equivalent. The primer shall be allowed to dry before assembly of the parts. All other surfaces shall be given one shop coat of zinc chromate primer made in accordance with United States Joint Army-Navy Specification JAN-P-735 or the equivalent and then shall be given a second shop coat of paint consisting of 2 lb of aluminum paste pigment (ASTM Specification D962-49, Type II, Class B) per gallon of varnish meeting Federal Specification TT-V-81b, Type II, or the equivalent. Sufficient Prussian blue shall be added to permit detection of an incomplete application of the subsequent paint coat. After erection, bare spots shall be touched up with zinc chromate primer followed by a touch-up coat of aluminum paint as specified above. The completed structure shall be finished according to one of the following methods:

1) One field coat of aluminum paint as specified above, except that Prussian blue shall be omitted from the field coat.

2) One or more field coats of alkyd base enamel pigmented to meet a desired color scheme.

I-7. Cleaning and Treatment of Metal Surfaces.—All surfaces to be painted shall be cleaned as follows:

a.—Surfaces of metal shall be cleaned immediately before painting by a method which will remove all dirt, oil, grease, chips, and other foreign substances.

b.—Either of the two following methods of cleaning may be used on exposed metal surfaces:

1) Chemical Cleaning.—Parts may be immersed in, or swabbed with, a solution of phosphoric acid and organic solvents diluted with water in the ratio of 1:3. The solution temperature shall be between 50° F and 90° F. The solution shall remain in contact with the metal not less than 5 min. Residual solution shall be removed with clear water.

2) Sandblasting.—Standard mild sandblasting methods may be used on sections more than 1/8 in. thick.

c.—For contacting surfaces only, the metal may be cleaned in accordance with Specification I-7b, or with a solvent such as mineral spirits or benzine.

d.—Flame cleaning is not permitted.

PART III. SPECIFICATIONS FOR WELDED STRUCTURES

Section J. Allowable Stresses for Welded Parts

Although the strength of alloy 6061-T6 is lowered locally by the heat of welding, its resistance to corrosion is not impaired and excellent results can be obtained. Welded members of alloy 6061-T6 are proportioned in accordance with the general rules of Part II, except that it is necessary to lower the allowable stresses in the heat-affected zone.

The heat-affected zone shall be considered to extend for a distance, in inches, equal to $(3+3t)$ on either side of the center line of the weld, where t is the thickness in inches of the material adjacent to the weld.

The allowable stresses in the zone extending for a distance of $(3+3t)$ on either side of the weld are as follows:

J-1. The basic allowable stress in tension is 8 kips per sq in.

J-2. The basic allowable stress in bearing against rivets, milled stiffeners, turned bolts in reamed holes and other parts in fixed contact is 15 kips per sq in.

J-3. Allowable compressive stresses are found from Figs. 2, 3, 4 and 8 in the usual manner except that a horizontal cutoff line is to be drawn at a stress of 8 kips per sq in., and all values above this cutoff line are to be ignored. Figs. 5 and 6, which are used for the determination of the stress f_1 in Formula 4, also have a horizontal cutoff line at 8 kips per sq in., and all values above this line are to be ignored.

J-4. Allowable shear stresses are taken from Fig. 7 in the usual manner except that a horizontal cutoff line is to be drawn at a stress of 5 kips per sq in., and all values above this cutoff line are to be ignored.

J-5. The allowable longitudinal shear stress on fillet welds shall be 4 kips per square inch. The allowable transverse shear stress on fillet welds shall be 4 kips per square inch, except that for double-fillet welds or other fillet welds designed so that the effects of bending are minimized, the allowable transverse shear stress shall be 5.5 kips per square inch. The shear stress in a fillet weld shall be taken to be the load divided by the throat area, regardless of the direction of loading.

Section K. Miscellaneous Design Rules

K-1. Fatigue tests indicate that welded members designed in accordance with the requirements of these specifications, and constructed so as to be free from severe re-entrant corners and other unusual stress raisers, will safely withstand at least 10,000 repetitions of maximum live load without fatigue failure regardless of the ratio of minimum to maximum load. Additional information on fatigue strength of welded joints is available in technical literature.^{4,5}

4. "Static and Fatigue Tests of Arc-Welded Aluminum Alloy 61S-T Plate," by E. C. Hartmann, M. Holt, and A. N. Zamboky, The Welding Journal Research Supplement, March, 1947, pp. 129-138.
5. "Fatigue Strength Butt Joints in 3/8-in. Thick Aluminum Alloy Plates," by E. C. Hartmann, M. Holt, and I. D. Eaton, The Welding Journal Research Supplement, January, 1954, pp. 21-30.

Section L. Fabrication

L-1. General.—These specifications are proposed for application to both field and shop welding operations. The general recommendations and regulations shown in the American Welding Society Specifications D2.0-47 "Welded Highway and Railway Bridges" 1947 and D1.0-46 "Code for Arc and Gas Welding in Building Construction" 1946 apply as well to welded 6061-T6 structures. Detail requirements in the above specifications apply only to steel structures. Detail requirements for welding alloy 6061-T6 are given in the following paragraphs.

L-2. Preparation for Welding.—Dirt, grease, forming or machining lubricants or any organic materials shall be removed from the areas to be welded by cleaning with a suitable solvent or by vapor degreasing.

Additional operations to remove the oxide coating just prior to welding are required when the inert gas tungsten arc welding method is used. This may be done by etching or by scratch brushing. The oxide coating may not need to be removed if the welding is done with the automatic or semi-automatic inert gas shielded metal arc.

Suitable edge preparation to ensure 100% penetration in butt welds shall be used. Flame cutting shall not be used. Sawing, chipping, machining or shearing may be used.

L-3. Welding Procedure.—Parts shall be welded with an arc or resistance welding process. No welding process that requires the use of a welding flux shall be used. The filler metal shall be aluminum alloy 4043 (ASTM designation S5B), 5154 (ASTM designation GR40A) or other approved alloy capable of meeting the qualification test requirements. Preheating for welding is permissible provided the temperature does not exceed 400° F for a total time of 30 min.

L-4. Qualification of Welding Procedure and Welding Operator.—The welding process and welding operators shall both meet a qualification test. The method of qualification shall be mutually agreed upon between the inspecting agency and the contractor or shall conform to the method described in the ASME Boiler and Pressure Vessel Code, Section IX, "Welding Qualifications," Part B, 1953. Aluminum Alloy 6061-T6 shall be used for the qualification test plates.

The minimum required tensile strength of reduced section specimens in the procedure qualification test is 24 kips per square inch. In addition to the tensile test, side-bend and face- and root-bend tests (either longitudinal or transverse) are required. Operators are qualified on the basis of bend tests and a fillet weld soundness test.

L-5. Rewelding Defects.—Portions of joints that have been rejected on inspection because of defects may be repaired only by rewelding. The defective area shall be removed by chipping or machining. Flame cutting shall not be used. Before rewelding, the joint shall be inspected to insure that all of the defective weld has been removed and that the joint is accessible so that the welding operator can obtain full penetration through the joint.

PART IV. EXPLANATION OF SPECIFICATIONS

Section A. Summary of Allowable Stresses

A-1. Basic Tensile Design Stress.—The basic tensile design stress of 15 kips per sq in. represents a factor of safety of 2.33 based on the specified tensile yield strength. This is a larger factor of safety with respect to yield strength than is ordinarily encountered in specifications for structural steel. In selecting this rather large factor of safety on yield strength, the committee was influenced to a considerable extent by the fact that there is a smaller spread between yield strength and tensile strength in this aluminum alloy than is commonly encountered in structural steels.

A-8, A-9, and A-13. Allowable Stresses on Rivets.—The allowable shearing and bearing stresses on rivets were selected on the basis of the results of numerous shearing and bearing tests. The factors of safety used are greater than those used for most of the other allowable stresses.

A-6, A-11, and A-12. Allowable Stresses in Pins.—The allowable bending, shearing, and bearing stresses on pins were selected to bear about the same relation to the corresponding properties of the material as is the case in standard steel specifications. It is not anticipated that any wide use of pins will be made in aluminum alloy structures but it is assumed that where they are used they will be of the same material as the structural members themselves, and that they would probably be obtained in the form of rolled rod, ASTM Specification B211-54 (GS11A).

Section B. Column Design

B-1. Curves for Allowable Compressive Stresses in Axially Loaded Column.—The curves in Fig. 2 are the tangent-modulus column curves with a factor of safety of 2.5 and with a cut-off at the basic allowable compressive design stress of 14 kips per sq in. The formulas for all three curves can be written^{6,7}

$$f_c = \frac{\pi^2 E_t}{2.5 \left(\frac{k L}{r} \right)^2} \dots \dots \dots (7)$$

in which:

f_c is the allowable compressive stress on the gross cross-sectional area in kips per square inch;

E_t is the tangent modulus taken from Fig. 1 at stress corresponding to $2.5(f_c)$, in kips per square inch;

L is the length of the column, in inches;

6. "Column Strength of Various Aluminum Alloys," by R. L. Templin, R. G. Sturm, E. C. Hartmann, and M. Holt, Aluminum Research Laboratories Technical Paper No. 1, Aluminum Co. of America, Pittsburgh, Pa., 1938.
7. "Inelastic Column Theory," by F. R. Shanley, Journal of the Aeronautical Sciences, Vol. 14, 1947, pp. 261-268.

r is the least radius of gyration of the column, in inches; and
 k is a factor describing the end conditions as defined in Fig. 2.

For values of slenderness ratio, L/r , greater than 91, the formula for the partial restraint curve in Fig. 2 reduces to

$$f_c = \frac{70,000}{\left(\frac{L}{r}\right)^2} \dots \dots \dots (8)$$

B-7. Formula for Combined Compression and Bending. Eq. 1 is based on an interaction formula that gives good agreement with the results of tests on aluminum alloy members subjected to combined compressive end load and bending.^{8,9} The formula is applicable to members in which the bending is applied about either the strong or the weak axis.

B-8. Formula for Transverse Shear on Columns.—Eq. 3a is based on the transverse component of the column load at the point of maximum slope of the column in its deflected position. A derivation by Mr. Hartmann has been published elsewhere.¹⁰

Section C. Curve for Allowable Compressive Stress in Beam and Girder Flanges

C-1. The curve in Fig. 3 is based on the theoretical solution for the critical bending moment in I-beams as given by S. Timoshenko.¹¹ It represents a factor of safety of 2.5 applied to the buckling strength of beams subjected to a uniform bending moment. It is assumed that at the ends of the laterally unsupported length there is partial restraint against rotation about a vertical axis and complete restraint against lateral displacement and against rotation about a horizontal axis parallel to the web. The effect of partial restraint at the ends of the span has been taken into account by substituting 0.75L for the length of the formula for buckling of the beam under uniform bending moment.

The part of the curve for values of $\frac{L}{\sqrt{B/S_c}}$ greater than 35 is based on elastic action, whereas the remainder is simply an extension of the same formula using tangent modulus rather than initial modulus. The curve has a cutoff at the basic allowable compressive design stress of 14 kips per sq in. It is important to note that the term L is defined as "laterally unsupported length," which is not necessarily the same as the span of the beam or girder.

The case of uniform bending moment on a simple beam has been used in setting up Fig. 3, because it is a good approximation of conditions frequently

8. "Plastic Buckling of Eccentrically Loaded Aluminum Alloy Columns," by J. W. Clark, Proceedings, ASCE, Separate No. 299, Vol. 79, October, 1953.
9. "Designing Aluminum Alloy Members for Combined End Load and Bending," by H. N. Hill, E. C. Hartmann, and J. W. Clark, Proceedings, ASCE, Separate No. 300, Vol. 79, October, 1953.
10. Discussion by E. C. Hartmann of "Rational Design of Steel Columns," by D. H. Young, Transactions, ASCE, Vol. 101, 1936, pp. 475-481.
11. "Theory of Elastic Stability," by S. Timoshenko, McGraw-Hill Book Co., Inc., New York, N. Y., 1936.

encountered in actual design, and because it is somewhat more conservative than many of the other cases that might have been selected. The provision that four-thirds times the length shall be used for L in the case of a cantilever beam has the effect of canceling the length reduction coefficient of 0.75 that was introduced to take account of the effect of lateral restraint in simple beams. Thus, the buckling strength of a cantilever beam is assumed to be equal to the strength of a simply supported beam of the same length subjected to uniform bending moment. This gives a conservative approximation to the strength of a cantilever beam.¹¹

For values of $\frac{L}{\sqrt{B/S_c}}$ greater than 35 the curve in Fig. 3 may be represented by the formula:

$$f_B = \frac{10,300}{\left(\frac{L}{\sqrt{B/S_c}}\right)^2} \dots \dots \dots (9)$$

The curve in Fig. 3 is based on a theoretical solution applicable only to I-beams having cross sections symmetrical about both axes. The modified interpretation of the term I_1 indicated in Specification C-1, however, permits the curve to be used without serious error for beams and girders having one flange differing in lateral stiffness from the other. It should be used with caution in cases of beams and girders which are unsymmetrical by a considerable margin. (In connection with this subject several supplementary references^{9,12,13,14,15} will be of interest.)

Section D. Curves for Design of Flat Plates, Legs and Webs

The curves of Figs. 4, 5 and 6 are based on values of critical stress compiled by Mr. Hill in 1940.¹⁶ Partial restraint along the supported edges and loaded edges was assumed in all cases except for the supported edge in Fig. 4 which was considered simply supported. Parts of the curves that represent critical buckling stresses above the elastic range are computed by using the tangent modulus instead of the modulus of elasticity, a procedure which is known to be conservative when applied to problems of plate buckling.¹⁷ A

12. "The Lateral Instability of Unsymmetrical I-Beams," by H. N. Hill, Journal of the Aeronautical Sciences, Vol. 9, 1942, pp. 175-180.
13. "The Lateral Stability of Equal-Flanged Aluminum-Alloy I-Beams Subjected to Pure Bending," by C. Dumont and H. N. Hill, Technical Note No. 770, National Advisory Committee for Aeronautics, Washington, D. C., 1940.
14. "Lateral Stability of Unsymmetrical I-Beams and Trusses in Bending," by George Winter, Transactions, ASCE, Vol. 108, 1943, pp. 247-268.
15. "Strength of Beams as Determined by Lateral Buckling," by Karl de Vries, ibid., Vol. 112, 1947, pp. 1245-1320.
16. "Chart for Critical Compressive Stress of Flat Rectangular Plates," by H. N. Hill, Technical Note No. 773, National Advisory Committee for Aeronautics, Washington, D. C., 1940.
17. "Buckling Stresses for Flat plates and Sections," by Elbridge Z. Stowell, George J. Heimerl, Charles Libove, and Eugene E. Lundquist, Transactions, ASCE, Vol. 117, 1952, pp. 545-575.

factor of safety of 2.5 against critical buckling has been used in all three charts and in all cases the curves have a cutoff at the basic allowable compressive design stress of 14 kips per sq in.

When a flat plate, leg, or web is built in along one or both edges to other parts of a compression member which offer partial edge restraint, the local buckling of the plate, leg, or web does not precipitate collapse of the member as a whole as it probably would in the case of a single-angle strut. For this reason it is proper to permit a decreased factor of safety against local buckling in such cases if suitable precautions are taken to avoid collapse. Step c of Specification D-2 provides a simple method for accomplishing this result by introducing the well known "effective width" concept. After a plate, leg, or web buckles, a part of its area is considered to be ineffective in supporting load, whereas a strip along each supported edge is considered still fully effective in working with the supporting material to which it is attached. The formula (Eq. 4) for effective width used in step c of Specification D-2 is generally more conservative than other accepted methods of computing effective width.^{18,19,20,21}

The limitation placed on the value of f_c in step f of Specification D-2 is intended to provide a factor of safety of at least 1.67 against local buckling at the design load.

Section E. Curves for Allowable Shear Stress in Webs

E-1.—The values of allowable stress in Fig. 7 are obtained by applying a factor of safety of 2 to the critical shear buckling stresses for flat plates with the edges about half way between the fixed and hinged conditions.^{11,22,23}

Those parts of the curves of Fig. 7 which represent critical buckling stresses above the elastic stress range are computed from formulas for elastic buckling with the tangent modulus substituted for the modulus of elasticity. For a given value of critical shear stress, the tangent modulus is that corresponding to an axial stress equal to $\sqrt{3}$ times the shear stress.²⁴ As in the case of compressive buckling of flat plates, the tangent modulus is conservative.

For values of allowable stress below 6 kips per sq in., the curves of Fig. 7

18. "The Strength of Thin Plates in Compression," by Theodor von Kármán, Ernest E. Sechler, and L. H. Donnell, Transactions, A.S.M.E., Vol. 54, 1932, pp. 53-57.
19. "The Apparent Width of the Plate in Compression," by Karl Marguerre, Technical Memorandum No. 833, National Advisory Committee for Aeronautics, Washington, D. C., 1937.
20. "Strength of Thin Steel Compression Flanges," by George Winter, Transactions, ASCE, Vol. 112, 1947, pp. 527-576.
21. "Performance of Thin Steel Compression Flanges," by George Winter, preliminary publication, 3d Cong. of the International Assn. for Bridge and Structural Engrs., Liège, Belgium, 1948.
22. "Formulas for Stress and Strain," by Raymond J. Roark, McGraw-Hill Book Co., Inc., New York, N. Y., 1938.
23. "Observations on the Behavior of Aluminum Alloy Test Girders," by R. L. Moore, Transactions, ASCE, Vol. 112, 1947, pp. 901-920.
24. "Critical Shear Stress of an Infinitely Long Plate in the Plastic Region," by Elbridge Z. Stowell, Technical Note No. 1681, National Advisory Committee for Aeronautics, Washington, D. C., 1948.

may be represented by the formula:

$$f_c = \frac{33,000}{(b/t)^2} \left[1 + 0.75 \left(\frac{b}{a} \right)^2 \right] \dots \dots \dots (10)$$

Section F. Plate Girder Design

F-6. Curves for Allowable Longitudinal Compressive Stress in Webs of Girders.—The curve in Fig. 8 for girders with no horizontal stiffeners is based on the critical buckling stress for rectangular flat plates under pure bending in the plane of the plate. Partial restraint is assumed at the toes of the flanges (about half way between the solution given by Mr. Timoshenko for the case of a plate simply supported on all four edges¹¹ and the solution of K. Nolke for a plate with the loaded edges simply supported and the other two edges fixed.²⁵

The curve in Fig. 8 for girders with a single horizontal stiffener is based on the critical buckling stress given by Mr. Timoshenko for plates simply supported on all four edges under combined bending and axial stress in the plane of the plate.¹¹ The simple support condition is used for this case because the horizontal stiffener would provide comparatively little restraint against rotation. The location of the horizontal stiffener shown in the sketch in Fig. 8 is chosen so that the parts of the plate above and below the stiffener will buckle at approximately the same load.

A factor of safety against buckling of 1.5 was used for the curves of Fig. 8. Although this factor of safety is not as large as some used elsewhere in these specifications, it is considered adequate in this instance since tests have shown that the critical bending stress for girder webs may be considerably exceeded without affecting the load carrying capacity of the girder.^{23,25} Use of Fig. 8, however, will prevent buckling from occurring at design stresses.

The curves of Fig. 8 may be represented by the following formulas: No horizontal stiffener—

$$f_a = \frac{190,000}{\left(\frac{h}{t} \right)^2} \dots \dots \dots (11)$$

and single horizontal stiffener—

$$f_a = \frac{750,000}{\left(\frac{h}{t} \right)^2} \dots \dots \dots (12)$$

The curves are cut off at the basic allowable compressive design stress of 14 kips per sq in.

F-8 and F-9. Curves for Spacing and Moment of Inertia of Vertical Stiffeners.—The curves for determining stiffener spacing, in Fig. 9, are merely replots of the data of Fig. 7. The curves of I_s/t^4 in Fig. 9 represent the following formula:

25. "Buckling of Webs in Deep Steel I-Girders," by Georg Wastlund and Sten G. A. Bergman, rept. of investigation made at the Royal Inst. of Technology, Stockholm, Sweden, 1947.

$$I_s = 8 \times 10^{-8} \times \frac{f_s h^3 t (s/h)}{1 + 5 (s/h)^3} \dots \dots \dots (13)$$

in which f_s is the average shear stress on the web in kips per sq in. Eq. 13 is designed to fit the theoretical solution of M. Stein and R. W. Fralich²⁶ for values of s/h between 0.2 and 1.0. This solution does not cover values of s/h greater than 1.0. In this range, however, Eq. 13 is conservative in comparison with the recommendations of L. S. Moisseiff.²⁷

F-10. Formula for Moment of Inertia of Stiffeners at Points of Bearings.—Eq. 5 simply states that the moment of inertia of a stiffener at a point of bearing should be equal to the sum of the moment of inertia required to resist the tendency of the web to buckle and the moment of inertia required for the stiffener to carry the bearing load as a column with length equal to the height of the web.

F-11. Formula for Moment of Inertia of Horizontal Stiffeners.—Eq. 6, for the moment of inertia of horizontal stiffeners, is based on the theoretical work of C. Dubas, reported by F. Bleich.²⁸

Section H. Miscellaneous Design Rules

H-4. Curves of Allowable Tensile Stress on Net Section for Various Numbers of Repetitions of Load Application.—The curves in Fig. 10 are plotted from the results of fatigue tests conducted at the Aluminum Research Laboratories of the Aluminum Company of America at New Kensington, Pa., on 6061-T6 butt joints with double straps joined with eight cold-driven 5/8-in. 6061-T6 rivets. The type of testing equipment and specimen (Type M1) used are illustrated in a paper by R. L. Templin²⁹ M. ASCE, in 1939, and a paper by E. C. Hartmann, J. O. Lyst, and H. J. Andrews,³⁰ Jun. ASCE, in 1944.

A factor of safety of 1.2 has been applied to the test data and all curves are cut off at the basic allowable tensile design stress of 15 kips per sq in. The right-hand part of the diagram is largely based on extrapolation of the data, but this is not considered to be a serious matter since the design of most members in this range will be governed primarily by Specification H-1 rather than by fatigue considerations.

26. "Critical Shear Stress of Infinitely Long, Simply Supported Plate with Transverse Stiffeners," by Manuel Stein and Robert W. Fralich, Technical Note No. 1851, National Advisory Committee for Aeronautics, Washington, D. C., 1949.
27. "Design Specifications for Bridges and Structures of Aluminum Alloy 27S-T," by Leon S. Moisseiff, Aluminum Company of America, Pittsburgh, Pa., 1940.
28. "Buckling Strength of Metal Structures," by Friedrich Bleich, McGraw-Hill Book Co., Inc., New York, N. Y., 1952.
29. "Fatigue Machines for Testing Structural Units," by R. L. Templin, Proceedings, A.S.T.M., Vol. 39, 1939, pp. 711-722.
30. "Fatigue Tests of Riveted Joints," by E. C. Hartmann, J. O. Lyst, and H. J. Andrews, Wartime Report W55, National Advisory Committee for Aeronautics, Washington, D. C., 1944.

Section J. Allowable Stresses for Welded Parts

The heat of welding lowers the strength of 6061-T6 parts in the vicinity of the weld by an amount that depends on how much heat is applied to the metal in making the weld. On the basis of tests of 6061-T6 welded joints,³¹ and the fact that Article L-4 specifies 24 kips per sq in. as the minimum tensile strength requirement to be met in a welding qualification test, the minimum tensile strength in the heat-affected zone has been assumed to be 24 kips per sq in. for design purposes. The corresponding minimum yield strength for design purposes has been selected as 15 kips per square inch. The values used for shear strength of fillet welds were 13 and 17 kips per square inch for longitudinal and transverse shear, respectively, based on test results.

Tests have shown that the extent of the region in which the strength of 6061-T6 parts is reduced by the heat of welding does not exceed a distance of (3+3t) on either side of the center line of the weld. Therefore, design stresses for material at greater distances from the weld are based on the strength of the fully heat-treated metal.

Section L. Fabrication

L-3. Welding Procedure. The use of alloy 5154 as a filler metal produces welds of greater strength and ductility than are generally obtained with alloy 4043. Welds in highly restricted locations may sometimes show cracking when 5154 filler metal is used. If this condition cannot be eliminated by adjustments of procedure or fixtures, the cracking tendency can be reduced by using 4043 filler metal. The allowable stresses given in Section J can be applied safely to welds made with either alloy.

L-4. Qualification of Welding Procedure and Welding Operator. The minimum requirement of 24 kips per sq in. for tensile strength of a reduced-section specimen used in a welding qualification test is the same as the minimum requirement in the ASME Boiler and Pressure Vessel Code.³²

Respectfully submitted,

F. Baron

E. H. Gaylord

W. A. Nash

P. E. Brandt

E. C. Hartmann

F. L. Plummer

R. Ebenbach

S. A. Kilpatric

W. K. Rey

C. N. Gaylord

R. B. B. Moorman

J. B. Scalzi

F. J. Tamanini

J. W. Clark, Chairman

31. "The Strength and Ductility of Welds in Aluminum Alloy Plate" by F. G. Nelson, Jr., and F. M. Howell, The Welding Journal Research Supplement, September, 1952, pp. 3-7.
32. "Qualification Standard for Welding Procedures, Welders, and Welding Operators," ASME Boiler and Pressure Vessel Code Section IX, 1953, paragraph QN-6, p. 14.

JOURNAL STRUCTURAL DIVISION

Proceedings of the American Society of Civil Engineers

SPECIFICATIONS FOR STRUCTURES OF ALUMINUM ALLOY 2014-T6

THIRD PROGRESS REPORT OF THE COMMITTEE OF THE STRUCTURAL DIVISION ON DESIGN IN LIGHTWEIGHT STRUCTURAL ALLOYS

FOREWORD

These specifications are a revised version of "Specifications for Heavy Duty Structures of High-Strength Aluminum Alloy," published as Proceedings, ASCE, Separate No. 22, June, 1950, and as Paper No. 2532, Transactions, ASCE, Vol. 117, 1952, p. 1253. Publication of these specifications as a progress report of the Committee on Design in Lightweight Structural Alloys has been approved by the Executive Committee of the Structural Division.

SYNOPSIS

These specifications cover allowable stresses, design rules, and fabrication procedures for riveted heavy duty structures built of the high-strength aluminum alloy known commercially as 2014-T6 (formerly 14S-T6). The basic allowable tensile working stress is 22 kips per sq in. based on a minimum yield strength of 53 kips per sq in. and a minimum tensile strength of 60 kips per sq in.

PART I. GENERAL

INTRODUCTION

These specifications cover the allowable stresses, the design rules, and the fabrication procedures for structures built of the high-strength aluminum alloy most commonly used for heavy duty structural purposes. In the preparation of these specifications the Committee has made use of the available theoretical and experimental work relating to this subject and especially to previous specifications by O. H. Ammann, Shortridge Hardesty, and the late Leon S. Moisseiff,¹ Members, ASCE.

Note: Please forward all comments on this report directly to J. W. Clark, Box 772, New Kensington, Pa. Paper 971 is part of the copyrighted Journal of the Structural Division of the American Society of Civil Engineers, Vol. 82, No. ST 3, May, 1956.

1. "Design Specifications for Bridges and Structures of Aluminum Alloy 27S-T," by Leon S. Moisseiff, Aluminum Co. of America, Pittsburgh Pa., 1940.

These specifications are confined to allowable stresses, design rules, and fabrication. No attempt has been made to cover the loading, erection, inspection, or nontechnical provisions included in many specifications, since such provisions are fairly well established in current good structural practice. Furthermore, no attempt has been made to include design rules which cover every detail of construction but rather those which are different from steel practice or which are needed for the sake of completeness. It is intended, of course, that structures built under these specifications will be designed, constructed, and erected by following the current good practice already well established for steel structures, except as modified herein.

It is believed that the designer can make more efficient use of a set of specifications if he knows the basis for its various provisions. For this reason, Part III, Explanation of Specifications, has been added. Part III contains background information and references concerning those paragraphs of the specifications for which some explanation seems required.

When the abbreviation "kip" is used in these specifications it denotes "kilo"-pounds, or "thousands of pounds."

Material

The principal material considered in these specifications is a high-strength aluminum alloy having the following nominal chemical composition:

Composition	Percentage by weight
Copper	4.4
Silicon	0.8
Manganese	0.8
Magnesium	0.4
Aluminum	93.6
Total	100.0

This material is covered by the American Society for Testing Materials (ASTM) Specifications Nos. B221-54T(CS41A), B235-54T(CS41A), B211-54T(CS41A), B247-54T(CS41A), and B209-54T (Clad CS41A). It is produced by several manufacturers under the commercial designation 2014-T6 and is available in the form of shapes, tubes, rods, bars, and forgings. It is also produced in the form of sheet and plate covered on both surfaces with an integral coating, or "cladding," of a corrosion-resistant aluminum alloy. In the latter form it is identified commercially by the designation, Alclad 2014-T6 (formerly Alclad 14S-T6 and R-301). All these products are given a solution heat treatment and a precipitation heat treatment before being shipped.

The specified minimum tensile properties of this material are not the same in all the various products (plate, shapes, etc.). The specified minimum tensile strengths vary from 60 kips per sq in. to 68 kips per sq in., and the specified minimum yield strengths vary from 53 kips per sq in. to 58 kips per sq in. The following are the lowest of the various specified minimum properties and have been used as a basis for the selection of allowable stresses in these specifications (in kips per square inch):

Description	Stress
Tensile Strength	60
Yield strength (offset 0.2%)	53

In addition to the specified minimum tensile properties, the engineer will be interested in some of the other mechanical properties not covered by specifications. The following are typical mechanical properties of this alloy and may be considered applicable to "nonclad" products, such as shapes, and to "clad" plate:

Shear strength, in kips per square inch	41
Modulus of elasticity in tension and compression, in kips per square inch	10,600
Modulus of elasticity in shear, in kips per square inch	4,000
Poisson's ratio	1/3
Coefficient of expansion per degree Fahrenheit	0.000012
Weight, in pounds per cubic inch	0.101

(The foregoing value of shear strength is typical as determined with steel shearing tools. The value determined by torsion tests is greater.)

Fig. 1 shows tensile and compressive stress-strain curves and the compressive tangent modulus curve for 2014-T6 material having the minimum properties listed in the second paragraph of this section.

Alloy 2014-T6 is the one principally considered in the preparation of these specifications and the one to which the allowable stresses for parts other than rivets and bolts apply. However, these specifications may be applied to structures built of other suitable aluminum alloys, provided such alloys meet the specified strengths and elongations listed in the ASTM specifications mentioned in the first paragraph of this section.

Rivets used in fabricating structures designed in accordance with these specifications shall be of aluminum alloy and may be either cold driven or hot driven. The alloys used are indicated in Table 1. Supplementary information on riveting was published² by E. C. Hartmann, M. ASCE, G. O. Hoglund, and M. A. Miller in 1944.

Permanent bolts used in structures designed in accordance with these specifications shall be of the aluminum alloy known commercially as 2024-T4. Such bolts have an expected minimum ultimate shear strength of 37 kips per sq in.

TABLE 1.—Alloys to Be Used for Rivets

Designation before driving	Driving procedure	Designation after driving	Typical shear strength ^a
2117-T4	Cold, as received	2117-T3	33
6061-T4	Hot, 990° F to 1,050° F	6061-T43	24

^aTypical ultimate shear strength of the driven rivet, in kips per square inch.

2. "Joining Aluminum Alloys," by E. C. Hartmann, G. O. Hoglund, and M. A. Miller, *Steel*, August 7, 1944, p. 84.

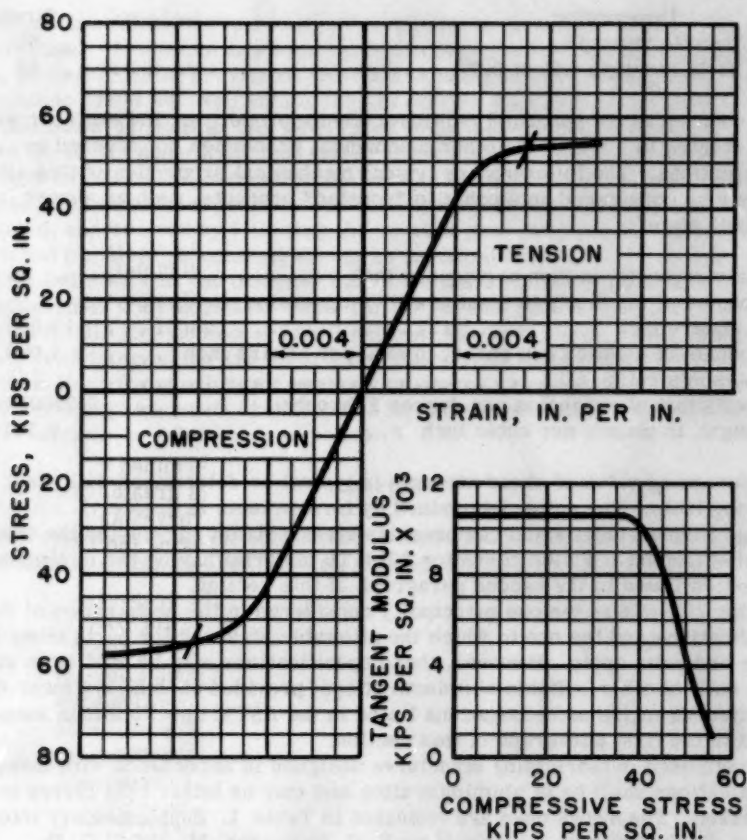


FIG. 1.—STRESS STRAIN AND TANGENT MODULUS CURVES

The materials covered by these specifications are heat treated for maximum strength. They cannot be welded without a considerable loss in strength. Structures designed under these specifications shall be assembled by riveting or bolting.

PART II. SPECIFICATIONS

Section A. Summary of Allowable Stresses

The allowable stresses to be used in proportioning the parts of a structure shall be as follows:

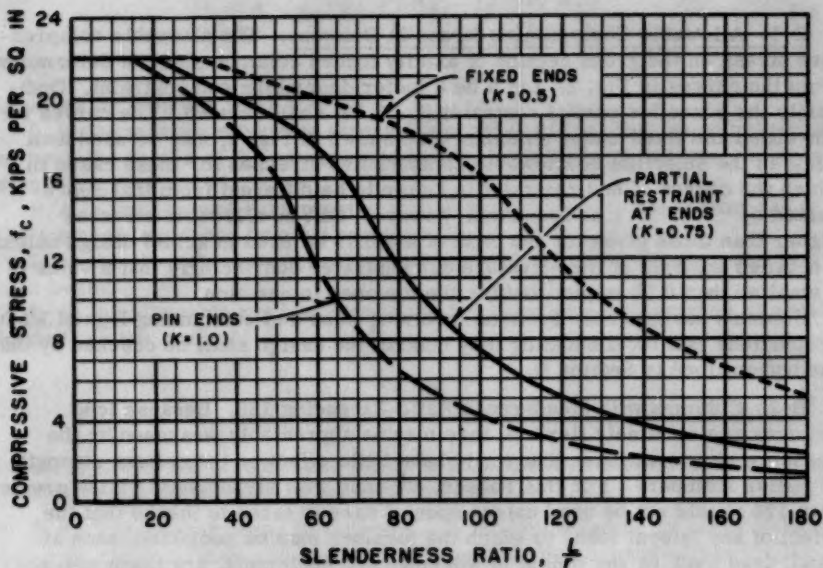


FIG. 2.—ALLOWABLE COMPRESSIVE STRESSES FOR AXIALLY LOADED COLUMNS (GROSS SECTION)

Specification	Description	Stress in kips per square inch
A-1	Avial tension, net section (see Specification H-4) . .	22
A-2	Tension in extreme fibers of shapes, girders, and built-up members subject to bending, net section (see Specification H-4)	22
A-3	Axial compression (see Section B)
A-4	Compression in extreme fibers of shapes, girders, and built-up members subject to bending (see Section C)
A-5	Compression in plates, legs, and webs (see Section D)
A-6	Stress in extreme fibers of pins	34
A-7	Shear in plates and webs (see Section E)
A-8	Shear in aluminum alloy 2117-T3 rivets, cold driven (see Tables 4 and 5)	10
A-9	Shear in aluminum alloy 6061-T43 rivets, driven at temperatures of from 990° F to 1,050° F (see Tables 4 and 6)	8
A-10	Shear in turned bolts of aluminum alloy 2014-T4 in reamed holes (see Table 4)	12
A-11	Shear in pins	16
A-12	Bearing on pins	30
A-13	Bearing on hot-driven or cold-driven rivets, milled stiffeners, turned bolts in reamed holes, and other parts in fixed contact (see Section G) . . .	36

Section B. Column Design

B-1. Allowable Compressive Stress in Columns.—The allowable compressive stress on the gross section of axially loaded columns shall be determined from the curves in Fig. 2. Let k be a factor describing end restraint. Ordinarily the curve for partial restraint ($k = 0.75$) shall be used. The curves for pin-ended and fixed-ended columns, also shown in Fig. 2, may be used as a guide in the selection of allowable compressive stresses for those cases in which the degree of end restraint is known to be different from that represented by $k = 0.75$. It is important, however, that no allowable stresses higher than those given for the case of $k = 0.75$ be used in actual design unless a detailed analysis of the structure demonstrates convincingly that a value of k smaller than 0.75 is justified for the member in question.

Columns having cross sections involving webs and outstanding legs of such proportions that local buckling may control the design shall be checked by the method outlined in Section D.

B-2. Columns with Slenderness Ratio Exceeding 120. Because long columns are relatively flexible, they may be appreciably weakened by the presence of lateral loads that would have little effect on the column strength of stiffer members. For this reason, columns with slenderness ratios greater than 120 should not be used unless special care is taken to insure that the effect of any lateral loads to which the member may be subjected, such as wind, dead load, or the weight of workmen and equipment, are taken into account by using the provision for combined compression and bending in Specification B-7.

B-3. Connections.—Compression members shall be so designed that the main elements of the section will be connected directly to the gusset plates, pins, or other members.

B-4. Compression Splices.—Members designed for compression, if faced for bearing, shall be spliced on four sides sufficiently to hold the abutting parts true to place. The splice shall be as near a panel point as practicable and shall be designed to transmit at least one half of the stress through the splice material. Members not faced for bearing shall be fully spliced for the computed stress. In either case, adequate provision shall be made for transmitting shear.

B-5. Stay Plates.—On the open sides of compression members, the flanges shall be connected by lacing bars, and there shall be stay plates as near each end as practicable. There shall be stay plates at intermediate points where the lacing is interrupted. The length of the end stay plates shall not be less than one and one-fourth times the distance between rivet lines. The thickness of stay plates shall not be less than one fortieth of the distance between rivet lines.

B-6. Diagonal Lacing.—The slenderness ratio of the part of the flange between the lacing bar connections shall be not more than two thirds of the slenderness ratio of the member.

B-7. Combined Compression and Bending.—The allowable stress in a member that carries bending moment in addition to uniform compression (as, for example, an eccentrically loaded column) shall be determined from the following formula:

$$f_b = f_B \left(1 - \frac{P/A}{f_C}\right) \left(1 - \frac{P/A}{f_{CE}}\right) \dots \dots \dots (1)$$

in which (in kips per sq in.):

f_b is the maximum bending stress (compression) that may be permitted at or near the center of the unsupported length, in addition to uniform compression, P/A ;

P/A is the average compressive stress on the gross cross section, A , of the member, produced by a column load, P ;

f_B is the allowable compressive working stress for the member considered as a beam;

f_C is the allowable working stress for the member considered as an axially loaded column; and

$$f_{CE} = \frac{74,000}{(L/r)^2} \dots \dots \dots (2)$$

in which L/r is the slenderness ratio for the member considered as a column tending to fail in the plane of the bending forces.

B-8. Transverse Shear in Columns.—In designing lacing or shear webs for columns, the maximum shear on the column shall be computed from the formula:

$$V = P \frac{4.5 r^2 (f_B - P/A)}{f_C L c} + V_t \dots \dots \dots (3a)$$

but shall not be taken less than

$$V = 0.02 P + V_t \dots \dots \dots (3b)$$

in which:

V is the maximum shear on any transverse section of a column in the outer eighth of the length at each end, in the direction of assumed bending, in kips;

r is the radius of gyration, in inches;

f_C is the allowable compressive stress taken from Fig. 2, in kips per square inch;

L is the length of the member, in inches;

c is the distance from the centroidal axis to the extreme fiber, in inches; and

V_t is the shear due to any transverse loads on a column, in kips.

The values of f_B , f_C , L , r , and c must be consistent with the direction of bending assumed.

Section C. Allowable Compressive Stresses in Flanges of Beams and Girders

C-1.—The allowable compressive stress in the extreme fiber (gross section) of single-web rolled shapes, extruded shapes, girders, and built-up sections, subject to bending, shall be determined from the curve in Fig. 3. The terms used in Fig. 3 are defined as follows:

L is the laterally unsupported length of beam (clear distance between supports at which the beam is prevented from lateral displacement), or, in the case of a cantilever beam with one end free, L is four thirds of the laterally unsupported length, in inches.

S_c is the section modulus for the beam about the axis normal to the web (compression side), in inches;

$$B = I_1 d \sqrt{11.7 + \frac{J}{I_1} \left(\frac{L}{d}\right)^2};$$

I_1 is the moment of inertia for the beam about the axis parallel to the web, in inches to the fourth power;

J is the torsion factor, in inches to the fourth power; and

d is the depth of beam, in inches.

In the case of beams having top and bottom flanges of different lateral stiffness, I_1 should be calculated as if both flanges were the same as the compression flange. Values of the torsion factor J are published for many standard shapes.³ Values of J for plates and shapes not published may be calculated by assuming the section to be composed of rectangles and taking the sum of the terms $b t^3/3$ for each rectangle, in which b equals the length and t , the thickness of the rectangle, both in inches. The value of J for a built-up member is the sum of the individual values of J of the sections of which it is composed.

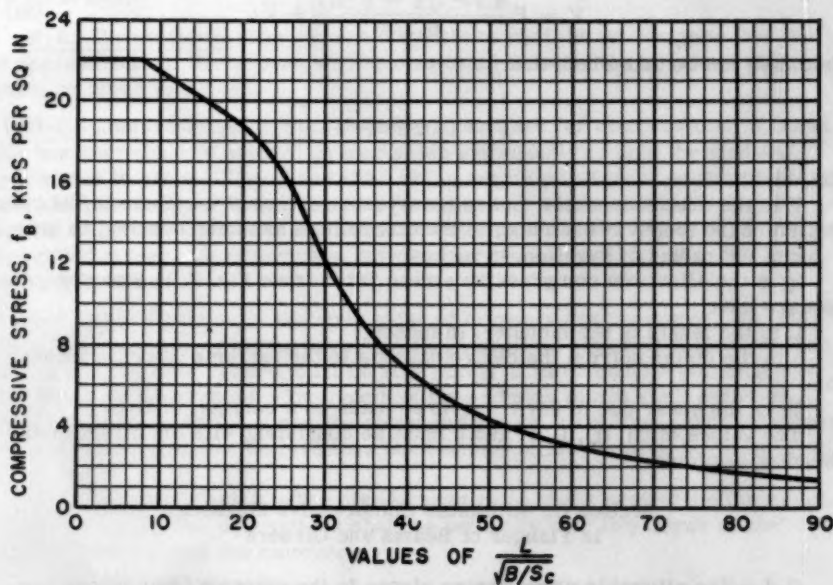


FIG. 3.—ALLOWABLE COMPRESSIVE STRESSES IN BEAM AND GIRDER FLANGES (GROSS SECTION)

3. "Alcoa Structural Handbook," Aluminum Co. of America, Pittsburgh, Pa., 1955, pp. 204-226.

The allowable stresses from Fig. 3 provide a safe margin against the lateral buckling type of failure. The outstanding compression flanges of the beams and girders should be checked for local buckling by the method outlined in Section D.

Table 2 lists values of allowable stress determined from Fig. 3 and Section D for various laterally unsupported lengths of a number of standard I-beams and H-beams. Table 3 lists similar values for standard channels.

Because of their tube-like cross section, double-web box girders are very still in torsion compared with single-web girders of comparable size, and hence, lateral buckling failures such as are considered in Fig. 3 do not occur in such girders. For double-web box girders it is necessary only to check for local buckling of the flanges by the method outlined in Section D.

Section D. Allowable Compressive Stress for Plates, Legs, and Webs

D-1.—For struts consisting of a single angle or a T-section, the compressive stress on the gross area shall not exceed the values given by the curves in Fig. 4 or Fig. 2, whichever is smaller.

D-2.—For compression members other than those consisting of a single angle or a T-section, the following procedure shall be followed to provide a suitable margin of safety against the weakening effects of local buckling of flat plates, legs, and webs:

a.—Compute the compressive stress f_c on the flat plate, leg, or web in question, based on the design loads and the gross area, without regard to local buckling. This stress must be within allowable limits as defined in Sections B and C.

b.—Find the limiting value of b/t corresponding to the stress, f_c , by the use of Fig. 5 or Fig. 6. If the flat plate, leg, or web has a ratio of unsupported width to thickness not exceeding this limiting value, local buckling is not a problem and the full gross area of the plate, leg, or web may be considered effective.

c.—If the flat plate, leg, or web has a ratio of unsupported width to thickness greater than the limiting $\frac{b}{t}$ -ratio found in step b, only a part of its unsupported width shall be included in computing its effective area. The part of the unsupported width of any individual flat plate, leg, or web which may be considered effective shall be found as follows:

$$b_e = b \frac{f_1}{f_c} \dots \dots \dots (4)$$

in which:

b_e is that part of the unsupported width considered effective, in inches;

b is the unsupported width, in inches;

f_c is the compressive stress based on gross area from step (a), in kips per square inch; and

f_1 is the stress found from Fig. 5 or Fig. 6 corresponding to the $\frac{b}{t}$ -value for the plate, leg, or web in question, in kips per square inch.

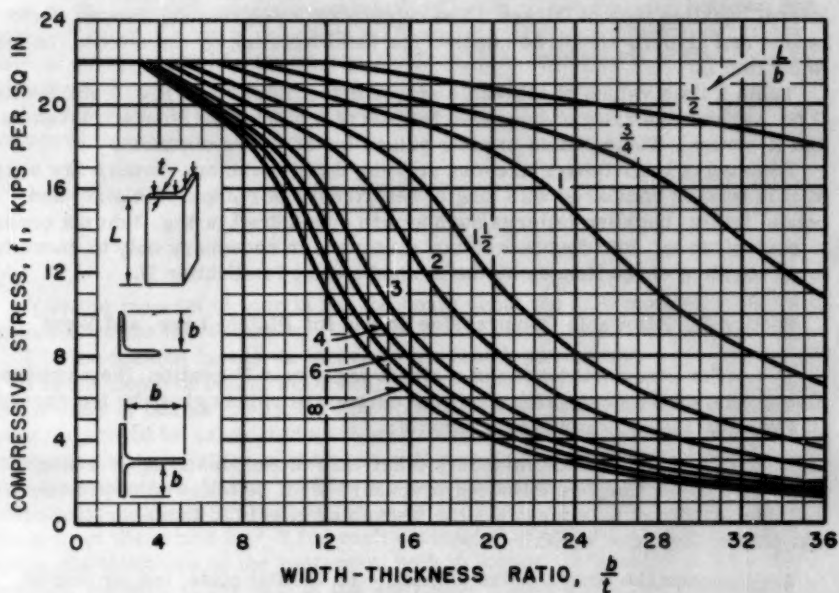


FIG. 4.—ALLOWABLE COMPRESSIVE STRESSES IN OUTSTANDING LEGS OF SINGLE-ANGLE AND T-SECTION STRUTS (GROSS SECTION)

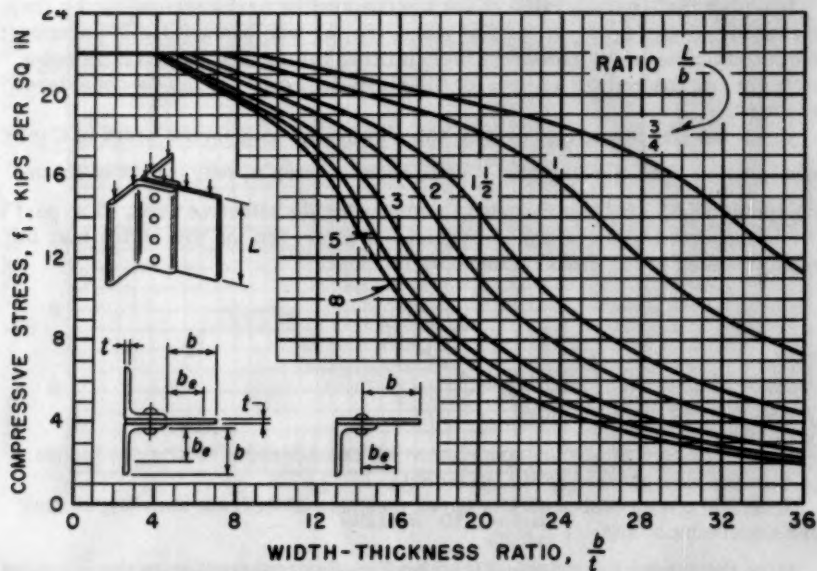


FIG. 5.—CHART FOR DETERMINING EFFECTIVE WIDTH FOR OUTSTANDING LEGS OF ANGLES BUILT INTO OTHER PARTS AND FOR PLATES BUILT IN ALONG ONE EDGE

TABLE 2.—Allowable Compressive Stress in Beam Flanges
for Various Values of Laterally Unsupported Length
of Compression Flange, L , in Inches

Procedure.—Maximum allowable bending moments are found by multiplying the allowable compressive stresses (in kips per square inch) by the gross section modulus of the beam. The stress on the net section of the tension flange must also be kept within allowable limits.												
Depth (in.)	Weight (lb per ft)	Section modulus (in. ³)	Values of L									
			16	32	64	96	128	160	192	256	352	480
(a) I-Beams												
2	0.78	0.481	13.1 ^a	12.1	9.4	5.8	4.2	3.3	2.7	2.0	1.4	...
2	1.43	0.782	13.7	12.7	11.4	10.4	8.6	6.8	5.7	4.2	3.1	2.3
2.5	1.80	1.162	13.8	12.9	11.9	11.1	10.3	9.0	7.5	5.6	4.1	3.0
3	1.96	1.68	13.8	12.7	11.1	9.5	7.1	5.6	4.6	3.5	2.5	1.8
3	2.59	1.95	13.9	12.9	11.7	10.8	9.5	7.8	6.5	4.8	3.5	2.6
4	2.64	3.03	13.9	12.8	11.1	9.1	6.6	5.2	4.3	3.1	2.3	1.7
4	3.63	3.59	13.9 ^a	13.0	11.7	10.7	9.3	7.4	6.1	4.6	3.3	2.4
5	3.43	4.90	13.9 ^a	12.9	11.2	9.3	6.7	5.2	4.2	3.1	2.3	1.6
5	5.10	6.09	13.9 ^a	13.2	11.9	10.9	9.8	8.0	6.6	4.9	3.6	2.6
6	4.30	7.36	13.9 ^a	13.1	11.4	9.6	6.9	5.3	4.3	3.1	2.3	1.6
6	5.96	8.77	13.9 ^a	13.2	11.8	10.7	9.1	7.2	5.9	4.4	3.1	2.3
7	5.27	10.48	13.9 ^a	13.2	11.6	10.0	7.2	5.5	4.4	3.2	2.3	1.6
7	6.92	12.12	13.9 ^a	13.3	11.8	10.7	8.8	6.8	5.6	4.1	2.9	2.1
8	6.35	14.39	13.9 ^a	13.4	11.8	10.4	7.7	5.8	4.6	3.3	2.4	1.7
8	8.81	17.18	13.9 ^a	13.4	12.0	11.0	9.6	7.6	6.2	4.5	3.2	2.3
9	7.51	19.09	13.9 ^a	13.5	12.0	10.7	8.2	6.1	4.9	3.5	2.4	1.8
9	10.37	22.75	13.9 ^a	13.5	12.2	11.1	9.8	7.8	6.3	4.6	3.3	2.4
10	8.76	24.68	13.9 ^a	13.6	12.1	10.9	8.8	6.5	5.1	3.6	2.5	1.8
10	12.10	29.41	13.9 ^a	13.6	12.3	11.2	10.1	8.2	6.6	4.8	3.4	2.4
12	10.99	36.35	13.9 ^a	13.6	12.2	11.0	9.2	6.7	5.2	3.6	2.5	1.8
12	17.28	50.81	14.0	13.8	12.6	11.6	10.8	9.6	7.9	5.6	4.0	2.9
(b) H-Beams												
4	4.71	5.36	13.8 ^a	13.6	12.5	11.6	11.0	10.2	9.1	6.8	4.9	3.5
5	6.45	9.53	13.7 ^a	13.7 ^a	12.8	12.0	11.3	10.6	9.7	7.2	5.2	3.7
6	7.81	14.69	13.6 ^a	13.6 ^a	13.1	12.2	11.5	10.9	10.0	7.6	5.3	3.8
6	9.14	15.81	13.6 ^a	13.6 ^a	13.1	12.3	11.7	11.1	10.5	8.5	6.0	4.3
8	11.19	28.23	13.3 ^a	13.3 ^a	13.0 ^a	12.6 ^a	12.0	11.3	10.7	8.6	5.7	3.9
8	12.95	30.23	13.3 ^a	13.3 ^a	13.0 ^a	12.7 ^a	12.1	11.5	10.9	9.3	6.4	4.4

^aThese values are governed by local buckling (see Section D). All other values are determined from Fig. 3, Section C.

d.—Compute the compressive stress on the effective area. In the case of an axially loaded column this is simply the axial load divided by the total effective area, which, in turn, is simply the sum of the effective areas of the component parts. In the case of a beam or girder the compressive stress on the effective area shall be determined as follows: Compute the compressive extreme fiber stress f_c for the gross section of the beam or girder and then multiply this value by the ratio of the gross compression flange area to the effective compression flange area, including in each flange area not only the flange proper but also one-sixth of the area of the web.

e.—The compressive stress on the effective area computed in accordance with step d shall not exceed allowable limits as defined in Sections B and C for the gross area.

TABLE 3.—Allowable Compressive Stress in Channel Flanges
for Various Values of Laterally Unsupported Length
of Compression Flange, L , in Inches

Procedure.—Maximum allowable bending moments are found by multiplying the allowable compressive stresses (in kips per square inch) by the gross section modulus of the beam. The stress on the net section of the tension flange must also be kept within allowable limits.

Depth (in.)	Weight (lb per ft)	Section modulus (in. ³)	Values of L									
			16	32	64	96	128	160	192	256	352	480
3	1.42	1.10	13.5	12.3	10.6	8.0	5.9	4.7	3.9	2.9	2.1	1.5
3	2.07	1.38	13.7	12.8	11.6	10.6	9.2	7.4	6.1	4.6	3.3	2.4
4	1.85	1.92	13.6	12.3	10.4	7.2	5.2	4.1	3.4	2.5	1.8	1.3
4	2.50	2.29	13.7	12.6	11.1	9.4	7.1	5.6	4.7	3.5	2.5	1.8
5	2.32	3.00	13.7	12.4	10.4	7.0	5.0	3.9	3.2	2.6	1.7	1.3
5	3.97	4.17	13.8a	12.9	11.6	10.5	8.9	7.1	5.9	4.4	3.2	2.3
6	2.83	4.37	13.7a	12.6	10.6	7.0	5.0	3.8	3.1	2.3	1.7	1.2
6	4.48	5.80	13.8a	12.9	11.4	9.9	7.6	6.0	4.9	3.7	2.7	1.9
7	3.38	6.08	13.7a	12.8	10.8	7.4	5.1	3.9	3.2	2.3	1.7	1.2
7	5.96	8.64	13.8a	13.0	11.6	10.4	8.5	6.7	5.5	4.1	2.9	2.1
8	4.25	8.46	13.8a	12.9	11.0	8.0	5.4	4.1	3.3	2.4	1.7	1.3
8	6.79	11.34	13.8a	13.1	11.6	10.4	8.2	6.4	5.2	3.9	2.8	2.0
9	4.60	10.60	13.8a	13.0	11.2	8.3	5.5	4.1	3.3	2.4	1.7	1.2
9	8.65	15.75	13.8a	13.2	11.8	10.7	9.0	7.1	5.8	4.3	3.1	2.2
10	5.28	13.47	13.8a	13.1	11.3	8.8	5.8	4.3	3.4	2.4	1.7	1.2
10	10.37	20.69	13.8a	13.3	12.0	10.9	9.5	7.6	6.2	4.6	3.3	2.3
12	7.41	21.97	13.8a	13.4	11.7	12.0	6.8	5.0	3.9	2.7	1.8	1.4
12	12.10	29.94	13.8a	13.5	12.0	10.9	9.2	7.1	5.7	4.1	2.9	2.1

aThese values are governed by local buckling (see Section D). All other values are determined from Fig. 3, Section C.

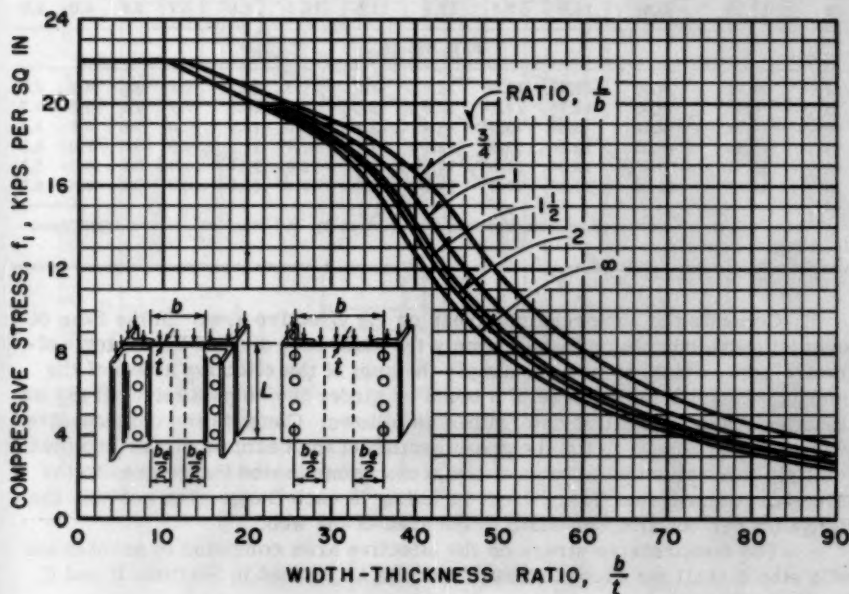


FIG. 6.—CHART FOR DETERMINING EFFECTIVE WIDTH FOR FLAT PLATES BUILT IN ALONG TWO EDGES

f.—Steps c, d and e provide a suitable factor of safety against collapse of the member as a whole, but do not necessarily provide complete protection against local buckling of individual flat surfaces at the design load. Where local buckling at the design load cannot be tolerated because of appearance, or for other reasons, the computed compressive stress on the gross area, f_c , shall not exceed $1.5f_1$, where f_1 is the compressive stress given in Fig. 5 or Fig. 6 for the b/t ratio in question. Regardless of whether or not this limitation is placed on f_c , the member must still be checked by the method outlined in Steps a through e to insure an adequate factor of safety against collapse.

Section E. Allowable Shear Stresses in Plates and Webs

E-1.—The allowable shear stress on flat webs shall not exceed the values given by the curves in Fig. 7. The values in Fig. 7 apply to the gross area of the web, but the shear on the net area shall not exceed 15 kips per sq in.

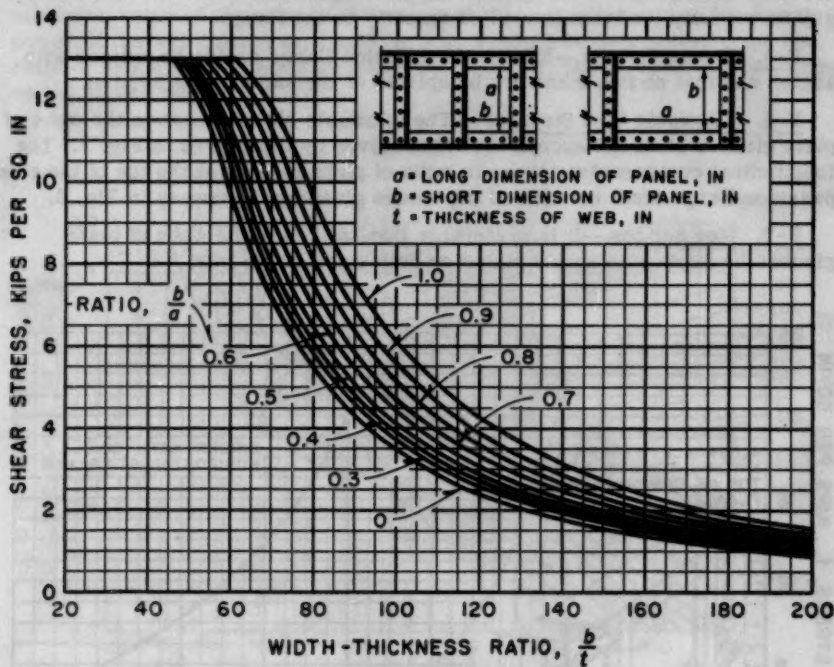


FIG. 7.—ALLOWABLE SHEAR STRESSES ON WEBS; PARTIAL RESTRAINT ASSUMED AT EDGES OF RECTANGULAR PANELS (GROSS SECTION)

Section F. Plate Girder Design

F-1. Proportioning Plate Girders.—Plate girders shall be proportioned by the moment of inertia method, with the gross section used to determine the moment of inertia.

The stress on the net area of the tension flange shall be found by

multiplying the stress on the gross section by the ratio of the gross area of the tension flange to the net area. In determining this ratio the tension flange shall be considered to consist of the flange angles and cover plates plus one-sixth of the web.

F-2. Allowable Flange Stress.—The allowable compressive stress in the extreme fiber of plate girders shall be determined as outlined in Sections C and D. The numerical value of the term $\sqrt{B/S_c}$, used in Fig. 3, is rarely less than one half of the width, in inches, of the compression flange for a plate girder. This fact is useful in preliminary design.

F-3. Flange Cover Plates.—Cover plates shall extend far enough to allow at least two extra rivets at each end of the plate beyond the theoretical end, and the spacing of the rivets in the remainder of the plate shall be such as to develop the required strength of the plate at any section.

F-4. Flange Rivets.—The flanges of plate girders shall be connected to the web with enough rivets to transmit the longitudinal shear at any point together with any load that is applied directly on the flange.

F-5. Flange Splices.—It is preferable that flange angles be spliced with angles and that no two members be spliced at the same cross section.

F-6. Allowable Web Stresses.—The allowable shear stress in the webs of plate girders shall not exceed the values given by the curves in Fig. 7. The longitudinal compressive stress in webs of plate girders at the toe of the compression flange shall not exceed the values given by the curves in Fig. 8.

F-7. Web Splices.—It is preferable that splices in the webs of plate girders be made with splice plates on both sides of the web.

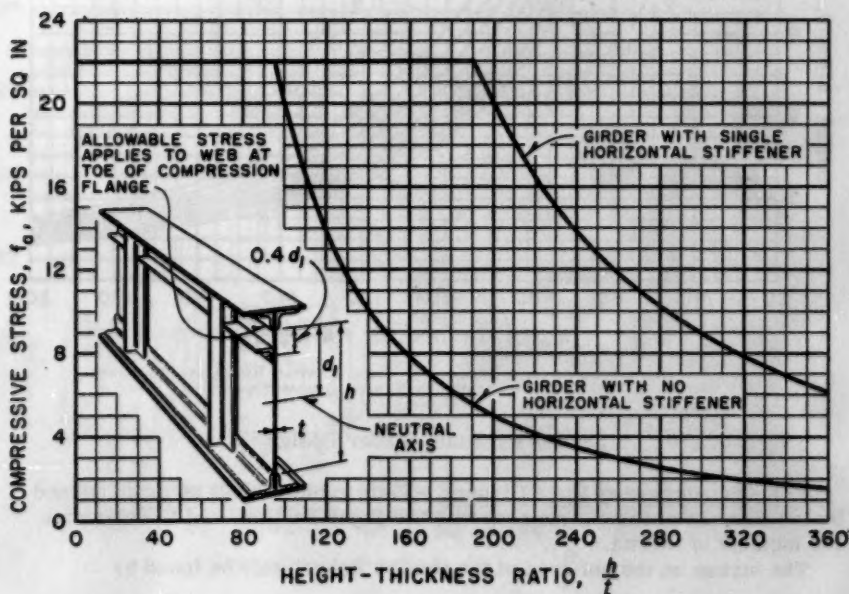


FIG. 8.—ALLOWABLE LONGITUDINAL COMPRESSIVE STRESSES FOR WEBS OF GIRDERS

F-8. Spacing of Vertical Stiffeners to Resist Shear Buckling.—The distance, s , between vertical stiffeners shall not exceed the values given by the solid curves in Fig. 9, which are replots of the curves in Fig. 7. The maximum value of the ratio of stiffener spacing to height of web, s/h , in Fig. 9 shall be determined from the ratio of clear height to thickness, h/t , and the computed shear stress on the girder web. Where a stiffener is composed of a pair of members, one on each side of the web, the distance s shall be the clear distance between the stiffeners. Where a stiffener is composed of a member on one side of the web only, the distance s shall be the distance between rivet lines. In determining the spacing of vertical stiffeners to resist shear buckling in panels containing a horizontal stiffener located as shown in Fig. 8, the distance h in Fig. 9 may be taken as 90% of the clear height between flanges.

F-9. Size of Vertical Stiffeners to Resist Shear Buckling.—Stiffeners applied to plate girder webs to resist shear buckling shall have a moment of inertia not less than the values given by the dotted curves in Fig. 9. The minimum value of the ratio of the stiffener moment of inertia to the fourth power of the web thickness, I_s/t^4 , in Fig. 9, shall be determined from the ratio of height of web to thickness of web, h/t , and the computed shear stress on the girder web.

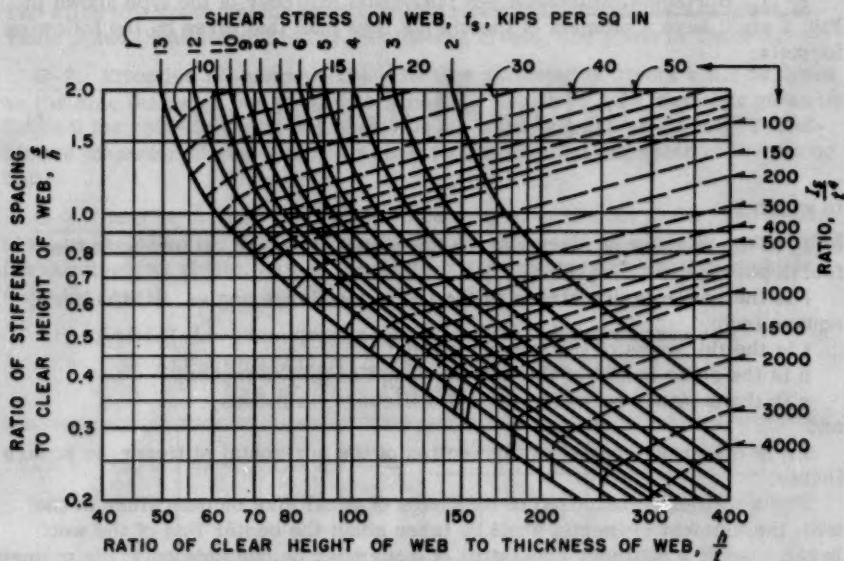


FIG. 9.—SPACING AND MOMENT OF INERTIA OF VERTICAL STIFFENERS TO RESIST SHEAR BUCKLING ON WEBS OF PLATE GIRDERS

For a stiffener composed of members of equal size on both sides of the web, the moment of inertia shall be taken about the center line of the web. For a stiffener composed of a member on one side only, the moment of inertia shall be taken about the face of the web in contact with the stiffener. In determining moment of inertia of stiffeners, the term h shall always be taken as

the full clear height between flanges, regardless of whether or not a horizontal stiffener is present.

F-10. Vertical Stiffeners at Points of Bearing.—Stiffeners shall be placed in pairs at end bearings of plate girders and at points of bearing of concentrated loads. They shall be connected to the web by enough rivets to transmit the load. Such stiffeners shall have a close bearing against the loaded flanges. Only that part of the stiffener cross section which lies outside the fillet of the flange angle shall be considered effective in bearing.

The moment of inertia of the stiffener shall not be less than that given by the formula:

$$I = I_s + \frac{P h^2}{74,000} \dots \dots \dots (5)$$

in which:

I_s is the moment of inertia, in inches to the fourth power, required to resist shear buckling (Fig. 9);

P is a local load concentration on the stiffener, in kips; and

h is the clear height of the web between flanges, in inches.

F-11. Horizontal Stiffeners.—A horizontal stiffener of the type shown in Fig. 8 shall have a moment of inertia not less than that given by the following formula:

$$I_h = f t h^3 \left[\left(16 + 90 \frac{A_h}{h t} \right) \left(\frac{s}{h} \right)^2 + 6 \right] \times 10^{-7} \dots \dots \dots (6)$$

in which:

I_h is the moment of inertia of the horizontal stiffener, in inches to the fourth power;

f is the compressive stress at the toe of the flange angles, in kips per square inch;

t is the thickness of the web, in inches;

h is the clear height of the web between flanges, in inches;

s is the distance between vertical stiffeners, in inches;

and

A_h is the gross area of cross section of the horizontal stiffener, in square inches.

For a stiffener composed of members of equal size on both sides of the web, the moment of inertia shall be taken about the center line of the web. In the case of a stiffener consisting of a member on one side only, the moment of inertia shall be taken about the face of the web in contact with the stiffener.

Eq. 6 must be solved by trial, since both the moment of inertia, I_h , and the area, A_h , of the stiffener are unknown. It is generally convenient to assume as a first approximation that the ratio $\frac{A_h}{h t}$ has the value of 0.1.

Section G. Riveted and Bolted Connections

G-1. Allowable Loads.—The allowable loads on rivets and bolts shall be calculated using the allowable shear and bearing stresses listed in Section A with the following exceptions:

a.—If a rivet or a bolt is used in relatively thin plates or shapes the allowable shear stress shall be reduced in accordance with the information given in Table 4.

b.—If the distance from the center of a rivet or bolt to the edge of a plate or shape toward which the pressure of the rivet or bolt is directed is less than twice the diameter of the rivet or bolt, the allowable bearing stress shall be reduced in accordance with the following:

Ratio of edge distance to rivet or bolt diameter	Allowable bearing stress, in kips per square inch
2 or more	36
1-3/4	33
1-1/2	30

The allowable loads calculated for cold-driven 2117-T3 rivets are given in Table 5 and those for 6061-T43, hot-driven rivets, are given in Table 6.

G-2. Effective Diameter.—The effective diameter of rivets shall be taken as the hole diameter but shall not exceed the values of hole diameter given in Table 5 for cold-driven rivets and in Table 6 for hot-driven rivets. The effective diameter of pins and bolts shall be the nominal diameter of the pin or bolt.

G-3. Bearing Area.—The effective bearing area of pins, bolts, and rivets shall be the effective diameter multiplied by the length in bearing; except that for countersunk rivets, half of the depth of the countersink shall be deducted from the length.

TABLE 4.—PERCENTAGE REDUCTION IN SHEAR STRENGTH
OF ALUMINUM ALLOY RIVETS RESULTING FROM THEIR
USE IN THIN PLATES AND SHAPES²

Ratio,* $\frac{D}{t}$	Loss in double shear ^b	Ratio,* $\frac{D}{t}$	Loss in double shear ^b	Ratio,* $\frac{D}{t}$	Loss in:		Ratio,* $\frac{D}{t}$	Loss in:	
					Single shear	Double shear		Single shear	Double shear
(1)	(3)	(1)	(3)	(1)	(2)	(3)	(1)	(2)	(3)
1.5	0	2.2	9.1	2.9	0	18.2	3.5	2.0	26.0
1.6	1.3	2.3	10.4	3.0	0	19.5	3.6	2.4	27.3
1.7	2.6	2.4	11.7	3.1	0.4	20.8	3.7	2.8	28.6
1.8	3.9	2.5	13.0	3.2	0.8	22.1	3.8	3.2	29.9
1.9	5.2	2.6	14.3	3.3	1.2	23.4	3.9	3.6	31.2
2.0	6.5	2.7	15.6	3.4	1.6	24.7	4.0	4.0	32.5
2.1	7.8	2.8	16.9

* Ratio of the rivet diameter, D , to the plate thickness, t . The thickness used is that of the thinnest plate in a single shear joint or of the middle plate in a double shear joint. ^b The percentage loss of strength in single shear is zero for D/t less than 3.0.

G-4. Arrangement and Strength of Connections.—Connections shall be arranged to minimize the eccentricity of loading on the member. Members and connections shall be proportioned to take into account any eccentricity of loading introduced by the connections.

G-5. Net Section.—The net section of a riveted tension member is the sum of the net sections of its component parts. The net section of a part is the product of the thickness of the part multiplied by its least net width. The net width for a chain of holes extending across the part in any straight or broken line shall be obtained by deducting from the gross width the sum of the diameters of all the holes in the chain and adding $\frac{s^2}{4g}$ for each gage space in the chain. In the correction quantity $\frac{s^2}{4g}$:

s is the spacing parallel to direction of load (pitch) of any two successive holes in the chain, in inches; and

g is the spacing perpendicular to direction of load (gage) of the same holes, in inches.

TABLE 5.—Allowable Design Load, in Kips per Rivet,
(Shear, 10 Kips per Sq In. and

Dimensions, in Inches	3/8	7/16	1/2	9/16				
Rivet diameter.....	0.386	0.453	0.516	0.578				
Hole diameter.....	W	29/64	33/64	37/64				
Drill size.....								
Thickness of plate, or shape, in inches:	RIVET IN SINGLE SHEAR (ss)							
	ss	ds	ss	ds	ss	ds	ss	ds
1/8	1.17	1.74 ^b	1.58 ^c	2.04 ^b	2.01 ^c	2.32 ^b	2.52 ^c	2.60 ^b
3/16	1.17	2.19 ^c	1.61	2.88 ^c	2.09	3.48 ^b	2.62	3.90 ^b
1/4	1.17	2.34	1.61	3.12 ^c	2.09	3.91 ^c	2.62	4.74 ^c
5/16	1.17	2.34	1.61	3.22	2.09	4.13 ^c	2.62	5.04 ^c
3/8	1.17	2.34	1.61	3.22	2.09	4.18	2.62	5.25
7/16	1.61	3.22	2.09	4.18	2.62	5.25
1/2	2.09	4.18	2.62	5.25
9/16	2.62	5.25
5/8
3/4
7/8
1

* Assuming distance from center of rivet to edge of member toward which the pressure of the rivet is directed is by bearing. ° These values are governed by reduced shear strengths as indicated in Table 4. All other values

The net section of the part is obtained from that chain which gives the least net width. The hole diameter to be deducted shall be the actual hole diameter for drilled or reamed holes.

For angles, the gross width shall be the sum of the widths of the legs less the thickness. The gage for holes in opposite legs shall be the sum of the gages from the back of the angle, less the thickness.

For splice members, the thickness shall be only that part of the thickness of the member that has been developed by rivets beyond the section considered.

G-6. Effective Sections of Angles.—If an angle in tension is connected on

one side of a gusset plate, the effective section shall be the net section of the connected leg plus one half of the section of the outstanding leg, unless the outstanding leg is connected by a lug angle. In the latter case the effective section shall be the entire net section of the angle, and there shall be at least two extra rivets in the lug angle beyond the gusset plate.

G-7. Grip of Rivets.—If the grip of rivets carrying calculated stress exceeds four and one-half times the diameter the allowable load per rivet shall be reduced. The reduced allowable load shall be the normal allowable load divided by $\left(\frac{1}{2} + \frac{G}{9D}\right)$, in which G is the grip and D the nominal diameter of the rivet. If the grip exceeds six times the diameter, special care shall be taken in driving the rivets to insure that the holes will be filled completely.

G-8. Pitch of Rivets in Built-Up Compression Members.—The pitch in the direction of stress shall be such that the allowable stress on the individual outside plates and shapes, treated as columns having a length equal to the rivet pitch in accordance with Fig. 2, exceeds the calculated stress. In no

for Cold-Driven 2117-T3 Rivets in 2014-T6 Structures
Bearing, 36 Kips per Sq In.²)

5/8 0.641 41/64		3/4 0.766 49/64		7/8 0.891 57/64		1 1.016 1 1/64		Dimensions, in Inches: Rivet diameter Hole diameter Drill size
OR IN DOUBLE SHEAR (ds)								Thickness of plate, or shape, in inches:
ss	ds	ss	ds	ss	ds	ss	ds	
2.88 ^b	2.88 ^b	1/8
3.18 ^b	4.33 ^b	4.42 ^b	5.17 ^b	5.82 ^b	6.02 ^b	3/16
3.23	5.62 ^b	4.61	6.89 ^b	6.11 ^b	8.02 ^b	7.78 ^b	9.14 ^b	1/4
3.23	6.03 ^b	4.61	8.14 ^b	6.24	10.02 ^b	8.04 ^b	11.43 ^b	5/16
3.23	6.31 ^b	4.61	8.62 ^b	6.24	11.12 ^b	8.11	13.72 ^b	3/8
3.23	6.45	4.61	8.97 ^b	6.24	11.66 ^b	8.11	14.58 ^b	7/16
3.23	6.45	4.61	9.22	6.24	12.07 ^b	8.11	15.16 ^b	1/2
3.23	6.45	4.61	9.22	6.24	12.39 ^b	8.11	15.64 ^b	9/16
3.23	6.45	4.61	9.22	6.24	12.47	8.11	16.00 ^b	5/8
....	4.61	9.22	6.24	12.47	8.11	16.22	3/4
....	6.24	12.47	8.11	16.22	7/8
....	8.11	16.22	1

not less than twice the nominal rivet diameter (see Specification G-1, exception b). ^b These values are governed by basic allowable shear stress.

case, however, shall the pitch in the direction of stress exceed six times the diameter of the rivets; and for a distance of one and one-half times the width of the member at each end, the pitch in the direction of stress shall not exceed three and one-half times the diameter of the rivets.

G-9. Stitch Rivets.—Where two or more web plates are in contact, there shall be stitch rivets to make them act in unison. In compression members, the pitch of such rivets in the direction of stress shall be determined as outlined in Specification G-8. The gage at right angles to the direction of stress shall not exceed twenty times the thickness of the outside plates. In tension members the maximum pitch or gage of such rivets shall be twenty times the

TABLE 6.—Allowable Design Loads, in Kips per Rivet,
(Rivets Driven at 990° F to 1,050° F; Shear, 8 Kips

Dimensions, in Inches:	3/8	7/16	1/2	9/16				
Rivet diameter.....	0.397	0.469	0.531	0.594				
Hole diameter.....	X	15/32	17/32	19/32				
Drill size.....								
	RIVET IN SINGLE SHEAR (ss)							
Thickness of plate, or shape, in inches:	ss	ds	ss	ds	ss	ds	ss	ds
1/8	0.99	1.60 ^b	1.35 ^b	2.05 ^b	1.70 ^b	2.39 ^c	2.08 ^b	2.67 ^c
3/16	0.99	1.85 ^b	1.38	2.47 ^b	1.77	3.01 ^b	2.22	3.57 ^b
1/4	0.99	1.98	1.38	2.68 ^b	1.77	3.31 ^b	2.22	4.00 ^b
5/16	0.99	1.98	1.38	2.76	1.77	3.50 ^b	2.22	4.26 ^b
3/8	0.99	1.98	1.38	2.76	1.77	3.54	2.22	4.43
7/16	1.38	2.76	1.77	3.54	2.22	4.43
1/2	1.77	3.54	2.22	4.43
9/16	2.22	4.43
5/8
3/4
7/8
1

* Assuming distance from center of rivet to edge of member toward which the pressure of the rivet is directed is by reduced shear strengths as indicated in Table 4. * These values are governed by bearing. All other values

thickness of the outside plates; and in tension members composed of two angles in contact, the pitch of the stitch rivets shall not exceed 10 in.

G-10. Minimum Spacing of Rivets.—The distance between centers of rivets shall not be less than three times the diameter of the rivets.

G-11. Edge Distance of Rivets.—The distance from the center of a rivet to a sheared, sawed, rolled, or planed edge shall be not less than one and one-half times the diameter, except in flanges of beams and channels, where the minimum distance may be one and one-fourth times the diameter. For rivets under computed stress, the distance from the center of the rivet to the edge of the plate or shape toward which the pressure of the rivet is directed should normally be at least twice the nominal diameter of the rivet. In cases where a shorter edge distance must be used, the allowable bearing stress shall be reduced in accordance with Specification G-1, exception b.

The distance from the edge of a plate to the nearest rivet line shall not exceed six times the thickness of the plate.

G-12. Sizes of Rivets in Angles.—The diameter of the rivets in angles whose size is determined by calculated stress shall not exceed one fourth of the width of the leg in which they are driven. In angles whose size is not so determined, 1-in. rivets may be used in 3-1/2-in. legs; 7/8-in. rivets, in 3-in. legs; and 3/4-in. rivets, in 2-1/2-in. legs.

G-13. Extra Rivets.—If splice plates are not in direct contact with the parts which they connect, there shall be rivets on each side of the joint in excess of the number required in the case of direct contact, to the extent of two extra lines for each intervening plate.

If rivets carrying calculated stress pass through fillers, the fillers shall be extended beyond the connected member and the extension secured by

for Hot-Driven 6061-T43 Rivets in 2014-T6 Structures
per Sq In.; and Bearing, 36 Kips per Sq In.^a)

5/8 0.656 21/32		3/4 0.781 25/32		7/8 0.922 59/64		1 1.063 1 1/16		Dimensions, in Inches: Rivet diameter Hole diameter Drill size
OR IN DOUBLE SHEAR (ds)								Thickness of plate, or shape, in inches:
ss	ds	ss	ds	ss	ds	ss	ds	
2.49 ^b	2.95 ^a					1/8
2.66 ^b	4.12 ^a	3.68 ^b	5.17 ^b	4.98 ^b	6.22 ^a	3/16
2.70	4.71 ^b	3.83	6.17 ^b	5.23 ^b	7.91 ^b	6.82 ^b	9.59 ^b	1/4
2.70	5.06 ^b	3.83	6.77 ^b	5.34	8.88 ^b	7.04 ^b	10.88 ^b	5/16
2.70	5.29 ^b	3.83	7.17 ^b	5.34	9.53 ^b	7.10	12.04 ^b	3/8
2.70	5.41	3.83	7.46 ^b	5.34	9.99 ^b	7.10	12.77 ^b	7/16
2.70	5.41	3.83	7.67	5.34	10.34 ^b	7.10	13.28 ^b	1/2
2.70	5.41	3.83	7.67	5.34	10.61 ^b	7.10	13.69 ^b	9/16
2.70	5.41	3.83	7.67	5.34	10.68	7.10	14.02 ^b	5/8
....	3.83	7.67	5.34	10.68	7.10	14.20	3/4
....	5.34	10.68	7.10	14.20	7/8
....	7.10	14.20	1

not less than twice the nominal rivet diameter (see Specification G-1, exception b). ^a These values are governed by basic allowable shear stress.

enough additional rivets to distribute the total stress in the member uniformly over the combined section of the member and filler.

Section H. Miscellaneous Design Rules

H-1. Reversal of Load.—Members subject to reversal of load under the passage of live load shall be proportioned as follows: Determine the tensile load and the compressive load and increase each by 50% of the smaller; then proportion the member and its connections so that the allowable stresses given in Sections A to G, inclusive, will not be exceeded by either increased load.

H-2. Slenderness Ratio of Tension Members.—Long slender members have little resistance to lateral loads. Therefore, tension members with values of slenderness ratio L/r greater than 150 shall not be used unless special care is taken to insure that such members are designed to resist any lateral loads such as wind, dead load, or the weight of workmen and equipment. Stresses caused by the combined bending and tensile loadings shall not exceed allowable limits.

H-3. Stay Plates for Tension Members.—Segments of tension members not directly connected to each other shall be stayed together. The length of the stay plate shall be not less than three fourths of the distance between rivet lines of the segments. Stay plates shall be connected to each segment of the tension member by at least three rivets. The distance between stay plates shall be such that the slenderness ratio of the individual segments of the member between stay plates does not exceed the slenderness ratio of the member as a whole.

H-4. Fatigue.—Tests indicate that riveted members designed in

accordance with the requirements of these specifications and constructed so as to be free from severe reentrant corners and other unusual stress raisers will safely withstand at least 100,000 repetitions of maximum live load without fatigue failure regardless of the ratio of minimum to maximum load. Where a greater number of repetitions of some particular loading cycle is expected during the life of the structure, the calculated net section tensile stresses for the loading in question shall not exceed the values given by the curves in Fig. 10. When using the curves in Fig. 10 the reversal-of-load rule in Specification H-1 should be ignored. The final member and connections selected, however, shall be strong enough to satisfy the requirements of Specification H-1.

In considering fatigue action on structures it is well to bear in mind the following points:

a.—The most severe combination of loadings for which a structure is designed (dead load, maximum live load, maximum impact, maximum wind, etc.) rarely occurs in actual service and is of little or no interest from the standpoint of fatigue.

b.—The loading of most interest from the fatigue standpoint is the steady dead load with a superimposed and repeatedly applied live load having an intensity consistent with day-to-day normal operating conditions.

c.—The number of cycles of load encountered in structures is usually small compared with those encountered in fatigue problems involving machine parts. It takes many years of service to accumulate even 100,000 cycles of any significant stress application in most structures as is indicated by the following examples: 100,000 cycles represent 10 cycles every day for 27 years; 10,000,000 cycles represent 20 cycles every hour for 57 years. Care must be taken not to overestimate grossly the number of cycles for any given load condition.

d.—Careful attention to details in design and fabrication pays big dividends in fatigue life. When a fatigue failure occurs in a structure it is usually at a point of stress concentration where the state of stress could have been improved with little or no added expense.

Section I. Fabrication

I-1. Laying Out.—

a.—Hole centers may be center-punched and cutoff lines may be punched or scribed. Center-punching and scribing shall not be used where such marks would remain on fabricated material.

b.—A temperature correction shall be applied where necessary in the layout of critical dimensions. The coefficient of expansion shall be taken as 0.000012 per degree Fahrenheit.

I-2. Cutting.—

a.—Material 1/2 in. thick or less may be sheared, sawed, or cut with a router. Material more than 1/2 in. thick shall be sawed or routed.

b.—Cut edges shall be true and smooth, and free from excessive burrs or ragged breaks.

c.—Edges of plates carrying calculated stresses shall be planed to a depth of 1/4 in. except in the case of sawed or routed edges of a quality equivalent to a planed edge.

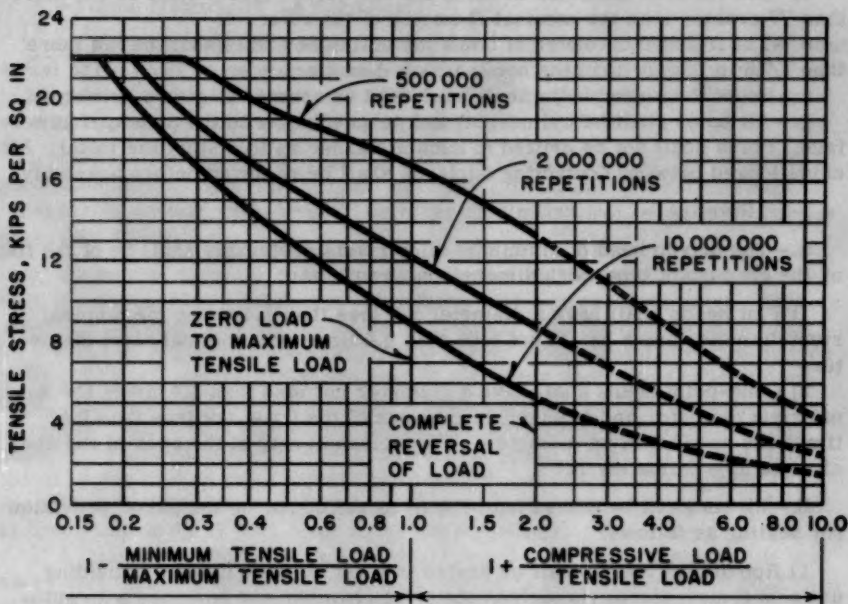


FIG. 10.—ALLOWABLE TENSILE STRESSES ON NET SECTION FOR VARIOUS NUMBERS OF REPETITIONS OF LOAD APPLICATION

d.—Reentrant cuts shall be avoided wherever possible. If used they shall be filleted by drilling prior to cutting.

e.—Flame cutting of aluminum alloys is not permitted.

I-3. Heating.—Structural material shall not be heated, with the following exceptions:

a.—Material may be heated to a temperature not exceeding 400° F for a period not exceeding 15 min to facilitate bending. Such heating shall be done only when proper temperature controls and supervision are provided to insure that the limitations on temperature and time are carefully observed.

b.—Hot-driven rivets shall be heated as specified in Section I-5.

I-4. Punching, Drilling, and Reaming.—Rules for punching, drilling, and reaming are as follows:

a.—Rivet or bolt holes in main members shall be subpunched or sub-drilled and reamed to finished size after the parts are firmly bolted together. The amount by which the diameter of a subpunched hole is smaller than that of the finished hole shall be at least one-quarter the thickness of the piece and in no case less than 1/32 in. If the metal thickness is greater than the diameter of the hole, punching shall not be used.

b.—Rivet or bolt holes in secondary material not carrying calculated stress may be punched or drilled to finished size before assembly.

c.—The finished diameter of holes for cold-driven rivets shall be not more than 4% greater than the nominal diameter of the rivet.

d.—The finished diameter of holes for hot-driven rivets shall be not more than 7% greater than the nominal diameter of the rivet.

e.—The finished diameter of holes for unfinished bolts shall be not more than 1/16 in. larger than the nominal bolt diameter.

f.—Holes for turned bolts shall be drilled or reamed to give a driving fit.

g.—All holes shall be cylindrical and perpendicular to the principal surface. Holes shall not be drifted in such a manner as to distort the metal. All chips lodged between contacting surfaces shall be removed before assembly.

I-5. Riveting.—

a.—The driven head of aluminum alloy rivets preferably shall be of the flat or the cone-point type, with dimensions as follows:

1) Flat heads shall have a diameter not less than 1.4 times the nominal rivet diameter and a height not less than 0.4 times the nominal rivet diameter.

2) Cone-point heads shall have a diameter not less than 1.4 times the nominal rivet diameter and a height, to the apex of the cone, not less than 0.65 times the nominal rivet diameter. The included angle at the apex of the cone shall be approximately 127°.

b.—Rivets shall be driven hot or cold as called for on the plans, provision for heating as follows:

1) Hot-driven rivets shall be heated in a hot air type furnace providing uniform temperatures throughout the rivet chamber and equipped with automatic temperature controls.

2) Hot-driven rivets shall be held at from 990° F to 1,050° F for not less than 15 min and for not more than 1 hour before driving.

3) Hot rivets shall be transferred from the furnace to the work and driven with a minimum loss of time.

c.—Rivets shall fill the holes completely. Rivet heads shall be concentric with the rivet holes and shall be in proper contact with the surface of the metal.

d.—Defective rivets shall be removed by drilling.

I-6. Welding.—Welding is not permitted.

I-7. Cleaning and Treatment of Metal Surfaces.—

a.—Surfaces of metal shall be cleaned immediately before painting by a method which will remove all dirt, oil, grease, chips, and other foreign substances.

b.—Either of the two following methods of cleaning may be used on exposed metal surfaces:

1) Chemical Cleaning.—Parts may be immersed in, or swabbed with, a solution of phosphoric acid and organic solvents diluted with water in the ratio of 1:3. The solution temperature shall be between 50° F and 90° F. The solution shall remain in contact with the metal not less than 5 min. Residual solution shall be removed with clear water.

2) Sandblasting.—Standard mild sandblasting methods may be used on sections more than 1/8 in. thick.

c.—For contacting surfaces only, the metal may be cleaned in accordance

with Specification I-7b, or with a solvent such as mineral spirits or benzine.

d.—Flame cleaning is not permitted.

I-8. **Painting.**—Specifications to control painting operations are as follows: Metal parts shall be painted as described in Specifications I-8a and I-8b (or in accordance with United States Military Specification MIL-T-704) except where the plans specifically permit a deviation.

a.—Where the aluminum alloy parts are in contact with, or are fastened to, steel members or other dissimilar materials, the aluminum shall be kept from direct contact with the steel or other dissimilar material by painting as described below:

1) Aluminum surfaces to be placed in contact with steel shall be given one coat of zinc chromate primer in accordance with United States Joint Army-Navy Specification JAN-P-735 or the equivalent. Zinc chromate paint shall be allowed to dry before assembly of the parts. Additional protection may be provided by the application of one coat of a suitable nonhardening joint compound, in addition to the zinc chromate primer. The steel surfaces to be placed in contact with aluminum shall be painted with good quality priming paint, such as red lead conforming to Federal Specification TT-P-86a, followed by one coat of paint consisting of 2 lb of aluminum paste pigment (ASTM Specification D962-49, Type II, Class B) per gallon of varnish meeting Federal Specification TT-V-81b, Type II, or the equivalent.

2) Aluminum surfaces to be placed in contact with wood, concrete, or masonry construction, except where the aluminum is to be imbedded in concrete, shall be given a heavy coat of an alkali-resistant bituminous paint before installation. The bituminous paint used shall meet the requirements of United States Military Specification MIL-P-6883. The paint shall be applied as it is received from the manufacturer without the addition of any thinner.

3) Aluminum surfaces to be imbedded in concrete shall, before installation, be given one coat of zinc chromate primer in accordance with United States Joint Army-Navy Specification JAN-P-735 or the equivalent. The paint shall be allowed to dry before the aluminum is placed in the concrete.

b.—All contacting metal surfaces other than those covered in Specification I-8a shall be painted before assembly with one coat of zinc chromate primer in accordance with United States Joint Army-Navy Specification JAN-P-735 or the equivalent. The primer shall be allowed to dry before assembly of the parts. All other surfaces shall be given one shop coat of zinc chromate primer made in accordance with United States Joint Army-Navy Specification JAN-P-735 or the equivalent and then shall be given a second shop coat of paint consisting of 2 lb of aluminum paste pigment (ASTM Specification D962-49, Type II, Class B) per gallon of varnish meeting Federal Specification TT-V-81b, Type II, or the equivalent. Sufficient Prussian blue shall be added to permit detection of an incomplete application of the subsequent paint coat. After erection, bare spots shall be touched up with zinc chromate primer followed by a touch-up coat of aluminum paint as specified above. The completed structure shall be finished according to one of the following methods:

1) One field coat of aluminum paint as specified above, except that Prussian blue shall be omitted from the field coat.

2) One or more field coats of alkyd base enamel pigmented to meet a desired color scheme.

PART III. EXPLANATION OF SPECIFICATIONS

Section A. Summary of Allowable Stresses

A-1. Basic Tensile Design Stress.—The basic tensile design stress of 22 kips per sq in. represents a factor of safety of 2.41 based on the specified tensile yield strength. This is a larger factor of safety with respect to yield strength than is ordinarily encountered in specifications for structural steel. In selecting this rather large factor of safety on yield strength, the committee was influenced to a considerable extent by the fact that there is a smaller spread between yield strength and tensile strength in this aluminum alloy than is commonly encountered in structural steels.

A-8, A-9, and A-13. Allowable Stresses on Rivets.—The allowable shearing and bearing stresses on rivets were selected on the basis of the results of numerous shearing and bearing tests. The factors of safety used are greater than those used for most of the other allowable stresses.

A-6, A-11, and A-12. Allowable Stresses on Pins.—The allowable bending, shearing, and bearing stresses on pins were selected to have about the same relation to the corresponding properties of the material as is the case in standard steel specifications. It is not anticipated that any wide use of pins will be made in aluminum alloy structures but it is assumed that where they are used they will be of the same material as the structural members themselves, and that they would probably be obtained in the form of rolled rod, ASTM Specification B211-54T(CS41A).

Section B. Column Design

B-1. Curves for Allowable Compressive Stresses in Axially Loaded Columns.—The curves in Fig. 2 are the tangent-modulus column curves with a factor of safety of 2.5 and with a cutoff at the basic allowable design stress of 22 kips per sq in. The formulas for all three curves can be written^{4,5}

$$f_c = \frac{\pi^2 E_t}{2.5 \left(\frac{kL}{r} \right)^2} \dots \dots \dots (7)$$

in which:

f_c is the allowable compressive stress on the gross cross-sectional area, in kips per square inch;

E_t is the tangent modulus taken from Fig. 1 at stress corresponding to 2.5 (f_c), in kips per square inch;

L is the length of the column, in inches;

r is the least radius of gyration of the column, in inches; and

4. "Column Strength of Various Aluminum Alloys," by R. L. Templin, R. G. Sturm, E. C. Hartmann, and M. Holt, Aluminum Research Laboratories Technical Paper No. 1, Aluminum Co. of America, Pittsburgh, Pa., 1938.

5. "Inelastic Column Theory," by F. R. Shanley, Journal of the Aeronautical Sciences, Vol. 14, 1947, pp. 261-268.

k is a factor describing the end conditions as defined in Fig. 2.

For values of slenderness ratio, L/r , greater than 72, the formula for the partial restraint curve in Fig. 2 reduces to

$$f_c = \frac{74,000}{\left(\frac{L}{r}\right)^2} \dots \dots \dots (8)$$

B-7. Formula for Combined Compression and Bending.—Eq. 1 is based on an interaction formula that gives good agreement with the results of tests on aluminum alloy members subjected to combined compressive end load and bending.^{6,7} The formula is applicable to members in which the bending is applied about either the strong or the weak axis.

B-8. Formula for Transverse Shear on Columns.—Eq. 3a is based on the transverse component of the column load at the point of maximum slope of the column in its deflected position. A derivation by Mr. Hartmann has been published elsewhere.⁸

Section C. Curve for Allowable Compressive Stress in Beam and Girder Flanges

C-1. The curve in Fig. 3 is based on the theoretical solution for the critical bending moment in I-beams as given by S. Timoshenko.⁹ It represents a factor of safety of 2.5 applied to the buckling strength of beams subjected to a uniform bending moment. It is assumed that at the ends of the laterally unsupported length there is partial restraint against rotation about a vertical axis and complete restraint against lateral displacement and against rotation about a horizontal axis parallel to the web. The effect of partial restraint at the ends of the span has been taken into account by substituting $0.75L$ for the length in the formula for buckling of the beam under uniform bending moment.

The part of the curve for values of $\frac{L}{\sqrt{B/S_c}}$ greater than 35 is based on elastic action, whereas the remainder is simply an extension of the same formula using tangent modulus rather than initial modulus. The curve has a cutoff at the basic allowable compressive design stress of 14 kips per sq in. It is important to note that the term L is defined as "laterally unsupported length," which is not necessarily the same as the span of the beam or girder.

The case of uniform bending moment on a simple beam has been used in setting up Fig. 3, because it is a good approximation of conditions frequently encountered in actual design, and because it is somewhat more conservative

6. "Plastic Buckling of Eccentrically Loaded Aluminum Alloy Columns," by J. W. Clark, *Proceedings, ASCE*, Separate No. 299, Vol. 79, October, 1953.
7. "Designing Aluminum Alloy Members for Combined End Load and Bending," by H. N. Hill, E. C. Hartmann, and J. W. Clark, *Proceedings, ASCE*, Separate No. 300, Vol. 79, October, 1953.
8. Discussion by E. C. Hartmann of "Rational Design of Steel Columns," by D. H. Young, *Transactions, ASCE*, Vol. 101, 1936, pp. 475-481.
9. "Theory of Elastic Stability," by S. Timoshenko, McGraw-Hill Book Co., Inc., New York, N. Y., 1936.

than many of the other cases that might have been selected. The provision that four-thirds times the length shall be used for L in the case of a cantilever beam has the effect of canceling the length reduction coefficient of 0.75 that was introduced to take account of the effect of lateral restraint in simple beams. Thus, the buckling strength of a cantilever beam is assumed to be equal to the strength of a simply supported beam of the same length subjected to uniform bending moment. This gives a conservative approximation to the strength of a cantilever beam.⁹

For values of $\frac{L}{\sqrt{B/S_c}}$ greater than 27.5, the curve in Fig. 3 may be represented by the formula:

$$f_B = \frac{10,900}{\left(\frac{L}{\sqrt{B/S_c}}\right)^2} \dots \dots \dots (9)$$

The curve in Fig. 3 is based on a theoretical solution applicable only to I-beams having cross sections symmetrical about both axes. The modified interpretation of the term I_1 indicated in specification C-1, however, permits the curve to be used without serious error for beams and girders having one flange differing in lateral stiffness from the other. It should be used with caution in cases of beams and girders which are unsymmetrical by a considerable margin. (In connection with this subject several supplementary references^{7,10,11,12,13} will be of interest.)

Section D. Curves for Design of Flat Plates, Legs and Webs

The curves of Figs. 4, 5, and 6 are based on values of critical stress compiled by Mr. Hill in 1940.¹⁴ Partial restraint along the supported edges and loaded edges was assumed in all cases except for the supported edge in Fig. 4, which was considered simply supported. Parts of the curves that represent critical buckling stresses above the elastic range are computed by using the tangent modulus instead of the modulus of elasticity, a procedure which is known to be conservative when applied to problems of plate buckling.¹⁵ A factor of safety of 2.5 against critical buckling has been used in all three

10. "The Lateral Instability of Unsymmetrical I-Beams," by H. N. Hill, Journal of the Aeronautical Sciences, Vol. 9, 1942, pp. 175-180.
11. "The Lateral Stability of Equal-Flanged Aluminum-Alloy I-Beams Subjected to Pure Bending," by C. Dumont and H. N. Hill, Technical Note No. 770, National Advisory Committee for Aeronautics, Washington, D. C., 1940.
12. "Lateral Stability of Unsymmetrical I-Beams and Trusses in Bending," by George Winter, Transactions, ASCE, Vol. 108, 1943, pp. 247-268.
13. "Strength of Beams as Determined by Lateral Buckling," by Karl de Vries, ibid., Vol. 112, 1947, pp. 1245-1320.
14. "Chart for Critical Compressive Stress of Flat Rectangular Plates," by H. N. Hill, Technical Note No. 773, National Advisory Committee for Aeronautics, Washington, D. C., 1940.
15. "Buckling Stresses for Flat Plates and Sections," by Elbridge Z. Stowell, George J. Heimerl, Charles Libove, and Eugene E. Lundquist, Transactions, ASCE, Vol. 117, 1952, pp. 545-575.

and in all cases the curves have a cutoff at the basic allowable design stress of 22 kips per sq in.

When a flat plate, leg, or web is built in along one or both edges to other parts of a compression member which offer partial edge restraint, the local buckling of the plate, leg, or web does not precipitate collapse of the member as a whole as it probably would in the case of a single-angle strut. For this reason it is proper to permit a decreased factor of safety against local buckling in such cases if suitable precautions are taken to avoid collapse. Step c of Specification D-2 provides a simple method for accomplishing this result by introducing the well-known "effective width" concept. After a plate, leg, or web buckles, a part of its area is considered to be ineffective in supporting load, whereas a strip along each supported edge is considered still fully effective in working with the supporting material to which it is attached. The formula (Eq. 4) for effective width used in step c of Specification D-2 is generally more conservative than other accepted methods of calculating effective width.^{16,17,18,19}

The limitation placed on the value of f_c in step f of Specification D-2 is intended to provide a factor of safety of at least 1.67 against local buckling at the design load.

Section E. Curves for Allowable Shear Stress in Webs

E-1.—The values of allowable stress in Fig. 7 are obtained by applying a factor of safety of 2 to the critical shear buckling stresses for flat plates with the edges about halfway between the fixed and hinged conditions.^{9,20,21}

Those parts of the curves of Fig. 7 which represent critical buckling stresses above the elastic stress range are computed from formulas for elastic buckling with the tangent modulus substituted for the modulus of elasticity. For a given value of critical shear stress, the tangent modulus is that corresponding to an axial stress equal to $\sqrt{3}$ times the shear stress.²² As in the case of compressive buckling of flat plates, the tangent modulus is conservative.

For values of allowable stress below 10.4 kips per sq in., the curves of

16. "The Strength of Thin Plates in Compression," by Theodor von Kármán, Ernest E. Sechler, and L. H. Donnell, Transactions, A.S.M.E., Vol. 54, 1932, pp. 53-57.
17. "The Apparent Width of the Plate in Compression," by Karl Marguerre, Technical Memorandum No. 833, National Advisory Committee for Aeronautics, Washington, D. C., 1937.
18. "Strength of Thin Steel Compression Flanges," by George Winter, Transactions, ASCE, Vol. 112, 1947, pp. 527-576.
19. "Performance of Thin Steel Compression Flanges," by George Winter, preliminary publication, 3d Cong. of the International Assn. for Bridge and Structural Engrs., Liege, Belgium, 1948.
20. "Formulas for Stress and Strain," by Raymond J. Roark, McGraw-Hill Book Co., Inc., New York, N. Y., 1938.
21. "Observations on the Behavior of Aluminum Alloy Test Girders," by R. L. Moore, Transactions, ASCE, Vol. 112, 1937, pp. 901-920.
22. "Critical Shear Stress of an Infinitely Long Plate in the Plastic Region," by Elbridge Z. Stowell, Technical Note No. 1681, National Advisory Committee for Aeronautics, Washington, D. C., 1948.

Fig. 7 may be represented by the formula:

$$f_v = \frac{35,000}{(b/t)^2} \left[1 + 0.75 \left(\frac{b}{a} \right)^2 \right] \dots \dots \dots (10)$$

Section F. Plate Girder Design

F-6. Curves for Allowable Longitudinal Compressive Stress in Webs of Girders.—The curve in Fig. 8 for girders with no horizontal stiffeners is based on the critical buckling stress for rectangular flat plates under pure bending in the plane of the plate. Partial restraint is assumed at the toes of the flanges (about halfway between the solution given by Mr. Timoshenko for the case of a plate simply supported on all four edges⁹ and the solution of K. Nolke for a plate with the loaded edges simply supported and the other two edges fixed.)²³

The curve in Fig. 8 for girders with a single horizontal stiffener is based on the critical buckling stress given by Mr. Timoshenko for plates simply supported on all four edges under combined bending and axial stress in the plane of the plate.⁹ The simple support condition is used for this case because the horizontal stiffener would provide comparatively little restraint against rotation. The location of the horizontal stiffener shown in the sketch in Fig. 8 is chosen so that the parts of the plate above and below the stiffener will buckle at approximately the same load.

A factor of safety against buckling of 1.5 was used for the curves of Fig. 8. Although this factor of safety is not as large as some used elsewhere in these specifications, it is considered adequate in this instance since tests have shown that the critical bending stress for girder webs may be considerably exceeded without affecting the load-carrying capacity of the girder.^{21,23} Use of Fig. 8, however, will prevent buckling from occurring at design stresses.

The curves of Fig. 8 may be represented by the following formulas: No horizontal stiffener—

$$f_a = \frac{200,000}{\left(\frac{h}{t} \right)^2} \dots \dots \dots (11)$$

and single horizontal stiffener—

$$f_a = \frac{800,000}{\left(\frac{h}{t} \right)^2} \dots \dots \dots (12)$$

The curves are cut off at the basic allowable design stress of 22 kips per sq in.

F-8 and F-9. Curves for Spacing and Moment of Inertia of Vertical Stiffeners.—The curves for determining stiffener spacing, in Fig. 9, are merely replots of the data of Fig. 7. The curves of I_s/t^4 in Fig. 9 represent the following formula:

23. "Buckling of Webs in Deep Steel I-Girders," by Georg Wastlund and Sten G. A. Bergman, rept. of investigation made at the Royal Inst. of Technology, Stockholm, Sweden, 1947.

$$I_s = 8 \times 10^{-6} \frac{f_s h^3 t \left(\frac{s}{h} \right)}{1 + 5 \left(\frac{s}{h} \right)^3} \dots \dots \dots (13)$$

in which f_s is the average shear stress on the web in kips per square inch.

Eq. 13 is designed to fit the theoretical solution of M. Stein and R. W. Fralich²⁴ for values of s/h between 0.2 and 1.0. This solution does not cover values of s/h greater than 1.0. In this range, however, Eq. 13 is conservative in comparison with the recommendations of L. S. Moisseiff.¹

F-10. Formula for Moment of Inertia of Stiffeners at Points of Bearing.—Eq. 5 simply states that the moment of inertia of a stiffener at a point of bearing should be equal to the sum of the moment of inertia required to resist the tendency of the web to buckle and the moment of inertia required for the stiffener to carry the bearing load as a column with length equal to the height of the web.

F-11. Formula for Radius of Gyration of Horizontal Stiffeners.—Eq. 6, for the moment of inertia of horizontal stiffeners, is based on the theoretical work of C. Dubas, reported by F. Bleich.²⁵

Section H. Miscellaneous Design Rules

H-4. Curves of Allowable Tensile Stress on Net Section for Various Numbers of Repetitions of Load Application.—The curves in Fig. 10 are plotted from the results of fatigue tests conducted at the Aluminum Research Laboratories of the Aluminum Company of America at New Kensington, Pa., on 2014-T6 butt joints with double straps joined with eight cold-driven 5/8-in. 2117-T6 rivets. The type of testing equipment and specimen (Type M1) used are illustrated in a paper by R. L. Templin,²⁶ M. ASCE, in 1939, and a paper by Mr. Hartmann, J. O. Lyst, and H. J. Andrews,²⁷ Jun. ASCE, in 1944.

A factor of safety of 1.2 has been applied to the test data and all curves are cut off at the basic allowable design stress of 22 kips per sq in. The right-hand part of the diagram is largely based on extrapolation of the data, but this is not considered to be a serious matter since the design of most

24. "Critical Shear Stress of Infinitely Long, Simply Supported Plate with Transverse Stiffeners," by Manuel Stein and Robert W. Fralich, Technical Note No. 1851, National Advisory Committee for Aeronautics, Washington, D. C., 1949.
25. "The Buckling Strength of Metal Structures," by Friedrich Bleich, McGraw-Hill Book Co., Inc., New York, N. Y., 1952, p. 422.
26. "Fatigue Machines for Testing Structural Units," by R. L. Templin, Proceedings, A.S.T.M., Vol. 39, 1939, pp. 711-722.
27. "Fatigue Tests of Riveted Joints," by E. C. Hartmann, J. O. Lyst, and H. J. Andrews, War-time Report W55, National Advisory Committee for Aeronautics, Washington, D. C., 1944.

members in this range will be governed primarily by Specification H-1 rather than by fatigue considerations.

Respectfully submitted,

F. Baron
P. E. Brandt
R. Ebenbach
C. N. Gaylord

E. H. Gaylord
E. C. Hartmann
S. A. Kilpatric
R. B. B. Moorman

W. A. Nash
F. L. Plummer
W. K. Rey
J. B. Scalzi
F. J. Tamanini

J. W. Clark, Chairman

Committee of the Structural Division on Design in Lightweight
Structural Alloys

JOURNAL
STRUCTURAL DIVISION
 Proceedings of the American Society of Civil Engineers

CONTENTS

DISCUSSION
 (Proc. Paper 972)

	Page
Foundation Failures in Residences and Small Structures, by Karl V. Taylor. (Proc. Paper 561. Prior discussion: 664. Discussion closed)	
by Karl V. Taylor (Closure)	972-3
Multiple Span Gabled Frames, by John D. Griffiths. (Proc. Paper 586. Prior discussion: 765. Discussion closed)	
by John D. Griffiths (Closure)	972-5
Bending Interaction in Suspension Bridges, by Haaren A. Miklofsky. (Proc. Paper 652. Prior discussion: 812. Discussion closed)	
by Haaren A. Miklofsky (Closure)	972-7
Influence Lines for Moment and Shear in a Continuous Beam, by Anthony Hoadley. (Proc. Paper 734. Prior discussion: 849. Discussion closed)	
Corrections to discussion by Benjamin C. F. Wei	972-9
Sequence Summation Factors, by Adrian Pauw. (Proc. Paper 763. Prior discussion: 878. Discussion closed)	
by Elio Giangreco	972-11
Report of ASCE-ACI Joint Committee on Ultimate Strength Design. (Proc. Paper 809. Prior discussion: 878, 924. Discussion closed)	
by P. W. Abeles	972-23
by L. W. Mensch	972-31
Determining Basic Wind Loads, by George F. Collins. (Proc. Paper 825. Prior discussion: none. Discussion closed)	
by Albert W. Hainlin	972-39
by T. C. Rathbone	972-40
(Over)	

Note: Paper 972 is part of the copyrighted Journal of the Structural Division of the American Society of Civil Engineers, Vol. 82, No. ST 3, May, 1956.

Introduction to Semi-Rigid Determinate Polygonal Trusses, by
Alexander H. Kenigsberg. (Proc. Paper 828. Prior discussion: 878.
Discussion closed)

by E. Neil W. Lane 972-45
by A. C. Scordelis 972-47

Analysis of Arches by Finite Differences, by Ephraim G. Hirsch
and E. P. Popov. (Proc. Paper 829. Prior discussion: none.
Discussion closed)

by Chiao-Lin Chang 972-53
by Herbert A. Sawyer, Jr. 972-54

Load Test of a Diagonally Sheathed Timber Building, by J. M. English
and C. F. Knowlton. (Proc. Paper 830. Prior discussion: none
Discussion closed)

by E. George Stern 972-59
by Norman B. Jones 972-60

Elasti-Plastic Design of Single-Span Beams and Frames, by Herbert
A. Sawyer. (Proc. Paper 851. Prior discussion: none. Discussion
closed)

by Bruce G. Johnston 972-61

Discussion of
"FOUNDATION FAILURES IN RESIDENCES
AND SMALL STRUCTURES"

by Karl V. Taylor
(Proc. Paper 561)

KARL V. TAYLOR,¹ M. ASCE.—The writer wishes to express his appreciation to Messrs. C. H. Clifton and A. H. Metcalfe for their discussions. Because this paper was originally prepared for oral presentation under definite time limitations a number of interesting aspects of the settlement problem were, of necessity, omitted. The author is indebted to the writers for the specific examples cited in amplification of generalized statements in the paper and particularly for the suggested structural treatments of foundation defects.

A number of instances of objectionable ground floor slab cracking and settlement in light manufacturing buildings for which the exterior foundation cuts were of sufficient depth and width to cause some 3 or 4 feet of the slab about the perimeter to bear on backfilled material have been observed by the author. He believes that in all these cases the slab failures could have been prevented merely by more careful attention to the backfilling procedures.

Mr. Clifton has mentioned as a cause of settlement the removal of ground water from the subsoil by trees in the proximity of structures. The author concurs since localized changes in ground water regimen are conducive to differential settlements. He has noted a few cases in which the assiduous watering of trees and shrubs adjacent to a house in an effort to preserve them during severe drouth has apparently caused sufficient retardation of subsoil shrinkage in local areas to result in minor differential settlement cracking in the structure.

Mr. Metcalfe cited several instances in which 8 to 15-foot long concrete-filled pipe piles were advantageously used to underpin and restore small structures. In the locale mentioned in the paper somewhat similar techniques for correcting settlements are used except that after the building has been shored and the excavation extended several feet beyond and beneath a portion of a continuous footing or individual column footing, auger holes, generally 8 to 12 inches in diameter, are bored beneath the footing to a depth of 10 to 15 feet by portable power operated flight augers. The holes are filled with concrete and the piles thus formed are capped with a reinforced concrete footing. After the building is jacked into proper alinement the space between the bottom of the old footing and top of the new footing is filled with concrete and the load permanently transferred to the pile foundation. In order to be effective in combating settlement caused by desiccation of the subsoil it is obviously necessary for the piles to extend well below the minimum water table elevation which would occur during years of severest drouth. The utilization of such small cast-in-place piles for the foundations of new

1. Supervising Eng., Bechtel Corp., Power Div., Los Angeles, Calif.

residences would not be excessively costly and would minimize settlement damage induced by soil shrinkage during periods of drouth.

The author would like to reiterate his belief that far too little attention is given to elementary practical soil mechanics in small building foundation construction, resulting in unnecessarily heavy maintenance costs to the owners.

Discussion of
"MULTIPLE SPAN GABLED FRAMES"

by John D. Griffiths
(Proc. Paper 586)

JOHN D. GRIFFITHS,¹ M. ASCE.—The alternate procedures recommended by Professor Diwan will be found helpful to many who must analyze multiple span frames on the basis of elastic theory. Basically, Professor Diwan suggests the use of fewer frame subdivisions. By the use of fewer subdivisions, the final Analysis by Parts is simplified due to the reduction in the number of joints to be relaxed. On the other hand, the subdivisions become more complex as their numbers are reduced. Each designer must decide for himself the degree of subdivision which will require the minimum total effort for any given structure.

It should be realized that basic data including stiffness and carry over factors for any subdivision may be obtained by Virtual Work, Strain Energy, Column Analogy or other similar procedures as well as by the "Concept of Equivalent Elastic Systems."

Advice has been received that the procedure outlined in the original paper has been used in the design of a number of structures such as the multiple span frames for the Kentucky State Fair Buildings at Louisville (Photograph on following page). The structural design for these Kentucky State buildings was done by Mr. Edwin R. Leonard (Member, ASCE) formerly associated with Fred Elwick & Associates of Louisville.

It is of course a source of satisfaction to the author to know that the procedure has been put to use in actual building construction. However, it should be again emphasized that the most worthwhile simplifications of design procedure will be based on plastic analysis rather than the above described elastic analysis.

1. Chf. Engr., Gate City Steel, Inc., Boise, Idaho.



1. The Tower, State City Hall, San Francisco, Calif.

Discussion of "BENDING INTERACTION IN SUSPENSION BRIDGES"

by Haaren A. Miklofsky
(Proc. Paper 652)

HAAREN A. MIKLOFSKY,¹ A.M. ASCE.—The writer thanks Messrs. Raab, Shearwood, Vincent, Robins and Sih for contributing their time and thoughts to the discussion of his paper.

Mr. Raab suggests that the relationship between shear and deflection be considered in proportioning web members of the stiffening truss. In long span bridges the truss is very flexible, and deflection of the cable is controlled primarily by the chord members of the truss. The writer has investigated the relative contribution of web members to the deflection of the Mount Hope truss, and finds that the web members contribute about 3 per cent of the deflection for the loading condition indicated in his paper. It does not seem necessary, therefore, to develop an interaction diagram for shear. The writer would proportion the web members to carry the entire maximum shear, unless minimum section governed the design.

Mr. Raab's suggestion, however, does raise the question of what to do about the web area of a stiffening girder when designing the chord sections for flexure. The writer offers the following answer.²

Stiffening girders are so deep that the required web area will probably be governed by buckling rather than shear. This means a limiting thickness to depth ratio of the web as governed by specifications. Let N be the specified ratio of web thickness, t_w , to depth, d . Also let K_i be the ratio of the moment of inertia of the flange to the moment of inertia of the web. Then:

$$N = \frac{t_w}{d} \quad \text{and} \quad K_i = \frac{I_{ff}}{I_{wb}} = \frac{A_f d^2 / 4}{t_w d^3 / 12} = \frac{3 A_f}{t_w d}$$

where A_f is the total flange area. Combining K_i and N :

$$K_i = \frac{3 A_f}{N d^2}$$

Since N is constant, K_i gives the ratio of flange area to depth, and an interaction diagram can now be drawn for a family of K_i curves instead of area curves. The total moment of inertia, I , of the cross section is:

$$I_t = \frac{A_f d^2}{4} + \frac{t_w d^3}{12} = \frac{K_i N d^4}{12} + \frac{N d^4}{12} = \frac{N d^4}{12} (K_i + 1)$$

1. Assoc. Prof. of Civ. Eng., Rensselaer Polytechnic Inst., Troy Bldg., Troy, N. Y.
2. The author thanks Mr. Omar Sotillo for contributing this idea from his doctorate thesis at R. P. I. on another subject.

When this expression is substituted for I_t in equations (13), (14), and (16) of the paper, a new set of curves (b), (c), and (d) of Fig. 5 result. The construction of the interaction diagram follows the same procedure as given in the paper, except that the interaction curves must be plotted from the new equations (13) and (16) instead of by proportion to Fig. 4. Once the limiting stress and deflection curves (h) and (k) of Fig. 7 are plotted, a suitable depth and K_1 value can be chosen, from which the area is found by the third equation above. Finally check the web section for shear, and revise N if necessary.

Mr. Shearwood suggests the use of a braced suspension bridge with diagonal ties of nearly equal inclination at each panel point and a stiff lower chord to replace the stiffening truss. The writer agrees that the diagonals may in some manner control the vibrations of the bridge due to wind. A similar system including the vertical hangers was used for such a purpose on the Deer Isle Bridge, Maine, 1943.³ However, since the diagonals are purely tension members of equal inclination, their effect on the cable is the same as a hanger for static loads, and the design of the stiffening truss or girder for limiting cable deflection due to static loads is still the same as described in the paper.

Mr. Vincent reemphasizes one of the important points the author hoped to convey in this paper; that "a clear picture is quickly gained of the effects of a wide range of stiffening truss area and depth, reducing substantially the number of more rigorous analysis to be made."

It is true that the same loss of precision in using parameters which are a compromise of a range of bridge design characteristics occur in this paper as in the Hardesty and Wessman paper. Modern design of suspension bridges, however, recognizes two types of design—preliminary design and final analysis. In the design of the Delaware Memorial Bridge the Hardesty and Wessman method was used for preliminary design while the final analysis was made in accordance with the Deflection Theory.⁴

Mr. Robins and Mr. Sih find lines joining points of equal moment of inertia useful aids to the interaction diagram, but each uses these lines for a different purpose. Mr. Robins uses these lines to find the least chord area that satisfies the limiting stress and deflection, while Mr. Sih uses these lines to plot the interaction curves. Both uses are ingenious and acceptable.

Mr. Sih further suggests the use of exact equations of deflection theory instead of the approximate methods in making the computations. The writer does not believe that this should be done. First of all the deflection theory equations contain a truss moment of inertia term in the evaluation of cable thrust; hence a moment of inertia must be assumed for plotting each point on the interaction diagram. Furthermore, even if graphs could simplify the computations, the writer believes that merely plotting curves (c) and (d) from the deflection theory formulas would not readily show the interaction relationship between the cable and truss.

The author is pleased to note that Mr. Robins visualizes the development of interaction diagrams for other complex structures besides long span bridges. The writer is in support of this type of research, and will appreciate personal suggestions for other important problems.

3. Steinman, D. B. "Suspension Bridges," *The American Scientist*, Vol. 42, July 1954, p. 407.

4. Howard, Needles, Tammen and Bergendoff, "The Delaware Memorial Bridge," Final Engineering Report, 1953, pages 98-99.

Discussion of
**"INFLUENCE LINES FOR MOMENT AND SHEAR
 IN A CONTINUOUS BEAM"**

by Anthony Hoadley
 (Proc. Paper 734)

Corrections to discussion by BENJAMIN C. F. WEI,¹ J. M. ASCE, in Proc. Paper 849.—On line 14, "enertia" should read "inertia."

In the first footnote on page 849-11, "D. B. Steinmen" should read "D. B. Steinman."

In Eq. 2, δ_{ap} should be δ_{bp}

At midpage on page 849-12,

$$\begin{aligned} \delta_{ap} = \delta_{pa} & \text{ should read } \delta_{ap} = \Delta_{pa} \\ \text{and } \delta_{bp} = \delta_{pb} & \text{ should read } \delta_{bp} = \Delta_{pb} \end{aligned}$$

Eq. 6 should read

$$x_b = \left(\frac{\delta_{ab}}{\delta_{aa} \delta_{bb} - \delta_{ab}^2} \right) \Delta P_a + \left(\frac{-\delta_{aa}}{\delta_{aa} \delta_{bb} - \delta_{ab}^2} \right) \Delta P_b$$

The last word in the footnote on page 849-12 should be the name "Kinne."

1. Structural Designer, D. B. Steinman, Cons. Engr., New York., N. Y.

Discussion of "SEQUENCE SUMMATION FACTORS"

by Adrian Pauw
(Proc. Paper 763)

ELIO GIANGRECO.¹—With reference to the paper by Mr. Pauw on Sequence Summation Factors, a few considerations on the topic may be added by the writer, who has been dealing with the subject since 1949.

As a matter of fact a close point to the subject was reached by the writer in the paper "Su di una generalizzazione del metodo Cross," which appeared on "Atti dell'Istituto di Scienza delle Costruzioni dell'Università di Napoli."

According to the paper, by moment distribution process in a framed structure the moment at the end of a member can be found by use of a sequence expression, whatever the structure and the load distribution, and with any degree of approximation.

Taking into consideration a joint in a frame, whatever the load and the end condition, (see Fig. 1), if a distributing moment is applied at the joint $-i$, in order to set the joint again in equilibrium a moment i must be applied to the joint, and this moment will be distributed among the members of the joint according to their stiffness distribution factor. In the beam il for instance the moment will be $-iK_{il}$, if K_{il} is the distribution factor. Part of the moment distributed will then be carried-over to the opposite end of the beam, and its value will be $-iK_{il}Z_{il}$, where Z_{il} is the carry-over factor. The procedure may be applied to any member of the joint i , thus generating a set of distributed moments:

$$-cK_{ci} \quad , \quad -hK_{hi} \quad , \quad -qK_{qi}$$

at the ends c , h and q and a set of carried-over moments at the opposite end i , each of the latter being affected by a carry-over factor:

$$-cK_{ci}Z_{ci} \quad , \quad -hK_{hi}Z_{hi} \quad , \quad -qK_{qi}Z_{qi}$$

The carried-over moments will again unbalance the joint and a new distribution takes place; there will be a new set of distributed moments $-iK_{il}$ and a correspondent set of carried over moments at the opposite end.

The procedure may be brought at any wanted degree of approximation. The final moments will be given by summation of accumulated moments at any end of a beam.

Referring to the member il only, that is to say to distribution between i and l , the value i' , i'' , $i''' \dots$, $i^{(n)}$, $i^{(n+1)}$, $i^{(n+2)}$, $i^{(n+3)}$, at successive operations would be:

1. Professor, Istituto di Scienza delle Costruzioni, Università Degli Studi di Bari, Italy.

$$i' = -\ell K_{\ell i}$$

$$\ell' = -i K_{i\ell} Z_{i\ell}$$

$$i'' = -\ell' K_{\ell i} Z_{\ell i} = i K_{i\ell} K_{\ell i} Z_{i\ell} Z_{\ell i} \quad \ell'' = \ell K_{i\ell} K_{\ell i} Z_{i\ell} Z_{\ell i}$$

$$i''' = -\ell'' K_{\ell i} Z_{\ell i} = -\ell K_{i\ell} K_{\ell i}^2 Z_{i\ell} Z_{\ell i}^2 \quad \ell''' = -i K_{i\ell}^2 K_{\ell i} Z_{i\ell}^2 Z_{\ell i}$$

$$i^{(n)} = -\ell^{(n-1)} K_{\ell i} Z_{\ell i} = i K_{i\ell}^2 K_{\ell i}^2 Z_{i\ell}^2 Z_{\ell i}^2 \quad \ell^{(n)} = \ell K_{i\ell}^2 K_{\ell i}^2 Z_{i\ell}^2 Z_{\ell i}^2$$

and the final moment at joint i is given by:

$$M_{i\ell} = \mu_{i\ell} - K_{i\ell} (i + i' + i'' + \dots + i^{(n-1)}) - K_{\ell i} Z_{\ell i} (\ell + \ell' + \ell'' + \dots + \ell^{(n-1)}) =$$

$$= \mu_{i\ell} - \left\{ K_{i\ell} (i - \ell K_{\ell i} Z_{\ell i}) + K_{\ell i} Z_{\ell i} (\ell - i K_{i\ell} Z_{i\ell}) \right\} \frac{1}{1 - K_{i\ell} K_{\ell i} Z_{i\ell} Z_{\ell i}}$$

where $\mu_{i\ell}$ denotes the fixed-end moment of beam $i\ell$ at joint i and

$\frac{1}{1 - K_{i\ell} K_{\ell i} Z_{i\ell} Z_{\ell i}}$ is the summation of the sequence:

$$1 + K_{i\ell} K_{\ell i} Z_{i\ell} Z_{\ell i} + K_{i\ell}^2 K_{\ell i}^2 Z_{i\ell}^2 Z_{\ell i}^2 +$$

Should the beam be of constant inertia, the carry-over factor would be equal to $1/2$ and the expression (1) of the moments becomes:

$$M_{i\ell} = \mu_{i\ell} - \left\{ K_{i\ell} \left(i - \frac{\ell K_{\ell i}}{2} \right) + \frac{K_{\ell i}}{2} \left(\ell - i \frac{K_{i\ell}}{2} \right) \right\} \frac{1}{1 - \frac{K_{i\ell} K_{\ell i}}{4}}$$

For the sake of simplicity we shall deal with constant section beams. In the most general case of beams with variable inertia, numerical factor disappears, and distribution factors must be multiplied by carry-over factors.

2) The procedure goes on as follows:

1st step:

The unbalanced moments at the ends of beams in each joint a, b, c, \dots are:

$$a, b, c$$

The moments at each end of member are:

$$M_{i\ell} = \mu_{i\ell} - i K_{i\ell} - \frac{\ell K_{\ell i}}{2}$$

$$M_{\ell i} = \mu_{\ell i} - \ell K_{\ell i} - i \frac{K_{i\ell}}{2}$$

2nd step:

The unbalanced moments at each joint a, b, c are:

$$h' = -\frac{1}{2}(bK_{bh} + gK_{gh} + iK_{ih} + pK_{ph})$$

$$i' = -\frac{1}{2}(cK_{ci} + hK_{hi} + lK_{li} + qK_{qi})$$

$$l' = -\frac{1}{2}(dK_{dl} + iK_{il} + mK_{ml} + rK_{rl})$$

$$m' = -\frac{1}{2}(eK_{em} + lK_{lm} + nK_{nm} + sK_{sm})$$

We may state at this point that each joint is affected by one half of the moment of the next joint, which lays at the opposite end of each beam.

The numerical coefficient 1/2 is the carry-over factor. Thus it is found that the moment at the end of the beam equals the moment of the first step, plus a certain quantity of the second step.

3rd step:

The unbalanced moments are found as in the previous step, and they are:

$$i'' = -\frac{1}{2}(cK_{ci} + h'K_{hi} + l'K_{li} + q'K_{qi})$$

$$l'' = -\frac{1}{2}(d'K_{dl} + i'K_{il} + m'K_{ml} + r'K_{rl})$$

or

$$i'' = \frac{1}{4} \{ i(K_{ic}K_{ci} + K_{ih}K_{hi} + K_{il}K_{li} + K_{iq}K_{qi}) + b(K_{bc}K_{ci} + K_{bh}K_{hi}) \\ + c(K_{cc}K_{ci} + d(K_{dc}K_{ci} + K_{de}K_{ei}) + gK_{gh}K_{hi} + p(K_{ph}K_{hi} + K_{pq}K_{qi}) \\ + mK_{ml}K_{li} + r(K_{rl}K_{li} + K_{rq}K_{qi}) + wK_{wq}K_{qi}) \}$$

$$l'' = \frac{1}{4} \{ l(K_{ld}K_{dl} + K_{li}K_{il} + K_{lm}K_{ml} + K_{lr}K_{rl}) + d(K_{dd}K_{dl} + hK_{hi}K_{il}) \\ + xK_{xr}K_{rl} + nK_{nm}K_{ml} + c(K_{cd}K_{dl} + K_{ci}K_{il}) + q(K_{qi}K_{il} + K_{qr}K_{rl}) \\ + s(K_{sm}K_{ml} + K_{sr}K_{rl}) + e(K_{ed}K_{dl} + K_{em}K_{ml}) \}$$

Let us take into consideration the expression of i ; i is generated by the second distribution in the joint i , when the joint is reached by unbalanced moments of the joint laying on the last but one members, as c, q, w, m, b, p, r, d , whatever the way to reach the joint i : unbalanced moments from g for

instance, may reach *i* only through *gh* and *hi*,² whilst the unbalanced moments of *b* may reach *i* both by *bc*; *ci* and *bh*, *hi*. The same joint then distributes the unbalanced moments to the same adjacent joints. The previous considerations on moment distribution may be applied for instance to joint *b*. The unbalanced moment from *b* to *i*, through *bc* and *ci* is:

$$b \frac{K_{bc} K_{ci}}{4} = b \frac{K_{bci}}{4}$$

the one from *b* to *i* through *bh* and *hi* is:

$$b \frac{K_{bh} K_{hi}}{4} = b \frac{K_{bhi}}{4}$$

Then for the unbalanced moments leaving and returning to the same joint we find the following four expressions:

$$\frac{i K_{ihi}}{4}, \quad \frac{i K_{ici}}{4}, \quad \frac{i K_{ili}}{4}, \quad \frac{i K_{iqi}}{4}$$

which relate to members *ih*, *ic*, *il*, *ig*.

We may also point out another important fact: that is to say that any joint laying at an odd number of members from *i* does not send any moment in this step; for instance *c*, *h*, *l* and *g* do not appear in the expression of *i*; the same applies to *b* and *d*, which lay at the next but two members: their unbalanced moments will only appear in the expressions of joints laying at the next but one members.

As a conclusion of our previous considerations we may state that by this particular way of applying the moment distribution method by Cross we can take advantage of two fundamental facts, which may not be focussed by the usual way:

a) Possibility of immediate determination of the moment in a joint at the end of a beam independently from the other joints.

b) Possibility of predicting the influence of unbalanced moments of other joints on the joint under consideration. In fact, by increasing the distribution steps, the symmetrical factor of distributions decreases as the terms which compose the factor itself are increasing and all of them do not reach as value unity.

3) Taking into consideration the frame of Fig. 2, which is similar to the one shown in Mr. Pauw's paper Fig. 2, we may compute final moments by means of the formulae which have lately been developed.

2. The unbalanced moment *g* could as well reach the joint *i* through members *gh*, *ab*, *bh*, *hi*, thus crossing four beams instead of two, the terms $g K_{ga} K_{ab} K_{bh} K_{hi}$ would then be found again together with the others in the expression of unbalanced moment in the joint *i* at the 4th step of the procedure.

3. It would be useful, in order to simplify formulae, to denote by K_{bci} the factors product $K_{bc} K_{ci}$, which may be introduced as the "synthetical distribution factor."

Let us indicate by a, b, c , the unbalanced moments in joints a, b, c ; carry-over factors are equal to $1/2$.

Then: $b = -86^k \text{ ft}$; $c = 150^k \text{ ft}$

Final moments at the ends of beam BC will be:

$$M_{bc} = \mu_{bc} - K_{bc}(b + b' + b'' + \dots) - \frac{K_{cb}}{2}(c + c' + c'' + \dots)$$

$$M_{cb} = \mu_{cb} - K_{cb}(c + c' + c'' + \dots) - \frac{K_{bc}}{2}(b + b' + b'' + \dots)$$

where:

$$b' = -c \frac{K_{bc}}{2}; \quad b'' = -c \frac{K_{cb}}{2} = b \frac{K_{bc} K_{cb}}{4}; \quad b''' = -c'' \frac{K_{cb}}{2} = -c \frac{K_{bc} K_{cb}^2}{8}$$

$$c' = -b \frac{K_{bc}}{2}; \quad c'' = -b \frac{K_{bc}}{2} = c \frac{K_{bc} K_{cb}}{4}; \quad c''' = -b'' \frac{K_{bc}}{2} = -b \frac{K_{bc}^2 K_{cb}}{8}$$

thus

$$\Sigma b = b + b' + b'' + \dots = b \left(1 + \frac{K_{bc} K_{cb}}{4} + \dots \right) - c \frac{K_{cb}}{2} \left(1 + \frac{K_{bc} K_{cb}}{4} + \dots \right)$$

$$\Sigma c = c + c' + c'' + \dots = c \left(1 + \frac{K_{cb} K_{bc}}{4} + \dots \right) - b \frac{K_{bc}}{2} \left(1 + \frac{K_{cb} K_{bc}}{4} + \dots \right)$$

The summation of $1 + x + x^2 + x^3 + \dots$ is $\frac{1}{1-x}$ when $x < 1$, thus:

$$\Sigma b = \left(b - c \frac{K_{cb}}{2} \right) \frac{1}{1 - \frac{K_{bc} K_{cb}}{4}} = -141,624^k \text{ ft}$$

$$\Sigma c = \left(c - b \frac{K_{bc}}{2} \right) \frac{1}{1 - \frac{K_{bc} K_{cb}}{4}} = +185,409^k \text{ ft}$$

The values are equal to $\Sigma K\theta$ values of Fig. 2c in Mr. Pauw's paper. Final moments M_{bc} and M_{cb} are then:

$$M_{bc} = \mu_{bc} - K_{bc} \Sigma b - \frac{K_{cb}}{2} \Sigma c = -150 + 70,812 - 55,623 = -134,811^k \text{ ft}$$

$$M_{cb} = \mu_{cb} - K_{cb} \Sigma c - \frac{K_{bc}}{2} \Sigma b = +150 - 111,245 + 35,406 = +74,161^k \text{ ft}$$

For the other members we have:

$$M_{ba} = \mu_{ba} - K_{ba} \Sigma b = +64 + 35,406 = +99,406^k \text{ ft}$$

$$M_{bc} = -K_{bc} \Sigma b = +35,406^k \text{ ft}$$

$$M_{cd} = -K_{cd} \sum c = -37,082 \text{ K ft}$$

$$M_{cf} = -K_{cf} \sum c = -37,082 \text{ K ft}$$

All values are equal to the ones found by Mr. Pauw's procedure, each number of summation being equal to the equivalent number of Mr. Pauw's paper (Fig. 2).

4) Let us consider now the frame of Fig. 3, which may be solved by Mr. Pauw's suggested method; carry-over factors are still $1/2$.

Unbalanced moments equal fixed end moments of member ab and their values are:

$$a = -b = -8340 \text{ Kgm.}$$

Relaxation of the unbalanced moment at a induce a moment at b equal to:

$$-a \frac{K_{ab}}{2} = +978,2820 \text{ Kgm.}$$

With the moment at g in balance, the total unbalanced moment at joint b is then 9318.2820.

The sequence summation factor for joint b is computed from:

$$\alpha_{ba} = \frac{0,2665 \times 0,2346}{4} = 0,0156$$

$$\beta_b^a = \frac{0,0156}{0,9844} = 0,0158$$

The moment to be relaxed at joint b must therefore be increased by:

$$9318,2820 \beta_b^a = 147,2288$$

and hence

$$\sum K_b \theta_b = 9318,2820 + 147,2288 = 9465,5108$$

The total moment relaxed at joint a is the sum of the initial unbalanced moment plus the moment induced by the relaxation of $\sum K_b \theta_b$. Thus:

$$\sum K_a \theta_a = -8340 - \frac{0,2665 \times 9465,5108}{2} = -9601,2793$$

These computations and the final cycle of moment distribution required to compute the support moments are shown in tabular form in Fig. 3c.

By our suggested method it would have been found by a faster procedure:

$$M_{ab} = a \left\{ 1 - \left(K_{ab} - \frac{K_{ba}}{2} + \frac{K_{ab} K_{ba}}{4} \right) \frac{1}{1 - \frac{K_{ab} K_{ba}}{4}} \right\} = -7348,8994 \text{ Kgm.}$$

$$M_{ba} = b \left\{ 1 - \left(K_{ba} - \frac{K_{ab}}{2} + \frac{K_{ba}K_{ab}}{4} \right) \frac{1}{1 - \frac{K_{ab}K_{ba}}{4}} \right\} = +6943,4837 \text{ Kgm.}$$

and for other members:

$$M_{ac} = -K_{ac} \left\{ \begin{array}{l} -K_{ac} \\ (a + a' + a'' + \dots) = -K_{ae} \end{array} \right\} = +3217,9783 \text{ Kgm.}$$

$$M_{ae} = -K_{ae} \left\{ \begin{array}{l} (a + a' + a'' + \dots) = -K_{ae} \\ (a - \frac{bK_{ba}}{2}) \frac{1}{1 - \frac{K_{ab}K_{ba}}{4}} \end{array} \right\} = +2252,2008 \text{ Kgm.}$$

$$M_{af} = -K_{af} \left\{ \begin{array}{l} -K_{af} \\ -K_{af} \end{array} \right\} = +1877,7940 \text{ Kgm.}$$

$$M_{bd} = -K_{bd} \left\{ \begin{array}{l} -K_{bd} \\ -K_{bd} \end{array} \right\} = -3152,9523 \text{ Kgm.}$$

$$M_{bg} = -K_{bg} \left\{ \begin{array}{l} (b + b' + b'' + \dots) = -K_{bg} \\ (b - \frac{aK_{ab}}{2}) \frac{1}{1 - \frac{K_{ab}K_{ba}}{4}} \end{array} \right\} = -2103,2303 \text{ Kgm.}$$

$$M_{bh} = -K_{bh} \left\{ \begin{array}{l} -K_{bh} \\ -K_{bh} \end{array} \right\} = -1686,7491 \text{ Kgm.}$$

5) The frame of Fig. 4 may be reduced owing to symmetry to the equivalent frame of Fig. 5. Suppose we want to find out the moment M_{ab} by means of joint next to a, that is b and c, without taking into account contribution by other joints as we find:

$$M_{ab} = \mu_{ab} - \frac{K_{ab}}{2} \left\{ \frac{a - bK_{ba}}{1 - \frac{K_{ab}K_{ba}}{2}} + \frac{a - cK_{ca}}{1 - \frac{K_{ac}K_{ca}}{2}} \right\}$$

$$- \frac{K_{ba}}{4} \left\{ \frac{b - aK_{ab}}{1 - \frac{K_{ab}K_{ba}}{2}} + \frac{b - dK_{db}}{1 - \frac{K_{bd}K_{db}}{2}} \right\} = +34400 - 10933,33 + 1342,95 = +24719,62 \text{ Kgm.}$$

The approximation, compared to the exact is 98,58 %.

If joint d is also taken into consideration, then the expression of M_{ab} depends also from a sequence, the value of which is given by the expression:

$$\frac{1}{1 - \frac{K_{ac}K_{dc}K_{cd}K_{ca}}{16}} \qquad \frac{1}{1 - \frac{K_{ab}K_{bd}K_{db}K_{ba}}{16}}$$

The approximation is in this case 99,32% of the exact value of the moment.

	z	t	n	f	f̄
	y	s	m	e	ē
	x	r	l	d	d̄
	w	q	i	c	c̄
	v	p	h	b	b̄
	u	o	g	a	ā

Figure 1.

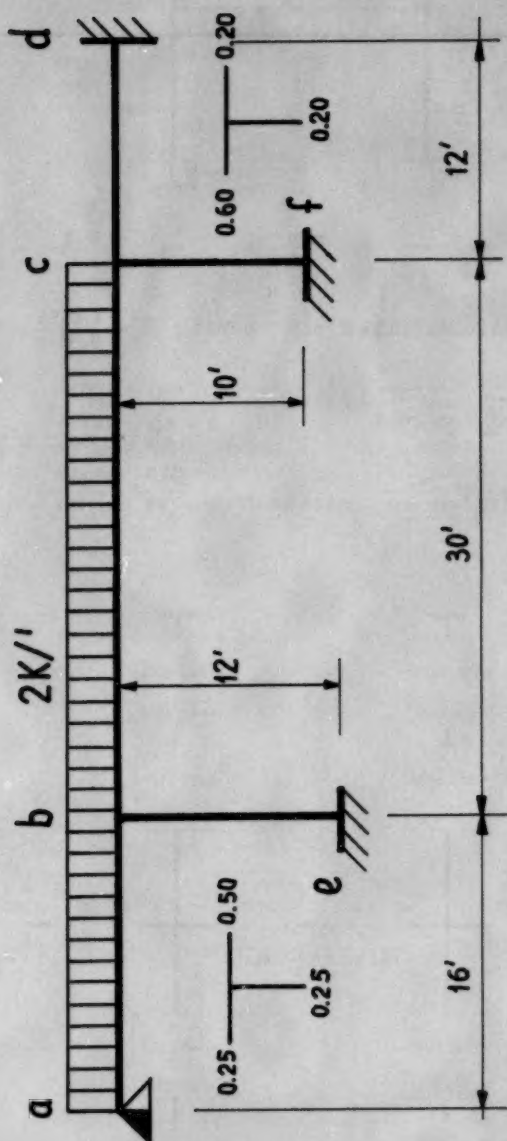
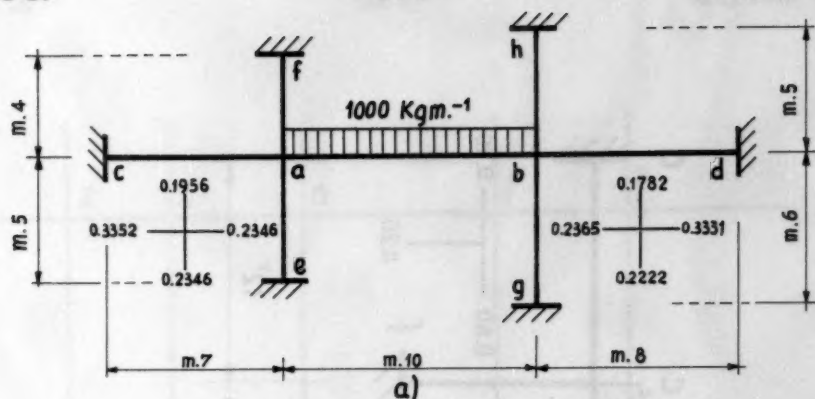


Figure 2.



$$\alpha_{ab} = 0.5 \times 0.2665 \times 0.5 \times 0.2346 = 0.0156 ; \beta_b^a = \frac{0.0156}{0.9844} = 0.0158$$

M_{ca}^U	-8340	$\times (-0.2346)(0.5)$	M_{ab}^U	+8340	
M_{ba}^U	-1261,2793		M_{ab}^U	+978,2820	
			ΣM^U	+938,2820	$\times (0.0158)$
			$\beta \Sigma M$	+147,2288	
$\Sigma K\theta$	-9601,2793	$\times (0.5)(-0.2665)$	$\Sigma K\theta$	+9465,5108	

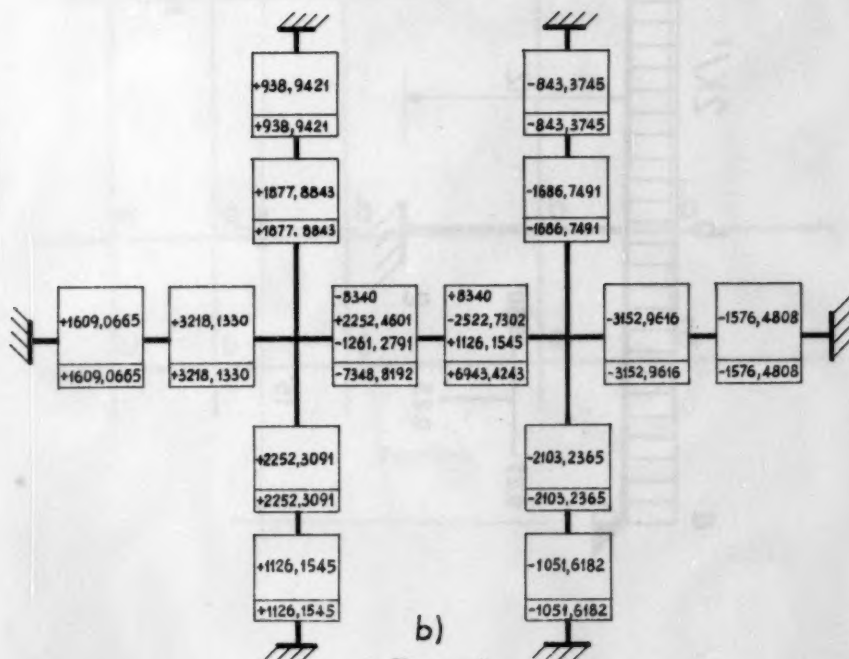
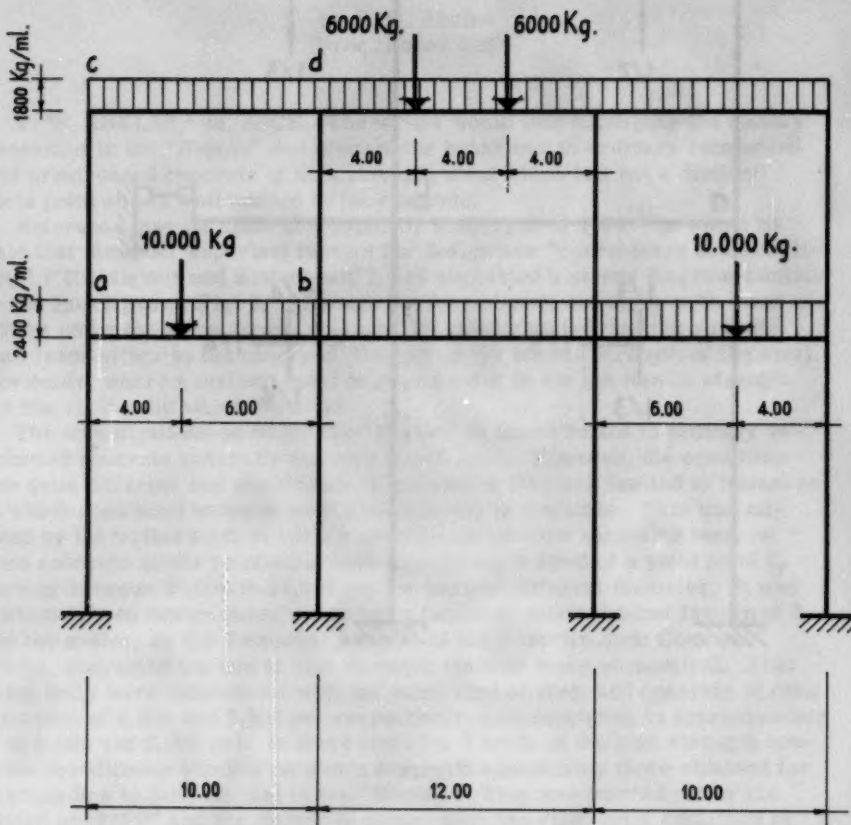


Figure 3.



$a = +34.400 \text{ Kg.m.}$; $b = -300 \text{ Kg.m.}$; $c = +15.000 \text{ Kg.m.}$; $d = +22.600 \text{ Kg.m.}$

Figure 4.

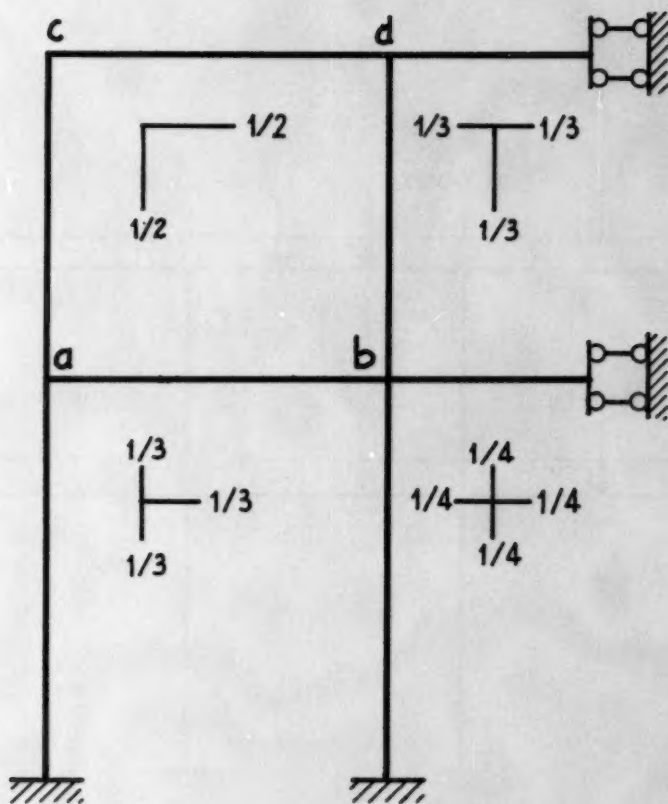


Figure 5.

Discussion of
"REPORT OF ASCE-ACI JOINT COMMITTEE
ON ULTIMATE STRENGTH DESIGN"

by P. W. Abeles
(Proc. Paper 809)

P. W. ABELES,¹ M. ASCE.—The writer would like to amplify the history presented in the "Report" and discuss the behaviour in ordinary reinforced and prestressed concrete of high strength steel which has not a distinct yield point and is well bonded to the concrete.

Reference may be made to a paper by Emperger of 1904⁽¹⁾ in which he said that the most important factors for design are "correctness and simplicity" ("Richtigkeit und Einfachheit"), and suggested a stress diagram similar to the 1st diagram, Fig. 2. Although his formulas do not agree with those of others using the same stress diagram, he clearly stated that the ultimate load leads either to the concrete strength or the tensile strength of the steel. Obviously, where a distinct yield point occurs it is not the tensile strength but the yield point which matters.

The investigations on which the "Report" is based relate to ordinary reinforced concrete generally on very broad lines. However, the conditions are quite different and much more favourable if they are limited to instances at which good bond between steel and concrete is available. This was noticed by the writer first in 1933/4 when he carried out extensive tests on spun concrete masts reinforced with high strength steel of a yield point f_y varying between 87,000 to 97,000 psi for bars of different diameter. It was permissible to design these masts for a factor of safety against failure of 3 and the writer, as the Technical Advisor of the Austrian Spun Concrete Works, suggested the use of high strength steel as more economical. Also beam tests were carried out with the same kind of steel and concrete of cube strengths of 8,000 and 2,500 psi respectively, corresponding to approximately f'_c of 6,000 and 2,000 psi. In these tests for 3 kinds of the high strength concrete the ultimate bending moments exceeded appreciably those obtained for f_y according to formula (2a) of the "Report". This was pointed out by the writer in 1935⁽²⁾ and the excess in stress over the yield point explained by the excellent bond between the high strength concrete and the steel. In consequence of this, the cracks remain relatively narrow up to failure and similar conditions are obtained as with fine notches in steel bars. If such a bar is loaded to failure, the calculated ultimate tensile stress at the notch will be in excess of the tensile strength in consequence of reduced necking at the notch, and this excess will be the greater, the narrower the notch is. Obviously the true stress at failure will be the same as the true ultimate stress in the remaining parts of the bar. This phenomenon was described by Timoshenko in 1926⁽³⁾ in a publication on comparative tests on notched ductile steel bars of 1 1/2 in. diameter, having a reduced diameter of 1/2 in.

1. Asst. Civ. Engr., British Rys., Eastern Region, London, England.

at the notches. The calculated ultimate stress (i. e. tensile strength) of 70,000 psi was increased by 61 % to 124,000 psi when the notch was 1/32 in. wide; by 24 % to 88,000 psi when the notch was 1/4 in. wide; but there was no increase when the notch was 1 in. wide.

Based on this early experience, the writer has noticed that for well bonded reinforcement Mr. Cox's formulas⁽⁴⁾ in which not $0.85 f'_c$ but the entire value f'_c is considered, give results. Moreover, he has amplified this by a suggestion to take into account the excess in stress of the steel by a stress distribution according to the writer's Fig. 1, in which by considering a nominal rectangular concrete tensile stress block the excess stress in the steel should be compensated. This stress distribution Fig. 1, suggested by the writer in 1942, is to a certain extent similar to that of Guerin (1941), shown in Fig. 2; however, it is not the actual concrete tensile bending strength (modulus of rupture) which is taken into account, as in the crack itself the concrete tensile resistance cannot co-operate. It is only a nominal concrete tensile stress which may be taken as a proportion of the compressive strength; i. e. $f_1 = f_{ct}/f'_c$. The equation (2a) reads according to Cox with a stress f'_c instead of $0.85 f'_c$ in slightly modified form as follows:

$$M_u = p.b.d^2.f_y (1 - 0.5q) \quad (2a')$$

and with $d_1 = t/d$ the following amplified formula is obtained:

$$M_u = b.d^2.f_y \frac{p(1 - 0.5q) + (f_1 \cdot p/2q) \cdot [d_1^2 - 2(d-1)q]}{1 + f_1} \quad (2a'')$$

for $d_1 = t/d = 1.1$ and $f_1 = f_{ct}/f'_c = 1/20$ equation (2a'') becomes

$$M_u = \frac{b.d^2.f_y}{1.05} [p(1 - 0.5q) + \frac{p}{40q} (1.2 - 0.2q)] \quad (2a''')$$

This formula (2a''') with a different notation has been shown in the writer's contribution to Mr. Cox's paper⁽⁴⁾ and again in 1944 in his discussion to Professor Evans' paper, mentioned in the Report, page 809-3. It has further been shown at the Congress Cambridge 1953.⁽⁵⁾ Nevertheless, this suggestion has been ignored in the summaries of stress distributions. It is, however, a means to take into account the excess strength, as will be seen in the following.

Before this is discussed in detail it will be shown that it is not the yield point but the ultimate strength which matters in cases where the steel has no distinct yield point and good bond is obtained. This was first clearly shown by Dr. Hajnal-Konyi⁽⁶⁾ in tests on concrete beams reinforced with work-hardened square twisted bars. In this paper it was discussed that it is also possible to break mild steel in special circumstances of extremely low percentages. On the other hand, with work hardened bars good bond conditions were obtained even with concrete of low strength (prism strength f'_c of 2,000 to 3,000 psi). With percentages of 0.214 an excess of stress over the strength up to 42 % was obtained and with $f'_c = 2000$ psi and higher percentages (0.353, 0.562, 0.750 and 0.938) an excess of 20-24.5 % was achieved. In some of the test specimens the steel fractured, but in other instances an excess of strength was obtained, without breaking of the steel. It is very important to bear in mind that in these conditions the ultimate strength f_u and not the yield point f_y should be considered. This applies also to pre-stressed concrete with well bonded wires.

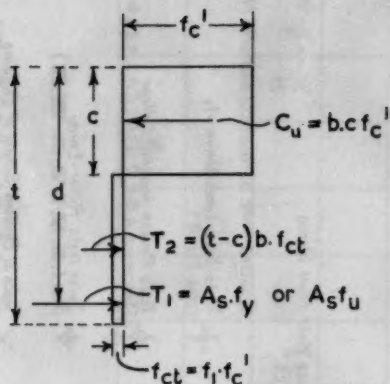


Figure 1.

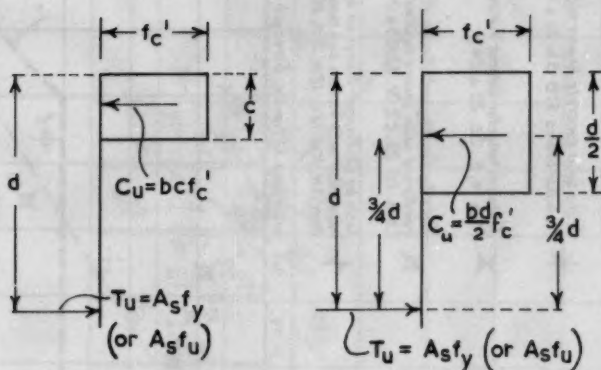


Figure 2.

In his paper⁽⁷⁾ the writer has investigated the ultimate resistance of a number of prestressed concrete and reinforced concrete beams, the latter having well bonded steel reinforcement. A simplified stress distribution according to Fig. 2 was taken into account with a rectangular stress block of f'_c with the limit depth $c = d/2$, which represents a further development of the Cox formula. This results in the formula (2b') corresponding to (2a'):

$$M_u = f'_c \cdot b \cdot d^2 \cdot q \cdot (1 - 0.5q) \quad (2b')$$

however, the limit reinforcement amounts to

$$p_u = 0.50 \frac{f'_c}{f_y} \quad \dots \text{ or } q = 0.50 \quad (3')$$

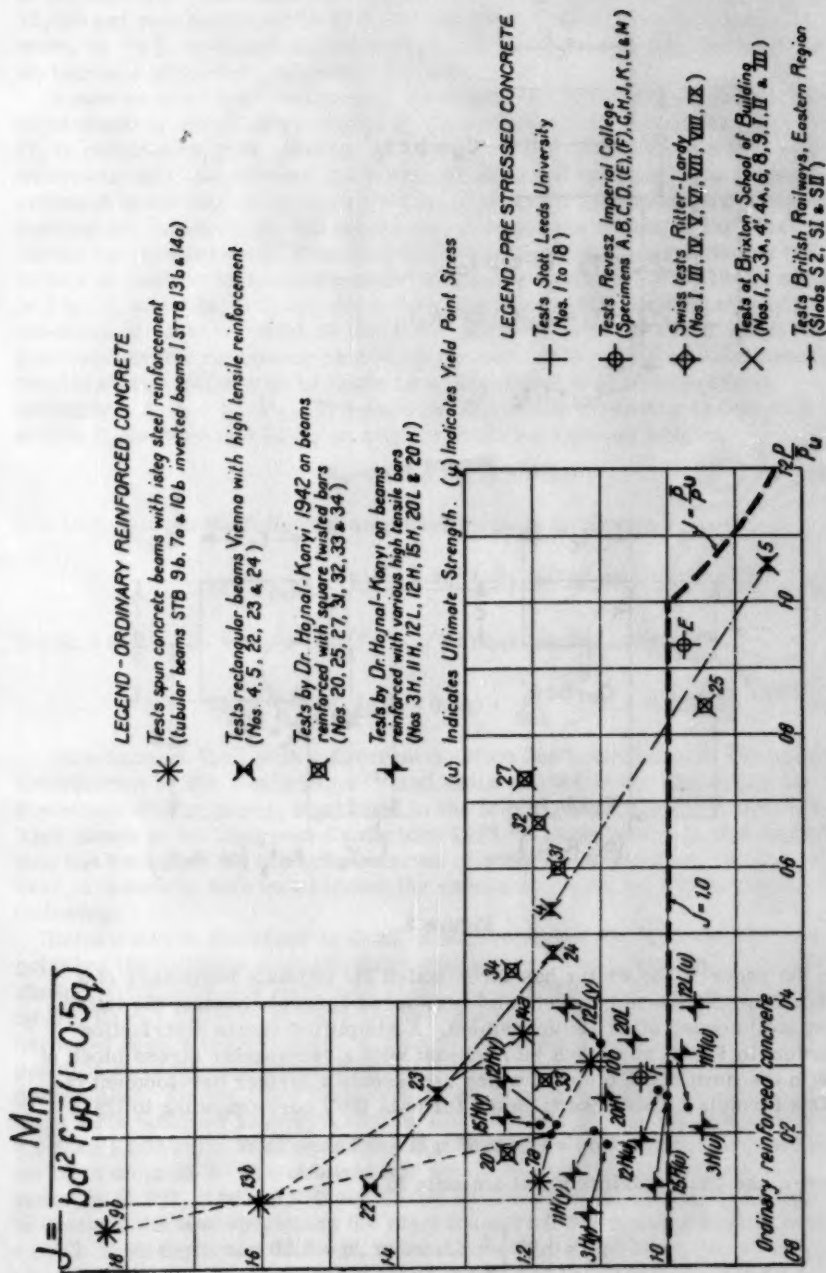


Figure 3 (part 1).

In this case the limit value $M_u/f'_c bd^2 = 0.375$ and not 0.306 as shown in Fig. 4 of the Report. In spite of this much higher value the investigations in paper (7) have shown that in almost all cases the actual failure moment was greater than the calculated moment. This is seen in Fig. 3 taken from Fig. 7 of paper (7) with adjustment of notation. Figure 3 shows the ratio between actual and calculated ultimate bending moment $J = M_m/M_u$ which is equivalent to the excess of steel stress over the yield point (or ultimate strength) in relation to the ratio of percentages p/p_u similar to the abscissa of Fig. 4 of the "Report". It may be mentioned that for the writer's tests on tubular spun concrete beams and on rectangular beams the yield point has been considered and for Dr. Hajnal-Konyi's tests on 1942 the ultimate strength has been taken into account. Only beam 25, which contained square twisted bars that were intentionally undertwisted, had a smaller bending moment than calculated as well as beam 5 of the writer's tests for which low strength concrete ($f'_c = 2000$ psi) was used with the consequence that the bond conditions were less satisfactory. The tests by Dr. Hajnal-Konyi of 1951⁽⁸⁾ related to beams reinforced with various high tensile bars of large diameter (1 in.) and consequently the bond was insufficient to consider the ultimate strength in all instances. In the graph both values are seen, those related to the yield point indicated by (y) and to ultimate strength indicated by (u). The former show in all cases excess of strength and the latter in most cases. With regard to prestressed concrete, there is an excess of strength in all cases, except for beams with non-bonded steel members. Reference may be made to an ordinary beam reinforced with high-tensile wire, indicated by (o.r.c.), which also shows slightly lower resistance.

From Fig. 3 it is thus clearly seen that in spite of the fact that in most cases the ultimate strength of the steel and the formulas (2a') and (2b') with the higher limit (3') have been taken into account, there is still an appreciable excess in strength of the actual failure values. It seems therefore justified to consider in such instances the excess of strength in accordance with the stress distribution according to Fig. 1, as suggested by the writer. In the paper (5) a supplement to (7), the writer reported on further tests carried out by British Railways on beams containing pre-tensioned wires 0.276 in. diameter. The results were investigated in accordance with the equation (2a'') for $f_1 = 1/20$ and $d_1 = t/d = 1.1$ and good agreement was reached with regard to the beam which failed solely in bending. It appears therefore appropriate to compare the carrying capacities obtained from stress diagrams (2) and (1) with that presented in the "Report". For that purpose 3 graphs A, B and C are shown in Fig. 4 of this contribution; graph A relates to M_{uL} corresponding to Fig. 4 of the original "Report".

The formula (2b') can be transformed to $M_u/f'_c bd^2 = \frac{0.50p}{p_u} \frac{(1 - 0.25p)}{p_u}$

with the limit of $M_u/f'_c bd^2 = 0.375$ according to the writer's suggestion and is shown in graph B distinguished by M_{uB} . It is possible to introduce formulas (2b') and (2b'') corresponding to (2a'') and (2a') which read as follows:

$$M_u = f'_c bd^2 \frac{q(1 - 0.5q) + f_1 [d_1^2 - 2(d-1)q]}{1 + f_1} \quad (2b'')$$

$$M_u = f'_c b d^2 \frac{40q (1 - 0.5q) + 1.21 - 0.2q}{42} \quad (2b'')$$

When introducing the same limit value, i. e. $p_u = \frac{0.50 f'_c}{f_y}$

the following equation is obtained

$$M_u / f'_c b d^2 = 1/42 \left[\frac{20p}{p_u} \left(1 - \frac{0.25p}{p_u} \right) + 1.21 - \frac{0.1p}{p_u} \right]$$

This relation, distinguished by M_{u3} , is plotted as graph C in Fig. 4 which also shows the excess of strength obtained by formula (2b'') (i. e. the ratio between bending moments obtained by formula (2b'') and that by formula (2b'), i. e. M_{u3} / M_{u2} .

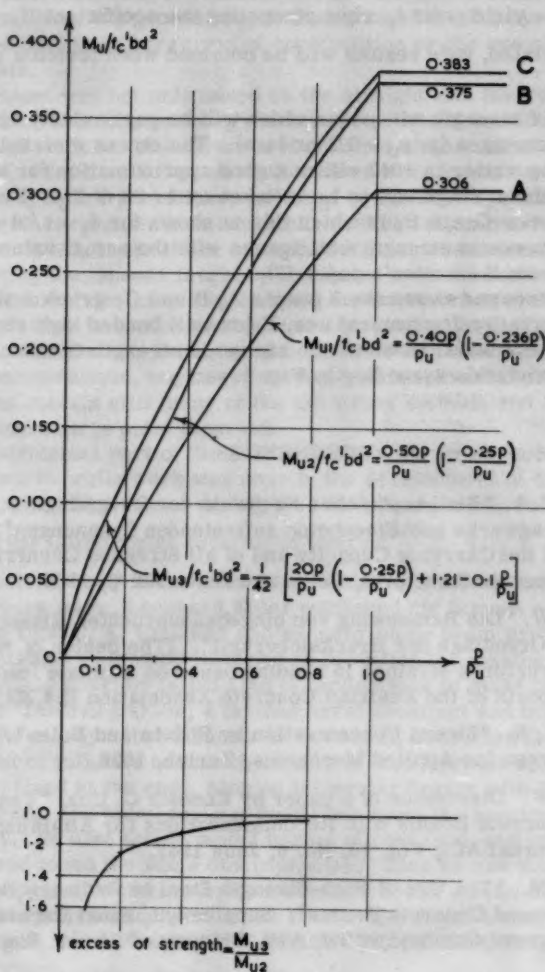


FIG. 4

Summing up, it can therefore be stated:

Fig. 4 of the "Report" shows that the design formulas suggested present satisfactory mean values for general conditions, the actual individual test results being to an extent above and below the graph except for ratios p/p_u less than 0.3, for which all test results are above the curve and thus indicate a greater ultimate resistance. From Fig. 3 of the present contribution it is seen that for well bonded high strength steel an excess in strength was obtained for such specimens for all percentages as compared with a calculated value based on Fig. 2 resulting in formula (2b'), i.e. the Cox formula with increased upper limit -

$$M_u / f'_c b d^2 = 0.375.$$

This formula is, therefore, a safe basis for the ultimate resistance of such special constructions. In such cases it is certainly permissible to take into account for steel members of limited size the ultimate steel strength f_u instead of the yield point f_y when computing the coefficient

$$q = \frac{f_y}{f'_c}. \text{ As stated, safe results will be obtained when formula (2b') is used,}$$

and an excess of strength will occur which will be particularly appreciable with small percentages ($p/p_u = 0.3$ or less). The stress distribution Fig. 1 suggested by the writer in 1942 offers a good approximation for this excess in strength, if the average stress f_{ct} is taken as $1/20$ of f'_c . From Fig. 4 of this contribution Graph C, in which this is shown for $d_1 = t/d = 1.1$, it is seen that the excess in strength well agrees with the actual values shown in Fig. 3, taken from the writer's paper (7).

Fig. 4 of this paper shows the 3 graphs A, B and C; graph A the "Report's" suggestion for general use, B for well bonded high strength steel giving safe results and C in which the excess in strength is taken into account by approximation according to Fig. 1.

REFERENCES

1. Emperger F. v. "Ein graphischer Nachweis der Tragfähigkeit und aller in einem Tragwerke aus Eisenbeton auftretenden Spannungen". (A graphical Proof of the Carrying Capacity and of all Stresses Occurring in a Reinforced Concrete Structure), Beton und Eisen No. 5, 1904.
2. Abeles, P. W. "Die Bemessung von biegebeanspruchten Eisenbetontragwerken auf Grundlage der Brucksicherheit". (The design of reinforced concrete structures strained in bending based on ultimate load conditions). Monthly Reports of the Austrian Concrete Association II.4 30th April 1935.
3. Timoshenko, S. "Stress Concentration by Fillets and Holes". International Congress for Applied Mechanics, Zurich, 1926.
4. Abeles, P. W. Discussion of a paper by Kenneth C. Cox, "Tests of Reinforced Concrete Beams with Recommendations for Attaining Balanced Design", Journal ACI, Vol. 13, No. 6, June 1942.
5. Abeles, P. W. "The Use of High-Strength Steel in Ordinary Reinforced and Prestressed Concrete Beams". Supplement, Final Report 1953, Fourth Congress Cambridge, Int. Ass. Bridge and Struct. Eng.

6. Hajnal-Konyi, K. "Tests on Square Twisted Steel Bars and Their Application as Reinforcement of Concrete". The Structural Eng., London, Sept. 1943.
7. Abeles, P. W., "The Use of High Strength Steel in Ordinary Reinforced and Prestressed Concrete Beams". Preliminary Publication, 1952, Fourth Congress Cambridge, Intern. Assoc. Bridge and Struct. Eng.
8. Hajnal-Konyi, K. "Comparative Tests on Various Types of Bars as Reinforcement of Concrete Beams". The Structural Engineer, May 1951.

L. J. MENSCH,¹ M. ASCE.—Soon after the Joint Committee report was published in 1940, the writer severely criticized it (Proceedings ASCE September, 1940) as lagging seriously behind the practice of the masters of the art and as a deterrent of economic development. In relation to the design of the various members of construction and the use of concrete and steel of various qualities, the general regulations proved inadequate and arbitrary and did not tend to better forms of construction or the use of better qualities of materials.

That report was not only based on the straight line theory but also on a great number of wrong notions, which were preached in all high schools of technical learning in the entire world as Bible truths and adopted by scholars as articles of faith with the result that there were raised up two generations of engineers, full of prejudices, and blind to the discrepancies of their theories with careful tests to destruction. When after the war costs of construction doubled, some of the more thinking engineers finally recognized that following the lessons taught by the tests, it would enable them to produce more economical designs; they induced the engineering societies to appoint a new committee to recommend proper changes in the prevailing codes. But, as the members of this committee had no actual experience with the new recommendations, engineers need not be surprised that the new recommendations contain still many of the old wrong notions, and it is the business of this discussion to point them out.

In the historical part of the report there is the wrong notion that for 180 years no worth-while work was done in the development of the theory of Elasticity. The fact is that during the lifetime of Hooke, Jacob Bernoulli developed the fundamental equation of flexure, $\frac{d^3 y}{dx^3} = \frac{M}{EI}$ and Christiaan Huygens solved many beam problems which are still reprinted in textbooks.

Fifty years later, Leonhard Euler published his famous column formula, and before 1800 C. A. Coulomb solved many more beam problems. The afore-mentioned mathematicians had no facilities for making tests at their disposition and possibly failed also of inclinations to make them. It remained for Thomas Barlow, a famous naval architect and investigator, to question the straight line theories of Bernoulli, Euber and Coulomb, by making test of full size beams of timber, of considerable spans, simply supported and fixed at the ends, also on triangular beams with the edge up and the edge down, and found serious deviations from the results of the straight line theory. He also tested model beams of cast iron, and other metals, also of glass, and found the same discrepancies. Then he had the brilliant idea to try to improve the theory by assuming parabolic stress blocks both in the tension and compression part of the section and found a very good agreement with his tests. (Ref. No. 99, THE STRENGTH OF TIMBER by Thomas

1. General Contractor, Evanston, Ill.

Barlow, Woolwich Arsenal, London, 1814)

Thus we see that the so-called plastic theory originated in England one hundred years before it was re-discovered in the U. S. A. It seems that continental authors entirely neglected Barlow's discovery, but English engineers of the old school, like James Watt of steam engine fame, and Sir William Fairbairn, both of whom were contractors for heavy warehouse buildings, consisting of cast iron columns, cast iron girders and beams and brick arches, were greatly influenced by Barlow's ideas, also Professor Hodgkinson and Professor Rankine.

The crude assumption of a rectangular stress block as shown in the first diagram in Fig. 2 was made by contractors who were no engineers like Hyatt, Ransome and Hennebique long before Professor Sueson and, besides, it was taught by Dr. F. V. Emperger in the Technische Hochschule in Vienna before 1900. (BETON KALENDER, 1906, page 56). The next two diagrams in Fig. 2 show the writer's assumptions which he used from 1910 to 1915. When more accurate tests, both European and American came to his knowledge, he changed them, as shown in Fig. 50.

Instead of a second degree parabola, he assumed a cubic parabola (Reference number 100, TRANSACTION ASCE Volume 83, 1919-20, page 1671, and reference number 101, ENGINEERING JOURNAL, April 1946, Montreal, Canada) also an extreme fiber stress in compression of $0.85 f'_c$ instead of f'_c (Reference number 102, ACI PROCEEDINGS, 1937, DISCUSSIONS, p. 4981) and the useful limit stress in the reinforcement f'_s instead of the yield point. This useful limit stress he assumed as the mean of the yield point and the ultimate strength or possibly the stress at a strain of 0.005 inch per inch.

The higher useful limit stress was adopted because it has often been observed in testing slabs, reinforced by wires, that the wires or high carbon bars broke at the ultimate load; besides, Professor F. E. Richart found it to be so in his tests. (Ill. Eng. Station Bulletins No. 314, page 47 and 60; No. 346, pages 56 and 57; No. 345, page 30). By inspection of Fig. 50 we can write

$$p b d f'_s = \frac{3}{4} k d x b x 0.85 f'_c \quad (100)$$

or

$$k d = 1.57 d p \frac{f'_s}{f'_c} \quad (101)$$

$$j d = d - 0.4 k d = d (1 - 0.6275 p \frac{f'_s}{f'_c}) \quad (102)$$

and the ultimate moment

$$M_u = A_s x j d x f'_s = b d^2 p f'_s (1 - 0.6275 p \frac{f'_s}{f'_c}) \quad (103)$$

The writer found that equation (103) agreed surprisingly closely with tests made by widely separated, experienced investigators.

No attention was paid to it for many years, but, when the literature on the plastic theory became fashionable, some authors got up similar equations of the type of equation (1) and to hide their plagiarism introduced unnecessary and confusing parameters k_1 , k_2 , k_3 in the hope that the undiscerning public will believe that their formulas being later must be more correct and being more complicated must be more scientific, when in fact they do not approach the truth as well as equation (103).

It must be confessed that equations (2a) and (103) are not as simple as the old Talbot formula

$$M_u = A_s \times \frac{7}{8} d \times f_r \quad (104)$$

which gave acceptable results at a time when low percentages of reinforcement were used, but for beams with higher percentages, the results varied considerably from tests.

To make the use of equation (103) as simple as Talbot's formula, the writer has given a table for $j d$ for various concrete strengths and various qualities of steel. (Reference numbers (101) and (102).) The report still retained the yield point in equation (1) which was a wrong notion of Koenen of 1886 and was also adopted by all later writers. To limit the yield point to 60,000 psi is another wrong notion of the committee. High yield point steel is used in prestressed concrete and its use in reinforced concrete can often compete with prestressed concrete. Sixty thousand pound steel makes the use of pre-cast transmission poles uneconomical. For fifty years a great number of poles have been built in France, Germany, and Switzerland with 100,000 pound steel. Long concrete piles would be more often used, were such steel permitted or encouraged. Engineers should be warned not to use often the balanced reinforcement in slabs as deflections might become too great and costs too high.

The problem of a girder with compression reinforcement has been a riddle for sixty years. A similar formula to equation (4) has been published long ago. (Reference number 102), and was declared incorrect by the writer, and now it appeared in slightly different form with the same wrong notions. That equation (4) is fundamentally wrong may be seen at once, when we consider a beam with the same reinforcement at top and bottom. Then $p = p'$ and the

term $\frac{0.59(p - p') f_y}{f'_c}$ which is the distance of the center of gravity of the

compression block from the top fiber evidently becomes zero in this case, which means the compression block disappears, which is against nature. Now we have tests by Dr. Hajnal Konyi (Reference number 104, REINFORCED CONCRETE REVIEW, Volume 3, 1955) on a number of beams with symmetrical compression reinforcement. Hajnal Konyi measured the distance from top of tension cracks to compression face just before failure and found the following values: for 4% reinforcement both at top and bottom of an intermediate grade steel of $f_y = 48,000$ psi and an ultimate strength of 79,000 psi, $k = 0.545$ instead of zero according to equation (4) and for 2% of high elastic limit steel both at top and bottom, $k = 0.326$; the latter steel had $f_y = 78,000$ psi and an ultimate strength of 91,500 psi. He computed the maximum tensile stress of the bottom steel at failure of the beams with intermediate steel as 50,000 psi and the maximum stress in the compression steel as 33,500 psi, very much less than f_y assumed in equation (4). For the high elastic limit steel he found the maximum tensile stress at the failure of the beam as 92,000 psi and the maximum stress in the compression steel as 39,000 psi.

The error in equation (4) is incurred by using the yield point in tension instead of the much larger useful limit stress and the yield point in compression instead of the much smaller useful limit stress. Another error is occasioned by not computing the location of the neutral axis from the condition that the sum of all stresses acting at a section must be zero, as shown by the writer long ago. (Reference number 102)

Not many tests have been published on slabs with compression reinforcement. The oldest, most elaborate and costliest has been made by the Austrian Engineering Society in 1892, and has been scientifically investigated by Joseph Anton Spitzer, Chief Engineer of G. A. Wayss & Co. of Vienna. (Reference number 105, ZEITSCHRIFT DES OESTERREICHISEN INGENIEUR & ARCHITECTEN VEREINES, 1896, No. 20) The tests were made on an arch of 76' span, 15.5' rise, 14" thick at the crown, 24" thick at the abutment, 39½" wide, and reinforced at top and on bottom with 3.75 square inch of mild steel. Spitzer computed all moments, thrusts and shears for the loads placed at one-half of the span at six points, also the rotations and the deflections at those points by Castigliano's Theorem and the straight line theory and found the following interesting results: viz: - for low loads before the slab cracked the rotations and deflections agreed with theory when E was taken at 2,030,000 psi and the modular ratio, $n = 15$. After considerable cracking, E was found = 470,000 psi and $n = 65$. As the arch had a rise of $\frac{1}{8}$ of the span and was loaded only on one-half of the span, the influence of the thrust was of minor importance and the bending moments were of governing influence on the behaviour of the arch.

Another early series of tests was made by Professor Bach at Stuttgart in 1910 (Reference number 106, MITTEILUNGEN UEBER FORSCHUNGSARBEITEN, Heft 90 and 91), which clearly showed that the ultimate stress of the steel in the compression zone was smaller than the yield point both for mild steel and for high elastic limit steel.

Equation (6) for concentrically loaded short columns is an improvement over the rule of the 1940 report, but the writer would have preferred that the useful limit stress had been used instead of f_y . Why the report recommended a smaller minimum eccentricity in spiral columns than in tied columns is not clear. In fact, this provision requires every column to be designed as an eccentrically loaded column by the help of equations 7a and 7b, which is a tremendous task. A very practical short-cut was given by the writer over thirty years ago (Reference number 107, TRANSACTION ASCE 1923, page 1195)

$$P_{exc} = \frac{P(axial)}{1 + 314 \frac{e}{d}} \quad (104)$$

for

$$\frac{e}{d} = 0.1, P_{exc} = \frac{P_{axial}}{1.314} = \text{approx. } 0.75 P_{axial} \quad (105)$$

which formula will be much preferred by all designing engineers.

It is more difficult to analyze the problem of an eccentrically loaded column by the plastic theory than by the straight line theory; but not sufficiently so as to require 70 equations of distinguished lengths and doubtful validity as done by this report to justify equations (7a) and (7b). Those two equations contain again the confusing parameters k_1 , k_2 , k_u and the yield point f_y , which latter was shown to introduce errors in the similar equation (4).

In order to make it possible for a designer to solve this problem more readily, the report offers five diagrams in Fig. (6) and Fig. (7) which with the text imposes on the reader's time, patience and close attention out of proportion with the necessity for it, seeing that the writer published more

than thirty years ago (Reference number 107) simple diagrams which at a glance gave a fair solution for the coefficient of reduction of the axial load to obtain the eccentric load for a given relative eccentricity $\frac{(e)}{d}$. This illustration is presented at the end of this discussion as Fig. 51.

This problem has a corollary in that of the strength of a long steel column. In the early days of structural engineering, Euler's formula with a factor of safety of 5 to 10 was used. Then some engineers tried to find a more rational solution and developed formulas of impractical lengths until Professor Rankine cut the Gordian knot by offering his parabolic formula

$$P_{\text{long}} = \frac{P_{\text{short}}}{1 + C \left(\frac{1}{r} \right)^2}. \quad \text{Let us hope this committee will imitate Rankine and}$$

offer a simpler solution of this problem.

The recommended load factor of 1.8 for girders, beams and slabs is entirely too low for American practice. Between the time of the inception of the project and many years after the completion, there occur many variations from perfect work. Some of these variations are the following:

A) In the design work.

- 1) Errors in computing live load and dead load on girders, beams and columns.
- 2) Errors in design by neglecting secondary stresses, temperature variations, shrinkage and flow.
- 3) Errors by following false notions of codes, especially in shear and length of positive reinforcement.
- 4) Errors by draftsman in following notes of the designer.
- 5) Errors by draftsman when making shop drawings.
- 6) Errors overlooked by checkers.

B) In materials of construction.

- 1) The quality of steel furnished may be inferior to that assumed by the designer.
- 2) The trussed bars may be incorrectly bent.
- 3) The ready made concrete is furnished with a low cement factor and a low water cement ratio to make the test cylinders come up to specifications. When the concrete is too dry to empty readily, the driver adds plenty of water which reduces strength.
- 4) During concreting heavy downpours sometimes occur, which weaken the concrete.
- 5) A sudden fall of temperature may occur in the months of October and April when no proper protection against freezing is provided.
- 6) When concreting is done during the winter months and the building has been enclosed by tarpaulins and is heated by salamanders, a big storm may occur and damage tarpaulins and in any case weaken outside columns and lintels.
- 7) In the summer months in the Southern States and the arid West, when the sun is shining on the fresh concrete and on the forms, cracking and weakening of the concrete is often caused.

C) Construction defects.

- 1) Form work often does not conform to working drawings, especially as to elevations and may not be properly supported.

- 2) The placing of the reinforcement may not follow shop drawings and negative bars are not properly held in place or may be displaced by concrete workers.
 - 3) Only rarely in American practice on medium sized jobs are competent engineers employed to watch the concrete and steel every moment.
- D. OTHER unfavorable influences.
- 1) Unequal settlements of foundations sometimes occur.
 - 2) Heavy construction loads of cement in bags, plaster, sand and steel are often placed on floors, which may seriously affect apartment and office floors, which are designed for a live load of only 40 to 50 pounds per square foot.
 - 3) The action of zero temperature on exposed reinforced concrete seriously damages concrete, when steel bars are too close to the surface.
 - 4) Owners and tenants often overload floors, especially when the use of buildings is changed.
 - 5) Owners, without consulting the architect or designer, have large openings cut in floors for additional elevators, machinery, et cetera.

In view of all these possibilities a factor of safety of $2\frac{1}{2}$ is the minimum which should be recommended and a factor of safety of 3 is much better. The latter factor was obtained by most contractors in the past fifty years who used rail bar steel or wire mesh reinforcement, provided they used enough stirrups in beams and girders.

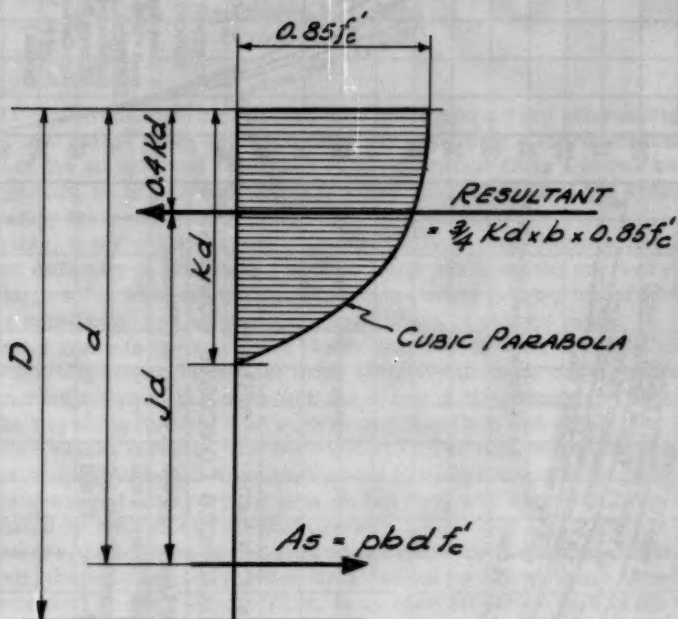


Figure 50.

Discussion of
"DETERMINING BASIC WIND LOADS"

by George F. Collins
(Proc. Paper 825)

ALBERT W. HAINLIN.¹—Mr. Collins has presented a very interesting, convincing, and useful piece of information. In providing a more precise estimation of the actual wind velocities at any elevation from a known velocity on the ground, he has given designers more assurance as to the actual factor of safety their structures possess.

This writer, however, disagrees with Mr. Collins in the implication that the greatest difficulty in designing for wind loads has been the correct evaluation of the precise wind velocities. There are other points, two of which seem more significant and about which more effort should be made.

The first of these is the so-called "form factor". In even the most elementary Fluid Mechanics Texts this more properly termed "drag coefficient" is shown to vary considerably with both the shape of the submerged object and with the Reynolds Number (for a given uniform fluid and object, the Reynolds Number varies directly with the velocity). The fact is that for some rectangular shaped items the drag coefficient can approach a value of 2.0. That is, the average force per unit area on the item will approach twice the value indicated by the velocity impact pressure.

Furthermore, in addition to the drag which might be measured on the object by itself, there is an interference drag caused by two or more objects in close proximity to each other. Thus, in an open structure as a radio tower which is a host of intersections, crosses, and irregular joints the matter of assigning the proper overall "form factor" is very difficult. Model studies in a high turbulence wind tunnel would be likely to provide the quickest source of reliable information.

The second of the points is that conventional calculations ignore the fact that our worst winds are accompanied by heavy rain. Computations show that for even relatively heavy rainfall (1 inch per hour) there is a negligible change in the overall density of the air whether the water is considered or not. This, of course, has led to the conclusion that rainfall has negligible effect on the structure. It is this conclusion which should be challenged for the following reasons:

- 1) During hurricanes there are tremendous quantities of wind borne water which never reach the ground at the point where highest winds occur. This water is carried on and deposited in a distant place as the hurricane subsides. It would seem that a computation of the density of the water in the air-water mixture based upon measured rainfall would have to be increased sharply to approach the correct value.

1. Professional Engr., Coral Gables, Fla.; formerly Assoc. Prof. of Mechanical Eng., Head, Fluid Mechanics Lab., and Director, Housing Research Lab., Univ. of Miami, Fla.

- 2) Since the water carried in the air is not a continuous fluid, it is unlikely that even by using a properly evaluated average mixture density and the correct "form factor" the correct result can be obtained. Probably a statistical summation of the effects of the impact from the individual drops will give some information as to the actual contribution the rain has to the total loads. Model studies in a high turbulence wind tunnel would again yield the more accurate design data once the actual rain density in a hurricane has been determined.

In addition to these two difficulties the other things which plague the designer are the directions the gusts and eddies take in a real storm. These occur both in the horizontal and vertical planes so that a tall structure is twisted and racked by many combinations of wind directions and velocities. Even in a steady breeze the designer may not relax because of the existence of vortices which form and detach themselves alternately from opposite edges of any submerged object. These cause small side thrusts which are harmless until they occur at some multiple of the resonance frequency of the structural member. This phenomena has been analyzed by von Karman and the stream pattern of these vortices now bears his name. A common example of its presence is exhibited in "singing" telephone wires.

In summary it is suggested that, although Mr. Collins has presented a very useful aid to the structural designer, much more effort is needed in the field before the problem can approach the "case closed" situation.

T. C. RATHBONE.¹—All additional efforts to extend existing knowledge of relationships between average wind velocities and true gust values with elevations above ground are welcome contributions to the literature in this field. Too many radio and TV towers in the past have been flattened by winds they supposedly should have withstood. Some failures can be laid to faulty structural design, or wind load ratings specified more in the interests of economy than safety. But inadequate information on true velocities to be anticipated, the potency of gusts, and increase of windspeeds with height may well be responsible for failures of other towers of supposedly conservative design. Now that TV towers are reaching for great heights, this subject is most timely.

The author describes the results of investigations made within a rather limited range, being confined to an elevation of 410 ft., and average ground velocities up to 65 mph,—considerably under common tower heights, and hurricane velocities as defined. Any conclusions drawn from the investigations under discussion should be restricted to the scope covered.

Within these limitations, a case is apparently made for the deficiency of the one-seventh power law in relating velocities at various elevations. This is most interesting, in view of the considerable past experience supporting this exponent. Although, not stated, it is presumed that both the height and gust factors were based on simultaneous records made with a number of anemometers at different elevations. To explore further the time-lag or drag effect on peak gusts as recorded by the "aerovanes", and to determine true gust durations, simultaneous records made with pressure-tube type anemometers alongside the aerovanes would become necessary.

The author's chart Fig. 3, which at first glance appears to exhibit a

1. Cons. and Research Engr., America Fore Ins. Group, New York, N. Y.

considerable diminution of the "gust factor" with increasing mean velocity, is a bit misleading. Actually, from the data presented, this rate variation is appreciable only for lower velocities, and becomes insignificant at higher wind speeds. If the data are plotted on rectangular coordinates, as gust versus average velocities, the values fall on a surprisingly straight line, as exhibited by the attached Fig. A. The resulting slope-intercept equation is almost precisely

$$G = 119.5 V + 9$$

where G = gust velocity, and V = 5 min. average. With such consistency, extrapolations beyond 65 mph by means of this equation would appear to be valid. The gust factor becomes 1.31 at 75 mph, and 1.27 at 100 mph, approaching an asymptote.

But extensions to higher elevations and base windspeeds on the selected velocity-profile chart Fig. 4, indicate that the computed and actual profiles start to diverge appreciably at elevations above 410 ft., suggesting further exploration. The Windspeed-Velocity Pressure-Elevation Chart Fig. 5, which is based on a nest of profiles as indicated in Fig. 4, cannot be extrapolated to higher elevations and higher base-wind speeds, without quickly leading to incredible values. Chart B, attached, is an extension of the author's chart Fig. 5, carrying the elevations to 1500 ft., and adding 30 ft.—base 5 min. average windspeed lines up to 120 mph. The added constructions are shown by broken lines. The straight "logarithmic" lines for the higher speeds follow the author's constructions, continuing the "a" value progression.

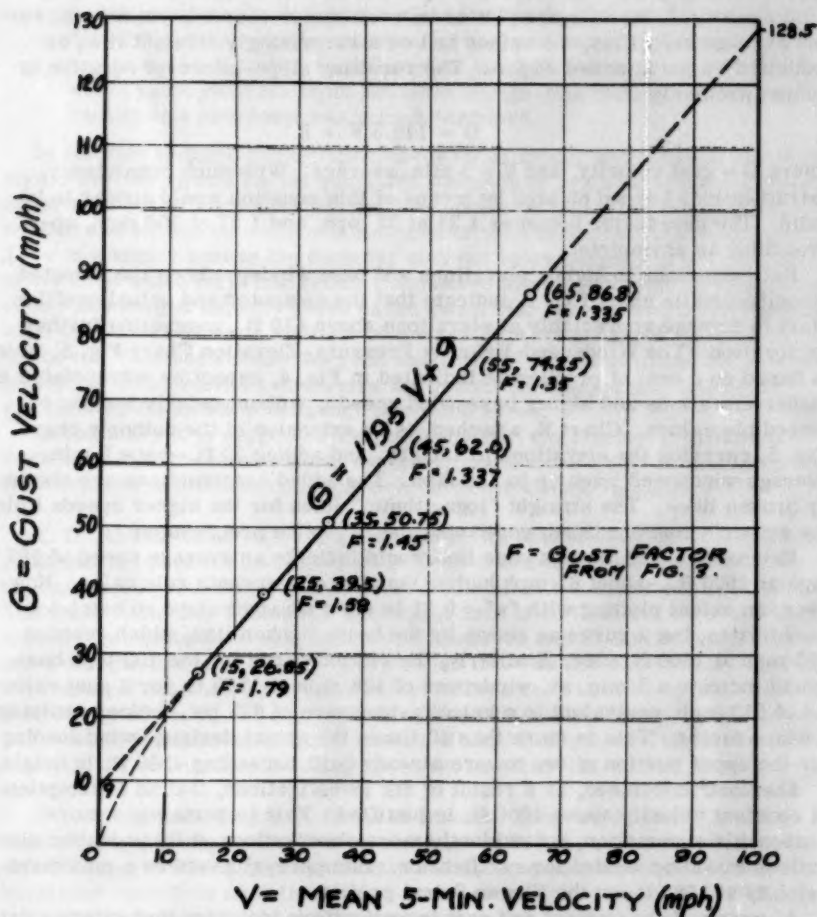
Extension of the 70 mph base line would indicate an average speed of 187 mph at 1500 ft.,—about 65 mph higher than the one-seventh rule value. However, an actual plotting with "a" = 0.31 is not a straight slope on semi-log coordinates, but a curve as shown by the heavy broken line, which reaches 235 mph at 1500 ft. elev. Similarly, the plotted curve for the 100 mph base would indicate a 5 min. av. windspeed of 426 mph at 1500 ft., or a gust velocity of 513 mph, equivalent to a velocity-pressure of 675 psf,—before applying a shape factor. This is more than 10 times the actual designed wind loading for the upper portion of two towers already built exceeding 1500 ft. in height.

Sherlock² concluded, as a result of his investigations, that an assumption of constant velocity above 1000 ft. is justified. This is certainly a more reasonable assumption, but evidently more observations at these higher elevations would be needed for verification. Humphreys³ assumes a maximum velocity at 1660 ft. on the Ekman Spiral profile.

A review of the present and past investigations indicates that existing data are inconsistent, and inadequate for use in basing rational wind loading for tall structures under realistic conditions, with assurance. Much more reliable information is needed on gust and height factors for the higher elevations and wind speeds, and on effective gust durations. It is to be hoped that some of the towers in the 1000-1500 ft. range can be utilized for such studies. This would entail a number of recording anemometers of both the standard and the pressure-tube type at various elevations, with provisions for making simultaneous records during severe storms as the opportunities occur.

2. Trans. ASCE, Vol. 118A, 1953, Paper No. 2553.

3. "Physics of the Air," W. J. Humphreys, McGraw-Hill Book Co.



RELATIONSHIP BETWEEN GUST AND MEAN VELOCITIES, DERIVED FROM GUST FACTORS TAKEN FROM AUTHOR'S CHART, FIG. 3.

FIGURE A.

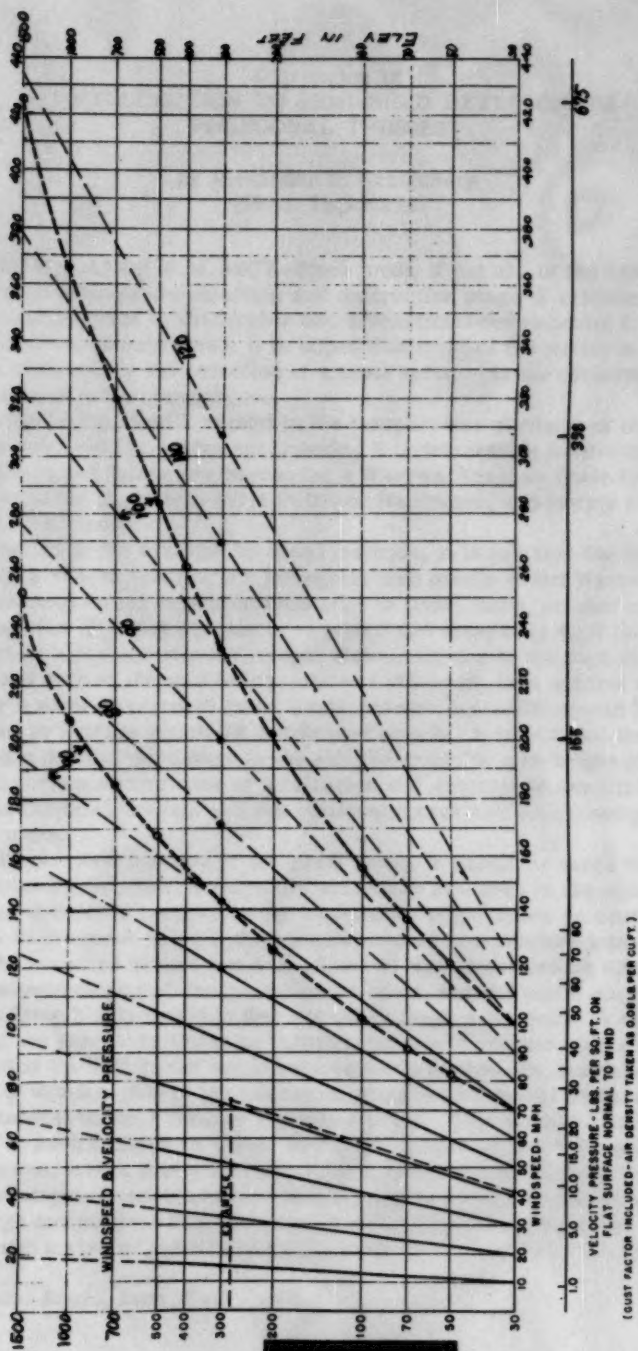
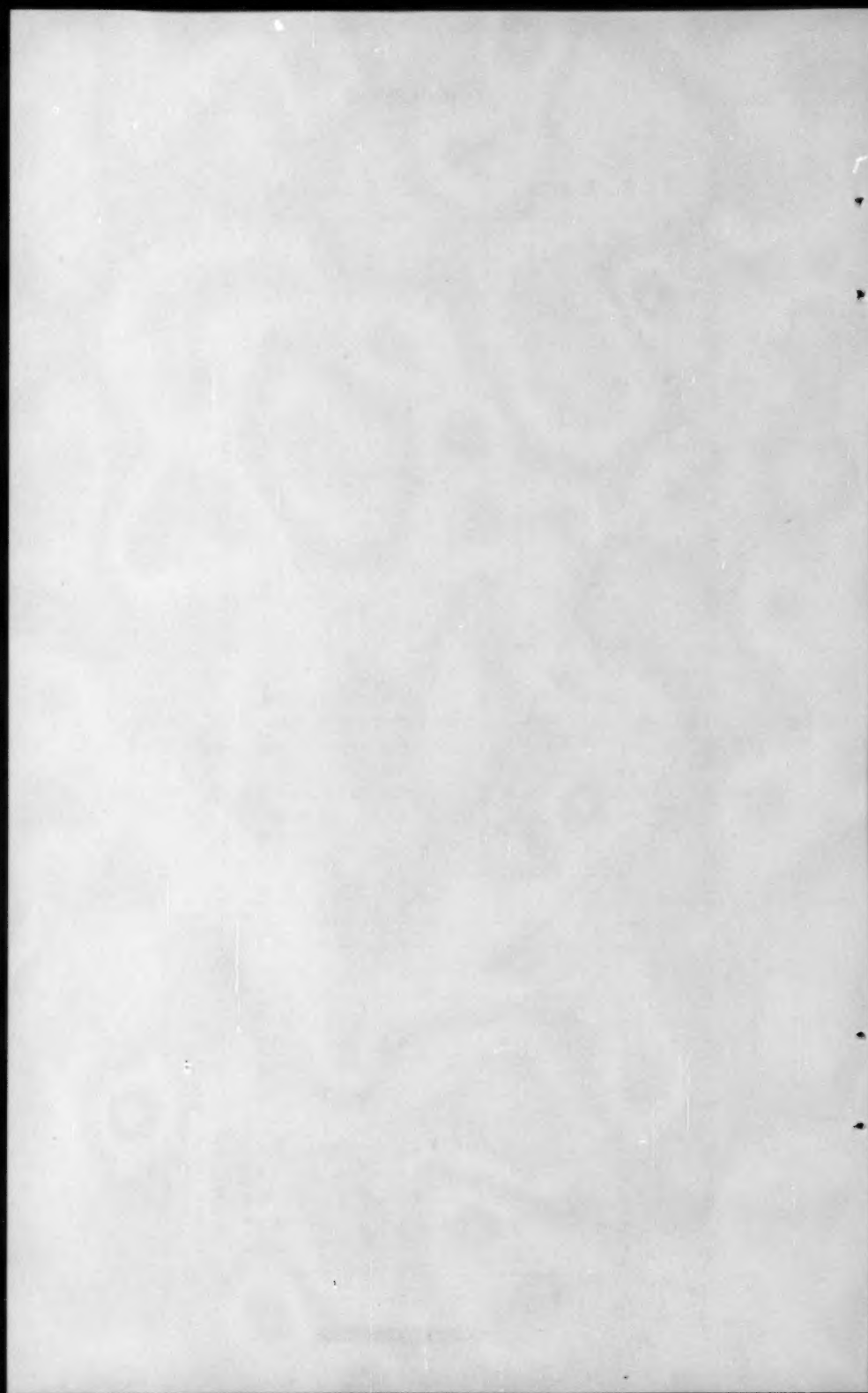


FIGURE B.



Discussion of
"INTRODUCTION TO SEMI-RIGID DETERMINATE
POLYGONAL TRUSSES"

by Alexander H. Kenigsberg
(Proc. Paper 828)

E. NEIL W. LANE,¹ A.M. ASCE—Since most, if not all, of the new and untried must go through the objection and obstruction stage of criticism and experimentation prior to its turning into a beneficial development for the betterment of those concerned, it is hoped that most of the writer's comments will be of some aid in the selection of a most suitable truss conformation and its design for a particular purpose.

Referring to Fig. 5 with regard to the comparative numbers of members and joints required for equivalent trusses, it is interesting to note that eleven less members and joints are needed for a Warren, Pratt or Howe frame; one member and nine joints less for a Pettit or Baltimore, and twenty each additional for a "K" truss.

With regard to the erection by usual methods, it is felt that the two self-supporting members forming the triangular web panels of the Warren, Pratt or Howe trusses would have a definite edge in time, labor, amount of scaffolding and size of lifting equipment required and especially so if the wye is assembled as a prefabricated element. Primarily due to the high moments to be contended with at the mid-height joints of the wyes, it is not felt as though the author's semi-Vierendeel truss could ever be competitive with long span tied arches or trusses requiring subdivided panels. It is felt that the latter would have a distinct advantage in the simplicity of the mid-height joints along with corresponding ease of fabrication and erection to say little of benefits as far as deflection and secondary stresses are concerned per unit weight of truss.

From linear deformations of the panel alone, it should be noted that top chord shortening will induce twice the secondary stresses in the upper arms of the wyes with their comparatively heavy mid-height joints as contrasted with those in the much more limber members and comparative joint-play found in the standard simple trusses. Some of this effect can be eliminated in erection procedure and design accommodation, but one could not eliminate its effects from highly variable line and other loads subsequent to erection. Increasing the section modulus by tapering the members and adding glange plates toward the "M" joints would only serve to accentuate a vicious cycle by means of which a part of the top chord compression would be carried in an uneconomical manner through the upper arms. This would be particularly important in such trusses as shown in Fig. 2. As far as the "M" joints themselves are concerned, this would necessitate heavier butt welds at the critical glange intersections where stress concentration and internal stresses are already high and suggest that annealing would probably be required. It is not felt as though a riveted substitute would likely be competitive. The author's

1. Structural Engr., Lodi, Calif.

method of designing the wyes as pin ended and detailing simple connections to the upper chord gussets is recognized as practical realism and as helping the situation even though it is in a somewhat undetermined manner. Any other method would obviate the patent. From these considerations, it is felt as though a large size model analysis or photoelastic study would throw some interesting side lights on appropriate avenues for study of the recommended design procedure.

Examination of Fig. 6 shows its immediate advantage in the stability of triangulation, especially for erection, and, as far as conformation of the member of the end panel is concerned, the result is stiffer than that shown in Fig. 5 (a) and has lower secondary stresses, though the joint LO is larger, and often more eccentric due to the member LO-M2. However, simple shifting of the support often remedies the effect on the panel as a whole, though not local parts composing the joint itself. All in all, it is believed that the stub-vertical collision post forming a part of the truss end-joint with the transverse floor beam is more economical framing, though not so picturesque or economical as its omission in favor of heavier exposed flange plates and greater bending stiffness in the decally used end post of the usual highway truss. Seldom has a collision strut saved a truss from accident, except in the case of light highway passenger cars and here the usual end post with its glancing blow has been found more suitable in several ways.

Such truss arrangements having short lower chord end panels adjacent to longer ones as in Fig. 1 (b) would cause serious increases in end-vertical compression stresses due to moving loads and uniformly spaced transverse floor beams except at the end. Should the transverse beams be connected at and between the lower wye legs to equalize the floor stringer spans, heavy bending stresses would be thrown into the lower chord likely necessitating the use of mid panel suspender rods partially prestressed to their attachment at the upper arms of the wye frames. Where the end panel is appreciably longer than the interior spaces as shown in Fig. 2 (b), 3 (b) and 4, one would obtain excessive secondary end-joint rotation unless counteracted again by partially prestressed ties, at least, and probably it would be found desirable to provide stiffness in these ties as the live load passes into the second panel reversing the bending otherwise passed into the lower chord member. True, this would not apply to the lower chord of a deck loaded roof truss, but the configuration is used to explain a consideration. For similar reasons, the connection of the end interior diagonal of the truss shown in Fig. 3 (a) would not be connected to the mid point of the end post, but to its upper end joining the top chord, and, being a full panel height strut, likewise, it would probably be economical to provide a secondary horizontal stiffener to the first interior "M" joint depending on actual stresses.

Double deck bridges, applying their floor loads uniformly at the upper and lower "M" joints of trusses, similar to those shown in Fig. 2, should find ready demand in a member of pleasing special and economic applications. However, in the interests of cost and stability, it is advised that two diagonals be added in the end panels running from the mid joints of the end posts to their respective "M" joints. This creates in effect a large-span Vierendeel truss with rigid triangulated "U" frames at the end, and triangular top and bottom chord units with built-in points of contraflexure at the mid-panel loci. The two layers of rigid "M" joints at the road levels with their stiff verticals would complete the picture of a highly desirable application where it might be suitable. The lateral and transverse framing could be nicely accommodated

in a most pleasing design and erection project, particularly adaptable say, to a gorge location or multi-level cross over in a typical congested city.

Another very favorable application for the semi-rigid polygonal truss could appear to be in field applications of the military forces or light and uniform loads, even though rhythmic at times and of long duration periodically. Although notoriously non-cognizant of load limitations, the military forces should likely be able to find some highly suitable war-zone uses for the portable, light weight metal bridges that could be built according to the author's scheme in prefabricated units along the lines of Fig. 5 (a). The span would probably be limited by the heaviest aluminum wye that could be carried by foot soldiers into place with two men at the "M" joint and one at the end of each leg. Such a bridge design could be easily packaged for convenient handling and shipping, and would be suitable for standing in a favorable manner, the adverse matters of rough and inexperienced handling, as well as undue corrosion from improper maintenance or atmospheric exposure.

A. C. SCORDELIS,¹ J. M. ASCE—The author has introduced an interesting new form of truss structure, which should stimulate considerable discussion regarding its merits. The writer wishes to confine his discussion to the section on truss deflections in which it is felt that the author leaves an erroneous impression that the polygonal truss is stiffer than a conventional truss and will thus deflect less under the same load.

In computing deflections the author uses the method of virtual work, sometimes called the unit dummy load method. This method consists of equating the external virtual work done by the external forces acting on the structure to the internal virtual work performed by the members of the truss. In a conventional truss in which all members are subjected only to axial load this leads to the expression:

$$1\delta \times \Delta = \sum u(AL) = \sum u \frac{SL}{AE}$$

However, in a polygonal truss since a number of members are subjected to bending moment as well as axial load the expression should be:

$$1\delta \times \Delta = \sum u \frac{SL}{AE} + \sum \int \frac{Mds}{EI}$$

Equations (1) and (2) may be found in any standard textbook on structural analysis and therefore the symbols are not defined herein. To be complete, equation (2) should also include the virtual work due to shear, but this is negligible when compared with that due to the axial load and the bending moment.

In determining the deflection in the polygonal truss the author fails to include the virtual work due to bending and thus the deflection obtained has little meaning. If one includes the effect of bending it will be found that the polygonal truss will have much higher deflections than the conventional truss.

In order to make a comparison of displacements in a polygonal truss and a conventional truss, the deflection of point B due to a one kip load at B will

1. Asst. Prof. of Civ. Eng., Univ. of California, Berkeley, Calif.

be obtained for the trusses shown in Fig. 1 and Fig. 2. So that the comparison may be valid an "exact" analysis has been made for the polygonal truss in Fig. 1. This structure is statically indeterminate to the second degree and an indeterminate analysis yields the axial loads and bending moments indicated on the figure. The axial loads developed in the members of a conventional Warren truss are shown in Fig. 2.

An application of Equations (1) and (2) is made in Table 1 in which the deflection of point B is obtained. Since this example is purely for purposes of comparison, the cross sectional area of all members has been assumed as 1 in² and the moment of inertia as 40 in⁴. It is recognized that in an actual structure the sizes of various members would differ but this would not change the conclusions obtained using the example chosen. The totals given in Table 1 are used below.

For the polygonal truss:

$$\begin{aligned}\Delta_B &= \sum \frac{uSL}{AE} + \sum \int \frac{Mm ds}{EI} \\ &= \frac{323.5}{E} + \frac{227.1}{E} = \frac{550.6}{E}\end{aligned}$$

For the Warren truss:

$$\Delta_B = \sum \frac{uSL}{AE} = \frac{270.8}{E}$$

These results definitely show that the conventional truss will deflect much less than the polygonal truss. A further investigation of the table indicates that the virtual work done by the chord members is essentially the same for the two types of trusses, but the strains in the web system of the polygonal truss contribute 65% of the total deflection whereas this figure is only 39% for the Warren truss. The above conclusions could have been predicted without the above analysis since it can be generally stated that if the members of a structure under a given load are subjected only to axial load, the structure will be stiffer and require less material than a similar structure in which the members are subjected to bending moment as well as axial load.

The polygonal truss of Fig. 1 has been analyzed by the approximate method described by the author and the results are shown in Fig. 3. A comparison of the results given in Fig. 1 and Fig. 3 indicates the degree of approximation involved for this case. The application of equation (2) using the axial loads and moments shown in Fig. 3 is made in Table 2 with the following results:

$$\begin{aligned}\Delta_B &= \sum \frac{uSL}{AE} + \sum \int \frac{Mm ds}{EI} \\ &= \frac{340.8}{E} + \frac{218.8}{E} = \frac{559.5}{E}\end{aligned}$$

The foregoing procedure was the same as that used by the author in his

example with the exception that he failed to include the effect of bending moment. While the above result is close to the value found for the "exact" solution it was obtained using an incorrect application of the principle of virtual work and thus in some cases this procedure may lead to highly incorrect answers.

The method of virtual work applies the deformations in the real structure to the forces and moments in the virtual structure. The deformations in the real structure must be compatible, while the only requirement of the force system in the virtual structure is that it be in static equilibrium.

The truss as analyzed in Fig. 3 does not satisfy the condition of compatible deformations. Considering triangle EFH, the relative displacement of E to F as obtained using the axial strain in member EF equals:

$$(\Delta L)_{EF} = \left(\frac{SL}{AE} \right)_{EF} + \frac{-0.916(96)}{(1) E} = \frac{-88.0}{E}$$

This same displacement may be obtained using the strains in members EH and EF. The effect of bending moment on this displacement cancels itself in these two members and thus only axial strains need be considered:

$$\begin{aligned} (\Delta L)_{EF} &= .707 \left(\frac{SL}{AE} \right)_{EH} + .707 \left(\frac{SL}{AE} \right)_{HF} \\ &= .707 \left[\frac{+.884(68)}{(1) E} \right] + .707 \left[\frac{+.530(68)}{(1) E} \right] = + \frac{68.0}{E} \end{aligned}$$

Similarly for triangle FIG, using the strain in member FG, the relative displacement of F to G is found to be $-32.0/E$, while if the strains in members FI and IG are used it equals zero. The difference in these values of the same displacement is a result of the approximations made in the stress analysis. This incompatibility of deformations does not exist in the "exact" analysis of Fig. 1.

In applying the method of virtual work this incompatibility of deformations should be reconciled before a deflection is found. This may be done by assuming some slip at the ends of members or some angle change between members forming into rigid joints. If this were to occur the virtual work due to these additional deformations would have to be included in the summations and thus the deflection found for point B would differ from that calculated above.

TABLE 1

DEFLECTION OF POINT B IN POLYGONAL TRUSS, FIG. 1, AND
WARREN TRUSS, FIG. 2

Bar.	L inches	A in ²	I in ⁴	Polygonal Truss Fig. 1				Warren Truss Fig. 2	
				S and u kips	$\frac{uSL}{A}$	M and m in.kips	$\int \frac{mMds}{I}$	S and u kips	$\frac{uSL}{A}$
AB	96	1	40	+333	10.7	0	0	+333	10.7
BC	96	1	40	+500	24.0	0	0	+500	24.0
CD	96	1	40	+166	2.7	0	0	+166	2.7
AE	107	1	40	-746	60.0	0	0	-746	60.0
EF	96	1	40	-861	71.0	0	0	-666	42.7
FG	96	1	40	-322	10.0	0	0	-333	10.7
GD	107	1	40	-373	15.0	0	0	-373	15.0
DH	48	1	40	+1,000	48.0	8.00	25.6	-	-
EH	68	1	40	+845	48.6	6.67	25.2	-	-
FH	68	1	40	+495	16.4	1.33	1.0	-	-
CI	48	1	40	0	0	16.00	102.4	-	-
FI	68	1	40	-363	9.0	7.45	31.4	-	-
GI	68	1	40	+345	8.1	8.55	41.5	-	-
EB	107	1	40	-	-	-	-	+746	60.0
FB	107	1	40	-	-	-	-	+373	15.0
FC	107	1	40	-	-	-	-	-373	15.0
GC	107	1	40	-	-	-	-	+373	15.0
Totals					323.5		227.1		270.8

TABLE 2

DEFLECTION OF POINT B IN POLYGONAL TRUSS, FIG. 3

Bar.	L inches	A in ²	I in ⁴	S and u kips	$\frac{uSL}{A}$	M and m in kips	$\int \frac{m M ds}{EI}$
AB	96	1	40	+333	10.7	0	0
BC	96	1	40	+500	24.0	0	0
CD	96	1	40	+166	2.7	0	0
AE	107	1	40	-746	60.0	0	0
EF	96	1	40	-916	80.6	0	0
FG	96	1	40	-333	10.7	0	0
GD	107	1	40	-373	15.0	0	0
BH	48	1	40	+1,000	48.0	8.00	25.6
EH	68	1	40	+884	53.0	4.00	9.1
FH	68	1	40	+530	19.1	4.00	9.1
CI	48	1	40	0	0	16.00	102.4
FI	68	1	40	-354	8.5	8.00	36.3
GI	68	1	40	+354	8.5	8.00	36.3
Totals					340.8		218.8

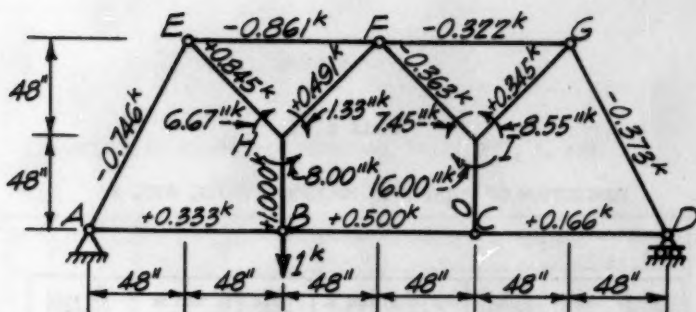


Fig. 1--"Exact" Analysis of Polygonal Truss

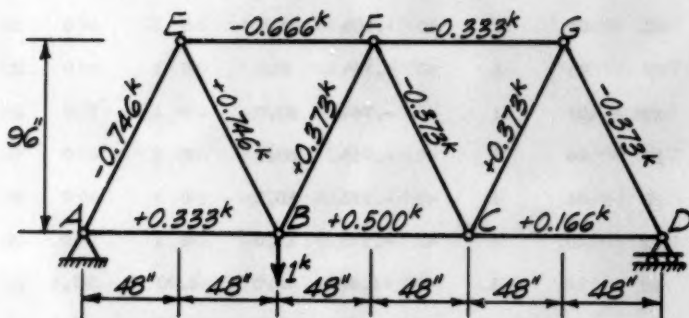


Fig. 2--Analysis of Conventional Warren Truss

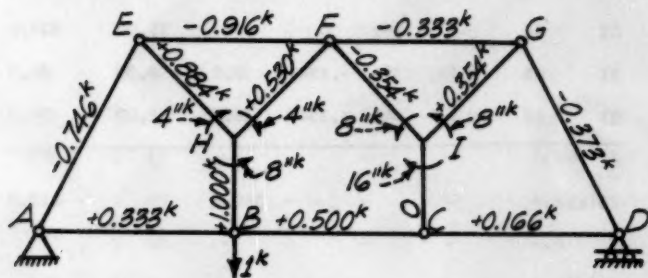


Fig. 3--Approximate Analysis of Polygonal Truss

Discussion of "ANALYSIS OF ARCHES BY FINITE DIFFERENCES"

by Ephraim G. Hirsch and E. P. Popov
(Proc. Paper 829)

CHIAO-LIN CHANG.¹ A.M. ASCE—The paper gives a very fine approach to arch analysis where horizontal as well as vertical deflections of arch rib are significant in increasing the bending stress in the arch. The use of Finite Differences in place of the original differential equations reduces the problem down to a set of simple linear simultaneous equations.

Engineers are entering a new era. With the development of electronic computers, a more exact analysis of a structure is no longer a task. Techniques such as successive approximations, by iteration or Relaxation, may no longer be a time saving device. But we should not lose sight of the physical behavior of the structure under load before it comes to equilibrium which is the basic foundation of successive approximations.

In the article, the example solved by Deflection Theory has 16 unknowns. They are seven vertical deflections η , seven horizontal deflections ξ , thrust H , and one vertical reaction, say V_L . It is assumed that the H and V_L are not affected by deflections and the values from Elastic Theory solution are used. There are also 16 continuity equations; seven in the form of Eq. 1a and nine in the form of Eq. 2a in cooperating with the boundary conditions. Two out of the latter nine equations are not used by the authors. They are at Sta. 4 and Sta. 5.

At Sta. 5

$$(\xi_6 - \xi_4) = -(\eta_6 - \eta_4) \times (-0.15625)$$

Combined with equations at Sta. 3 and Sta. 7

$$[0.46875 \eta_6 + 0.15625 (\eta_4 + 2 \eta_2)] = +0.15625 (\eta_6 - \eta_4)$$

or

$$3 \eta_6 + \eta_4 + 2 \eta_2 - \eta_6 + \eta_4 = 0$$

$$\eta_2 + \eta_4 + \eta_6 = 0 \quad (a)$$

At Sta. 4

$$(\xi_5 - \xi_3) = -(\eta_5 - \eta_3) \times 0$$

or

$$\xi_5 = \xi_3$$

Combined with equations at Sta. 2 and Sta. 6

$$\eta_1 + \eta_3 + \eta_5 + \eta_7 = 0 \quad (b)$$

It is clear that the basic assumption of this analysis is that the sum of vertical deflection at odd stations is zero and the sum of vertical deflection at even stations is also zero. The exact relation should be that the total

1. Design Engr., Richardson, Gordon and Associates, Cons. Engrs., Pittsburgh, Pa.

downward deflection equals the total upward deflection. As illustrated by Fig. A,

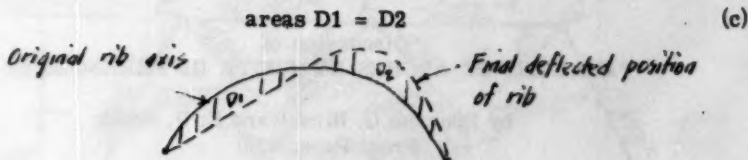


Fig. A

The larger the number of segments used, the closer equations (a) and (b) approach (c).

A good way to check the correctness of the mathematics involved and also the accuracy of the solution in assuming the values of H and V_L from Elastic Theory is by substituting the results into equations (a) and (b).

eq. (a) becomes

$$-0.0843 - 0.0005 + 0.0825 = -0.0023' \neq 0$$

eq. (b) becomes

$$-0.0626 - 0.0583 + 0.0569 + 0.0610 = -0.0030 \neq 0$$

using $H = 552.96$ lb.

$$552.96 \times 0.0030 = 1.66 \text{ ft. lb.}$$

This small moment shows the results obtained by the authors are rather accurate.

It is well to point out that the Deflection Theory presented does not apply to Tied Arch or Self-Anchored Suspension Bridge analysis. The position of the thrust in the tie does not remain fixed. It deflects practically the same amount as that of the arch rib or cable.

HERBERT A. SAWYER, JR.,¹ M. ASCE.—A practical, efficient, and general deflection-theory method of arch analysis has been clearly presented in this paper, for which its authors deserve great credit.

This paper also serves to re-emphasize the important fact that, unlike secondary stresses from deflection of a truss, "secondary" stresses from the deflection of an arch are commonly of primary importance and magnitude.

Since this paper is concerned with analysis rather than design, the authors did not discuss the determination of the loading for the illustrative example. For a deflection-theory analysis stresses are not proportional to loads, and to prevent an unsafe design the loads used for analysis must be obtained by multiplying the working loads of the standard specifications by a factor of safety or load factor.

For the sake of completeness, the writer would suggest that another term related to axial and transverse strains be added to basic Eq. 1. The addition of this term does not, however, affect the discussion and illustrative examples following Eq. 1 of the paper, all of which neglected the effect of axial strains. The derivation of this term follows.

Consider the infinitesimal length of member, ds , shown in Fig. 6, which

1. Prof. of Civ. Eng., Univ. of Connecticut, Storrs, Conn.

before deformation has a radius of curvature R and describes a central angle $d\theta$. If this length is subjected to a transverse contractive unit strain of ϵ_t from any cause, points A and B would move toward the member's axis a distance $\epsilon_t c$ to new positions A' and B' . Since fiber AB does not change length, lines AA' and BB' must be parallel. At the same time, as shown by Fig. 6, line AD rotates through an angle $d\phi_t$ with respect to line BE in assuming its new position $A'D'$, causing a corresponding change in $d\theta$:

$$d\phi_t = d\theta' - d\theta \quad (14)$$

but, using similar triangles:

$$d\theta' = \frac{ds}{R'} = \frac{c}{(1+\epsilon_t)c} \frac{ds}{R} = (1+\epsilon_t)d\theta$$

Substituting this value into Eq. 14:

$$d\phi_t = +\epsilon_t d\theta \quad \text{or} \quad \frac{d\phi_t}{ds} = \frac{\epsilon_t}{R} \quad (15)$$

It has been shown previously* that an axial contractive strain of ϵ_a will cause a change in a central angle $d\theta$ of

$$d\phi_a = -\epsilon_a d\theta \quad \text{or} \quad \frac{d\phi_a}{ds} = -\frac{\epsilon_a}{R} \quad (16)$$

Thus the total rate of change in the central angle from flexure and axial and transverse strains will be:

$$\frac{d\phi}{ds} = \frac{M}{EI} + \frac{\epsilon_t - \epsilon_a}{R} \quad (17)$$

For a combination of axial thrust and temperature change:

$$\epsilon_a = \frac{N}{EA} - \alpha t \quad \epsilon_t = -\frac{\mu N}{EA} - \alpha t$$

where μ is Poisson's ratio. Eq. 1 may now be revised by replacing the original M/EI term of Eq. 1 by the complete expression of Eq. 17, using the above values of unit strain:

$$\frac{d^2\eta}{dx^2} = \left[\frac{M}{EI} - \frac{N(1+\mu)}{EAR} \right] \sec \theta - \left(\frac{N}{EA} - \alpha t \right) \frac{d^2y}{dx^2} \quad (1-A)$$

2. "Modern Framed Structures, Part II", J. B. Johnson, C. W. Bryan, and F. E. Turneure, Wiley, New York, Tenth Edition, 1929, p. 129.

Since $1/R$ is of the same order of magnitude as d^2y/dx^2 , the added term for thrust is of the same order of magnitude as the original term for thrust in Eq. 1. Thus, if the effects of thrust strains are included in an analysis, Eq. 1-A should be used.

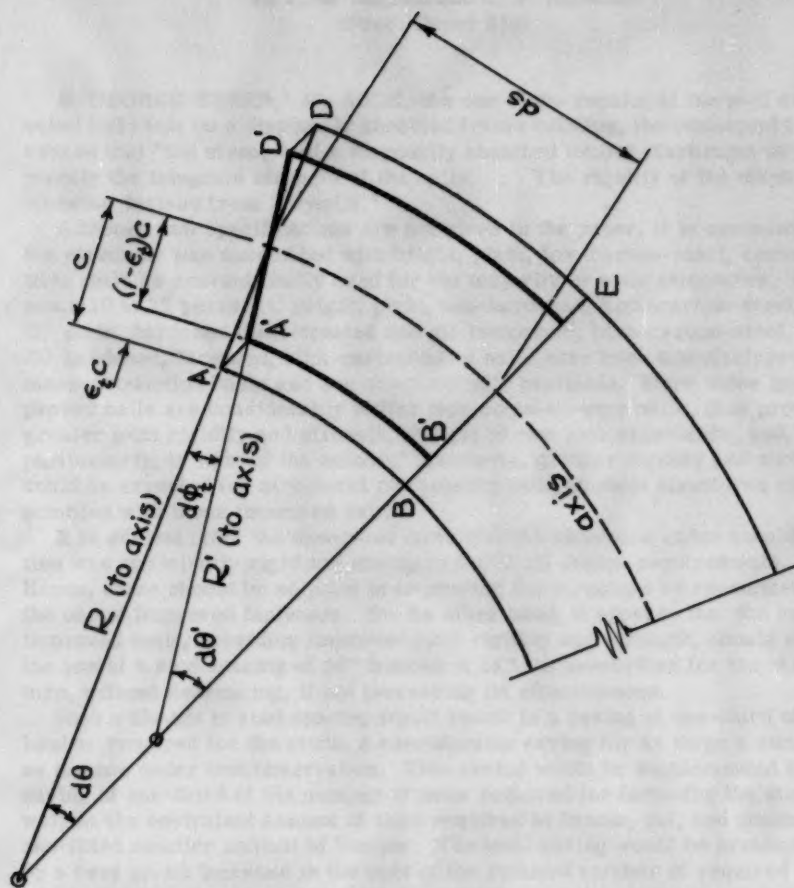


Fig. 6. Deformation from Transverse Strain.

Figure 10.10 shows a curve in the first quadrant of a Cartesian coordinate system. The curve starts at the origin O and passes through points A , B , C , D , and E . The area under the curve from O to E is divided into four regions by vertical lines through A , B , and C . The regions are labeled R_1 , R_2 , R_3 , and R_4 from left to right. The total area under the curve from O to E is denoted by A . The area of region R_1 is denoted by A_1 , the area of region R_2 is denoted by A_2 , the area of region R_3 is denoted by A_3 , and the area of region R_4 is denoted by A_4 . The width of each region is denoted by Δx . The height of each region is denoted by $f(x_i)$ for $i = 1, 2, 3, 4$. The area of region R_1 is given by $A_1 = \Delta x \cdot f(x_1)$. The area of region R_2 is given by $A_2 = \Delta x \cdot f(x_2)$. The area of region R_3 is given by $A_3 = \Delta x \cdot f(x_3)$. The area of region R_4 is given by $A_4 = \Delta x \cdot f(x_4)$. The total area A is given by $A = A_1 + A_2 + A_3 + A_4$.

FIGURE 10.10 The area under a curve



Discussion of
"LOAD TEST OF A DIAGONALLY SHEATHED TIMBER BUILDING"

by J. M. English and C. F. Knowlton
(Proc. Paper 830)

E. GEORGE STERN,¹ M. ASCE.—As one of the results of the well executed field test on a diagonally sheathed frame building, the statement is advanced that "the strength of a diagonally sheathed timber diaphragm is merely the integrate strength of the nails. . . . The rigidity of the diaphragm likewise derives from the nails."

Although nail specifications are not given in the paper, it is assumed that the structure was assembled with bright, plain, low-carbon-steel, common-wire nails as conventionally used for the majority of wood structures. Since some 10 to 15 years, (1) bright, plain, non-hardened, high-carbon-steel, (2) plain, hardened (heat-treated and oil-tempered), high-carbon-steel, and (3) hardened, threaded, high-carbon-steel nails have been manufactured on a mass-production basis and are commercially available. Since these improved nails are considerably stiffer than common-wire nails, thus provide greater joint rigidity and strength, in light of previous experience, and, particularly, in light of the authors' statement, greater rigidity and strength could be expected for structural components and complete structures assembled with these improved nails.²

It is evident from the described tests that the structure under consideration was sufficiently rigid and strong to fulfill all design requirements. Hence, there should be no point in improving the structure by recommending the use of improved fasteners. On the other hand, it appears that the use of improved nails, providing improved joint rigidity and strength, should allow the use of a stud spacing of 24" instead of 16", as prescribed for the structure, without decreasing, if not increasing its effectiveness.

Such a change in stud spacing would result in a saving of one-third of the lumber required for the studs, a considerable saving for as large a structure as the one under test observation. This saving would be supplemented by a saving of one-third of the number of nails required for fastening the studs as well as the equivalent amount of time required to handle, cut, and assemble a one-third smaller amount of lumber. The total saving would be accomplished by a very small increase in the cost of the reduced number of required nails, which should amount to a very small percentage of the savings achieved.

Under given conditions, the use of properly threaded, hardened nails might allow even the use of a smaller number of such nails per joint than called for by the use of common-wire nails. Such a reduction in number of nails required would result in an additional saving in field labor.

The potential saving for the particular structure under consideration would be sufficient to justify a detailed analysis of this recommendation to

1. Research Prof., Virginia Polytechnic Inst., Blacksburg, Va.
2. "Grooved Nails Strengthen House Frames, by E. George Stern, Engineering News-Record, April 6, 1950.

use improved nails for the assembly of the framing as well as for fastening the sheathing to the framing. The economies involved on a nationwide basis, however, are far more important, when consideration is given to the tremendous amount of lumber used for conventional framing with studs spaced 16" apart, especially at a time when 1,200,000 and more houses are built in this country during a year, in addition to the numerous commercial frame structures.

NORMAN B. JONES.¹ J. M. ASCE.—A valuable study of the action of a diagonally sheathed building under lateral loading has been presented in this paper. However, the writer believes that certain valuable information has been omitted and some of the conclusions are in error.

It would be very interesting to see a detail sketch of the manner in which the roof diaphragm was connected to the end shear walls. Another detail of interest is that provided for the roof diaphragm ridge caused by the last bow-string truss parallel to the North end wall. As indicated on pages 830-2 and 830-5, the building was in general of very special design.

One item of detail observation by the author deserves especial emphasis to the designing engineer in seismic areas. At the end of the fourth paragraph on page 830-8, there is this statement; "This was a compression region which indicated that the straps were carrying the load rather than the blocks which had been designed for that purpose."

On page 830-23, there appear the following statements. "The total deflection at the center measured from the initial zero was 5 inches. This represents 1/480th of the span, well within the allowable limit for a plastered wall. Also, such a deflection in proportion to the wall height would lie within reasonable limits for the support of a masonry wall cantilevered from a wall footing."

The writer is not certain what is intended by "a masonry wall cantilevered from a wall footing." It is certain, however, that any conventional design of a masonry or tilt-up concrete wall for this building would presume support of the top of the walls by the roof diaphragm. In tilt-up work it could easily happen also that a wood diaphragm chord might be provided. By usual building codes such walls plus the roof dead load would impose a seismic load on the roof diaphragm which compares very closely with that represented by the "Full Load" curve of the author's Fig. 7. A center deflection on the order of the 5 inches reported is about 3 times as large as the maximum allowable for such walls based on usual design procedure.² Before such deflection could actually take place the roof diaphragm would be pulling on the side walls for support. Serious damage would undoubtedly occur.

The writer is dubious that even a plastered wall could sustain with little damage the total roof diaphragm and shear wall deflections indicated for full wind load, particularly if the loading were opposite to the apparent permanent set of about 1 1/2 inches which resulted from the diaphragm testing.

In conclusion it is interesting to note that the chord deflection data of this test compares fairly well with similar information on the recently tested 20' x 80' diaphragm.³ In making this comparison, it must be noted that the author's Fig. 7 does not contain a directly comparable amount of residual deflection effects. The author's report shows that this test produced no deflection which may be compared to the end post deflection of the 20' x 80' diaphragm test.⁴

1. Structural Engr., Whittier, Calif.

2. Technical Bulletin Number 1, "Horizontal Bracing Systems in Buildings Having Masonry or Concrete Walls," by Struct. Engrs. Assn., Southern Calif.

3. Oregon Forest Products Laboratory Report No. T-12, Oct. 1955, Table 1.

4. *Ibid.*, Table 2.

Discussion of
"ELASTI-PLASTIC DESIGN OF SINGLE-SPAN
BEAMS AND FRAMES"

by Herbert A. Sawyer, Jr.
(Proc. Paper 851)

BRUCE G. JOHNSTON,¹ M. ASCE.—It is unfortunate that Mr. Sawyer should cast an aura of doubt on all possible applications of plastic analysis in design when he opens his paper with the remark "Limit design is unreliable in obtaining collapse loads". It would be better to say that limit design is reliable in obtaining collapse loads only within a framework of certain limitations involving the possibilities of fatigue failure, brittle fracture, local instability, and/or excessive deflection. Mr. Sawyer is certainly correct in pointing out that when and if the ultimate moment occurs at rather low levels of localized angular rotation a severe limitation is prescribed on the application of limit design. This deficiency has sometimes been termed a lack of "rotation capacity". (25)

One may conclude from Mr. Sawyer's paper that this is especially important in reinforced concrete construction.

In the case of steel construction, the accumulated results of research of the past 10 years have made it possible to stipulate the requirements that will insure "rotation capacity" without fall off of moment due to local buckling. In the work at Lehigh University (25), since 1945, it has always been emphasized that real progress would be made in the application of plastic analysis to steel design when and only when the limitations on it are quantitatively evaluated. Mr. Sawyer makes the claim that elasti-plastic analysis leads to a better understanding of structural behavior. If one were to go to elasti-plastic design the great advantage of the simplicity in "plastic design" would be lost. On the other hand, if the limitations to plastic design are fully recognized and spelled out in a code of practice, then there can be a safe and reliable use of plastic design that will lead to real economy in certain areas of steel construction. No claim is made here that plastic design will generally replace elastic design but (contrary to the inference in Mr. Sawyer's paper) it does seem applicable as a supplementary procedure for industrial and tier buildings of continuous welded steel construction provided the application is controlled by a proper code of plastic design practice.

1. Prof. of Structural Eng., Civ. Eng. Dept., Univ. of Michigan, Ann Arbor, Mich.

The first of these is the fact that the...
the second is the fact that the...
the third is the fact that the...

It is also true that the...
the fact that the...
the fact that the...

It is also true that the...
the fact that the...
the fact that the...

It is also true that the...
the fact that the...
the fact that the...

It is also true that the...
the fact that the...
the fact that the...

It is also true that the...
the fact that the...
the fact that the...

It is also true that the...
the fact that the...
the fact that the...

It is also true that the...
the fact that the...
the fact that the...

It is also true that the...
the fact that the...
the fact that the...

It is also true that the...
the fact that the...
the fact that the...

It is also true that the...
the fact that the...
the fact that the...

It is also true that the...
the fact that the...
the fact that the...

JOURNAL STRUCTURAL DIVISION

Proceedings of the American Society of Civil Engineers

DYNAMIC STRESSES IN CONTINUOUS PLATE GIRDER BRIDGES

Roy C. Edgerton,¹ A.M. ASCE and Gordon W. Beecroft,² J.M. ASCE
(Proc. Paper 973)

SYNOPSIS

This paper describes and presents results of tests conducted by the Bureau of Public Roads and the Oregon State Highway Department on two three-span continuous plate girder bridges in Oregon. Measurements include deflection of the girders and strain in the girders, stringers and floor beams under test vehicles approximating the AASHO H20-S16-44 truck at speeds of 5 to 45 miles per hour. The test records provide values of frequency of vibration, amplitude of vibration, and amplitude of strain oscillation. Test data are presented in curves showing variation of stress and deflection with speed. Comparisons are made with stresses and deflections calculated according to existing specifications. Measured stresses in general are found to be lower than calculated values. Analytical work pertaining to theoretical frequencies and amplitudes of vibration is summarized. A good correlation was obtained between measured and computed frequencies of vibration. Calculations relative to the amplitude of vibration do not provide a correlation with the measured values; however, they strongly suggest that a substantial part of the vibration can be attributed to deck roughness. Measured strains are used to determine the degree of fixity of the ends of the floor beams, and measured deflections are used to evaluate the torsional rigidity of the structures.

Bridge specifications have been based on calculated static load stresses, empirical impact allowances, and satisfactory past performance. The need for strain measurements in structural members under moving loads has been recognized. Since the development and application of electronic strain recording equipment made these measurements possible, a number of reports of tests of bridges under moving loads have been published. The present report adds two three-span continuous plate girder bridges to the growing list of dynamic bridge studies.

Note: Discussion open until October 1, 1956. Paper 973 is part of the copyrighted Journal of the Structural Division of the American Society of Civil Engineers, Vol. 82, No. ST 3, May, 1956.

1. Research Engr., State Highway Dept., Salem, Ore.
2. Assistant Research Engineer, State Highway Dept., Salem, Ore.

During 1952, the Physical Research Branch of the U. S. Bureau of Public Roads completed the assembly of a portable bridge test unit. The unit, contained in a house trailer, consists of the equipment necessary to record varying strains and deflections. Agreement was reached between the Bureau of Public Roads and the Oregon State Highway Department for the test unit to be employed on an Oregon highway bridge during the summer of 1953 as a co-operative project of the two agencies. The North Dillard Bridge over the South Umpqua River on the Pacific Highway (US 99) in Douglas County was selected for the test. At the conclusion of the tests on the North Dillard Bridge, it was decided to repeat a portion of the test program on the Troutdale Bridge over the Sandy River on the Columbia River Highway (US 30) in Multnomah County. The tests on the two bridges will be described in the order mentioned.

The North Dillard Bridge is a three-span continuous plate girder bridge with two variable depth girders. The selection of this particular bridge was based primarily on three factors: (1) an appreciable amount of vibration had been observed in the structure, (2) most of the floor panels had transverse deck cracks, indicating the possibility that some damage was being caused by the vibration, and (3) no previous work known to the authors had covered dynamic stresses and vibrations on a bridge of this type. The bridge was designed for H20-S16-44 loading and utilized ASTM A242-46 steel having an allowable working stress of 27,000 p.s.i. The spans are 121 feet, 160 feet, and 121 feet, center to center of bearing. The girder depth, back to back of flange angles, varies from 5 feet 10-1/2 inches at the outside ends of the side spans and at the center of the center span to 9 feet 2-1/2 inches over the interior piers. The four piers, of dumbbell pattern, are founded on rock. The heights from footing to bearing are about 35 feet for the exterior piers, 43 feet for the north interior pier, and 38 feet for the south interior pier. There is a 50-foot 3-inch reinforced concrete approach span at each end. The deck is 30 feet wide with two 3-foot 6-inch sidewalks. Figure 1 shows principal details of the structure. The bridge is on tangent. The profile of the bridge is a 600-foot convex vertical curve with the deck grade varying from level to 0.8 percent. The south end is 2.77 feet lower than the north end.

The bridge was opened to traffic on November 29, 1950. The average daily traffic is 7,000 vehicles with 13 percent heavy trucks and combinations. The south city limit of the town of Winston is 0.2 mile north of the bridge, and the edge of the unincorporated town of Dillard is 0.5 mile south. Along the highway between the two towns are three roadside fruit stands, several residences, and road connections to a sawmill and a gravel plant. These features were important considerations in the operation of test vehicles since they necessitated additional precautions to prevent traffic interference.

The program consisted of four series of tests with vehicles approximating the H20-S16-44 truck travelling at speeds of 5 to 45 miles per hour. In the interest of public safety, speeds greater than 45 miles per hour were not attempted due to the restrictions imposed by the towns and roadside development described above. In Series I, girder deflections and positive moment strains were measured. Negative moment girder strains were measured in Series II. Stringer strains were measured in Series III and floor beam strains in Series IV.

Magnetic strain gages were used in Series I and II. SR-4 resistance strain gages were used in Series III and IV. The deflectometers operated on the same principle as a magnetic strain gage. A coil housed in a pipe coupling

was attached to the lower girder flange. An iron core in the coil was attached by a brass rod to a pipe mast from the ground or stream bed. Deflection of the girder produced relative motion between the coil and the core, thereby producing a change in the characteristics of the circuit and, ultimately, a galvanometer deflection.

The strain recording equipment consisted of a power supply, bridge and attenuator panels, and two oscillographs. Light-beam galvanometers in the oscillographs exposed the strain traces on sensitized paper. Each oscillograph was connected to handle 15 active traces. A separate power supply and separate bridge and attenuator panels were provided for the deflectometers. The output was wired to the same two oscillographs used for strain recording. Dark room facilities for developing the oscillograms were provided in the trailer.

The magnetic strain gages and the deflectometers were calibrated with dial indicators before installation and after removal. The strain recording equipment contained calibrating facilities for SR-4 resistance strain gages.

Road tubes were installed across the bridge deck at each pier and at the center of the center span. The road tubes operated air switches which recorded the progress of the test vehicle on one trace on each oscillogram. This record and the one-tenth second lines that were printed automatically on every oscillogram permitted accurate determination of the location of the test vehicle at all times. It also made possible an accurate determination of vehicle speed.

The strain gages and the strain recording equipment, including the oscillographs, were components of the Bureau of Public Roads test unit. The deflectometers, deflectometer power supply, and bridge and attenuator panels were loaned to the project by the Institute of Traffic and Transportation Engineering of the University of California.

Two test vehicles were used. Vehicle A was a logging truck and trailer unit based on a 2-1/2-ton military-type truck chassis. The vehicle was loaded with steel sheet piling. Vehicle B was a diesel truck-tractor with an equipment semi-trailer. The load was a track-type tractor. Figure 2 shows essential dimensions and axle loads of the two vehicles.

For Series I, six deflectometers and 24 magnetic strain gages were installed. A deflectometer was installed on the outside lower flange of each girder at the center of each span. Strain gages were installed on the inside and outside top and bottom flanges of each girder at the center of each span. They were installed on the lower surface of the top flanges and on the upper surface of the bottom flanges. The axis of each gage was located seven-eighths inch from the outside edge of the outstanding leg of the flange angle.

Series I was divided into four subseries. Series Ia was a set of runs with the test vehicle centering the roadway centerline. Runs were started with Vehicle A. Four or six runs, two or three in each direction, were made at each multiple of 5 miles per hour from 5 to 30 miles per hour by the speedometer. The highest speed attainable by Vehicle A under the test conditions was about 30 miles per hour. Vehicle B was then procured and runs with it were made at 5 miles per hour and at each multiple of 5 miles per hour from 20 to 45 miles per hour by the speedometer. There was some variation between speedometer speed and actual speed as calculated from the air switches and the oscillogram time lines. The highest actual speed was about 43 miles per hour.

For an understanding of the terms used on the curves and in the discussion

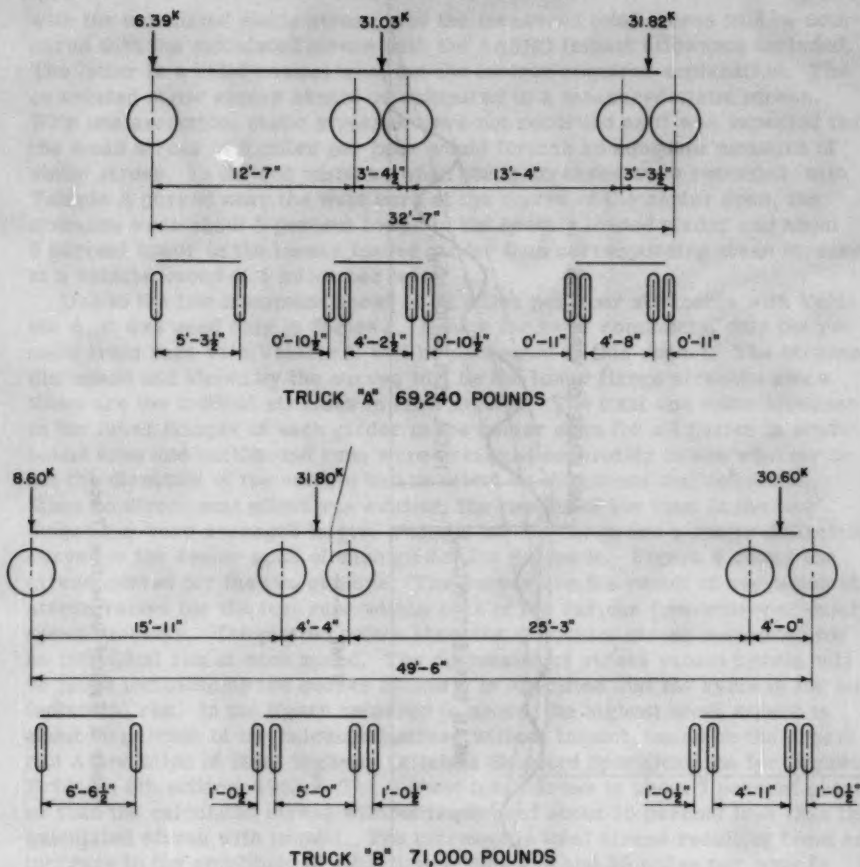


Figure 2. Test Vehicles.

of the test results, attention is invited to Figure 3. This is a typical deflection trace from an oscillogram. For clarity of illustration, the ratio of ordinate to abscissa of the trace has been doubled for the figure. The trace takes the form of a vibration curve with a frequency of about two cycles per second superimposed on a deflection curve representing the passage of the vehicle across the center span. To take the results from a trace, envelopes are drawn to the vibration curve. The maximum ordinate of the upper envelope and the maximum ordinate of a line midway between the envelopes are converted to deflection by the calibration curve and are termed the total deflection (Δ_t) and the mean deflection (Δ_m). The difference between the total deflection and the mean deflection is the amplitude of vibration. Strain traces are analyzed in an identical manner. Strains are converted to stress by an assumed modulus of elasticity of 30,000,000 p.s.i. The terms used are total stress (σ_t), mean stress (σ_m), and amplitude of stress oscillation. In the discussion of the test results, the measured mean stress will be compared

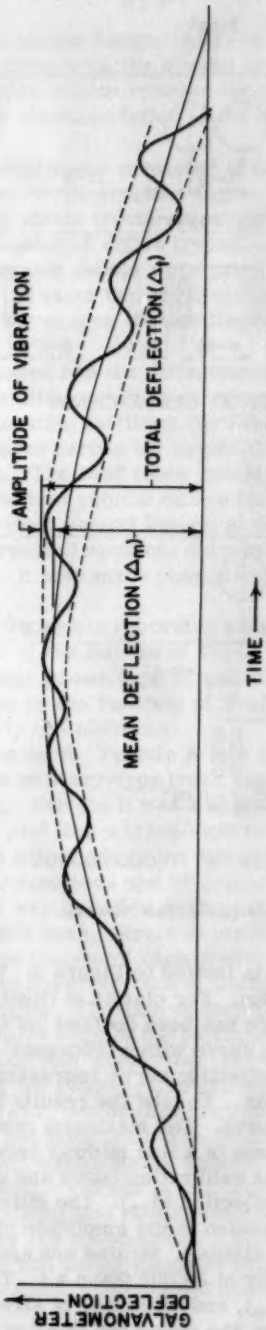


Figure 3. Typical Deflection Trace.

with the calculated static stress, and the measured total stress will be compared with the calculated stress with the AASHO impact allowance included. The latter is a valid comparison, but the former requires explanation. The calculated static stress should be compared to a measured static stress. With one exception, static stresses were not recorded as it was expected that the mean stress at 5 miles per hour would furnish an adequate measure of static stress. In the one instance when static stresses were recorded, with Vehicle A parked near the west curb at the center of the center span, the stresses were about 2 percent lower in the heavily loaded girder and about 6 percent lower in the lesser loaded girder than corresponding mean stresses at a vehicle speed of 5 miles per hour.

Due to the low maximum speed of 30 miles per hour attainable with Vehicle A, it was used only in Series I. Except for brief comments, only the results from runs with Vehicle B will be presented in this report. The stresses discussed and shown by the curves will be the lower flange stresses since these are the critical stresses in each section. The total and mean stresses in the lower flanges of each girder in the center span for all Series Ia southbound runs and northbound runs were averaged separately to see whether or not the direction of the vehicle had an effect on the stress and deflection. Since no directional effect was evident, the results of the runs in the two directions were averaged to give a single stress curve and a single deflection curve for the center span of each girder for Series Ia. Figure 4 shows the stress curves for the two girders. The curves are the result of averaging the stress values for the test runs within each of the various five-mile-per-hour speed brackets. The plotted points show the maximum stress measured for an individual run at each speed. The discussion of stress values herein will be those indicated by the curves unless it is specified that the value is for an individual run. In the figure referred to above, the highest mean stress is about 90 percent of the calculated stress without impact, based on the American Association of State Highway Officials Standard Specifications for Highway Bridges, 6th edition, 1953.³ The highest total stress is about 7 percent greater than the calculated stress without impact but about 10 percent less than the calculated stress with impact. The increase in total stress resulting from an increase in the amplitude of vibration between 20 and 30 miles per hour is typical of the span. For Series Ia, the maximum stress measured for Vehicle A in the center span was about 3 percent higher than the calculated stress without impact but about 13 percent lower than the calculated stress with impact. The maximum stress for an individual run is about 6 percent less than the calculated stress with impact for Vehicle B. Figure 5 shows the deflection curves for Series Ia with Vehicle B in the center span. The deflection follows the same general pattern as the stress except that a sharp increase in amplitude in the east girder occurs about 29 to 35 miles per hour. The greatest observed deflection is 0.55 inch and the greatest amplitude of vibration is 0.13 inch, both occurring at about 42.6 miles per hour in the east girder. The maximum amplitude of vibration for Vehicle A in the center span was 0.04 inch.

3. Since shear developing angles were used at 21-inch to 24-inch spacing in the region of positive moment, the calculated girder stresses and deflections presented in this report are those obtained by considering composite action of the girder with that portion of the deck allowed under AASHO specifications. A value of $n=10$ was used in computing both stresses and deflections.

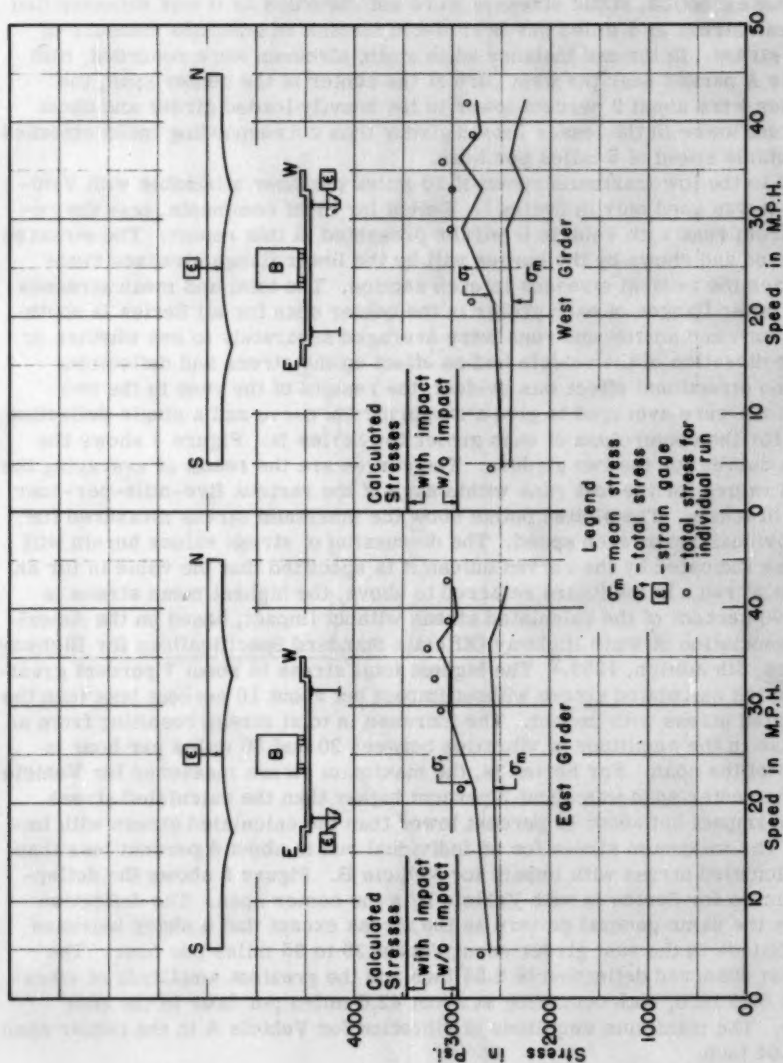


Figure 4. North Dillard Bridge Stress Curves, Series Ia, Vehicle B, Center Span.

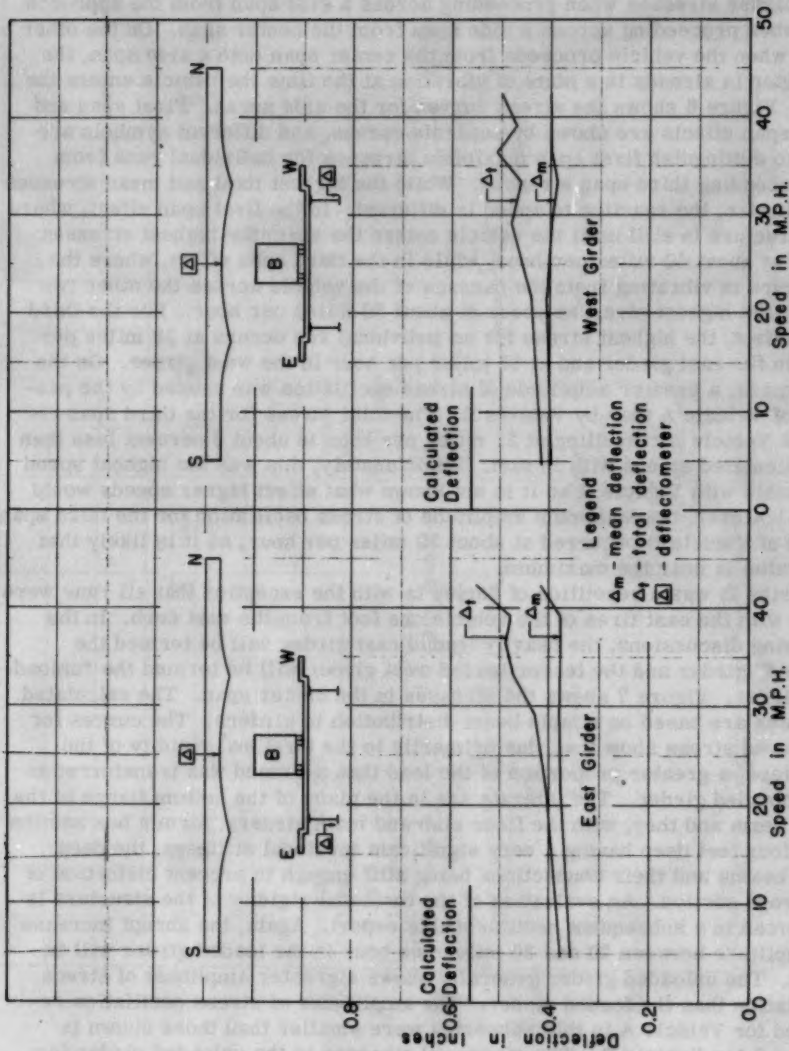


Figure 5. North Dillard Bridge Deflection Curves, Series 1a, Vehicle B, Center Span.

In the case of the side spans, a difference in stress and deflection characteristics due to the direction of the vehicle might be expected for two reasons. The influence line for moment at the mid-point of the end span of a continuous series is not symmetrical, nor is the axle and load arrangement of the vehicle longitudinally symmetrical. Calculations indicate that the vehicle should produce higher stresses when proceeding across a side span from the approach than when proceeding across a side span from the center span. On the other hand, when the vehicle proceeds from the center span onto a side span, the side span is already in a state of vibration at the time the vehicle enters the span. Figure 6 shows the stress curves for the side spans. First span and third span effects are shown by separate curves, and different symbols are used to distinguish first span maximum stresses for individual runs from corresponding third span stresses. While the highest total and mean stresses are similar, the reaction to speed is different. In the first span effect, where the structure is still until the vehicle enters the span, the highest stresses occur at about 40 miles per hour; while in the third span effect, where the structure is vibrating from the passage of the vehicle across the other two spans, the highest stresses occur at about 30 miles per hour. For the third span effect, the highest stress for an individual run occurs at 38 miles per hour in the east girder and at 33 miles per hour in the west girder. On the side spans, a greater amplitude of stress oscillation was caused by the passage of Vehicle A than by Vehicle B. The total stress for the third span effect of Vehicle A travelling at 31 miles per hour is about 3 percent less than the calculated stress with impact. Unfortunately, this was the highest speed attainable with Vehicle A so it is not known what effect higher speeds would have; however, the maximum amplitude of stress oscillation for the third span effect of Vehicle B occurred at about 30 miles per hour, so it is likely that this value is near the maximum.

Series Ib was a repetition of Series Ia with the exception that all runs were made with the east tires of the vehicle one foot from the east curb. In the following discussions, the heavily loaded east girder will be termed the "loaded" girder and the lesser loaded west girder will be termed the "unloaded" girder. Figure 7 shows the stresses in the center span. The calculated stresses are based on simple beam distribution to girders. The curves for measured stress show that, due primarily to the torsional rigidity of the structure, a greater proportion of the load than assumed was transferred to the unloaded girder. The laterals are in the plane of the bottom flange of the floor beam and they, with the floor slab and main girders, form a box section over four feet deep having a very significant torsional stiffness, the deep floor beams and their connections being stiff enough to prevent distortion of the cross section. An evaluation of the torsional rigidity of the structure is presented in a subsequent section of this report. Again, the abrupt increase in amplitude between 20 and 30 miles per hour in the loaded girder will be noted. The unloaded girder generally shows a greater amplitude of stress oscillation than the loaded girder. The amplitudes of stress oscillation recorded for Vehicle A in this subseries were smaller than those shown in Figure 7 for Vehicle B. The measured stresses in the unloaded girder for individual runs show a high degree of scatter. The maximum value for an individual run is about twice as high as the mean stress at 5 miles per hour (approximately equal to the static stress), indicating an impact of 100 percent. This extreme value is attributed to the fact that the girder is very lightly loaded.

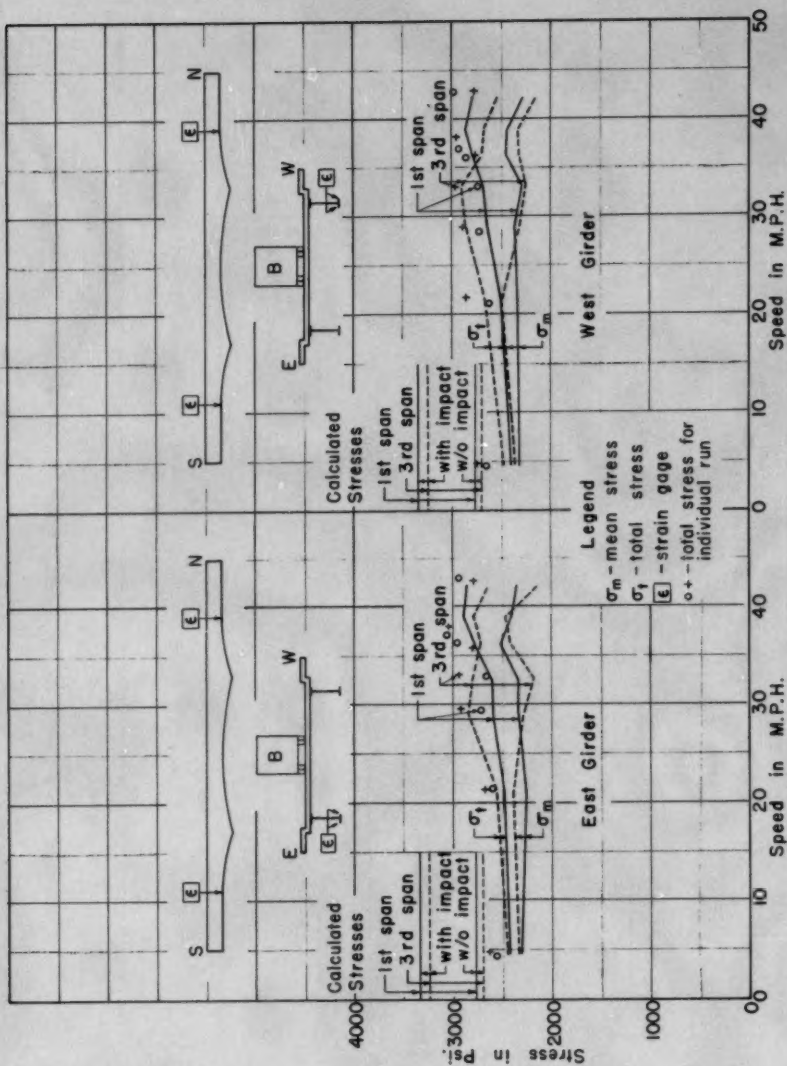


Figure 6. North Dillard Bridge Stress Curves, Series Ia, Vehicle B, Side Spans.

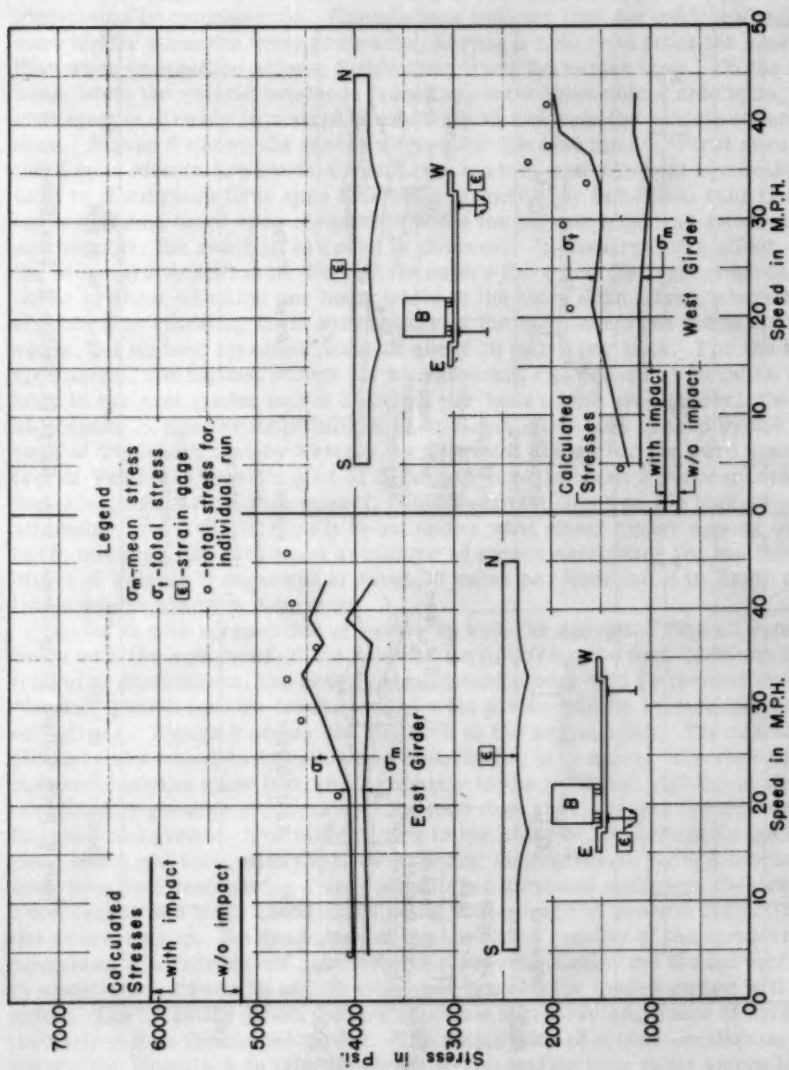


Figure 7. North Dillard Bridge Stress Curves, Series 1b, Vehicle B, Center Span.

To determine the damping effect of stationary mass or dead load on the vibration of the structure, Vehicle A was parked at the center of the center span with tires touching the west curb. Series Ib was then repeated as Series Ic with Vehicle B making all the runs. Figure 8 shows the stress curves under these conditions. New strain and deflection zeros were established after Vehicle A was parked on the span. The stresses in Figure 8 are those caused by the moving vehicle only. They do not include the stress caused by the parked vehicle. The highest total stresses in the loaded girder occur at a different speed than in Series Ib, but the magnitude of these stresses is virtually unchanged by the parked vehicle. The maximum stress in the unloaded girder for an individual run is about 12 percent lower than the corresponding value for Series Ib.

The fourth subseries under Series I was It, readings taken under normal heavy truck traffic on the bridge. The traffic was allowed to flow undisturbed during this testing, resulting in numerous records in which several passenger vehicles were on the bridge in addition to a truck. A few records were obtained with two trucks on the structure. The tabulated data from these records were carefully examined to locate any unusually high stresses or vibrations. No stresses or deflections greater than those measured in the loaded girder in Series Ib were found.

For Series II, the twelve strain gages were removed from the inside girder flanges and were installed on the girder flanges near the north interior pier. Eight gages were installed in the center span on the inside and outside of top and bottom flanges on both girders. Four gages were installed in the north span on the outside of top and bottom flanges of both girders. All gages were installed 2 feet 6 inches from the pier centerline. This distance was necessary to avoid the special girder details at the pier. Figure 9 shows the stress curves for the bottom flange gages on the center span side of the pier. The negative moment stresses show a higher degree of uniformity and less oscillation at higher speeds than the positive moment stresses. Disregarding composite action, since this measurement is for negative moment stresses, the calculate stresses without impact are almost identical to the measured mean stress. The amplitude of stress oscillation is greater than the specified impact allowance, resulting in a maximum measured stress 16 percent higher than the calculated stress with impact. Because of the measured position of the neutral axis, the composite moment of inertia was used in calculating the stresses presented in a partial report previously published on this project. The mean upper flange stress, computed from measured strains, is only 34 percent of the calculated stress based on the moment of inertia of the steel girder only. Apparently, the concrete slab and its reinforcement contribute an appreciable tensile resistance; however, the measured lower flange stresses are higher than would be expected for a section having a moment of inertia as large as that indicated by the position of the neutral axis. This apparent inconsistency may be due to experimental error or to local stress conditions caused by the special girder details at the pier.

For Series III, resistance strain gages were installed on both sides of the top and bottom flanges of the three stringers at two cross sections of the bridge. One cross section was at the center of the second floor panel from the north end of the north span, and the other cross section was over the floor beam next south. Runs were made with the vehicle centered on the deck, hence, centered over the center stringer, and with the west wheels of the vehicle directly over the center stringer. At the center of the panel,

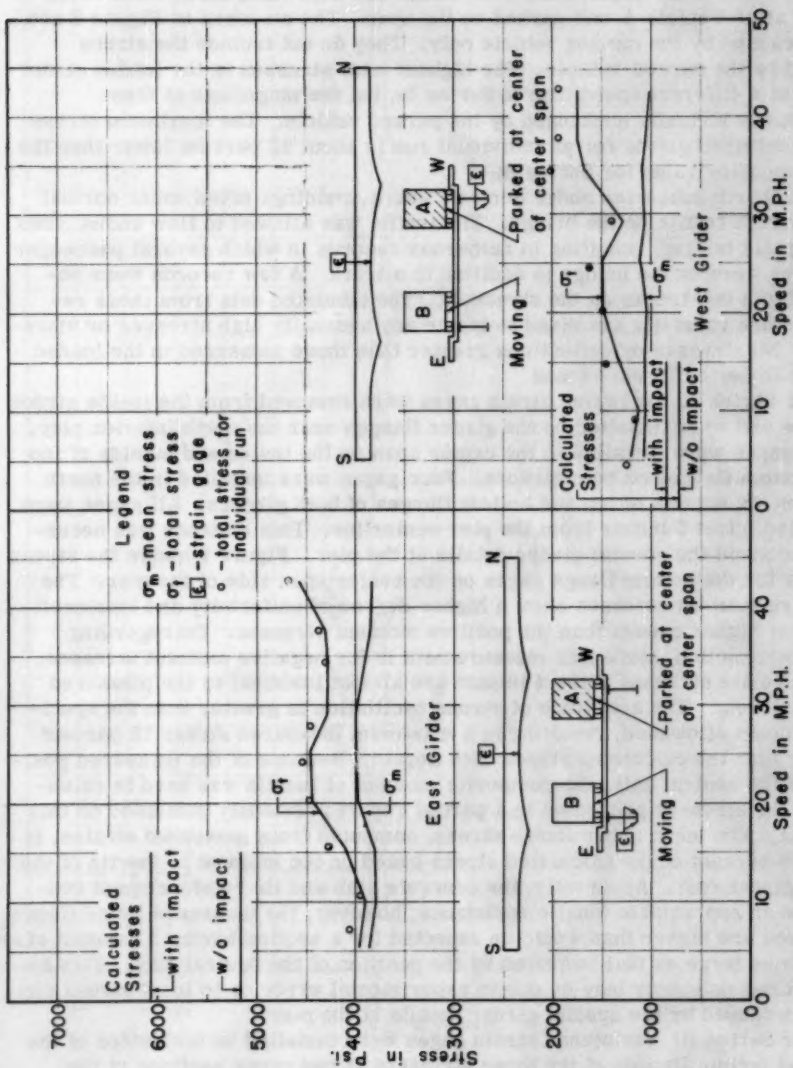


Figure 8. North Dillard Bridge Stress Curves, Series 1c, Center Span. Stresses from moving vehicle only.

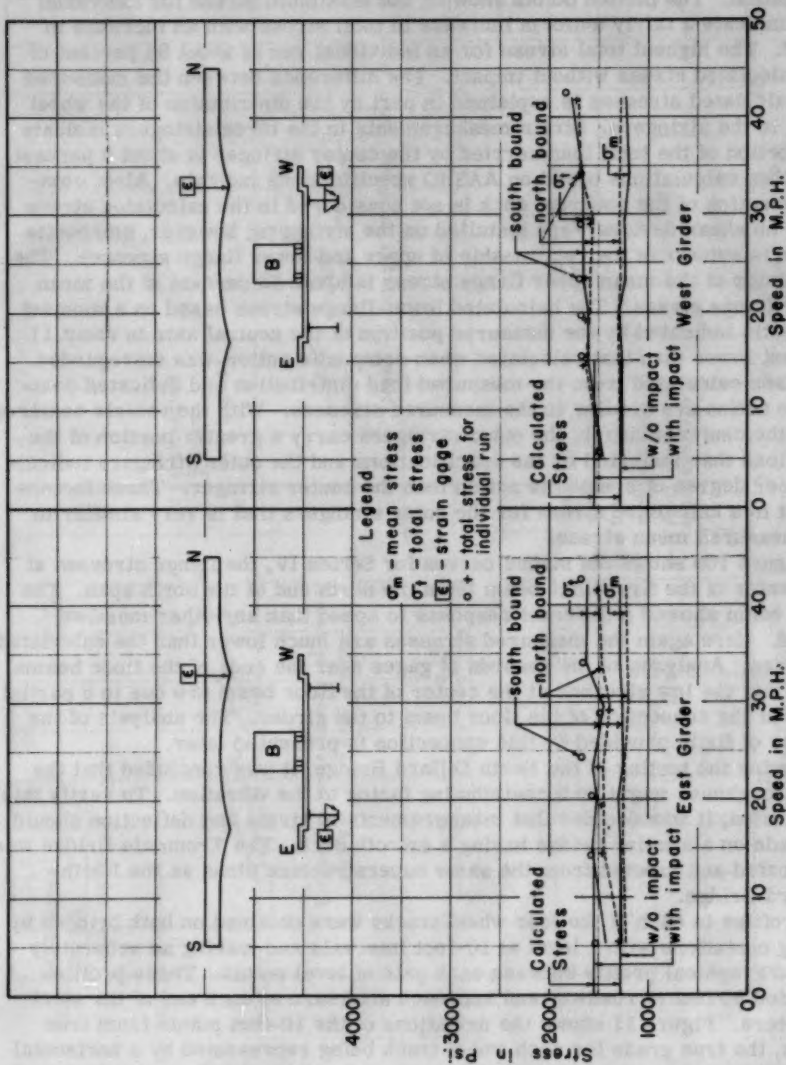


Figure 9. North Dillard Bridge Stress Curves, Series IIa, Vehicle B, Center Span.

maximum stresses were produced in the lower flange of the center stringer with the vehicle centered over the stringer. Figure 10a shows these stresses. The unusual feature of these curves is the variation of both mean and total stress with speed and the comparative uniformity of the amplitude of stress oscillation. The plotted points showing the maximum stress for individual runs indicate a fairly uniform increase in total stress with an increase in speed. The highest total stress for an individual run is about 94 percent of the calculated stress without impact. The difference between the measured and calculated stresses is explained in part by the distribution of the wheel loads to the stringers. Strain measurements in the three stringers indicate the portion of the total load carried by the center stringer is about 8 percent less than calculations based on AASHO specifications indicate. Also, composite action of the concrete deck is not considered in the calculated stress since no shear devices were installed on the stringers; however, composite action is evident in the relationship of upper and lower flange stresses. The magnitude of the mean upper flange stress is about 75 percent of the mean lower flange stress. The calculated lower flange stress based on a moment of inertia indicated by the measured position of the neutral axis is about 11 percent lower than that calculated when composite action was disregarded. Stresses calculated from the measured load distribution and indicated composite action are similar to the measured stresses. With the vehicle centered over the center stringer, the outer stringers carry a greater portion of the total load than indicated by the specifications and the outer stringers indicate a lesser degree of composite action than the center stringer. These factors result in a calculated stress for the outer stringers that is very similar to the measured mean stress.

Figure 10b shows the stress curves for Series IV, the flange stresses at the center of the first floor beam from the north end of the north span. The floor beam showed a different response to speed than any other member tested. Here again the measured stresses are much lower than the calculated stresses. Analyses of the records of gages near the ends of the floor beams show that the low stresses at the center of the floor beam are due to a partial fixity at the connection of the floor beam to the girder. The analysis of the degree of fixity provided by this connection is presented later.

During the testing of the North Dillard Bridge, it was concluded that the deck roughness might be a contributing factor to the vibration. To verify this conclusion, it was decided that measurements of strain and deflection should be made on a similar bridge having a smooth deck. The Troutdale Bridge was fabricated and erected from the same superstructure plans as the North Dillard Bridge.

Profiles in each of the four wheel tracks were obtained on both bridges by taking elevations with a level at 10-foot intervals and making an accurately traced graphical profile between each pair of level points. These profiles included 60 feet of roadway and approach structure at each end of the steel structure. Figure 11 shows the deviations of the 10-foot points from true grade, the true grade for each wheel track being represented by a horizontal line. To arrive at a numerical comparison of the roughness of the two structures, total deviations from true grade at the 10-foot points were computed. The total deviations in 520 feet for the four wheel tracks at North Dillard were 2.02 feet, 2.09 feet, 2.05 feet, and 2.00 feet—for an average of 2.04 feet. The deviations at Troutdale were 1.37 feet, 1.08 feet, 0.84 feet, and 0.84 feet—for an average of 1.03 feet. On the basis of this comparison, the Troutdale

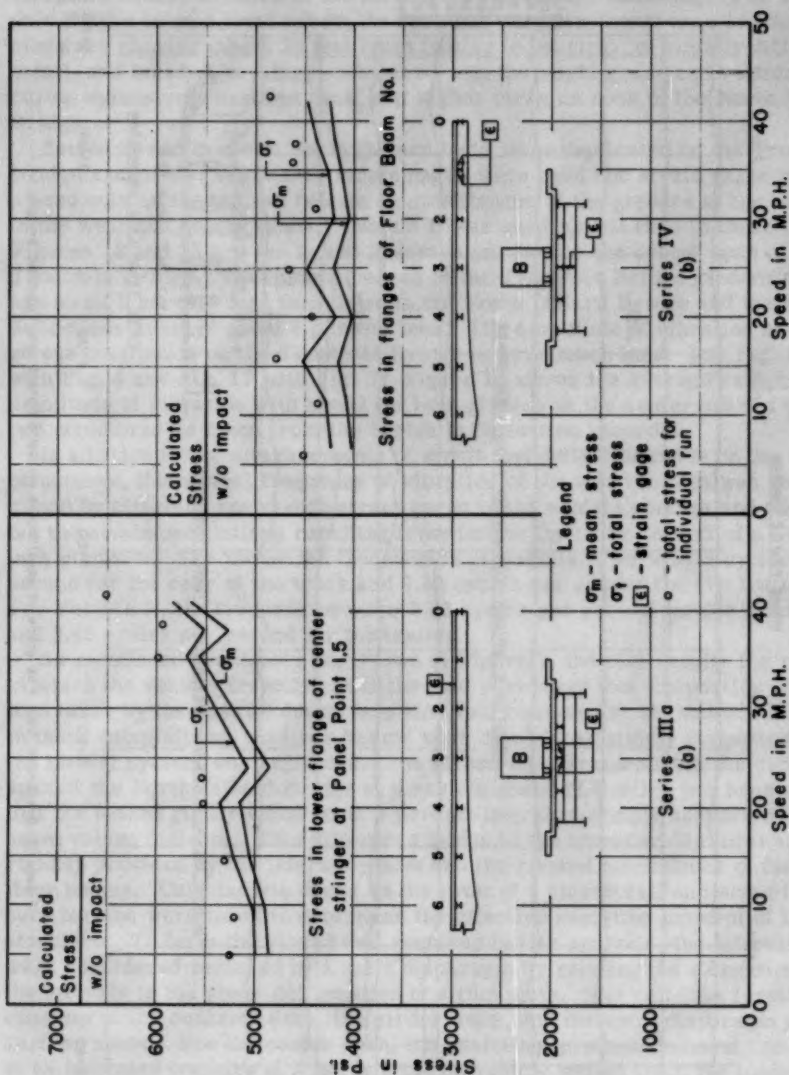


Figure 10. North Dillard Bridge Floor System Stress Curves, Vehicle B, North Span.

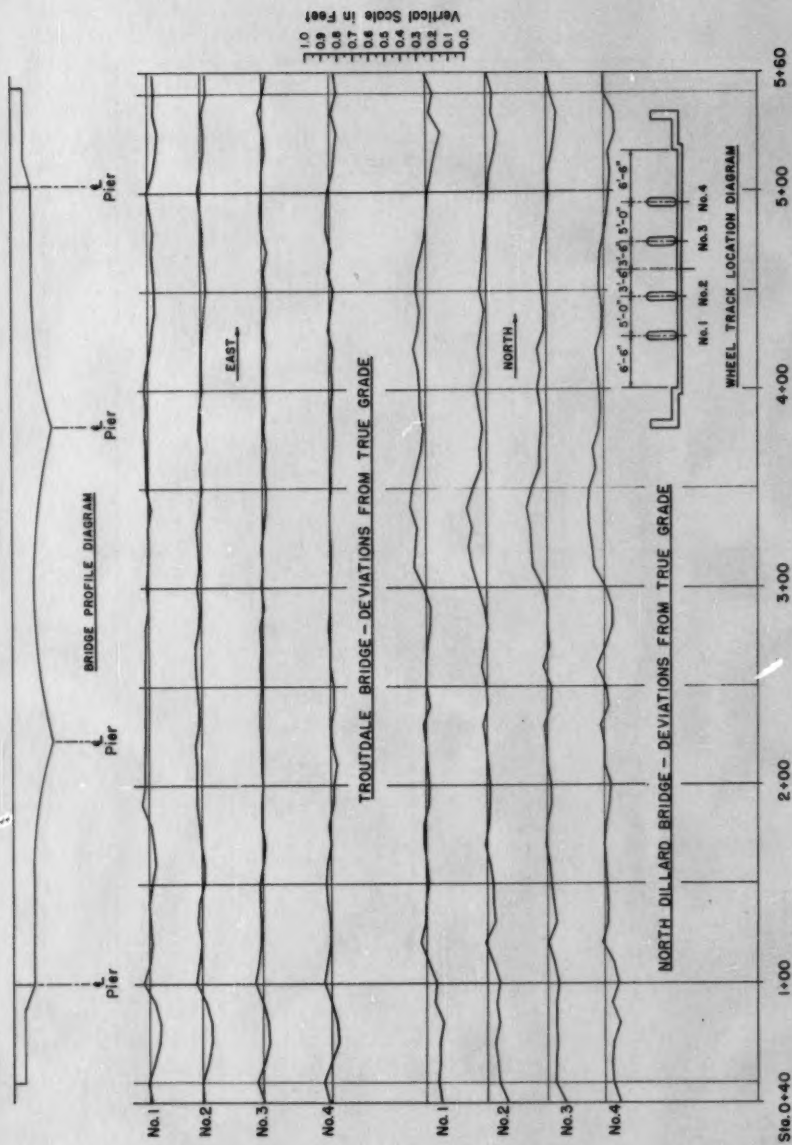


Figure 11. Deviations from true grade of wheel tracks on North Dillard and Troutdale bridges.

Bridge was selected for making comparable measurements of strain and deflection.

Differences other than deck roughness that might be significant in the vibratory characteristics of the structures include the following. The Troutdale Bridge is on a level grade; its deck has very few transverse cracks; its piers are shorter (about 28 feet from footing to bearing), of slightly different detail, and founded on piling—compared with the slight grade and vertical curve, extensively cracked deck, and higher piers on rock of the North Dillard Bridge.

Series Ia and Ib of the North Dillard tests were duplicated on the Troutdale Bridge except that resistance strain gages were used and strain gages were placed only on the top and bottom outside flanges of the girders at the centers of the west and center spans. Vehicle B was used for all runs in these tests. Figures 12 and 13 are the Ia and Ib stress curves for the center span of the Troutdale Bridge. The mean stresses in the Troutdale Bridge girders average about 5 percent less than those in the North Dillard Bridge and the mean deflections average about 4 percent less. The amplitude of vibration and stress oscillation on the Troutdale Bridge is very much less. (cf. Fig. 12 with Fig. 4 and Fig. 13 with Fig. 7) Figure 14 shows the average variation in amplitude of vibration with speed for both girders in the center span of the two structures as taken from the Series Ia deflection records.

In addition to the measurements of strain and deflection made on the two structures, the natural frequency of vibration of the test vehicles was determined by attaching resistance strain gages to the vehicle springs and recording the strain oscillations resulting from letting the truck roll off of a four-inch platform. The measured frequencies of Vehicle A were 3.29 cycles per second for the rear of the truck and 3.42 cycles per second for the trailer. For Vehicle B, the frequencies were 2.36 cycles per second for the tractor and 2.41 cycles per second for the trailer.

As mentioned previously and shown in Figure 7, the test results for runs in which the vehicle travelled near the east curb show that the portion of the load taken by the east girder is less than that indicated by the calculations. In these calculations, the floor beams were considered simply supported and the lateral system was neglected. The stress measurements for the center span of the North Dillard Bridge at a vehicle speed of 5 miles per hour show that the loaded girder takes about 9 percent less than simply supported floor-beam values indicate. This difference is due to the considerable torsional rigidity provided by the lateral system and the riveted connections of the deep floor beams. Calculations based on the twist of a closed cell subjected to pure torsion were made to determine the effective resisting moment of the structure. To form the closed cell required in this analysis, the laterals were considered replaced by a solid diaphragm by relating the elongation of the laterals to the shear deformation of a thin plate. The cell thus formed consists of the concrete deck, the girder webs, and the solid diaphragm described above. For the center span, the resisting torsional moment results in an indicated transfer of 7 percent of the vehicle weight from the loaded to the unloaded girder for a 10-foot vehicle eccentricity. A simple beam stress distribution for this vehicle position shows the east girder would take 87.7 percent of the total load. The load transferred from this girder due to torsional rigidity reduces the calculated value to 80.7 percent. The measured value, based on relative strains, shows that 78.5 percent of the total load is carried by the east girder. The calculation of the load transfer due to

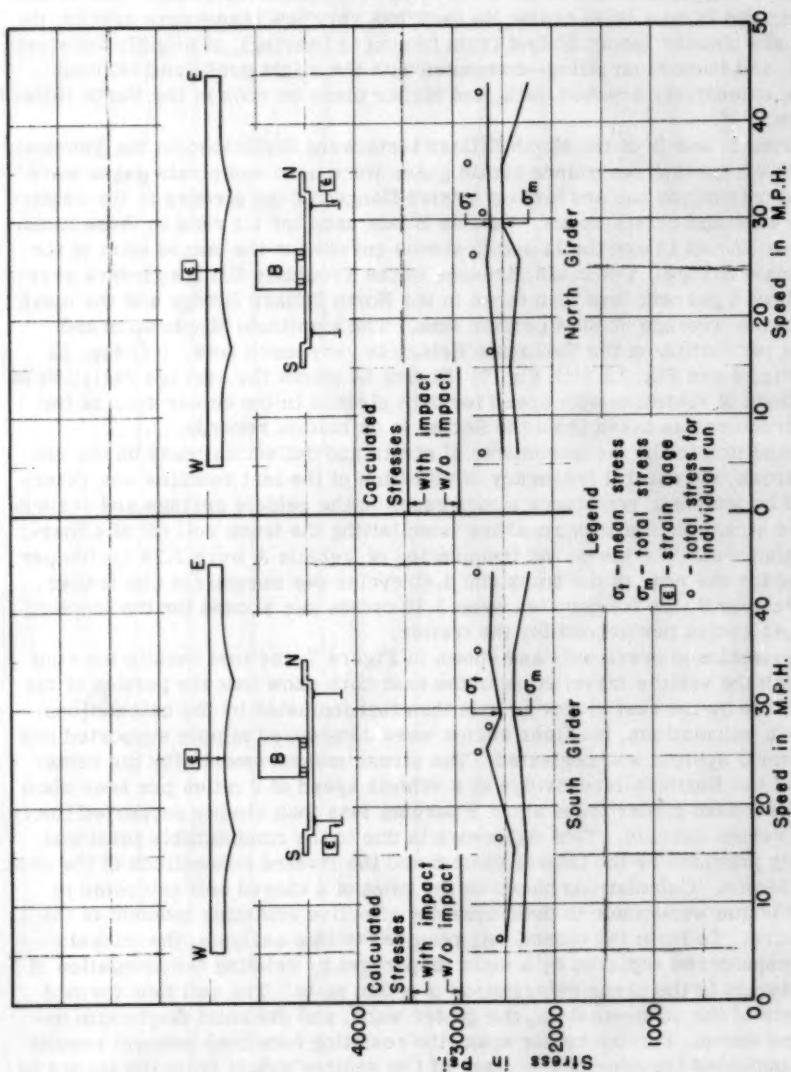


Figure 12. Troutdale Bridge Stress Curves, Series 1a, Vehicle B, Center Span.

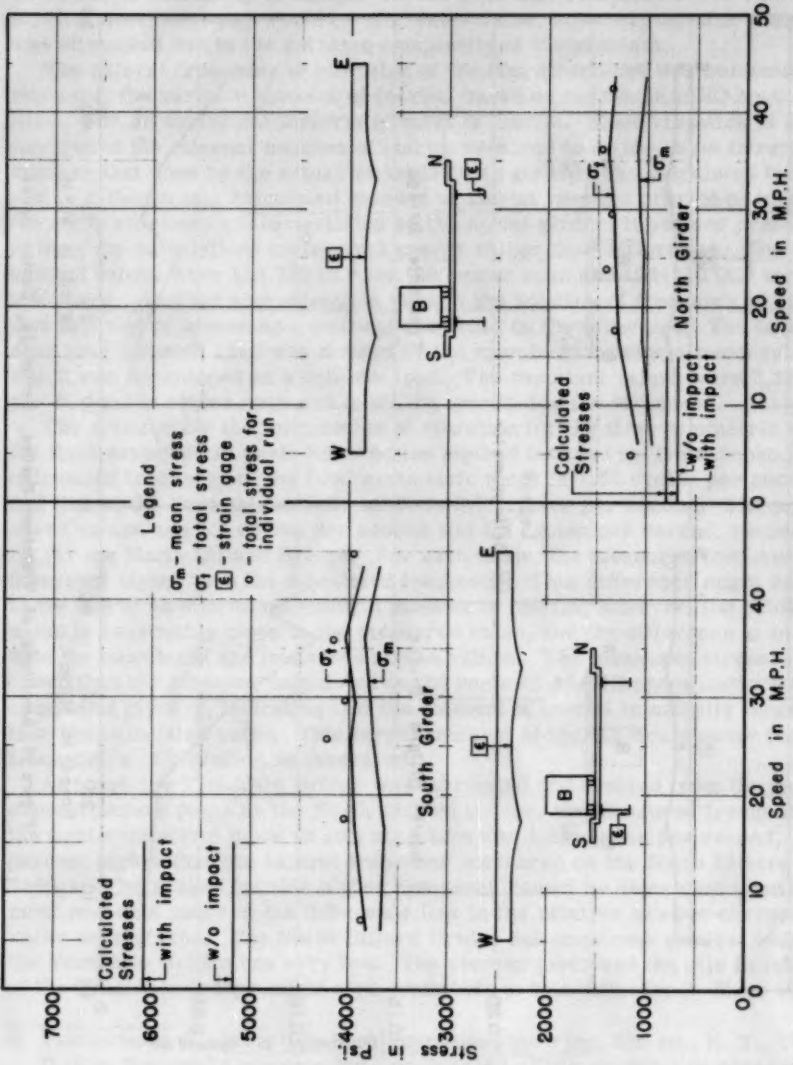


Figure 13. Troutdale Bridge Stress Curves, Series Ib, Vehicle B, Center Span.

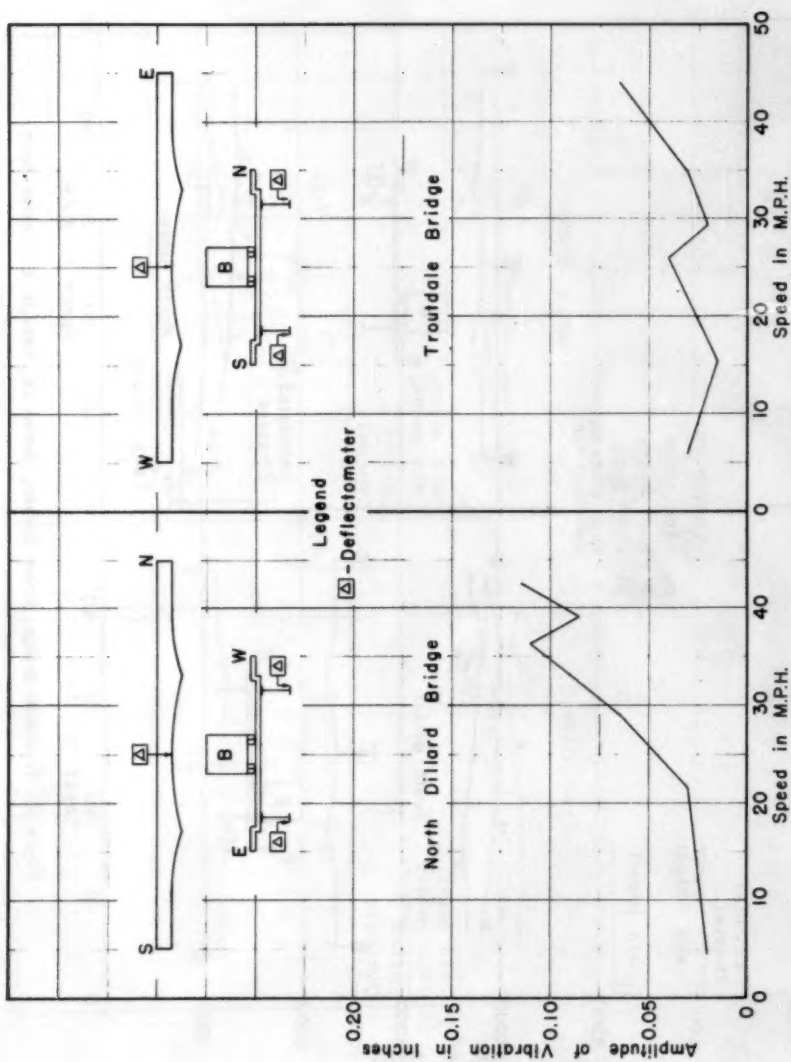


Figure 14. Amplitude of Vibration Curves, Series 1a, Center Spans.

torsional rigidity was based on measurements of the differential deflection of the girders. Therefore, the calculations explain the deviation from a simple-beam distribution in the test structure, but the method cannot be applied to predict the behavior of another bridge except for estimates that might be justified due to similarity of design. An analysis that considered deflection and torsion simultaneously would be of greater value; however, no such analysis was attempted due to the extreme complexity of the problem.

The natural frequency of vibration of the test structures was computed by replacing the variable moment of inertia, based on current AASHO specifications, with an equivalent uniform moment of inertia. Since vibration is a function of the internal moment of inertia required to do the same internal work as that done by the actual variable depth girders was calculated for each span. Although this calculated moment of inertia may not provide precisely the same vibratory characteristics as the actual girder, it seemed preferable to base the calculations on internal energy rather than deflections. The calculated values were 132,720 in.⁴ for the center span and 124-310 in.⁴ for the end spans. Another approximation used in the solution of frequency of vibration was that of assuming a uniform dead load on the structure. The total dead load for each span was divided by the span length giving a mean value which was considered as a uniform load. The resultant values were 2,320 lbs. per ft. for the center span and 2,297 lbs. per ft. for the end spans.

The solution for the frequencies of vibration for the first symmetric and the first asymmetric mode followed the method outlined by Timoshenko.⁴ The calculated frequency of the first symmetric mode is 1.57 cycles per second and that of the first asymmetric mode is 2.50 cycles per second. The measured values are 1.7 cycles per second and 2.7 cycles per second, respectively, for the North Dillard Bridge. For each mode, the measured frequency is 8 percent higher than the calculated frequency. This difference might be due to the use of an equivalent uniform moment of inertia; however, the calculated value is reasonably close to the measured value, and the difference is in line with the calculated and measured stress values. The measured stresses were lower than the stresses calculated on the basis of AASHO specifications for composite girders, indicating that the moment of inertia is actually larger than the calculated value. This larger moment of inertia would cause higher frequencies of vibration as measured.

Although the Troutdale Bridge was fabricated and erected from the same superstructure plans as the North Dillard Bridge, the measured frequency of the first symmetric mode on this structure was 1.87 cycles per second, 10 percent higher than the natural frequency measured on the North Dillard Bridge. The reason for this higher frequency cannot be determined, but the most probable cause of the difference lies in the relative number of transverse deck cracks. The North Dillard Bridge has numerous cracks, while the Troutdale Bridge has very few. The shorter piers and the pile foundation of the Troutdale Bridge might also contribute to this difference. Since the

4. Timoshenko, S., *Vibration Problems in Engineering*, 2nd ed., N. Y., 1937, D. Van Nostrand Company, Inc., pp 345-348. This material is presented assuming each span has the same unit weight and moment of inertia. To apply the method to the present study, it was necessary to include the ratio of the k values for the center and end spans as well as the span lengths in obtaining the trial and error solution. The k value is defined in equation number 126, p. 333 in the text cited above.

measured mean stresses averaged about five percent lower in the Troutdale Bridge, a slightly higher frequency could be expected for this bridge. No records for the Troutdale Bridge were observed in which a residual vibration in the first asymmetric mode was evident. Many of the records for the North Dillard Bridge tests indicate this mode very clearly. Since the same test vehicle was used in testing both bridges, the factor that provides the most plausible reason for this difference is the excessive roughness of the North Dillard Bridge deck. This roughness, in conjunction with the oscillation of the vehicle load on its springs, may cause the asymmetric mode of vibration to be impressed on the structure before the truck leaves the span, and this vibration persists at its natural frequency after the passage.

The existing theory pertaining to amplitudes of vibration of highway bridges is very limited. No one approach can begin to cover the innumerable variables that might be encountered in multiple-span highway structures. There are some basic theoretical concepts that might be applied with reasonable success to simple-span structures, providing enough information about the bridge and vehicle characteristics was available. Several of these concepts, modified by the relationship between the static deflections of the simple-span and the multiple-span structures, were applied to the test bridges. Due to the complexity of the problem, no correlation between measured and computed amplitudes of vibration was accomplished. However, calculations based on an assumed deck contour indicate that the excessive vibration of the North Dillard Bridge can be attributed to deck roughness. With one exception, the calculations were made on the assumption that the test vehicle acted as a single concentrated load as it crossed the structure. Obviously, this is a radical deviation from the actual case since the axle spacing or the pitching action of the load on its springs may in some cases contribute more to the vibration than the speed or natural vibration of the vehicle.

To determine whether the amplitude of vibration could be correlated with the frequency of application of the axle loads, the vehicle velocities required to make the application of the axle loads coincide with the frequency of the bridge were calculated. The speeds at which a point of resonance is indicated by these calculations are about 35 miles per hour for the North Dillard Bridge and 38 miles per hour for the Troutdale Bridge. As shown in Figure 14, an increased amplitude of vibration occurs in the North Dillard Bridge at a speed near this point of resonance, but the Troutdale Bridge shows an increased vibration at a speed appreciably different than this resonant speed. The maximum amplitudes of vibration on both bridges occurred at the maximum test speed obtained. The fact that the North Dillard Bridge has an increased amplitude near the point of resonance while the Troutdale Bridge does not indicates the possibility that deck roughness may cause the application of the axle loads to act as a pulsating force being applied to a point on the bridge.

Assuming a smoothly rolling, concentrated load on a smooth deck, a maximum deflection of 1.11 times the static deflection was calculated for a vehicle speed of 37 miles per hour for the North Dillard Bridge. For the condition of load and surface described, this value is approximately equal to the worst case in which the forced vibration is in phase and is added to the free vibration.⁵ The average total deflection for the two girders at this speed was 1.32

5. Refer to S. Timoshenko, *Vibration Problems in Engineering*, 2nd ed., p. 360, and to equation number 156. In this equation, the static deflection was substituted for $\frac{2P l^3}{EI \pi^4}$ in obtaining the approximate value presented above.

times the static deflection (mean deflection at 5 miles per hour). The speed of 37 miles per hour was used in the calculations because a maximum total deflection occurs in both girders of the North Dillard Bridge at about this speed. A similar analysis was made for the Troutdale Bridge at a vehicle speed of 43 miles per hour since the maximum total deflection occurred at this speed. The calculated ratio of total deflection to static deflection was 1.12 and the measured ratio was 1.13 for this bridge. This approach to calculating the amplitude of vibration was not considered applicable to the North Dillard Bridge because of the roughness of the deck. The calculations were made for purposes of comparison only.

As shown in Figure 11, the profiles of the wheel tracks of the two bridges show that the North Dillard Bridge is considerably rougher than the Troutdale Bridge. Since the greater amplitudes of vibration were measured on the North Dillard Bridge, it seems probable that the deck roughness is a contributing factor to the vibration. It was found that the excess vibration of the rougher bridge could be quite closely accounted for by a mathematical analysis involving a number of approximations and simplifying assumptions.

The continuous profiles of the wheel tracks do not follow a pattern that can be conveniently expressed as an equation; therefore, it would be extremely difficult to base any calculations on the actual deck contour. To determine whether the amplitude of vibration can be attributed to deck roughness, it was assumed that the deck contour could be represented by a sinusoidal curve, and an approximate solution was obtained for the increased force on the bridge due to the wavy contour of the deck surface.⁶ In arriving at a value for this increased force, it was necessary to separate the sprung portion of the load from the unsprung portion. For this purpose, it was assumed that the unsprung weight of Vehicle B was 6,000 pounds. The action of the individual axles was not considered; the total weight was assumed to be a concentrated load. Assuming a wave length of 25 feet and a height of 1/4 inch for the deck contour and a speed of 37 miles per hour, the calculated value of the increased force on the deck was 36,600 pounds, about 51 percent of the vehicle weight. The value of 1/4 inch used for the height of the waves is less than the average height on the actual deck. However, the additional force on the structure would probably be appreciably less than this calculated value due to the different axles being out of phase, the yielding of the bridge deck, and the fact that the actual roughness is variable both in the length and the amplitude of the waves. From these calculations, it is conceivable that a pulsating force of 20,000 pounds might exist, which is the approximate value of force required to cause the measured impact deflections. Calculations for the total deflection were made assuming a 20,000-pound pulsating force was acting in addition to the 71,000-pound weight of the test vehicle. This resulted in a total deflection 31 percent greater than the static deflection.⁷ The measured total deflection at the vehicle speed used in this analysis was 32 percent greater than the static deflection.

In regard to the damping characteristics of the structures, the logarithmic decrement was calculated from deflectometer traces for the two obvious modes in the North Dillard Bridge and for the first symmetric mode in the Troutdale Bridge. The logarithmic decrement for the North Dillard Bridge vibrating in the first symmetric mode is about 0.065, and for the first

6. Timoshenko, S., Vibration Problems in Engineering, 2nd ed., pp. 238-240.

7. Timoshenko, S., Vibration Problems in Engineering, 2nd ed., pp. 356-357.

asymmetric mode about 0.076. The value for the Troutdale Bridge vibrating in the first symmetric mode averaged about 0.063. The fact that the damping in the first symmetric mode (the only mode observed at Troutdale) was about the same on both bridges would seem to eliminate the difference in piers as a factor of any consequence affecting the relative amplitudes of vibration.

The instrumentation used in the tests of the deck system of the North Dillard Bridge consisted of gages at the midpoint and at one end of each stringer and at the midpoint and at points 2 feet from each end of two adjacent floor beams. To determine the degree of fixity of the ends of the floor beams, the relative stringer stresses were used to estimate the portion of the total load being applied to the floor beam at each stringer connection. Having thus established the load being applied at each quarter point, the slopes of the bending moment diagram were calculated. Using these slopes and the measured strains at points 2 feet from the ends of the floor beams, the points of contraflexure were calculated to be 2.19 feet from the ends. From this analysis, the negative moment at the ends of the floor beam was found to be 34.95 foot kips. Under the same assumed load distribution, the negative moment for full fixity would be 92.34 foot kips. The ratio of these values indicates the floor beam connection and torsional stiffness of the girder provides 38 percent fixity. Continuing the analysis, the calculated stress at the center of the floor beam is 4,500 pounds per square inch. The mean stress at this point, computed from measured strains, is 4,030 pounds per square inch—11 percent lower than the value found above. This is considered a satisfactory agreement since the actual load distribution would vary somewhat from the values calculated from stringer strains. The total truck load was applied to the three stringers; no allowance was made for the load going directly to the girders. The stress at the center, calculated from the assumption of hinged end connections, is 5,775 pounds per square inch for the load distribution discussed above. This stress is approximately 43 percent higher than the measured value. The rigidity of the riveted floor beam connections is apparent from this comparison.

The tests that were conducted on the North Dillard Bridge and the Troutdale Bridge provide much valuable information concerning the action of continuous three-span bridges under moving loads. However, no recommendations for changes in design procedures are considered warranted on the basis of this limited information. The need for additional information and verification of the findings of this project is obvious. Only through the consolidation of the results of many such tests can definite conclusions and recommendations for modifications in design practices be provided. The information derived from these bridge tests may be summarized as follows:

- 1) The measured stresses are generally lower than stresses calculated on the basis of current AASHO specifications. At the center of the center span of the North Dillard Bridge, the moment of inertia calculated from measured strains was nine percent higher than the value calculated according to specifications for composite sections. For these bridges, the indication is that the specifications defining the portion of deck to be considered in the composite girder are conservative, but not overly so. Measured stresses at the center of the floor beams were appreciably lower than computed values. This difference is explained by the fixity of the riveted floor beam connection and the torsional stiffness of the girder. Although no shear keys were used between stringer and deck, measurements show that partial composite action

does exist. Also, the fact that the deck is continuous over the stringers causes the portion of the total load carried by the center stringer to be less than the value calculated according to specifications. Because of these factors, the stress calculated for the center stringer was appreciably higher than the measured value. The calculated stress for the outer stringers was similar to the measured mean stress. The portion of the total load carried by the outer stringers was greater than the calculated value, and the degree of composite action was less for these stringers than for the center one.

2) For the stresses calculated from measured strains in the North Dillard Bridge girders, the amplitude of stress oscillation (that is, the excess of the instantaneous stress over the mean) is, in some cases, greater than the allowance provided by the AASHTO impact formula. However, this stress oscillation was caused by a single vehicle, and it would be very unlikely that the high percentage increase would apply to the total design load for the structure. Including the specified impact allowance, the calculated stresses were higher than maximum stress values obtained from measured strains in all cases except for the lesser loaded girder under eccentric loading and negative moment stresses in the lower girder flanges. The total stresses in the floor beams and stringers were lower than total stresses calculated according to specifications. For the Troutdale Bridge, all measured stress oscillations were lower than the corresponding calculated impact allowances. It was concluded that the deck roughness of the North Dillard Bridge contributed much to the impact stresses.

3) The natural frequencies of vibration of bridges of this type can be calculated with reasonable accuracy by using a uniform moment of inertia that provides an equivalent internal energy. The frequency of vibration of the structures during the passage of the test vehicles remained close to the natural frequency of the bridge. No forced vibration with a frequency similar to that of the test vehicle was detected. No conclusive point of resonance is apparent from the various stress curves.

4) The greater mean deflection and mean stress and the lower natural frequency of vibration of the North Dillard Bridge could all be explained by a lesser moment of inertia which could be attributed to the greater cracking of the deck slab of that bridge as compared with the Troutdale Bridge. Its greater amplitude of vibration and stress oscillation appear to be largely due to the greater roughness of its deck surface.

The original test program was prepared by Mr. Neil Van Eenam of the Bureau of Public Roads. Mr. Van Eenam was present during the early phases of testing and assisted in the general organization of the project. The Bureau of Public Roads' test unit was assembled by Mr. E. G. Wiles, who accompanied the unit to the test site and supervised its operation during the tests. Mr. G. S. Vincent represented the Bureau of Public Roads on the project, assisted in the field work, and consulted with the authors at frequent intervals during the analyses of data and offered helpful suggestions in the preparation of the report.

JOURNAL
STRUCTURAL DIVISION
Proceedings of the American Society of Civil Engineers

EARTHQUAKE STRESSES IN SPHERICAL DOMES AND IN CONES

E. P. Popov,¹ A.M. ASCE
(Proc. Paper 974)

SYNOPSIS

Formulas for the primary or membrane stresses in spherical domes and cones due to earthquake loading are given in this paper. The earthquake forces are assumed to act in a horizontal direction and in magnitude are equal to a fraction of the dead weight of the structure itself. Such an assumed earthquake loading is commonly used in the design of structures in areas of seismic activity. It is also shown how the ordinary flexure formula may be used directly in determining the meridional membrane stresses.

INTRODUCTION

Most of the technical literature on structural thin-walled domes and cones is devoted to the analysis of stresses resulting from the dead weight of the structure itself and due to the applied vertical live loads. To a lesser degree stresses caused by assumed wind loads were also studied.^(1,2) To simplify the solution of this problem anti-symmetrical wind loading is usually assumed, i.e., pressure on the windward side and suction on the leeward side act simultaneously. Moreover, the absolute intensity of the wind pressure is assumed to vary in a mathematically convenient manner^(2,3) with the wind invariably acting perpendicularly to the surface of the shell. The solution based on this type of wind distribution, accepted in Europe⁽⁴⁾ but at variance with the American building codes, finds reasonable substantiation with aerodynamic experiments,⁽⁴⁾ and may be used in practice. A few other anti-symmetrical loadings^(3,5) have been also analyzed.

Another type of an anti-symmetrical loading of a dome or a cone with a vertical axis results if distributed forces acting in the same horizontal direction are assumed which are proportional to the dead weight of the shell. Thus, if the weight of a shell of constant wall thickness is w lb. per sq.ft., the

Note: Discussion open until October 1, 1956. Paper 974 is part of the copyrighted Journal of the Structural Division of the American Society of Civil Engineers, Vol. 82, No. ST 3, May, 1956.

1. Prof. of Civ. Eng., Univ. of California, Berkeley, Calif.
2. Numbers in parentheses refer to the Bibliography at the end of the paper.

horizontal force is p lb. per sq.ft. of the same surface. For the entire shell the ratio of p to w is assumed constant. This type of loading is commonly assumed⁽⁶⁾ to simulate an effect of an earthquake on a structure, and there appears to be no readily available solutions for this type of loading applicable to domes and cones. This paper develops the stress analysis formulas first for a spherical dome and then, for a cone subjected to the above type lateral loading. The formulas developed are for the primary or membrane stresses. The shell thicknesses are assumed constant.

A direct technique using the usual flexure formula to obtain the meridional stresses is also illustrated for the two types of shells having the form of a surface of revolution.

NOTATION

a	- radius of a spherical dome
b	- height of a conical shell
C_1, C_2, C_3, C_4	- constants of integration
M	- bending moment
N_ϕ	- meridional force per unit length
N_θ	- hoop force per unit length
$N_{\theta\phi}$	- shearing force per unit length
p	- equivalent weight of the shell per unit of surface area assumed to act horizontally for simulating the effect of an earthquake.
r_0, r_1, r_2	- radii
s	- distance along the generatrix of a cone
S	- area of the middle surface of a dome or a cone
w	- weight of a shell per unit of surface area
X, Y, Z	- components of the applied load per unit of area
α, θ, ϕ	- angles
ϕ, ψ	- special functions of ϕ

Spherical Dome

The basic differential equations of equilibrium for a spherical shell considered acting as a membrane are^(1,3)

$$\frac{\partial N_\theta}{\partial \theta} + \frac{\partial N_{\theta\phi}}{\partial \phi} \sin \phi + 2N_{\theta\phi} \cos \phi + Xa \sin \phi = 0 \quad (1)$$

$$\frac{\partial N_{\theta\phi}}{\partial \theta} - N_\theta \cos \phi + \frac{\partial N_\phi}{\partial \phi} \sin \phi + N_\phi \cos \phi + Ya \sin \phi = 0 \quad (2)$$

$$N_\theta + N_\phi = -Za \quad (3)$$

and, as may be seen from Figs. 1a and b, for the assumed earthquake loading

$$X = p \sin \theta \quad (4)$$

$$Y = -p \cos \phi \cos \theta \quad (5)$$

$$Z = p \sin \phi \cos \theta \quad (6)$$

Equations 1, 2, and 3 must be solved for the three unknowns N_θ , $N_{\theta\phi}$ and N_ϕ and because of their structure this can be accomplished(3) by prescribing the form of the expression for two of the unknowns as

$$N_\phi = \bar{\Phi} \cos \theta \quad (7)$$

$$N_{\theta\phi} = \bar{\Psi} \sin \theta \quad (8)$$

where $\bar{\Phi}$ and $\bar{\Psi}$ are functions of ϕ only, and then following a rather standardized procedure.(3,1)

Thus, by substituting Eqs. 7 and 8 into Eqs. 1, 2, and 3 and eliminating N_θ , with the aid of Eqs. 4, 5, and 6, one obtains

$$\frac{d\bar{\Psi}}{d\phi} + 2\bar{\Psi} \cot \phi + \frac{\bar{\Phi}}{\sin \phi} + 2pa = 0 \quad (9)$$

$$\frac{d\bar{\Phi}}{d\phi} + 2\bar{\Phi} \cot \phi + \frac{\bar{\Psi}}{\sin \phi} = 0 \quad (10)$$

Then, by defining new terms

$$U_1 = \bar{\Phi} + \bar{\Psi} \quad (11)$$

$$U_2 = \bar{\Phi} - \bar{\Psi} \quad (12)$$

and by first adding and then subtracting Eqs. 9 and 10, one obtains

$$\frac{dU_1}{d\phi} + \left[2 \cot \phi + \frac{1}{\sin \phi} \right] U_1 + 2pa = 0 \quad (13)$$

$$\frac{dU_2}{d\phi} + \left[2 \cot \phi - \frac{1}{\sin \phi} \right] U_2 - 2pa = 0 \quad (14)$$

The solution of these equations is

$$U_1 = (C_1 + 2pa \cos \phi + pa \sin^2 \phi) \frac{1 + \cos \phi}{\sin^3 \phi} \quad (15)$$

$$U_2 = (C_2 - 2pa \cos \phi + pa \sin^2 \phi) \frac{1 - \cos \phi}{\sin^3 \phi} \quad (16)$$

and, from Eqs. 11 and 12, for use in Eq. 7, one obtains

$$\begin{aligned} \Phi &= \frac{1}{2}(U_1 + U_2) \\ &= \frac{1}{2} \left[(C_1 + C_2) + (C_1 - C_2) \cos \phi + 4pa \cos^2 \phi + 2pa \sin^2 \phi \right] \frac{\cos \theta}{\sin^3 \phi} \end{aligned} \quad (17)$$

Here, however, since N_ϕ at $\phi = 0$ must be finite, the expression in the square brackets for $\phi = 0$ must equal zero. This condition yields

$$C_1 = -2pa \quad (18)$$

Moreover, since $\sin \phi$ in the denominator of Eq. 17 is to the third power, first and second derivatives of the expression in the square brackets must also be equal to zero. The last condition yields

$$C_2 = 2pa \quad (19)$$

These constants may be verified using in the same manner the expression for Ψ or by the more usual procedure of using the conditions of static equilibrium for the whole dome.

On the above bases the membrane stresses in a spherical dome subjected to an assumed earthquake loading given by Eqs. 4, 5, and 6 are

$$N_\phi = \Phi \cos \theta = pa \frac{\tan^2 \frac{\phi}{2}}{\sin \phi} \cos \theta \quad (20)$$

$$N_{\theta\phi} = \Psi \sin \theta = pa(-2 + 2 \cos \phi + \sin^2 \phi \cos \phi) \frac{\sin \theta}{\sin^3 \phi} \quad (21)$$

$$N_\theta = -Za - N_\phi = -pa \left(\sin \phi + \frac{\tan^2 \frac{\phi}{2}}{\sin \phi} \right) \cos \theta \quad (22)$$

The nature of the variation of these quantities along some sections of a dome is shown in Fig. 2.

It is of considerable interest to note that Eq. 20 may be derived directly using flexure formula. Thus, noting that the area S of the middle surface of a spherical dome is

$$\bar{y} = \frac{1}{2} a (1 + \cos \phi) \quad (23)$$

and that the centroid of such an area is given by

$$S = 2\pi a^2 (1 - \cos \phi) \quad (24)$$

as shown in Fig. 3a. Then the bending moment M caused by the horizontal load of p lb. per unit of surface area around a horizontal axis A in the plane of a cut is

$$\begin{aligned} M &= 2\pi a^2 (1 - \cos \phi) p \left[\frac{1}{2} a (1 + \cos \phi) - a \cos \phi \right] \\ &= p\pi a^3 (1 - \cos \phi)^2 \end{aligned} \quad (25)$$

This moment M is resisted by the vertical components of the forces N_ϕ , and on the basis of the flexure formula the following relation holds true

$$N_\phi \sin \phi = \frac{My}{I} \quad (26)$$

where I is the moment of inertia of a line in a form of a circle of radius $a \sin \phi$ which is $\pi a^3 \sin^3 \phi$. Then, since $y = a \sin \phi \times \cos \theta$, see Fig. 3b, one finds directly

$$N_\phi = \frac{1}{\sin \phi} \frac{My}{I} = \frac{pa \tan^2 \frac{\phi}{2}}{\sin \phi} \cos \theta \quad (27)$$

which is the same expression as before found more simply.

After N_ϕ is determined, N_θ may be found from Eq. 3. Finally, using Eq. 2, the expression for $N_\theta \phi$ may be determined. This, then, is an alternative procedure for obtaining Eqs. 20, 21, and 22.

Conical Shell

The basic differential equations of equilibrium for a conical shell may be established directly by considering an infinitesimal element of a cone or by carrying out a limiting process for the general equations^(1,3) of equilibrium for shells in the form of a surface of revolution where for a cone, see Fig. 4,

$$\phi = \frac{1}{2} \pi - \alpha = \text{Const.} \quad (28)$$

$$r_1 = \infty \text{ and } r_2 = \frac{r_0}{\cos \alpha} \quad (29)$$

$$\frac{d}{d\phi} = r \frac{d}{ds} \quad (30)$$

The three pertinent differential equations are

$$\frac{\partial N_\theta}{\partial \theta} + \frac{\partial(N_{\theta\phi} r_0)}{\partial s} + N_{\theta\phi} \sin \alpha + X r_0 = 0 \quad (31)$$

$$\frac{\partial(N_{\phi} r_0)}{\partial s} + \frac{\partial N_{\theta\phi}}{\partial \theta} - N_\theta \sin \alpha + Y r_0 = 0 \quad (32)$$

$$N_\theta + \frac{r_0}{\cos \alpha} Z = 0 \quad (33)$$

For the assumed earthquake loading, from Eq. 4, 5, and 6 one obtains

$$X = p \sin \theta \quad (34)$$

$$Z = p \cos \alpha \cos \theta \quad (35)$$

$$Y = -p \sin \alpha \cos \theta \quad (36)$$

and since $r_0 = s \sin \alpha$, from Eq. 33 one gets

$$N_\theta = -ps \sin \alpha \cos \theta \quad (37)$$

which is one of the expressions sought. Then again as for a spherical dome, because of the nature of the differential Eqs. 31 and 32, N_ϕ and $N_{\theta\phi}$ must be assumed to be of the form given by Eqs. 7 and 8. Whence substituting Eqs. 8 and 37 into 31, upon simplification, one obtains

$$\frac{d\Psi}{ds} + 2\frac{\Psi}{s} + 2p = 0 \quad (38)$$

The solution of this differential equation is

$$\Psi = \frac{C_3}{s^2} - \frac{2}{3}ps \quad (39)$$

where C_3 is a constant of integration which must be taken equal to zero to yield finite value of $N_{\theta\phi}$ at $s = 0$. Hence, from Eqs. 8 and 39

$$N_{\theta\phi} = -\frac{2}{3}ps \sin \theta \quad (40)$$

Finally, the substitution of Eqs. 7, 37, and 40 into 32 and simplification yields

$$\frac{d\bar{\Phi}}{ds} + \frac{\bar{\Phi}}{s} - \frac{2p}{3s\sin\alpha} = 0 \quad (41)$$

the solution of which is

$$\bar{\Phi} = \frac{C_4}{s} + \frac{ps}{3s\sin\alpha} \quad (42)$$

where again the constant C_4 must be set equal to zero to yield finite answer for N_ϕ at $s = 0$. Therefore,

$$N_\phi = \bar{\Phi} \cos\theta = \frac{ps}{3s\sin\alpha} \cos\theta \quad (43)$$

The nature of the variation of N_θ , $N_{\theta\phi}$ and N_ϕ as given by Eqs. 37, 40, and 43 is shown in Fig. 5.

For a conical shell the internal forces in the cone may be found with the aid of the flexure formula much the same as for a spherical dome. Thus, note that the surface area S of a cone, see Fig. 6, is

$$S = \pi b^2 \tan\alpha \sec\alpha \quad (44)$$

and that the centroid of such an area is

$$\bar{z} = \frac{2}{3}b \quad (45)$$

On this basis the bending moment M around an axis passing through point A is

$$M = \frac{1}{3}p\pi b^3 \tan\alpha \sec\alpha \quad (46)$$

whence by applying Eq. 26 with $y = b \tan\alpha \cos\theta$, one obtains

$$N_\phi = \frac{1}{\sin\phi} \frac{My}{I} = \frac{ps}{3s\sin\alpha} \cos\theta \quad (47)$$

As shown earlier, N_θ follows directly from Eq. 33, whereas with N_ϕ and $N_{\theta\phi}$ known, either Eq. 31 or 32 can yield the expression for $N_{\theta\phi}$.

Another case where knowledge of the membrane stresses due to an earthquake loading of the type considered in this paper is important occurs in cylindrical shells. The available(1,7) solutions for the membrane stresses caused by the shell's own weight, however, provide the necessary information using angles 90° out of phase with the gravity loading.

ACKNOWLEDGMENT

The author is indebted to Joseph Cham, a graduate student in Civil Engineering at the University of California, for checking the work.

BIBLIOGRAPHY

1. "Theory of Plates and Shells" by S. Timoshenko, Chapter X, McGraw-Hill, (New York), 1940.
2. "Handbuch für Eisenbetonbau" by Fr. Dischinger, Vol. 6, Chapter 2, 4th Edition, Ernst U. Sohn, (Berlin), 1928.
3. "Flächentragwerke" by Karl Girkmann, pp. 365-372, 3rd Edition, Springer, (Wien), 1954.
4. "Einführung in die Schalenstatik" by Alf Pfluger, pp. 14 and 33, Schroedel, (Hannover), 1948.
5. "Scienza delle Costruzioni" by O. Belluzzi, Vol, III, Zanichelli, (Bologna), 1951.
6. "Uniform Building Code," Pacific Coast Building Officials' Conference, 1952 Edition.
7. "Design of Cylindrical Concrete Shell Roofs," ASCE Manual of Engineering Practice No. 31, 1952.

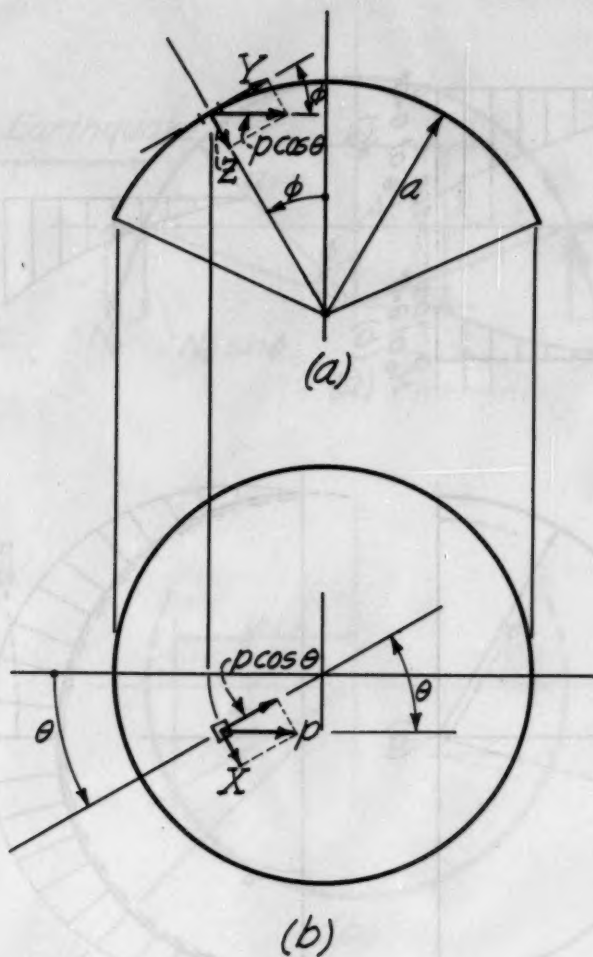


Fig. 1

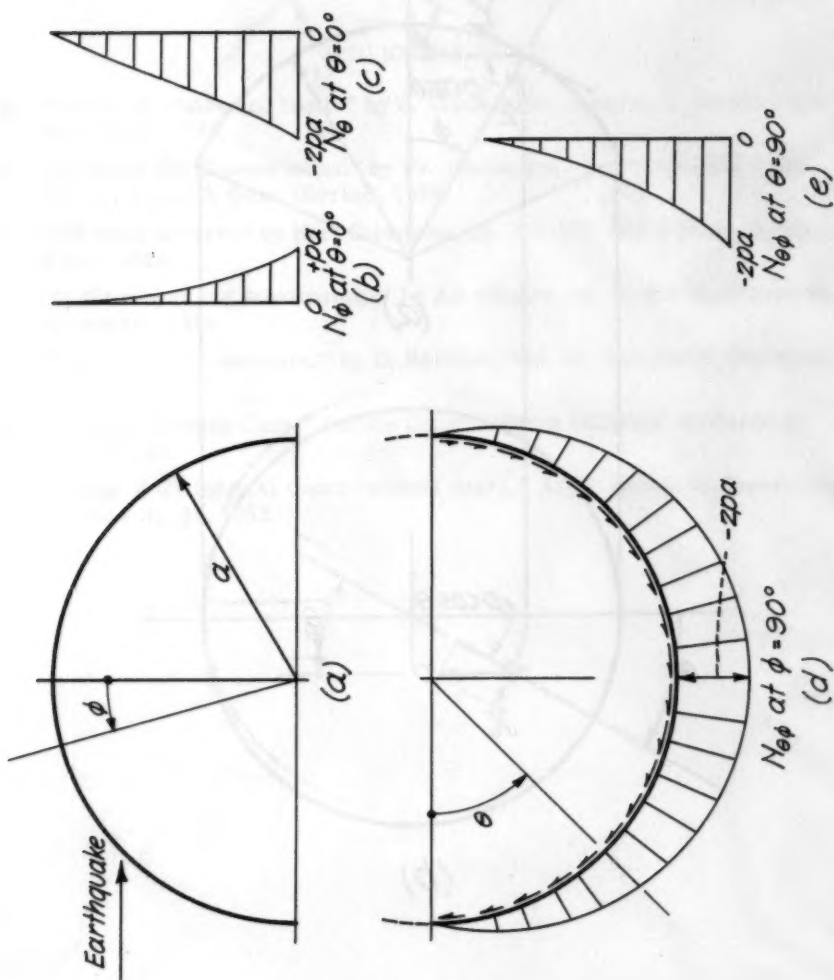


Fig. 2

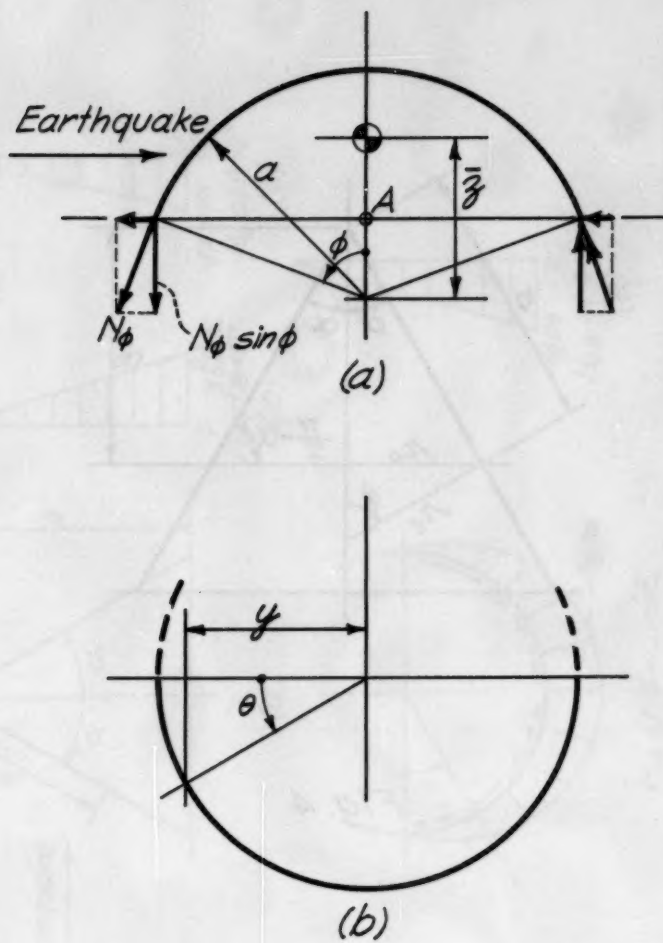


Fig. 3

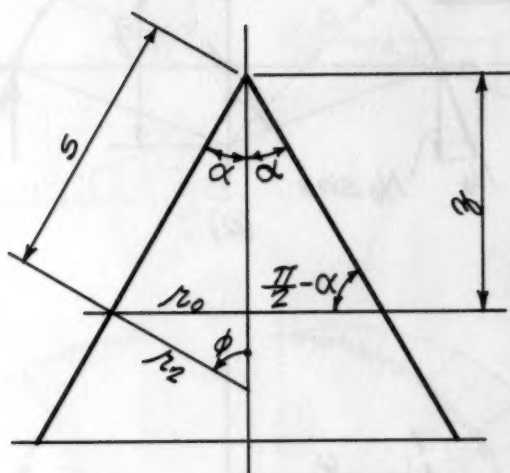


Fig. 4

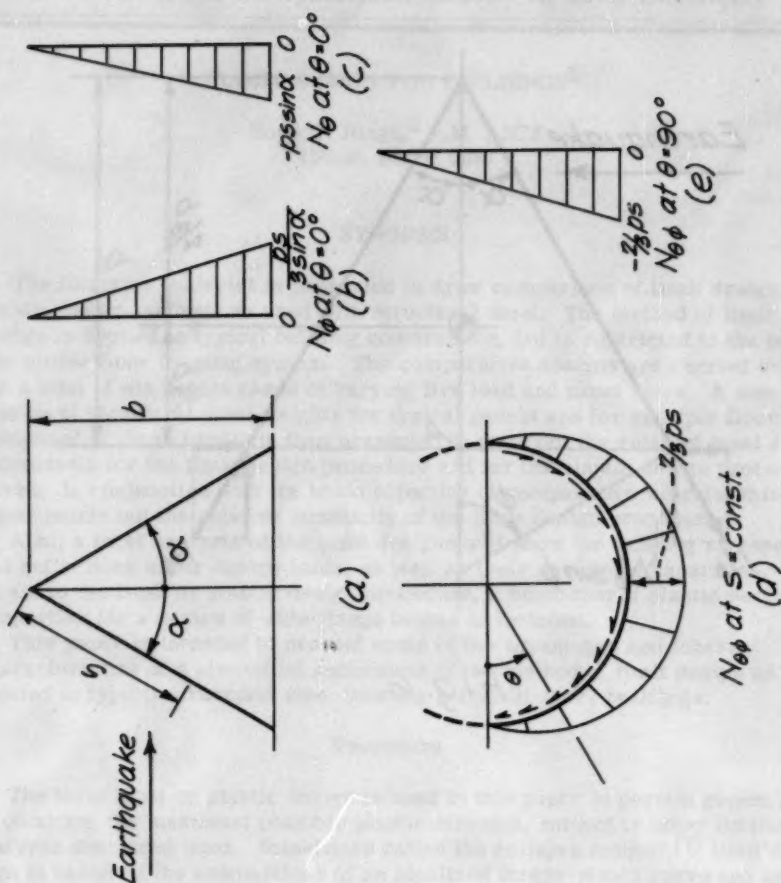


Fig. 5

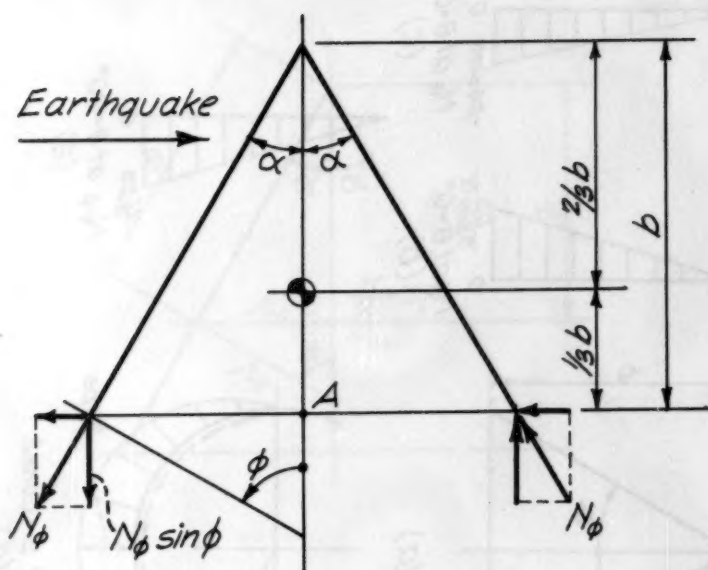


Fig. 6

JOURNAL STRUCTURAL DIVISION

Proceedings of the American Society of Civil Engineers

LIMIT DESIGN FOR BUILDINGS¹

Boyd C. Ringo,² J.M. ASCE
(Proc. Paper 986)

SYNOPSIS

The following material is presented to draw comparison of limit design to elastic design methods as used with structural steel. The method of limit design is applied to typical building construction, but is restricted to the beam and girder floor framing system. The comparative designs are carried out for a total of six design cases of varying live load and panel sizes. A summation of structural steel weights for typical panels and for multiple floors composed of these panels is then presented to point out the relative steel requirements for the limit design procedure and for the elastic design procedures. In conjunction with the basic objective of comparative weights, this paper points out the relative simplicity of the limit design procedure.

Also, a brief analysis of the limit designs will show the existing stresses and deflections under design loads, as well as their remaining capacities. As an aid to the limit or plastic design procedure, a tabulation of plastic section properties for a series of wide-flange beams is included.

This paper is intended to present some of the advantages and inherent characteristics of a simplified application of the method of limit design as applied to typical structural steel framing for multi-story buildings.

Procedure

The term limit or plastic design is used in this paper to pertain generally to obtaining the maximum possible plastic strength, subject to other limiting features discussed later. Sometimes called the collapse method,⁽⁷⁾ limit design is based on the assumptions of an idealized stress-strain curve and an idealized plastic stress distribution for a section under full ductility.⁽⁸⁾ The introduction of a safety factor is made by multiplying the design load by a load factor, this product being the limit load. The structure, in this case the

Note: Discussion open until October 1, 1956. Paper 986 is part of the copyrighted Journal of the Structural Division of the American Society of Civil Engineers, Vol. 82, No. ST 3, May, 1956.

1. Based on a thesis presented to Washington University at St. Louis, Mo., in May, 1954, in partial fulfillment of the degree of Master of Science.
2. Instructor of Civil Eng., Michigan State Univ., East Lansing, Mich.

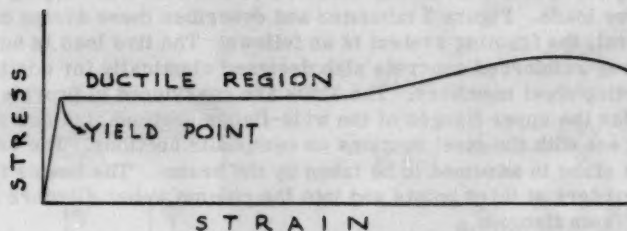
beam and girder framing, is then designed to fail under the action of this limit load. Failure is taken as that point at which excessive deformations appear. In the case of the beams and girders, these deformations will begin to occur when full plastic hinges are developed at each support of the member and at its mid-span, thus forming a system which is free to deflect under little or no increase in the applied load.

A proper value for the load factor, termed q , must be chosen for use in the limit design procedure. In the case of a simply-supported beam under any condition of transverse static loading, there exists a safety factor of 1.85 based on A.S.T.M. A7 steel and an average shape factor of 1.12. This shape factor was computed by the author. The sense of this is that the load may be increased by 85% above that load dictated by an A.I.S.C. design before a flexural failure, in the form of excessive deformations, will occur. The shape factor is defined as the ratio of plastic section modulus to elastic section modulus. The average shape factor, k , of 1.12 is taken from the plastic section properties of the fifty-three wide-flange beams tabulated in this paper. Since this safety factor of 1.85 is a minimum value for general beam loadings, this value is taken as an approximate value for the load factor q . Due to the variables existing, the value of 1.85 will be rounded off to 1.90. Subsequent investigations may produce a more accurate or more logical value for q , but for the comparative purposes of this paper, the value of 1.90 will be used. This load factor is applied to the total design load, LL plus DL ; thus, omitting the inclusion of comparative live load to dead load ratios.

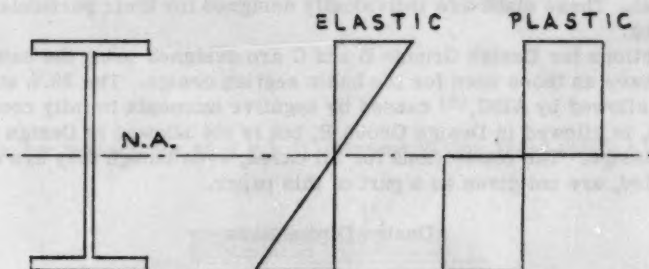
There is no established code for the use of limit design in this country; therefore, it is necessary to choose limiting values for stresses and deflections. The limit designs in this paper are based on the following: The flexural yield point shall be a minimum of 33.0 ksi (A.S.T.M. A7 structural steel).⁽¹⁾ The yield point in shear shall be 19.0 ksi. The load factor shall be taken as 1.90 as previously stated. In addition to these requirements, the following criterion is established at a load factor of 1.00: The maximum deflection shall not exceed the span divided by 360. The maximum flexural stress shall not exceed the yield point of 33.0 ksi.

There are two methods of elastic design presented. One is an elastic design assuming all beams and girders simply supported. The other is an elastic design assuming full continuity through the supporting members. Although the logical comparison is between limit design and the elastic design assuming continuity, the comparison with the elastic design assuming simply supported members is made as an additional point of interest. Connections are designed in accordance with the particular design group to which they apply. Both methods of elastic design are handled under the A.I.S.C. specifications (1952),⁽⁶⁾ with deflections being limited to the span divided by 360. In the computations of deflections for the elastic design cases and for the plastic design cases under the load factor of 1.00, these deflections are based on a five-span continuous beam. Column restraint is neglected and extreme end supports are considered hinged. This same five-span continuous beam is the basis for the elastic design assuming continuity.

The design methods are compared through their application to six design cases. The methods themselves will be referred to as design groups. Design Group A refers to the method of elastic analysis assuming simply-supported members. Design Group B refers to the method of elastic analysis assuming continuity through supporting members. Design Group C refers to the method



Idealized Stress-Strain Relationship



Idealized Stress Distributions

FIGURE 1

Identification of Design Cases

Case	Panel Size	Live Load	Design Group
Case I	35' x 35'	75. psf	A, B, & C
Case II	35' x 35'	200. psf	A, B, & C
Case III	35' x 35'	400. psf	A, B, & C
Case IV	25' x 25'	75. psf	A, B, & C
Case V	25' x 25'	200. psf	A, B, & C
Case VI	25' x 25'	400. psf	A, B, & C

FIGURE 2

of limit design as previously described. The six design cases, numbered I through VI, refer to two basic bay sizes under the action of varying magnitudes of live loads. Figure 2 tabulates and describes these design cases.

In general, the framing system is as follows: The live load is supported on a one-way reinforced concrete slab designed elastically for continuity over the supporting steel members. The slabs are considered to provide lateral restraint for the upper flanges of the wide-flange sections, but are not considered to act with the steel sections as composite sections. The entire dead load of the slabs is assumed to be taken by the beams. The beams frame into the steel girders at third points and into the column webs. Girders frame into the column flanges.

The reinforced concrete slabs are designed under the ACI Building Code 318-51,⁽²⁾ using the coefficients of the ASCE Joint Committee Specifications of 1940.⁽⁴⁾ Compressive strength of concrete is taken at 3,000. psi for the 28-day cylinder strength. Allowable reinforcing steel strength is taken at 20,000. psi. These slabs are individually designed for their particular span and loading.

Connections for Design Groups B and C are designed using the same allowable stresses as those used for the basic section design. The 20% stress increase allowed by AISC,⁽⁶⁾ caused by negative moments in fully continuous members, is allowed in Design Group B, but is not allowed in Design Group C on limit design. The connections for all cases, even though they are designed and detailed, are not given as a part of this paper.

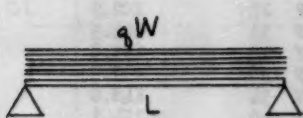
Design Discussions

Design Group C is the consideration of each of the six design cases by the method of limit design. The procedure followed for each of these cases is illustrated in Figure 5 for the specific Design Case V, a 25' by 25' panel with a LL of 200. psf. All beams and girders are considered fully continuous through their supporting members. Figure 3 lists the expressions used in the limit designs. Figure 4 tabulates the plastic section properties of a series of WF shapes.

Each beam and girder is first selected using a limit design procedure. After determination of the ultimate moment and shear for the given loads is made, the members themselves are selected from the plastic section property table previously noted. Computation of both the ultimate moment and the ultimate shear is simple and quick. After the specific section is chosen, a check is then made of the maximum flexural stress, maximum shear stress, and the maximum centerline deflection at a load factor of 1.00. These characteristics are based on the premise that stresses will remain within the minimum yield point under working loads and are therefore based on the five-span continuous beam. This procedure is followed for both beams and girders in all design cases. The value for deflection is given both as an absolute value and as related to span length in order to check the limiting deflection criterion. Figure 6 summarizes the results for Design Group C.

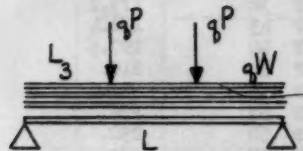
Elastic Design Group B is based on the five-span fully continuous beam, neglecting column restraint. Dead load moments are, of course, computed on the basis of all spans loaded. Live load moments are computed on the basis of alternate span loading for the worst possible moments both at center span and over supports. Centerline deflections are also computed on the

Design Expressions



$$M_{ULT} = \frac{qWL}{16}$$

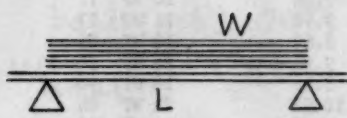
$$V_{ULT} = \frac{qW}{2}$$



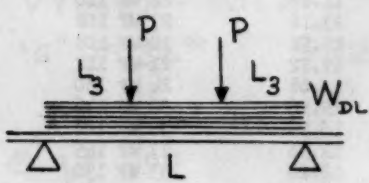
$$M_{ULT} = \frac{qPL}{6} + \frac{qWL}{16}$$

$$V_{ULT} = qP + \frac{qW}{2}$$

Check for Deflections at $q = 1$ (stresses within yield point)



$$\Delta_{\epsilon} = \frac{L^3}{EI} \left\{ .00316 W_{DL} + .00728 W_{LL} \right\}$$



$$\Delta_{\epsilon} = \frac{L^3}{EI} \left\{ .00448 P_{DL} + .01561 P_{LL} + .00316 W_{DL} \right\}$$

Maximum deflection computed with LL on alternate spans

Expressions for Limit Design

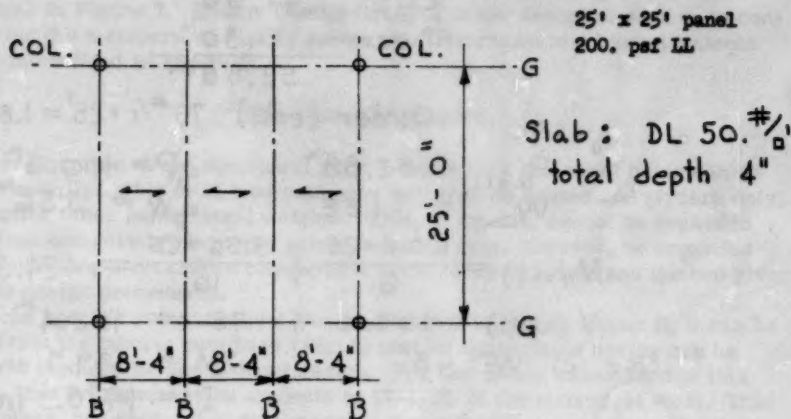
FIGURE 3

Plastic Section Properties for use in Limit Design

Z in. ³	A _p in. ²	WF Section	M (ult.) ft.k.
37.4	2.68	12 WF 27	102.9
38.0	2.60	10 WF 33	104.5
46.4	3.54	14 WF 30	127.8
50.0	3.34	12 WF 36	137.5
53.8	3.76	14 WF 34	148.0
56.0	3.20	12 WF 40	154.1
63.0	4.48	16 WF 36	173.2
67.8	3.88	14 WF 43	186.4
71.8	4.60	16 WF 40	197.5
76.4	4.28	14 WF 48	210.
81.0	5.20	16 WF 45	223.
85.4	4.66	14 WF 53	235.
90.8	5.70	16 WF 50	250.
100.0	6.02	18 WF 50	275.
100.4	4.78	14 WF 61	276.
110.8	6.58	18 WF 55	305.
116.2	6.44	16 WF 64	320.
122.2	7.02	18 WF 60	336.
130.2	7.08	16 WF 71	358.
142.4	7.90	21 WF 62	392.
143.2	7.24	18 WF 70	394.
157.8	8.48	21 WF 68	434.
158.8	7.84	18 WF 77	437.
170.2	9.98	21 WF 73	468.
176.0	8.68	18 WF 85	484.
198.4	9.92	24 WF 76	546.
204.2	8.46	18 WF 96	562.
222.0	10.58	24 WF 84	610.
239.4	11.06	21 WF 96	658.
250.4	11.60	24 WF 94	688.
273.8	12.46	27 WF 94	753.
274.8	10.50	24 WF 100	757.
275.4	10.16	21 WF 112	758.
304.2	11.46	24 WF 110	837.
304.6	13.16	27 WF 102	838.
341.6	15.52	30 WF 108	938.
353.2	12.72	21 WF 142	972.
365.8	12.68	24 WF 130	1006.
373.2	15.96	30 WF 116	1027.
403.4	16.56	30 WF 124	1109.
445.2	14.96	27 WF 145	1226.
460.8	18.20	33 WF 130	1267.
494.6	16.36	27 WF 160	1360.
507.6	19.00	33 WF 141	1397.
572.8	21.22	36 WF 150	1574.
585.6	18.14	30 WF 172	1611.
616.4	22.16	36 WF 160	1693.
651.4	19.68	30 WF 190	1790.
660.2	23.12	36 WF 170	1816.
707.8	24.62	36 WF 182	1947.
727.0	21.48	30 WF 210	2000.
762.4	26.16	36 WF 194	2090.
905.0	25.50	36 WF 230	2489.

FIGURE 4

Limit Design Procedure - Design Case V



Beam : LL 200 $\frac{\#}{ft^2}$ x 25' x 8.33' = 41.66^k
 slab 50 $\frac{\#}{ft^2}$ x 25' x 8.33' = 10.42^k
 beam (est.) 70 $\frac{\#}{ft^2}$ x 25' = 1.75^k

$$W_{DL+LL} = 53.83^k$$

$$q_b = 1.90 \quad \therefore q_b W = 102.3^k$$

$$M(ULT.) = \frac{102.3 \times 25}{16} = 156.2^{1k}$$

$$V(ULT.) = 51.2^k$$

Use 16" WF 36[#]

$$SM = 56.3 \text{ in}^3$$

$$I = 446.3 \text{ in}^4$$

$$W_{DL} = 0.80^k$$

$$@ q_b = 1.00$$

$$M_{DL} = -.079 \times 11.22 \times 25' = -22.16$$

$$M_{LL} = -.117 \times 41.66 \times 25 = -121.80$$

$$f = \frac{143.96 \times 12}{56.3} = \pm 30.7 \text{ ksi}$$

$$\Delta_t = \frac{2.7 \times 10^7}{30(10^3)(446.3)} \left\{ .00316[11.22] + .00728[41.66] \right\} = 0.689'' = \frac{L}{436}$$

FIGURE 5

Girder :

slab	10.42 ^k
LL	41.66 ^k
Beam	0.80 ^k
	<hr/> 52.88 ^k

 $q_b = 1.90$ Girder (est.) $75\#1 \times 25' = 1.88^k$

$$P_{DL+LL} = 52.88^k$$

$$q_b P = 100.6^k$$

$$W_{DL} = 1.88^k$$

$$q_b W = 3.56^k$$

$$M(ULT.) = \frac{100.6 \times 25}{6} + \frac{3.56 \times 25}{16} = 424.3^{IK}$$

$$V(ULT.) = 100.6 + 1.78 = 102.4^k$$

Use 21" WF 68"

$$SM = 139.9 \text{ in}^3$$

$$I = 1478.3 \text{ in}^4$$

$$W_{DL-G} = 1.70^k$$

@ $q_b = 1.00$

$$M_{DL} = -.211 \times 11.22 \times 25' = -59.2^{IK}$$

$$M_{LL} = -.298 \times 41.66 \times 25 = -310.4^{IK}$$

$$M_{DL-G} = -.079 \times 1.70 \times 25 = -3.4^{IK}$$

$$-373.0^{IK}$$

$$f = \frac{373.0 \times 12}{139.9} = \pm 32.0 \text{ ksi}$$

$$\Delta_{\pm} = \frac{2.7 \times 10^7}{30(10^3)(1478.3)} \left\{ .00448(11.22) + .01561(41.66) + .00316(1.70) \right\}$$

$$\Delta_{\pm} = 0.430'' = \frac{L}{698}$$

FIGURE 5

Summary - Limit Design Group C

Case	LL	Panel	Slab	Beam	Girder
I	75 psf	35' x 35'	4"	16 WF 50	24 WF 84
II	200 psf	35' x 35'	5"	21 WF 73	33 WF 130
III	400 psf	35' x 35'	7"	30 WF 108	36 WF 230
IV	75 psf	25' x 25'	4"	12 WF 27	16 WF 45
V	200 psf	25' x 25'	4"	16 WF 36	21 WF 68
VI	400 psf	25' x 25'	5"	18 WF 55	27 WF 102

FIGURE 6

basis of alternate span loading for the maximum possible centerline deflection of the member under consideration. Results of Design Group B are summarized in Figure 7. Elastic Design Group A is the design of each case considering the members as simply supported. Structural steel requirements are summarized in Figure 8.

Discussion of Weights

A comparison of the structural steel weights on a per panel basis can be made initially. This dead load summary will include beams and girders only, neglecting other lesser steel weights. This, of course, cannot be regarded as a true measure of economic comparison. It may, however, be regarded as establishing a maximum comparison between limit design and the two given elastic design procedures.

In the specific comparison of Design Group C to Design Group B, it can be seen from the tabular summary (Fig. 9) that an appreciable saving can be realized through the use of limit design. For the design cases used in this paper, this averaged saving amounts to 17-1/2% of the structural steel. This percentage, however, takes no account of the columns, connection materials, or fabrication wastes.

In order to further establish a sense of value concerning the relative merits of limit design, these basic panel designs will be applied to three typical multi-floor building units. Each unit consists of two, three, or four floors, roof, and supporting columns. In assembling of structural steel weights of these units, supplementary designs of a roof frame and supporting columns are required. Although this paper does not include a presentation of these elements individually, the basis for their design is as follows: The roof frame is designed as simply supported members under the specifications of the A.I.S.C. Steel Construction Code with a uniform LL of 30. psf and DL of 50. psf. This design is constant for all design cases and groups and its framing is identical to that of the floor systems. All columns are chosen from the A.I.S.C. code considering each column to be axially loaded, neglecting any moments induced because of alternate floor panel loadings. The weights of the members chosen by these roof framing and column designs are then included in the building panel weights presented. The roof members and column selections are summarized for Case V, Design Group C in Figure 10.

The structural steel weights for the elements of each of the three building panels are summarized in Figure 11. These dead load weights are given in terms of pounds per square foot of usable floor area based on column centerline dimensions. All total weights are rounded off to the nearest ten pounds, but the unit weights are allowed to remain at normal slide rule accuracy.

Figure 11, tabulating these structural steel dead weights, shows, as anticipated, the unit weights to vary little with the addition of floors, but to depend principally on the combination of design case and design group. Referring again to the comparison between limit design and Design Group B, a savings of approximately 16% can be realized. This figure, although it does not include consideration of connection materials, does account in a general way for roof and column weights. Considering the three floor building under Design Case V (25' x 25' panel; 200. psf LL), the weight differential between limit design and elastic design assuming continuity is 3,980. pounds for each bay. If a building of this type 75' by 150' were erected, there would be a total

Summary - Design Group B
(fully continuous elastic design)

Case	LL	Panel	Slab	Beam	Girder
I	75 pef	35' x 35'	4"	18 WF 55	24 WF 100
II	200 pef	35' x 35'	5"	24 WF 94	36 WF 170
III	400 pef	35' x 35'	7"	33 WF 130	36 WF 280
IV	75 pef	25' x 25'	4"	14 WF 30	18 WF 50
V	200 pef	25' x 25'	4"	16 WF 45	24 WF 94
VI	400 pef	25' x 25'	5"	21 WF 68	30 WF 124

FIGURE 7

Summary - Design Group A
(simply supported elastic design)

Case	LL	Panel	Slab	Beam	Girder
I	75 pef	35' x 35'	4"	21 WF 73	33 WF 130
II	200 pef	35' x 35'	5"	30 WF 108	36 WF 230
III	400 pef	35' x 35'	7"	36 WF 160	36 WF 260
					2- 1 $\frac{1}{2}$ " x 15" FL wgt = 308. #/ft
IV	75 pef	25' x 25'	4"	16 WF 36	21 WF 68
V	200 pef	25' x 25'	4"	18 WF 60	30 WF 108
VI	400 pef	25' x 25'	5"	24 WF 84	36 WF 150

FIGURE 8

Dead Load Summary Per Panel

Design Case	Design Group		
	A elastic	B elastic	C limit
I	12,220. #	9,280. #	8,190. #
II	19,390. #	15,830. #	12,120. #
III	27,590. #	23,460. #	19,390. #
IV	4,400. #	3,500. #	3,150. #
V	7,200. #	5,730. #	4,400. #
VI	10,050. #	8,200. #	6,680. #

FIGURE 9

Design Case V
Roof Framing Members and Column Selections

Roof Framing Members :	Beam	12 WF	27
	Girder	18 WF	50
Column supporting roof		8 WF	24
Column supporting 4th floor		10 WF	49
Column supporting 3rd floor		12 WF	85
Column supporting 2nd floor		14 WF	119
Column supporting 1st floor		14 WF	150

Design Group C Limit Design

Design Case V

25' x 25' panel
200. psf LL

FIGURE 10

Building Weights
Unit weights per square foot of usable floor area

Case	Design Group	Weight in Pounds per sq. ft.		
		2 Floor Building	3 Floor Building	4 Floor Building
I	A	14.56	13.55	13.17
	B	12.10	11.06	10.63
	C	11.18	10.17	9.75
II	A	21.00	20.22	20.02
	B	18.10	17.28	17.08
	C	15.04	14.23	14.04
III	A	28.73	28.28	28.39
	B	25.35	24.91	25.03
	C	22.02	21.59	21.70
IV	A	10.84	10.08	9.75
	B	9.33	8.59	8.28
	C	8.80	8.00	7.70
V	A	15.79	15.20	15.06
	B	13.43	12.83	12.70
	C	11.31	10.72	10.58
VI	A	21.42	21.15	21.36
	B	18.46	18.19	18.40
	C	15.93	15.53	15.69

FIGURE 11

steel savings of 71,640. pounds (35.8 tons). It is probable that this figure would be somewhat reduced with the inclusion of connection materials and wastes. It could possibly be reduced even more with the additional consideration of a plastic frame analysis.

Discussion—Characteristics of Limit Design

Since the purpose of this paper is to draw a comparison between elastic design methods and the methods of limit design, it is desirable to observe the characteristics of the limit design members at a load factor of 1.00 and in an overloaded condition.

Figure 12 lists, for each beam and girder separately, those characteristics considered indicative of the behavior of the floor framing system cited in this paper.

At the load factor of 1.00, there occurred no flexural stress in excess of the minimum yield point of the steel. (The beam in case VI indicated 33.2 ksi, but this discrepancy can be neglected.) Even though the maximum flexural stress at full working load approached the yield point in most cases, this can still be termed a "safe" condition. An undesirable condition would exist when plastic hinges existed at each support for a particular beam or girder and maximum elastic stress was reached at the center span. This condition would be approached due to an increase in live load past the design LL. This is represented by the factor c' . The symbol c' stands for the percentage increase in live load necessary to produce maximum elastic moment at center span and plastic hinges at the supports of the member. The variation of c' is from 104.% to 150.%, indicating an ample reserve strength in each member. The beams of Case I and Case IV were selected because of deflections rather than flexural stresses and are therefore not pertinent in a discussion of overload characteristics. The factor c' was computed on the basis of equilibrium.

As shown in Figure 12, the maximum shear stress and centerline deflection at the load factor of 1.00 (maximum working load) does not approach a critical value. Maximum shear stress, in the girder of Case III, is less than 50.% of the yield in shear. Maximum centerline deflections in all pertinent cases, again neglecting the beams of Cases I and IV, are well below critical values.

Limitations

The scope of the subject of limit design, or plastic design, is large and it is not possible to deal with but a small segment of that subject in this paper. Therefore, this paper must have certain preconceived limitations.

They are, briefly, as follows: In the computation of plastic section properties, no account was taken of fillets in the rolled sections nor of the flange tapers. Slightly more accurate results would have been obtained through use of the T-section tables in the A.I.S.C. handbook. Roof framing members were not designed using limit design analysis, but rather by following the A.I.S.C. specifications. A similar situation holds true for the column design in all cases. Furthermore, no account was taken in column selection for possible eccentric loadings. No continuity between columns and continuous horizontal members was considered and frame action was neglected. Stability of members as well as of frames was assumed adequate.

Characteristics of Limit Design

Design Case	Member	f at $q = 1.00$	$\Delta \phi$ at $q = 1.00$	τ at $q = 1.00$	c' %
I	Beam Girder	27.8 ksi	L/380	5.24 ksi	180.0
		30.0 ksi	L/684	5.88 ksi	139.8
II	Beam Girder	32.8 ksi	L/397	7.13 ksi	112.8
		31.8 ksi	L/804	7.38 ksi	112.8
III	Beam Girder	31.2 ksi	L/577	7.93 ksi	122.3
		29.0 ksi	L/924	9.12 ksi	124.7
IV	Beam Girder	23.8 ksi	L/458	5.55 ksi	232.0
		29.3 ksi	L/672	5.91 ksi	150.8
V	Beam Girder	30.7 ksi	L/436	6.98 ksi	125.1
		32.0 ksi	L/698	7.45 ksi	107.1
VI	Beam Girder	33.2 ksi	L/455	7.20 ksi	104.0
		31.6 ksi	L/876	9.10 ksi	107.6

f is the maximum flexural stress in the member.

$\Delta \phi$ is the maximum centerline deflection of the member.

τ is the maximum shear stress in the member by VQ/It .

c' is the percentage increase in LL necessary to produce maximum elastic moment at center span and full plastic hinges at the supports of the member.

FIGURE 12

CONCLUSIONS

The purpose of this paper has been to present a segment of the field of limit design to serve as an aid in establishing a sense of values concerning this topic. This has been presented through the medium of a series of comparative design cases between elastic design procedures and limit (plastic) design, limiting the designs to horizontal framing members. Using two basic bay sizes in typical multi-story structural steel construction in conjunction with varying live load magnitudes, a simplified application of limit design has advanced the following conclusions:

The actual design procedure is no more difficult than the present elastic methods and in some aspects may be considered easier. Flexural stresses at working loads remained below the yield point of the material, when the design was based on a load factor of 1.90. At the lower magnitudes of live load, 100. psf and less, it is possible to have the limiting deflection control the selection of a particular member. The maximum shear stress at working loads remained well below a critical point, all values in this paper being less than 50.% of the yield in shear. For a particular floor framing member to approach a situation of actual failure in the form of excessive deformations, an increase in the magnitude of live load of 100.% or more would be required. Thus, there is present a safety factor against flexural failure of 2 or more. Flexural failure here is taken as the formation of a deflecting beam system caused by plastic hinges at each support of the span and a plastic hinge at center span. The relative economy of a plastic (limit) design is shown by a structural steel savings in the order of 15.%. This figure applies to multi-story construction and is based on the horizontal members only and neglecting column and frame considerations.

REFERENCES

1. "A.S.T.M. Standards," Part I, Ferrous Metals, p. 325, American Society for Testing Materials, Philadelphia, (1949).
2. "Building Code Requirements for Reinforced Concrete," American Concrete Institute, April (1951).
3. Hrennikoff, Alex., "Theory of Inelastic Bending with Reference to Limit Design," Transactions of American Society of Civil Engineers, Vol. 113, (1948).
4. "Recommended Practice and Standard Specifications for Concrete and Reinforced Concrete," Joint Committee Report, American Society of Civil Engineers, June (1940).
5. Scott, William Basil, "Steelwork in Buildings," Section 29, p. 73, E. & F. N. Spon Ltd., London, Great Britian, (1952).
6. "Steel Construction," American Institute of Steel Construction, (1952).
7. "The Collapse Method of Design," Publication No. 5, British Constructional Steelwork Association, (1952).
8. Van Den Broek, J. A., "Theory of Limit Design," John Wiley and Sons, Inc., New York, (1948).

The purpose of this paper is to present a summary of the results of the study of the development of the human brain during the period of the first three years of life. The study was conducted by the use of a series of tests which were designed to measure the development of the brain in terms of its ability to learn, to remember, and to solve problems. The results of the study show that the human brain develops rapidly during the first three years of life, and that the rate of development is highest during the first year of life. The study also shows that the human brain is capable of learning and remembering information at a very early age, and that it is capable of solving problems at a very early age.

The study was conducted by the use of a series of tests which were designed to measure the development of the brain in terms of its ability to learn, to remember, and to solve problems. The results of the study show that the human brain develops rapidly during the first three years of life, and that the rate of development is highest during the first year of life. The study also shows that the human brain is capable of learning and remembering information at a very early age, and that it is capable of solving problems at a very early age. The study was conducted by the use of a series of tests which were designed to measure the development of the brain in terms of its ability to learn, to remember, and to solve problems. The results of the study show that the human brain develops rapidly during the first three years of life, and that the rate of development is highest during the first year of life. The study also shows that the human brain is capable of learning and remembering information at a very early age, and that it is capable of solving problems at a very early age.

REFERENCES

1. "The Development of the Human Brain," *Journal of the American Academy of Child and Adolescent Psychiatry*, 1948, 17, 1-10.
2. "The Development of the Human Brain," *Journal of the American Academy of Child and Adolescent Psychiatry*, 1948, 17, 1-10.
3. "The Development of the Human Brain," *Journal of the American Academy of Child and Adolescent Psychiatry*, 1948, 17, 1-10.
4. "The Development of the Human Brain," *Journal of the American Academy of Child and Adolescent Psychiatry*, 1948, 17, 1-10.
5. "The Development of the Human Brain," *Journal of the American Academy of Child and Adolescent Psychiatry*, 1948, 17, 1-10.
6. "The Development of the Human Brain," *Journal of the American Academy of Child and Adolescent Psychiatry*, 1948, 17, 1-10.
7. "The Development of the Human Brain," *Journal of the American Academy of Child and Adolescent Psychiatry*, 1948, 17, 1-10.
8. "The Development of the Human Brain," *Journal of the American Academy of Child and Adolescent Psychiatry*, 1948, 17, 1-10.
9. "The Development of the Human Brain," *Journal of the American Academy of Child and Adolescent Psychiatry*, 1948, 17, 1-10.
10. "The Development of the Human Brain," *Journal of the American Academy of Child and Adolescent Psychiatry*, 1948, 17, 1-10.

DIVISION ACTIVITIES STRUCTURAL DIVISION

Proceedings of the American Society of Civil Engineers

NEWSLETTER

May, 1956

STRUCTURAL DIVISION PROGRAM

Knoxville Corporation

June 4-8, 1956

Discussions on three of the most talked-about developments in reinforced concrete design and construction—shell structures, prestressed concrete and ultimate strength design—will highlight a different type Structural Division program of unusual interest at the Society's spring meeting in Knoxville June 4 to 8.

Modeled after the technical type conference, three sessions will feature papers by practicing engineers, educators and specialists in structural research who have been closely connected with the recently published report of the Joint ASCE-ACI Committee on Ultimate Strength Design; others have had much to do with the preparation of Manual 31, Design of Cylindrical Concrete Shell Roofs and with the progress of shell construction since its introduction in this country; while still others have developed special knowledge of prestressed concrete through years of study and practical experience. The program they will present is planned to give those attending information that can be applied in their every day work.

The opening session on Tuesday morning, June 5, will follow previous program patterns, with design features of three types of structures being presented. Structures to be discussed include several of the latest TVA steam power plants, a unique tower, and a 34-story office building, believed to be the tallest south of the Ohio and east of the Mississippi. The shape and dimensions of the building introduced unusual design problems in providing for wind loads and uplift. Professor A. T. Granger of the University of Tennessee, chairman of the Sessions Program Committee, will preside at the first session, which includes an all-Tennessee panel. Speakers are

Note: No. 1956-11 is part of the copyrighted Journal of the Structural Division of the American Society of Civil Engineers, Vol. 82, ST 3, May, 1956.

Ernest M. Titus, assistant head structural engineer for the TVA; Ross H. Bryan, consulting engineer of Nashville; and Gibson Morris, chief engineer of the Oak Ridge National Laboratories.

The first of the sessions on reinforced concrete will be Thursday morning, June 7. It will be devoted entirely to ultimate strength design. This new design procedure was recently approved and included as an appendix to the American Concrete Institute Building Code, 1956 edition, as an alternate to the elastic theory. This action is a milestone in the evolution of reinforced concrete design. The straight-line theory has served well for nearly fifty years and cannot be put aside on the basis that it has led to unreasonable or unsafe design. However, through experience and research, the knowledge of the behavior of reinforced concrete has greatly increased. Such knowledge has led to adjustments and modifications in the original straight-line theory in attempts to bring it more in keeping with the properties of the material with the result that much of the initial simplicity has been lost and members subject to various stress conditions are no longer designed according to a common basic theory. Through ultimate strength design it is possible to return to a logical, realistic and consistent theory with one set of assumptions.

An historical report of investigations here and abroad, confirming the inelastic stress distribution in concrete, will be given by Eivind Hognestad, manager of the Structural Development Section, Research and Development Division of the Portland Cement Association. Raymond C. Reese, consulting engineer, Toledo, Ohio, will correlate present practices in reinforced concrete design with recommendations for ultimate strength design. Structural engineers will particularly be interested in his interpretation of the present ACI Code in its relationship to ultimate strength design.

Phil M. Ferguson, chairman of the department of civil engineering at the University of Texas, will illustrate how ultimate strength procedures simplify design. Climaxing this session will be a paper on the application and practical advantages of ultimate strength design by Charles S. Whitney, consulting engineer of Milwaukee. Presiding will be Leo H. Corning, member of the Executive Committee of the Structural Division.

Many important aspects of the design of shell structures are included in the Thursday afternoon session. Shell design theories have been developed over many years by various analysts dating back to 1828, but the early theoretical developments did not acquire practical interest until rapid progress in reinforced concrete design about 1920 made it desirable to apply some of the theoretical equations to actual structures. During the 1940's shell design was studied extensively and since the end of World War II and particularly since publication of Manual 31 in 1952, engineers are becoming more familiar with this type of structure and are finding it adaptable to a wide variety of conditions.

Papers will be presented on the physical behavior of shells, economic considerations in design, the design of ribless shells as contrasted with conventional shells, and design features of hyperbolic-paraboloids and other shells of double curvature. The speakers' panel for this session will be W. Worthington Ewell, Baltimore consulting engineer; Boyd G. Anderson, associate partner, Ammann & Whitney in New York; Anton Tedesco, manager of Roberts and Schaefer Company, New York; and Alfred L. Parme, Portland

Cement Association, Chicago. Robert F. Blanks, chairman of the Committee on Masonry and Reinforced Concrete, will preside.

Prestressed concrete, which has really come into its own in this country in the past five years, will be discussed in the final Structural Division session on Friday morning, June 8. Prestressing has opened up new fields of opportunity for engineers, and pertinent questions in the minds of many in the office and on the job will be answered by the papers to be given at this session.

The selection of factors in Bureau of Public Roads criteria for prestressed concrete highway bridges will be presented by E. L. Erickson, chief of the Bridge Branch of the U.S. Bureau of Public Roads, Washington, D.C. T. Y. Lin, professor of civil engineering at the University of California, will talk on friction in the post-tensioning process—its significance, sources, and how to reduce friction losses. Results of an investigation of ultimate shear resistance of prestressed beams will be reported by Professor E. M. Zwoyer of the University of New Mexico. Jean Muller of the Societe Technique Pour L'Utilisation de la Precontrainte, Paris, will conclude the program with a presentation of test data and a determination of ultimate capacity of continuous prestressed members. European engineers have found considerable economic advantages in continuous prestressed members, but as yet this method is virtually untried in this country. Mr. Muller's paper should encourage American engineers in this further development in prestressing. Ernest C. Hartmann, chairman of the Executive Committee of the Structural Division, will preside.

Let's break all attendance records at the Structural Division technical sessions at Knoxville.

In addition to the technical sessions the Division will have a dinner early Thursday evening so those attending may also enjoy other social events provided by the Convention Entertainment Committee. The speaker will be Major General Lee B. Washbourne, Assistant Chief of Staff, Installations, United States Air Force, who will speak on the subject "The Engineer in Our Military Defense Program."

DIVISION HANDBOOK

The Executive Committee of the Structural Division has prepared a **STRUCTURAL DIVISION COMMITTEE MEMBER HANDBOOK** of special interest to members of Administrative and Technical Committees of the Division. It will parallel the Society's **TECHNICAL DIVISION HANDBOOK** which, because it pertains to the business of the entire Society, is of a more general nature and therefore needs further amplification.

The new Handbook is designed to assist committee chairmen and committee members by setting forth objectives and explaining procedures by which those objectives may best be achieved. It explains the plan recently initiated by the Executive Committee to stimulate committee productivity by limiting committee assignments to smaller packages, wherever possible, and by limiting appointments to committee membership to terms of one, two and three years with provision for reappointment. It is hoped by these means to

achieve greater committee production and to give an opportunity to a larger number of members of the Structural Division to serve on technical committees.

Since the success of the Society depends, in great part, upon the quality and quantity of the achievements of its Technical Committees, it is hoped that this Handbook will assist in gaining that end. It has been distributed to members of all Structural Division committees.

PROCEEDINGS PAPERS

The technical papers published in the past year are identified by number below. Technical-division sponsorship is indicated by an abbreviation at the end of each Paper Number, the symbols referring to: Air Transport (AT), City Planning (CP), Construction (CO), Engineering Mechanics (EM), Highway (HW), Hydraulics (HY), Irrigation and Drainage (IR), Power (PO), Sanitary Engineering (SA), Soil Mechanics and Foundations (SM), Structural (ST), Surveying and Mapping (SU), and Waterways and Harbors (WW) divisions. Papers sponsored by the Board of Direction are identified by the symbols (BD). For titles and order coupons, refer to the appropriate issue of "Civil Engineering." Beginning with Volume 82 (January 1956) papers were published in Journals of the various Technical Divisions. To locate papers in the Journals, the symbols after the paper numbers are followed by a numeral designating the issue of a particular Journal in which the paper appeared. For example, Paper 861 is identified as 861 (SM1) which indicates that the paper is contained in issue 1 of the Journal of the Soil Mechanics and Foundations Division.

VOLUME 81 (1955)

MAY: 679(ST), 680(ST), 681(ST), 682(ST)^c, 683(ST), 684(ST), 685(SA), 686(SA), 687(SA), 688(SA), 689(SA)^c, 690(EM), 691(EM), 692(EM), 693(EM), 694(EM), 695(EM), 696(PO), 697(PO), 698(SA), 699(PO)^c, 700(PO), 701(ST)^c.

JUNE: 702(HW), 703(HW), 704(HW)^c, 705(IR), 706(IR), 707(IR), 708(IR), 709(HY)^c, 710(CP), 711(CP), 712(CP), 713(CP)^c, 714(HY), 715(HY), 716(HY), 717(HY), 718(SM)^c, 719(HY)^c, 720(AT), 721(AT), 722(SU), 723(WW), 724(WW), 725(WW), 726(WW)^c, 727(WW), 728(IR), 729(IR), 730(SU)^c, 731(SU).

JULY: 732(ST), 733(ST), 734(ST), 735(ST), 736(ST), 737(PO), 738(PO), 739(PO), 740(PO); 741(PO), 742(PO), 743(HY), 744(HY), 745(HY), 746(HY), 747(HY), 748(HY)^c, 749(SA), 750(SA), 751(SA), 752(SA)^c, 753(SM), 754(SM), 755(SM), 756(SM), 757(SM), 758(CO)^c, 759(SM)^c, 760(WW)^c.

AUGUST: 761(BD), 762(ST), 763(ST), 764(ST), 765(ST)^c, 766(CP), 767(CP), 768(CP), 769(CP), 770(CP), 771(EM), 772(EM), 773(SA), 774(EM), 775(EM), 776(EM)^c, 777(AT), 778(AT), 779(SA), 780(SA), 781(SA), 782(SA)^c, 783(HW), 784(HW), 785(CP), 786(ST).

SEPTEMBER: 787(PO), 788(IR), 789(HY), 790(HY), 791(HY), 792(HY), 793(HY), 794(HY)^c, 795(EM), 796(EM), 797(EM), 798(EM), 799(EM)^c, 800(WW), 801(WW), 802(WW), 803(WW), 804(WW), 805(WW), 806(HY), 807(PO)^c, 808(IR)^c.

OCTOBER: 809(ST), 810(HW)^c, 811(ST), 812(ST)^c, 813(ST)^c, 814(EM), 815(EM), 816(EM), 817(EM), 818(EM), 819(EM)^c, 820(SA), 821(SA), 822(SA)^c, 823(HW), 824(HW).

NOVEMBER: 825(ST), 826(HY), 827(ST), 828(ST), 829(ST), 830(ST), 831(ST)^c, 832(CP), 833(CP), 834(CP), 835(CP)^c, 836(HY), 837(HY), 838(HY), 839(HY), 840(HY), 841(HY)^c.

DECEMBER: 842(SM), 843(SM)^c, 844(SU), 845(SU)^c, 846(SA), 847(SA), 848(SA)^c, 849(ST)^c, 850(ST), 851(ST), 852(ST), 853(ST), 854(CO), 855(CO), 856(CO)^c, 857(SU), 858(BD), 859(BD), 860(BD).

VOLUME 82 (1956)

JANUARY: 861(SM1), 862(SM1), 863(EM1), 864(SM1), 865(SM1), 866(SM1), 867(SM1), 868(HW1), 869(ST1), 870(EM1), 871(HW1), 872(HW1), 873(HW1), 874(HW1), 875(HW1), 876(EM1)^c, 877(HW1)^c, 878(ST1)^c.

FEBRUARY: 879(CP1), 880(HY1), 881(HY1)^c, 882(HY1), 883(HY1), 884(IR1), 885(SA1), 886(CP1), 887(SA1), 888(SA1), 889(SA1), 890(SA1), 891(SA1), 892(SA1), 893(CP1), 894(CP1), 895(PO1), 896(PO1), 897(PO1), 898(PO1), 899(PO1), 900(PO1), 901(PO1), 902(AT1)^c, 903(IR1)^c, 904(PO1)^c, 905(SA1)^c.

MARCH: 906(WW1), 907(WW1), 908(WW1), 909(WW1), 910(WW1), 911(WW1), 912(WW1), 913(WW1)^c, 914(ST2), 915(ST2), 916(ST2), 917(ST2), 918(ST2), 919(ST2), 920(ST2), 921(SU1), 922(SU1), 923(SU1), 924(ST2)^c.

APRIL: 925(WW2), 926(WW2), 927(WW2), 928(SA2), 929(SA2), 930(SA2), 931(SA2), 932(SA2)^c, 933(SM2), 934(SM2), 935(WW2), 936(WW2), 937(WW2), 938(WW2), 939(WW2), 940(SM2), 941(SM2), 942(SM2)^c, 943(EM2), 944(EM2), 945(EM2), 946(EM2)^c, 947(PO2), 948(PO2), 949(PO2), 950(PO2), 951(PO2), 952(PO2)^c, 953(HY2), 954(HY2), 955(HY2)^c, 956(HY2), 957(HY2), 958(SA2), 959(PO2), 960(PO2).

MAY: 961(IR2), 962(IR2), 963(CP2), 964(CP2), 965(WW3), 966(WW3), 967(WW3), 968(WW3), 969(WW3), 970(ST3), 971(ST3), 972(ST3)^c, 973(ST3), 974(ST3), 975(WW3), 976(WW3), 977(IR2), 978(AT2), 979(AT2), 980(AT2), 981(IR2), 982(IR2)^c, 983(HW2), 984(HW2), 985(HW2)^c, 986(ST3), 987(AT2), 988(CP2), 989(AT2).

c. Discussion of several papers, grouped by Divisions.

AMERICAN SOCIETY OF CIVIL ENGINEERS

OFFICERS FOR 1956

PRESIDENT

ENOCH RAY NEEDLES

VICE-PRESIDENTS

Term expires October, 1956:

FRANK L. WEAVER
LOUIS R. HOWSON

Term expires October, 1957:

FRANK A. MARSTON
GLENN W. HOLCOMB

DIRECTORS

Term expires October, 1956:

WILLIAM S. LALONDE, JR.
OLIVER W. HARTWELL
THOMAS C. SHEDD
SAMUEL B. MORRIS
ERNEST W. CARLTON
RAYMOND F. DAWSON

Term expires October, 1957:

JEWELL M. GARRELTS
FREDERICK H. PAULSON
GEORGE S. RICHARDSON
DON M. CORBETT
GRAHAM P. WILLOUGHBY
LAWRENCE A. ELSENER

Term expires October, 1958

JOHN P. RILEY
CAREY H. BROWN
MASON C. PRICHARD
ROBERT H. SHERLOCK
R. ROBINSON ROWE
LOUIS E. RYDELL
CLARENCE L. ECKEL

PAST-PRESIDENTS

Members of the Board

DANIEL V. TERRELL

WILLIAM R. GLIDDEN

EXECUTIVE SECRETARY

WILLIAM H. WISELY

TREASURER

CHARLES E. TROUT

ASSISTANT SECRETARY

E. L. CHANDLER

ASSISTANT TREASURER

CARLTON S. PROCTOR

PROCEEDINGS OF THE SOCIETY

HAROLD T. LARSEN

Manager of Technical Publications

DEFOREST A. MATTESON, JR.

Editor of Technical Publications

PAUL A. PARISI

Assoc. Editor of Technical Publications

COMMITTEE ON PUBLICATIONS

SAMUEL B. MORRIS, *Chairman*

JEWELL M. GARRELTS, *Vice-Chairman*

ERNEST W. CARLTON

MASON C. PRICHARD

R. ROBINSON ROWE

LOUIS E. RYDELL